

ROLE OF *rocA* POLYMORPHISMS ON VIRULENCE AND PATHOGENESIS OF
SEROTYPE M28 GROUP A *Streptococcus*

A Dissertation

by

PAUL EDWARD BERNARD

Submitted to the Graduate and Professional School of
Texas A&M University
in partial fulfillment of the requirements for the degree of

DOCTOR OF PHILOSOPHY

Chair of Committee,	Randall J. Olsen
Committee Members,	David P. Huston
	L. Garry Adams
	Sara D. Lawhon
	James M. Musser
Head of Program,	Carol Vargas

May 2022

Major Subject: Medical Sciences

Copyright 2022 Paul Edward Bernard

ABSTRACT

Group A *Streptococcus* (*Streptococcus pyogenes*, GAS) is a human-specific pathogen that causes a wide range of diseases and significant morbidity and mortality worldwide. Despite over a century of research, no licensed human vaccine exists to protect against GAS infection, which may be due, in part, to the complex regulation of its many virulence factors and surface exposed proteins. Several virulence regulators have been well described for GAS, including the CovRS (control of virulence regulator/sensor) two-component system. CovRS is a negative regulator of virulence in GAS. That is, CovS phosphorylates CovR to repress virulence gene expression. Whereas CovRS has been extensively studied over the past two decades, my research efforts have focused on RocA (regulator of Cov), an accessory protein to the CovRS two-component system. RocA is believed to interact with CovS to increase CovR phosphorylation, although the molecular mechanism of this phenomenon remains unknown.

Recent whole-genome population-based sequencing studies of serotype M28 GAS invasive disease clinical isolates identified an unusually high number of polymorphisms in *rocA* compared to other serotypes. Thus, I hypothesized that amino acid changes in RocA result in altered RocA-RocA and RocA-CovS protein interactions, giving rise to an altered global transcriptome and increased virulence in serotype M28 GAS. I used naturally-occurring clinical isolates and constructed isogenic *rocA* GAS mutant strains for transcriptome sequencing (RNA-seq), *in vitro* virulence factor assays, and *in vivo* animal infection model studies. Additionally, I performed substituted cysteine accessibility method as applied to transmembrane orientation (SCAMTM) to determine the membrane topology of

RocA and bacterial adenylate cyclase-based two-hybrid (BACTH) assays to study RocA protein-protein interactions.

My results demonstrate that deletion of *rocA* results in a significantly altered GAS transcriptome and significantly increased virulence *in vivo*. Naturally-occurring polymorphisms in *rocA* also altered the global GAS transcriptome and increased strain virulence. The observed virulence phenotypes are the result of altered RocA-RocA and RocA-CovS protein interactions. Taken together, the data add important new understanding of the molecular pathogenesis of RocA in serotype M28 GAS.

DEDICATION

For Mom, Dad, James, Abi, Katie, Torie, and Jensen

ACKNOWLEDGEMENTS

First, I would like to thank my committee chair, Dr. Olsen, and my committee members, Dr. Huston, Dr. Adams, Dr. DeLeo, Dr. Lawhon, and Dr. Musser, for their guidance and support throughout the course of this research.

Second, thanks go to the Fondren Foundation at Houston Methodist and the American Heart Association for financial support of this research.

Third, thanks go to my colleagues in laboratory of Dr. Musser and the Department of Pathology and Genomic Medicine at the Houston Methodist Research Institute for their support and assistance with this research, and also for making the four years in the lab a great experience. Additionally, thanks to Dr. Amy Wright and her team in the Houston Methodist Academic Institute, and the laboratory of Dr. Bogdanov at the University of Texas Health Science Center at Houston McGovern Medical School.

Fourth, thanks go to my undergraduate summer interns Zaid Kajani, Jessica Madry, and Amey Duarte. All of you provided me an invaluable teaching experience, and I wish the best of luck to each of you in your promising future endeavors.

Fifth, thanks go to my colleagues in the Texas A&M Health Science Center College of Medicine MD/Ph.D. program, the program coordinators, and Dr. Leibowitz and Dr. Cannon for their support and guidance during the course of my time in the program.

Finally, thanks go to my immediate family, Mom, Dad, James, Abi, Katie, Torie, and Jensen, and all of my extended family across the country, for their encouragement, support, and patience while I conducted this research.

CONTRIBUTORS AND FUNDING SOURCES

Contributors

This work was supervised by a dissertation committee consisting of Dr. Randall J. Olsen (advisor) and Dr. James M. Musser of the Department of Pathology and Genomic Medicine, Houston Methodist Research Institute and Houston Methodist Hospital; Dr. David P. Huston of the Department of Microbial Pathogenesis and Immunology, College of Medicine; and Dr. L. Garry Adams and Dr. Sara D. Lawhon of the Department of Veterinary Pathobiology, College of Veterinary Medicine. Dr. Frank R. DeLeo (Chief, Laboratory of Bacteriology, Rock Mountain Laboratories, National Institutes of Health) served as a guest member of the dissertation committee.

The research conducted in Chapter 2 was performed in conjunction with my co-authors Priyanka Kachroo, Luchang Zhu, Stephen B. Beres, Jesus M. Eraso, Zaid Kajani, Z. Wesley Long, James M. Musser, and Randall J. Olsen. Technical assistance was provided by Matthew Ojeda Saavedra, Sarah Linson, Concepcion Cantu, and Kathryn Stockbauer.

The research conducted in Chapter 3 was performed in conjunction with my co-authors Priyanka Kachroo, Jesus M. Eraso, Luchang Zhu, Jessica E. Madry, Sarah E. Linson, Matthew Ojeda Saavedra, Concepcion Cantu, James M. Musser, and Randall J. Olsen. Technical assistance was provided by Samantha Kubiak, Hoang Nguyen, and Sasha M. Pejerrey.

The research conducted in Chapter 4 was performed in conjunction with my co-authors Amey Duarte, Mikhail Bogdanov, James M. Musser, and Randall J. Olsen. Technical assistance was provided by Nishanth Makthal, Hackwon Do, Prasanti Yerramilli,

Layne Pruitt, Matthew Ojeda Saavedra, Concepcion Cantu, Sasha M. Pejerrey, and Heather McConnell. Additionally, Daniel Ladant provided a plasmid for these experiments.

Figure 5-1 in Chapter 5 was created by Heather McConnell.

All other work conducted for the dissertation was completed by the student independently.

Funding Sources

Graduate study was supported by the Texas A&M Health Science Center College of Medicine MD/Ph.D. Program and the Houston Methodist Academic Institute.

This work was also made possible in part by a Fondren Foundation Medical Scientist Trainee Fellowship (Houston Methodist Hospital) and an American Heart Association Predoctoral Fellowship (award number 19PRE34380820). Its contents are solely the responsibility of the authors and do not necessarily represent the official views of the Fondren Foundation and American Heart Association.

TABLE OF CONTENTS

Page

ABSTRACT ii

DEDICATION iv

ACKNOWLEDGEMENTS v

CONTRIBUTORS AND FUNDING SOURCES..... vi

TABLE OF CONTENTS viii

LIST OF FIGURES xii

LIST OF TABLES xiv

1. INTRODUCTION..... 1

 1.1. Group A *Streptococcus*: A major cause of morbidity and mortality worldwide 1

 1.1.1. Serotype M28 GAS: Overrepresentation in puerperal sepsis and female genital tract infections, yet underrepresentation in molecular pathogenesis research... 2

 1.2. Two-component systems: Major gene expression regulatory systems in bacteria 3

 1.2.1. TCSs of GAS..... 6

 1.3. Accessory proteins to TCSs: An added layer of regulatory complexity to TCSs 16

 1.3.1. RocA: An accessory protein to the CovRS TCS in GAS..... 19

 1.4. Overarching hypothesis..... 21

 1.5. References 23

2. ROCA HAS SEROTYPE-SPECIFIC GENE REGULATORY AND PATHOGENESIS ACTIVITIES IN SEROTYPE M28 GROUP A STREPTOCOCCUS 50

 2.1. Summary 50

 2.2. Introduction 51

 2.3. Results 53

 2.3.1. *rocA* is unusually polymorphic in serotype M28 GAS 53

 2.3.2. Creation of an isogenic *rocA* deletion mutant strain 55

 2.3.3. Deletion of *rocA* in M28 GAS strain MGAS28426 results in a substantial transcriptome change..... 55

 2.3.4. RocA directly or indirectly regulates transcription regulators involved in virulence in serotype M28 GAS 58

 2.3.5. RocA directly or indirectly regulates transcription regulators and virulence factors involved in the stress response in serotype M28 GAS 59

2.3.6. Deletion of <i>rocA</i> results in differential transcript levels of multiple GAS virulence factors	61
2.3.7. Deletion of <i>rocA</i> results in increased virulence in a mouse model of necrotizing myositis	63
2.4. Discussion	64
2.5. Materials and methods	71
2.5.1. Determination of SNPs in <i>rocA</i> in serotype M28 GAS strains	71
2.5.2. Construction of an isogenic <i>rocA</i> deletion strain	72
2.5.3. RNA-seq analysis	72
2.5.4. SOF activity assay	74
2.5.5. Growth under acidic conditions	74
2.5.6. Western immunoblot analysis of SPN and SLO in culture supernatant.....	75
2.5.7. SPN and SLO activity assays	75
2.5.8. PAF acetylhydrolase activity assay	75
2.5.9. SKA activity assay	76
2.5.10. Mouse model of necrotizing myositis	76
2.5.11. Hyaluronic acid capsule assay	77
2.5.12. Accession number(s)	77
2.6. References	78
3. POLYMORPHISMS IN REGULATOR OF COV CONTRIBUTE TO THE MOLECULAR PATHOGENESIS OF SEROTYPE M28 GROUP A <i>STREPTOCOCCUS</i>	93
3.1. Summary	93
3.2. Introduction	94
3.3. Materials and methods	96
3.3.1. RNA-seq analysis	96
3.3.2. Generation of isogenic <i>rocA</i> polymorphism strains	99
3.3.3. Growth in acidic conditions	100
3.3.4. Western immunoblot analysis of SPN and SLO in culture supernatants	101
3.3.5. Activity assays.....	101
3.3.6. Quantitative RT-PCR analysis	101
3.3.7. Animal infection models	102
3.3.8. Statistical analysis	103
3.3.9. Data availability	103
3.4. Results	103
3.4.1. Naturally occurring polymorphisms in <i>rocA</i> are associated with altered transcriptomes in serotype M28 GAS strains	103
3.4.2. Selection and construction of isogenic <i>rocA</i> polymorphism strains	105
3.4.3. Polymorphisms in <i>rocA</i> result in an altered transcriptome in M28 GAS strains.....	108
3.4.4. Polymorphisms in <i>rocA</i> confer two distinct responses to acid stress in M28 GAS	109

3.4.5. Polymorphisms in <i>rocA</i> confer different virulence factor expression and enzymatic activity profiles in M28 GAS strains	110
3.4.6. Polymorphisms in <i>rocA</i> confer different secreted streptokinase activities	111
3.4.7. Polymorphisms in <i>rocA</i> confer two distinct virulence phenotypes in a mouse model of necrotizing myositis	114
3.4.8. Polymorphisms in <i>rocA</i> result in altered virulence in a NHP model of necrotizing myositis	116
3.5. Discussion	116
3.6. References	121
4. SINGLE AMINO ACID REPLACEMENTS IN ROCA DISRUPT PROTEIN-PROTEIN INTERACTIONS TO ALTER THE MOLECULAR PATHOGENESIS OF GROUP A <i>STREPTOCOCCUS</i>	138
4.1. Summary	138
4.2. Introduction	139
4.3. Results	141
4.3.1. Multiple <i>in silico</i> membrane topology algorithms predict a consensus RocA membrane topology	141
4.3.2. SCAM TM recapitulates the predicted <i>in silico</i> topology of RocA	143
4.3.3. RocA-PhoA-LacZ α protein fusions are consistent with the <i>in silico</i> algorithm predictions and SCAM TM results	146
4.3.4. Summary of the RocA protein topology experiments	147
4.3.5. RocA interacts with RocA and CovS, but not CovR	148
4.3.6. Amino acid changes in RocA differentially alter the interaction of RocA with itself and CovS	150
4.3.7. Polymorphisms in the C-terminus of RocA are function-altering	153
4.4. Discussion	156
4.5. Experimental procedures	161
4.5.1. Strains and culture conditions	161
4.5.2. <i>In silico</i> modeling and prediction of RocA membrane topology	162
4.5.3. Construction of cysteine-engineered RocA-FLAG-tag plasmids and strains	162
4.5.4. Membrane topology studies: Substituted-cysteine accessibility method as applied to transmembrane orientation (SCAM TM)	163
4.5.5. Western immunoblot analysis	165
4.5.6. Membrane topology studies: PhoA-LacZ α protein fusions	165
4.5.7. Bacterial adenylate cyclase-based two-hybrid (BACTH) assays	167
4.5.8. Generation of isogenic C-terminal <i>rocA</i> polymorphism strains	168
4.5.9. <i>In vitro</i> virulence factor activity assays	168
4.5.10. Mouse model of necrotizing myositis	168
4.5.11. Statistical analyses	169
4.6. References	169
5. CONCLUSIONS	184

5.1. RocA: An important virulence regulator in the molecular pathogenesis of GAS..	184
5.2. Polymorphisms in <i>rocA</i> differentially effect molecular pathogenesis	184
5.2.1. RocA R258K and V420I	185
5.2.2. RocA P97L	186
5.2.3. RocA G184W and G184E	189
5.2.4. RocA T442I, T442P, and Q443*	191
5.3. Polymorphisms in <i>covS</i> that result in altered RocA-CovS interaction.....	193
5.4. RocA as a global accessory protein: Potential interactions with other TCSs	194
5.5. Streptokinase regulation in serotype M28 GAS.....	195
5.6. Conclusions	196
5.7. References	197
APPENDIX A FIGURES.....	210
APPENDIX B TABLES	220

LIST OF FIGURES

	Page
Fig. 1-1 Predicted structure of the GAS CovS (control of virulence sensor) HK cytoplasmic domain.	5
Fig. 1-2 <i>rocA</i> polymorphisms in serotype M28 GAS strains.	22
Fig. 2-1 <i>rocA</i> is unusually polymorphic in serotype M28 GAS strains.	53
Fig. 2-2 Deletion of <i>rocA</i> significantly alters the GAS transcriptome.	56
Fig. 2-3 Deletion of <i>rocA</i> significantly increases the transcript levels of genes in the Mga regulon.	59
Fig. 2-4 Deletion of <i>rocA</i> significantly increases the transcript levels of genes encoding transcription regulators and proteins involved in the stress response.	60
Fig. 2-5 Deletion of <i>rocA</i> significantly increases GAS virulence factor levels and activity in the culture supernatant.	63
Fig. 2-6 Deletion of <i>rocA</i> increases GAS virulence in a mouse model of necrotizing myositis.	64
Fig. 2-7 Model of RocA contribution to the molecular pathogenesis of serotype M28 GAS.	65
Fig. 3-1 Clinical isolates with naturally occurring <i>rocA</i> polymorphisms have altered global transcriptomes.	97
Fig. 3-2 Polymorphisms in <i>rocA</i> significantly alter the GAS transcriptome.	107
Fig. 3-3 Polymorphisms in <i>rocA</i> result in an altered virulence phenotype <i>in vitro</i>	110
Fig. 3-4 Polymorphisms in <i>rocA</i> result in decreased <i>ska</i> transcript levels and streptokinase (SKA) activity, in part, due to altered <i>fasX</i> regulation.	113
Fig. 3-5 Polymorphisms in <i>rocA</i> result in altered virulence in mouse and nonhuman primate (NHP) models of necrotizing myositis.	115
Fig. 3-6 Model of RocA contribution to the molecular pathogenesis of serotype M28 GAS.	117
Fig. 4-1 The predicted membrane topology model of RocA has a seven transmembrane helical architecture.	142

Fig. 4-2 RocA interacts with itself and CovS, but not CovR.	149
Fig. 4-3 Single amino acid replacements in RocA alter the interaction between RocA and itself and CovS.	151
Fig. 4-4 Polymorphisms in the C-terminus of RocA are function-altering.	152
Fig. 4-5 Polymorphisms in the C-terminus of RocA result in altered virulence in a mouse model of necrotizing myositis.	155
Fig. 4-6 Single amino acid replacements in RocA alter RocA-RocA and RocA-CovS interactions, leading to altered gene expression and virulence.	157
Fig. 5-1 RocA is an accessory protein to the CovRS two-component system in group <i>A Streptococcus</i>	185

LIST OF TABLES

	Page
Table 2-1 GAS transcription regulator genes (proven and inferred) directly or indirectly regulated by RocA at mid-exponential (ME) and early-stationary (ES) growth phases.....	57
Table 2-2 Selected proven and putative virulence factors of GAS regulated by <i>rocA</i> at mid-exponential (ME) and early-stationary (ES) growth phases.	62
Table 3-1 Primers used in this study.	100
Table 4-1 Experimentally determined cellular location for RocA residues, as determined by SCAM TM	145
Table 4-2 Normalized activity ratios (NARs) and experimentally determined cellular location for RocA residues.	147

1. INTRODUCTION

1.1. Group A *Streptococcus*: A major cause of morbidity and mortality worldwide

Group A *Streptococcus* (*Streptococcus pyogenes*, GAS) is a human-specific pathogen responsible for an immense disease burden worldwide. GAS asymptotically colonizes the throat and skin (1, 2). It causes a wide range of diseases, from superficial infections, such as pharyngitis (“strep-throat”), impetigo, and scarlet fever, to invasive life-threatening infections, such as streptococcal toxic shock syndrome (STSS) and necrotizing fasciitis (“flesh-eating” disease) (1-3). GAS infection can also lead to serious post-infectious immune sequelae, such as acute rheumatic fever, rheumatic heart disease, and post-streptococcal glomerulonephritis (1, 2).

The disease burden of GAS globally is substantial. An estimated 111 million skin infections, 616 million cases of pharyngitis, 1.78 million new cases of invasive and post-infectious sequelae, and 517,000 deaths occur annually worldwide (4). The World Health Organization ranks GAS as the ninth leading cause of infectious mortality (2). Over the years, the incidence of post-infectious sequelae has decreased due to the use of antibiotics (1). However, rheumatic heart disease is still estimated to affect 2.4 million children aged five to fourteen (4), making rheumatic heart disease the most common cause of preventable pediatric heart disease worldwide (2). Despite the large disease burden, and over a century of GAS pathogenesis research (1, 2), no commercially licensed vaccine is available (5).

GAS strains are most commonly classified by the *emm* gene, encoding the highly polymorphic and antiphagocytic M protein (2, 6). GAS serotypes were historically identified using antisera against the M protein, but they are now more often identified by sequencing

the *emm* gene (1, 7). Over 220 GAS serotypes have been characterized to date (7), with variation in the disease rate caused by GAS strains of differing serotypes (8). In high income and industrialized countries, such as the United States and Western Europe, the majority of GAS disease is caused by a few serotypes (2, 8, 9). In contrast, countries in Africa and the Pacific Islands have no dominant serotype(s) (8).

The GAS genome is approximately 1.9 Mb in size, regardless of serotype (3). GAS strains of different serotypes have approximately 90% shared gene content (the core genome), with the remaining 10% being located in mobile genetic elements such as prophages and integrative and conjugative elements (3). While the core genomes of GAS strains of different serotypes differ from one another on the order of tens of thousands of single nucleotide polymorphisms (SNPs) and insertions/deletions (indels) (3, 10), GAS strains within the same serotype differ by tens to hundreds of SNPs and indels (10-14). Minute genetic differences between GAS strains may cause drastic differences in virulence, as best demonstrated by the genomic events driving the current epidemics of serotype M1 and M89 GAS strains (12, 13, 15, 16).

1.1.1. Serotype M28 GAS: Overrepresentation in puerperal sepsis and female genital tract infections, yet underrepresentation in molecular pathogenesis research

Serotype M28 GAS strains are among the more common serotypes causing GAS pharyngitis and invasive disease in the United States and Western Europe (2, 8, 9, 17-19). Additionally, serotype M28 GAS are overrepresented in puerperal sepsis and female genital tract infections (14, 17, 19-25). The overabundance may be due, in part, to the region of difference 2 (RD2) element in the genome of most serotype M28 GAS strains (22, 26). RD2 is a 37.4 kb mobile genetic element that encodes 7 putative extracellular proteins and has

high homology to *Streptococcus agalactiae*, a common cause of neonatal infections (22). Despite being a common cause of GAS infections, knowledge of the molecular pathogenesis of serotype M28 GAS is lacking compared to other numerically important serotypes, such as serotype M1 and M3 GAS (5, 11, 12, 14, 26-32).

1.2. Two-component systems: Major gene expression regulatory systems in bacteria

Two-component systems (TCSs) are fundamental regulatory systems used by bacteria to sense stimuli in the environment and alter gene expression (33, 34). Classically, a TCS is comprised of two proteins: a histidine kinase (HK) and a response regulator (RR) (33, 34). HKs typically function as homodimers and sense a stimulus in the environment, resulting in autophosphorylation of a conserved histidine residue. The phosphate group is then transferred to a conserved aspartic acid residue of the RR, resulting in a conformational change of the RR and altered expression of genes under its regulatory control (33, 34). In pathogenic and non-pathogenic bacteria alike, TCSs are major regulators of many different virulence factors and other transcription regulators and genes that control diverse cellular phenotypes (33, 35, 36). Almost all bacterial species studied to date encode TCSs (33, 37), and the apparent lack of HKs in the animal kingdom make them a possibly favorable target for designing novel antimicrobial therapies (33, 37, 38).

HKs are most commonly composed of two main domains: an N-terminal sensing domain and a C-terminal kinase domain. Most HKs reside in the cellular membrane, typically having two transmembrane domains with an extracellular sensing domain in the N-terminus (34, 35, 37), though for many HKs the exact stimulus that is sensed remains unknown (35, 36). Not all HKs have a large extracellular loop between the transmembrane domains. The intramembrane HKs are hypothesized to sense stimuli in the membrane (35).

Little to no conservation of the N-terminal sensing domain sequences is observed, suggesting a great diversity of stimuli that can be detected (34, 35). In comparison, the C-terminal kinase domains are relatively well conserved (37, 39). Two main regions of highly conserved sequences exist in the kinase domain (Fig. 1-1): the phosphorylatable histidine (the H box) and the ATP binding sites (the N, D, F, and G boxes) (33, 34, 37, 39). The conserved sequences are used for classification of HKs (35, 37), but they do not typically predict stimuli sensed or regulatory output (35). The exact mechanism of signal transduction from the extracellular N-terminal sensing domain through the membrane to the C-terminal kinase domain remains unknown (34); however, many models have been proposed (40).

RRs are most commonly composed of two domains: an N-terminal receiver domain and a C-terminal effector domain (33, 34). The N-terminal receiver domain is the site of the phosphorylatable aspartic acid residue and the site of the RR dimerization interface (33, 34). The aspartic acid residue resides in an acidic pocket that catalyzes the phosphotransfer from the HK histidine to the RR aspartic acid (33, 37). Phosphorylation of the RR results in global conformation changes in the entire protein, shifting the RR from an inactive to active state (33). Most RRs are transcription regulators, containing a C-terminal DNA-binding motif (33). Therefore, sensing of a stimulus by a HK will result in direct changes in gene expression due to altered DNA-binding affinity and/or dimerization potential of the RR (33). While most phosphorylation of RRs is carried out by phosphotransfer from HKs, small phosphate donors, such as acetyl phosphate, can phosphorylate RRs *in vivo*, though at a much slower rate (34).

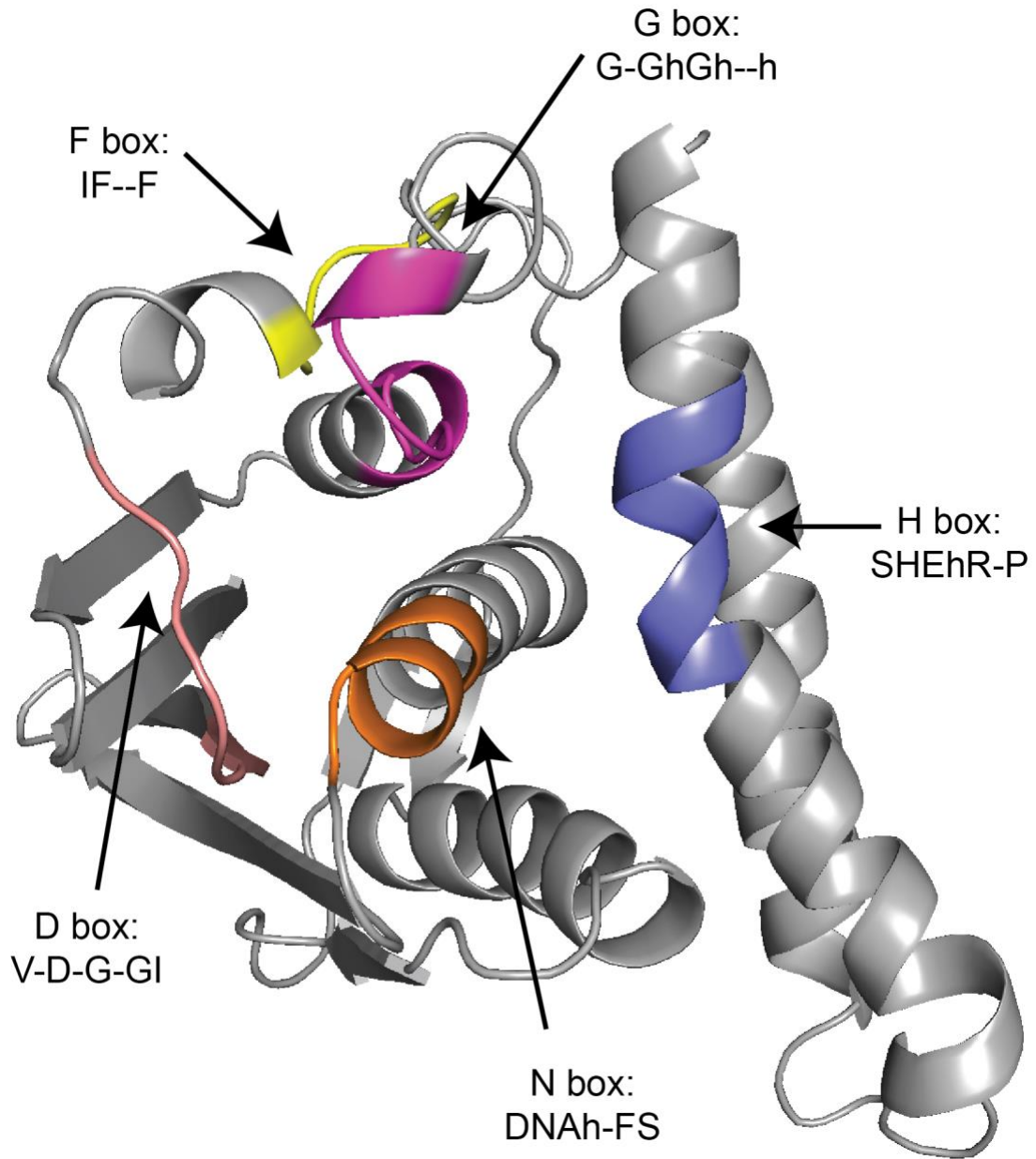


Fig. 1-1 Predicted structure of the GAS CovS (control of virulence sensor) HK cytoplasmic domain. The location of highly conserved sequences are indicated: H box (purple), N box (orange), D box (pink), F box (yellow), and G box (magenta) (41, 42). Consensus sequences are depicted for the HPK1a family (h, hydrophobic residue) (37).

Most HKs are activated from a “kinase-off” state to a “kinase-on” state by stimuli (33, 34). That is, activation of HKs by stimuli will result in increased phosphorylation and activation of RRs. While all HKs are kinases, some also possess phosphatase activity (37). Bifunctional kinases are able to phosphorylate and dephosphorylate a RR, providing an

added layer of regulatory control (37). While all HKs participate in phosphotransfer through a common mechanism, one HK acts on one RR (34). The cognate HK-RR pair is typically organized in the same operon within the bacterial genome, making identification of the pairs relatively facile (37).

TCSs have a documented role in pathogenesis for several bacterial species (36). While many TCSs can act independently to regulate a specific response to a specific stimulus, often times multiple TCSs will work in tandem to deliver a shared phenotype (34). For example, a single hybrid HK and RR regulate virulence gene expression in *Bordetella pertussis* (36). In contrast, several TCSs function in a phosphorelay to regulate sporulation in *Bacillus subtilis*, and in tandem to regulate virulence determinants in *Salmonella enterica* (36, 43). Thus, although a TCS may have a documented role in virulence, the mechanism for the observed phenotype is not common to all HKs (36). Understanding TCSs remains an active field for molecular pathogenesis research.

1.2.1. TCSs of GAS

A recent analysis of 64 closed GAS genomes of varying serotypes identified 14 TCSs (44), of which 12 TCSs are conserved (i.e., full-length intact operon present in > 85% of strains) across serotypes (45). Of note, serotype M28 GAS typically have 13 TCSs (22). While not all GAS TCSs have been studied to similar extents, several have proven roles in GAS molecular pathogenesis.

1.2.1.1. M28_Spy0761-0762: Regulator of a mannose/fructose-type PTS system

M28_Spy0761-0762 is the only unnamed TCS in GAS. Deletion of the TCS RR, *M28_Spy0762*, resulted in differential expression of approximately 15% of GAS genes across 4 growth phases in a nutrient-rich medium (45). The largest difference in expression

was for the TCS itself, *M28_Spy0761-0762*, and an upstream operon, *ptsABCD*, encoding a mannose/fructose-type PTS system (45). Deletion of *M28_Spy0762* did not result in significantly different mouse mortality in a bacteremia infection model (45). Further study in other *in vitro*, *ex vivo*, or *in vivo* environments may elucidate regulatory roles besides sugar metabolism.

1.2.1.2. YesMN: Role in cell physiology and metabolism

The YesMN TCS has not been well-studied. Expression of *yesN* (the RR of the TCS) *in vivo* in human patients with GAS pharyngitis is not striking (46). Deletion of *yesN* resulted in differential expression of approximately 40% of GAS genes across 4 growth phases in a nutrient-rich medium (45). Besides demonstrating YesN to be a repressor of the YesMN TCS, more genes were differentially expressed at later time points, suggesting a role for YesMN as a regulator in the stationary growth phase (45, 47). Despite a large change in gene expression, deletion of *yesN* did not result in a significantly different mouse mortality in a bacteremia infection model (45).

1.2.1.3. VicKR: Role in osmotic stress response

The VicKR TCS has not been as well-studied as other TCSs in Gram-positive bacteria, as *vicKR* are essential in *B. subtilis* and *Streptococcus pneumoniae*, and *vicR* is essential in *Streptococcus mutans* (48-50). Although *vicR* was demonstrated to be essential in GAS (51, 52), an unstable *vicR* deletion mutant was generated in one study (53). Deletion of either *vicR* or *vicK* in GAS decreased growth in non-immune human blood and serum and decreased mouse mortality in a soft tissue infection model (53). VicKR may play a role in regulating the osmotic stress response, as deletion of *vicR* increased expression of *opuAA* and *opuABC*, genes encoding proteins of an osmoprotectant transporter (53, 54).

Additionally, a very recent study identified VicK as being essential for a nonhuman primate (NHP) *in vivo* vaginal colonization model (55).

1.2.1.4. MaeKR/DpiBA: Regulation of malate utilization

The MaeKR TCS, also referred to as the DpiBA TCS, is implicated in malate utilization. MaeR is an activator of *maeKR* expression and the adjacent two gene operon *maePE* (45). MaeP is a malate-Na⁺ symport, and MaeE is a NAD-dependent malic enzyme that converts malate to pyruvate (45, 56). Based on transcript expression data in *maeR* and *maeK* deletion mutants, MaeK may sense malate and low pH to activate *maePE* expression (56). The role of MaeKR in virulence remains elusive, as conflicting studies, under the conditions tested, have demonstrated no difference in mouse mortality (45) and decreased mouse mortality (56) in similar soft tissue infection models. A study of GAS clinical isolates causing pediatric STSS found a significant correlation between *emm87* STSS isolates and a nonsynonymous mutation in *maeK* (57), suggesting a possible role for the MaeKR TCS in invasive disease pathogenesis.

1.2.1.5. SrtKR and SalkR: Regulation of repurposed lantibiotic biosynthesis operons

Two GAS TCSs are located within lantibiotic biosynthesis operons. Lantibiotics are antimicrobial peptides that are synthesized by Gram-positive bacteria to act against other closely related Gram-positive bacteria (58).

The first TCS, SrtKR, is associated with a lantibiotic biosynthesis operon that produces streptin (59). Not all GAS serotype genomes encode *srtKR* or have an intact operon, and, therefore, not all GAS serotypes produce streptin (59). Besides regulating streptin biosynthesis, SrtKR play a role in defense against nisin A, a lantibiotic produced by *Lactococcus lactis*. Deletion of *srtKR* increased susceptibility to nisin A (60). Nisin A

induces expression of *srtFEG*, an ABC transporter, through SrtKR (60), suggesting that, in GAS strains that do not produce streptin, the streptin lantibiotic locus has evolved from a role in lantibiotic biosynthesis to defense.

The second TCS, SalKR, is associated with the lantibiotic biosynthesis operon that produces salivaricin (58). The *sal* locus is not intact in any GAS serotype, and thus, no GAS strains produces salivaricin (58, 61). A transposon mutagenesis screen identified *salK* and *salY*, an ABC transporter of the *sal* locus, as attenuated mutants in a zebrafish infection model (62). Deletion of *salY* decreased intracellular survival in macrophages (62), and deletion of *salK* decreased survival in human blood and polymorphonuclear leukocytes (63). SalR is a repressor of the *sal* locus, which is induced by an unknown heat-stable human serum component (63).

1.2.1.6. SptRS: Role in persistence in human saliva

The function of the SptRS TCS in GAS pathogenesis was determined after a transcriptomic study of GAS grown *ex vivo* in human saliva (64). *sptRS* had the highest expression among all TCSs, which increased over time (64). Deletion of *sptR* resulted in decreased persistence in human saliva, most likely due to altered expression of carbon utilization genes (64). Additionally, *sptR* was highly expressed *in vivo* in human patients with GAS pharyngitis (64), suggesting an important role for the SptRS TCS in GAS survival in the oropharynx. A later study determined that SptR is a repressor of *sptRS* expression, and deletion of *sptR* results in increased mouse mortality in a soft tissue infection model (45). Also, SptS is essential for a NHP *in vivo* vaginal colonization model (55).

1.2.1.7. Ihk-Irr: Detection and evasion of the human innate immune response

The function of the Ihk-Irr TCS was identified in a study of GAS gene expression during phagocytosis by human polymorphonuclear leukocytes (PMNs) (65). Expression of both *ihk* and *irr* increased in response to PMN exposure, and deletion of *irr* resulted in increased killing by PMNs (65). Irr regulates approximately 20% of the GAS transcriptome, including genes involved in cell wall biosynthesis and oxidative stress response (66). Deletion of *irr* increased susceptibility to H₂O₂, LL-37, and cathepsin G, and decreased virulence in mouse and NHP necrotizing myositis infection models (5, 66). Expression of *ihk* and *irr* is induced by primary neutrophil granules (66), and they are highly expressed *in vivo* in human patients with GAS pharyngitis (65), suggesting that the Ihk-Irr TCS plays a key role in evasion of the human innate immune response.

1.2.1.8. CiaHR: Role in stress response in GAS

CiaHR is a TCS that has been relatively well studied in *S. pneumoniae*, where they regulate competence, β -lactam resistance, and stress response (67, 68). Additionally, 5 small regulatory RNAs (sRNAs) are regulated by CiaHR in *S. pneumoniae*, which facilitate the control of competence (68, 69). In GAS, CiaHR play a role in acidic and oxidative stress response (67, 70). Very recently, CiaH was demonstrated to be vital in GAS virulence in mouse and NHP necrotizing myositis infection models (5), and to be essential in NHP *in vivo* vaginal colonization and *ex vivo* uterine wall infection models (55). A few of the CiaHR-regulated sRNAs have been identified in a serotype M3 GAS strain by sequence homology but remain unstudied (69). The sRNAs are likely to have novel regulatory roles compared to their counterparts in *S. pneumoniae*, since GAS is not naturally competent (67).

1.2.1.9. TrxTSR: Regulation of the Mga regulon

A study of the TrxRS TCS found that TrxR is a negative regulator of *mga*, a well-studied stand-alone regulator (71-73). Mga controls the expression of a well-studied set of virulence factors involved in tissue adherence and immune modulation (6, 74-80). Deletion of *trxR* decreased virulence in a mouse model of soft tissue infection (71). Additional study of the TrxRS phosphorelay did not identify a requirement of TrxR phosphorylation for regulation of the Mga regulon (81), although it may be necessary for regulation of other GAS genes. Unlike most GAS TCSs, *trxSR* is co-transcribed with an upstream open reading frame, *trxT* (81). Deletion of the conserved hypothetical membrane protein resulted in a partial *trxR* deletion phenotype, suggesting a possible involvement of TrxT in the TrxRS signaling pathway (81). TrxTSR may sense asparagine to alter gene expression of virulence factors (82).

1.2.1.10. LiaFSR: Role in acid stress response, biofilm formation, and pilus regulation

LiaS is a unique HK in GAS. It is the only GAS HK belonging to the intramembrane-sensing family (44). The LiaFSR system has been very well studied in *B. subtilis*, where it was originally characterized (83, 84). In *B. subtilis*, LiaS is activated by cell membrane and envelope damage by lipid II antibiotics, such as bacitracin, leading to LiaR phosphorylation and altered gene expression (83, 84). LiaF, a membrane protein co-transcribed with *liaSR*, acts as a negative regulator of LiaSR (83). In *S. mutans*, LiaFSR play a role in resistance to cell membrane damaging agents, acid stress response, and biofilm formation (85).

In GAS, deletion of *liaS* increased susceptibility to bacitracin, decreased acid stress response, and decreased mouse mortality in a soft tissue infection model (86, 87). A study of asymptomatic carriage strains identified a polymorphism in *liaS* that increased mouse

nasopharyngeal colonization and adherence to human epithelial cells *in vitro* (88). Transcriptome studies demonstrated that LiaFSR regulate *spxA2*, a transcriptional anti-activator that regulates stress responses and virulence factor expression (88, 89). Further studies discovered that LiaFSR is activated by bacitracin and, similar to *S. agalactiae* and *S. pneumoniae*, regulates the expression of pilus and biofilm formation (90, 91). Very recently, LiaF was found to be essential for a NHP *in vivo* vaginal colonization model (55).

1.2.1.11. FasBCA/*fasX*: Colonization/dissemination phenotype regulation by a sRNA

The FasBCA/*fasX* system (fibronectin/fibrinogen binding/hemolytic activity/streptokinase regulator) is unusual compared to other TCSs in GAS because 1) it has two HKs (FasB and FasC) and 2) the main effector of the system is a sRNA, *fasX*. Initial studies demonstrated that deletion of *fasX* results in a similar phenotype to deletion of *fasBCA* (92), and all three proteins, FasBCA, are needed for expression of *fasX* (32). The FasBCA/*fasX* system regulates several cellular phenotypes, including fibrinogen binding, streptokinase activity, and cell adherence (92, 93). *fasX* functions by binding to the 5' untranslated region (UTR) of mRNA transcripts and altering mRNA stability. *fasX* binds to the 5' UTR of *ska* mRNA transcript, the gene encoding streptokinase, and increases the stability of the mRNA, resulting in increased secreted streptokinase protein levels and activity (94, 95). In contrast, *fasX* binds to the 5' UTR of mRNA transcripts for genes of the FCT locus, encoding genes for pilus and fibronectin binding, and blocks the ribosomal binding site, reducing translation of the mRNA and decreasing cell adherence (93, 95, 96). Deletion of *fasX* decreased mouse mortality in a plasminogen-humanized bacteremia infection model (95), demonstrating the importance of the FasBCA/*fasX* system to GAS pathogenesis.

1.2.1.12. CovRS: Regulation of virulence in GAS

Since its identification over 20 years ago (97-99), the CovRS TCS (control of virulence regulator/sensor), also referred to as the CsrRS TCS (capsule synthesis regulation), has been the most well-studied TCS from GAS. Initially identified as a negative regulator of hyaluronic acid capsule synthesis, transcriptomic studies have demonstrated that CovRS regulates approximately 10-15% of the GAS genome (14, 100-103). Of note, the CovRS regulon differs slightly among strains of different serotypes (see below). CovRS represses expression of many proven and putative virulence factors, such as *hasABC* (hyaluronic acid capsule synthesis genes) (104), the *sag* operon (streptolysin S and biosynthesis genes) (105, 106); *speB* (streptococcal pyrogenic exotoxin B, a secreted cysteine protease) (107, 108), *ska* (streptokinase) (109, 110), *grab* (protein-G-related α_2 -macroglobulin binding protein) (111), *mac* (IgG endopeptidase and inhibitor of reactive oxygen species generation) (112, 113), *spyCEP* (interleukin-8 protease) (114), *nga* (NAD⁺-glycohydrolase) (115), and *slo* (streptolysin O) (115). Additionally, CovRS regulates the expression of several transcription regulators, including many of the TCSs mentioned above (100, 102). Since CovRS negatively regulates the expression of many virulence factors, deletion of *covRS* results in significantly increased virulence in multiple animal infection models (14, 101, 103, 107, 116-118).

Several mechanistic studies of CovR and CovS have been published, giving a detailed understanding of their molecular pathogenesis. The *covRS* operon is transcribed as two different transcripts (*covR* and *covRS*) (119), and CovR is a repressor of *covRS* transcription (120). CovR binds to the promoter of several genes it regulates at AT-rich sites (98, 105, 109, 116, 120-125), with a consensus binding site of ATTARA (122).

Phosphorylation of CovR at aspartic acid 53 (D53), the site of phosphorylation by CovS (123, 126, 127), results in oligomerization and increased DNA binding affinity (98, 116, 120-123). CovR can also be phosphorylated at threonine 65 (T65) by a serine/threonine kinase (Stk), which precludes phosphorylation of D53 by CovS (127). CovR mutants with single amino acid changes have been characterized, resulting in altered phosphorylation of CovR by CovS, signaling from CovS to CovR, or DNA binding affinity (116, 123, 125-128). CovR mutant strains can either function more similar to a *covR* deletion strain or *covS* deletion strain, depending on the mutation (see below) (116, 125, 127-129). Additionally, not all CovR mutations result in identical transcriptome and virulence profiles (116, 129), suggesting that the regulatory output is dependent on the location and severity of the mutation (14, 116, 128). CovS is a bifunctional histidine phosphatase/kinase (126, 128, 130, 131). That is, CovS can both phosphorylate and dephosphorylate CovR at D53. Transcriptomic studies of CovS kinase and phosphatase deficient mutants and CovR phosphate site mutants revealed that differential gene expression by CovRS is dictated by CovR phosphorylation level (128, 131).

Although the exact stimulus of the CovRS TCS *in vivo* is unknown, two environmental cues have been identified *in vitro* (132, 133). Supraphysiological concentrations of cationic magnesium (Mg^{2+}) result in activation of the CovRS system, leading to increased CovR phosphorylation and increased repression of CovRS regulated genes (131, 132, 134, 135). In comparison, subinhibitory concentrations of the human cathelicidin peptide LL-37 result in inactivation of the CovRS system, leading to decreased CovR phosphorylation and decreased repression of CovRS regulated genes (128, 131, 133, 135, 136). Serotype-specific differences in response to both Mg^{2+} and LL-37 have been

demonstrated, which likely results from differences in basal levels of CovR phosphorylation (128, 131). Little is known about the mechanism of action of Mg²⁺ on CovRS, though it can antagonize the effect of LL-37 (133, 135). A ten amino acid peptide of LL-37, RI-10, binds to acidic residues of the CovS extracellular domain (136), suggesting that LL-37 functions by specifically binding to CovS, rather than by damaging the cell membrane. Additionally, CovS phosphatase knockout mutants show no altered CovR phosphorylation in response to LL-37, suggesting that binding of LL-37 (or fragments of LL-37 containing RI-10) to CovS activates its phosphatase activity to alleviate gene repression (128).

As observed with responses to environmental cues, serotype-specific differences in gene regulation by CovRS have been documented (102, 103, 127, 137, 138). Although minor changes are to be expected due to differences in gene content, a noteworthy difference is regulation of the Mga regulon (103). The Mga regulon is regulated by CovRS to a much greater extent in GAS serotypes that do not express hyaluronic acid capsule (103), suggesting that a regulatory function of the CovRS TCS is to remodel the cell surface.

Although CovS is the main factor altering CovR phosphorylation, deletion of *covS* does not result in absence of phosphorylated CovR (131). That is, CovR is phosphorylated *in vivo* by other mechanisms besides CovS, most likely by small phosphate donors. As such, subtle transcriptomic changes differ between CovR and CovS mutant strains (103, 127, 129). For example, *speB* transcription and secreted enzymatic activity is increased in a GAS strain with deletion of *covR*, but decreased in a GAS strain with deletion of *covS* (129). A mechanistic study of CovRS *speB* regulation has suggested that non-phosphorylated CovR is dominant to phosphorylated CovR in repressing *speB* transcription (139).

Population-based studies of GAS clinical isolates have identified *covRS* as highly polymorphic genes (11, 12, 14). A recent population transcriptomic study demonstrated that naturally-occurring CovRS mutants are not identical in gene expression and *in vivo* virulence profiles, although a majority do result in a significant increase in virulence (14). Additionally, neutrophils may select mutant *covRS* strains *in vivo* (140). However, *covRS* mutation decreases survivability in competition assays with wild-type strains (102, 129), and decreases adherence to human cells *in vitro* and mouse tissue *in vivo* (137, 141). Thus, mutation of CovRS may decrease transmissibility, which is uncommon in population-based studies (142).

1.3. Accessory proteins to TCSs: An added layer of regulatory complexity to TCSs

While TCSs function in a linear fashion to sense and respond to the environment, they are not completely isolated (34). In addition to working in tandem with one another for more complex response regulation, the phosphorelay of TCSs can be modified by accessory proteins (also referred to as auxiliary proteins) (43). Accessory proteins are non-HKs and non-RRs that act on the signal transduction pathway of TCSs (43). The diversity in protein sequence of accessory protein mirrors their diversity in mechanistic function. Accessory proteins act at multiple sites of the TCS phosphorelay, including assisting in sensing stimuli and signal transduction, and altering phosphotransfer reactions (43, 143). The added complexity of regulation allows for integration of multiple stimuli and regulatory proteins for a fine-tuned cellular response (43, 143). Several accessory proteins from other bacterial species have been well-characterized.

In *Escherichia coli*, the PhoQP TCS responds to extracellular Mg^{2+} and Ca^{2+} to regulate ion uptake, whereas the EvgSA TCS confers acid and multidrug resistance (144).

EvgSA TCS activation activates the PhoQP TCS via SafA (145). SafA is a small inner membrane protein whose expression is induced by the EvgSA TCS and interacts directly with PhoQ to increase autophosphorylation and activate the PhoQP TCS (145, 146). In *Sinorhizobium meliloti*, the FeuPQ TCS is required for symbiotic infection. Within the *feuPQ* operon is a third gene, *feuN*, encoding a small essential protein that inhibits the FeuPQ TCS (147). FeuN is only essential in the presence of a functional FeuQ (the HK of the TCS), suggesting that FeuN interacts with FeuQ to alter FeuQ enzymatic activity (147). FeuN may interact with the transmembrane domains of FeuQ, as mutations in and around the transmembrane domains of FeuQ decrease sensitivity to FeuN (147). Thus, small accessory proteins alter TCS regulation through transmembrane interactions.

In *B. subtilis*, the essential YycFG TCS regulates genes involved in cell wall metabolism. Two accessory proteins, YycH and YycI, interact with YycG (the HK of the TCS) to modulate kinase activity (148). While both are large membrane anchored proteins, only the transmembrane domains of YycH and YycI together are required for function (149). Modeling and mutagenesis studies of YycGHI transmembrane domain interactions suggest that YycH and YycI interact with one another and YycG to alter YycG kinase activity (149). Thus, two accessory proteins act in tandem to regulate TCS kinase activity through interaction of transmembrane domains.

Several accessory proteins have functional roles in regulating pilus formation. In *E. coli*, CpxP is a periplasmic accessory protein whose crystal structure has been determined (150). CpxP dimerizes to form a cap-like structure, and each face of the dimer has different functionality (150). The concave surface is able to bind to the periplasmic domain of CpxA (the HK of the TCS), inhibiting activation of the CpxAR TCS, while the convex surface

binds to misfolded proteins in the periplasm and directs them to be degraded, activating the CpxAR TCS and expression of pilus biogenesis and stress response proteins (150). In *Pseudomonas aeruginosa*, the major type IV pilin PilA interacts with PilS (the HK of the PilSR TCS) via transmembrane domains in the inner membrane (151). The PilA-PilS interaction activates PilS phosphatase activity, resulting in decreased PilR phosphorylation and decreased expression of *pilA* (151). Thus, accessory proteins are involved in feedback regulation of pilus biosynthesis TCS regulators.

In *Staphylococcus aureus*, several different accessory proteins of multiple TCSs have been characterized. The SaeRS TCS consists of an intramembrane HK that is induced by human neutrophil peptides to regulate virulence determinants (152). Two accessory proteins, SaeP, a lipoprotein, and SaeQ, a membrane protein, directly interact with SaeS to promote SaeS phosphatase activity (153). The GraSR TCS consists of an intramembrane HK that controls cationic antimicrobial peptide resistance (154). GraX, a cytoplasmic protein, and VraFG, a repurposed ABC transporter, are accessory proteins that sense cationic antimicrobial peptides and signal through GraS to activate GraR (155). The essential WalKR TCS is involved in regulation of cell wall metabolism (156). SpdC, an Abi-domain membrane protein, interacts with WalK (the HK of the TCS) and negatively regulates WalKR activity (157). Additionally, SpdC interacts with nine other HKs of *S. aureus* through transmembrane domain interactions, suggesting that SpdC is a universal accessory protein involved in several regulatory pathways (157).

In *S. agalactiae*, the CovRS TCS regulates virulence determinants in a manner similar to the CovRS TCS in GAS. A recent study identified Abx1 as an accessory protein to the CovRS TCS system in *S. agalactiae* (158). Abx1, an Abi-domain membrane protein,

interacts directly with CovS transmembrane domains (158). Abx1 acts as an antagonist to the CovRS TCS, either by inhibiting CovS kinase or enhancing CovS phosphatase activity (158). *abx1* is present in the core genome of *S. agalactiae*, but a homolog is not found in the GAS genome (158). Animal infection studies using strains with either deletion or overexpression of *abx1* decreased mortality, suggesting that protein levels of Abx1 are tightly regulated and important for pathogenesis (158). Sequencing studies of *S. agalactiae* clinical isolates have identified protein truncation mutations of Abx1, but the molecular pathogenesis of the Abx1 variants has not been determined (159).

Altogether, accessory proteins are diverse in amino acid composition and mechanism of action toward TCSs in many bacterial species. Further study of the molecular mechanisms of TCS regulation will undoubtedly lead to the identification of more accessory proteins with new modes of regulation (43).

1.3.1. RocA: An accessory protein to the CovRS TCS in GAS

In GAS, three proposed accessory proteins have been studied. The first two, LiaF and TrxT, are discussed above. The third has become more well-characterized in the last few years, including many new discoveries reported in this dissertation. RocA (regulator of Cov) is an accessory protein to the CovRS TCS in GAS. It was initially identified in a transposon mutagenesis study (160). RocA is a 451 amino acid protein unique to GAS with homology to quorum sensing histidine kinases of other Gram-positive bacteria. RocA has a predicted N-terminal transmembrane domain and predicted C-terminal putative histidine kinase ATPase domain missing several key residues for ATP binding (160). Further study of RocA identified truncated *rocA* alleles in serotype M3 and M18 GAS strains (161-164). In all serotype M18 GAS studied to date, a SNP in *rocA* results in insertion of an early stop codon

and truncation of RocA to 89 amino acids (161). In all serotype M3 GAS studied to date, a single nucleotide deletion results in a frameshift mutation and truncation of RocA to 416 amino acids (164). Both the M18 and M3 *rocA* alleles increased virulence factor expression and activity *in vitro* and increased virulence in animal infection models similar to isogenic mutant strains lacking *rocA* (161-164), providing evidence that RocA is a negative regulator of virulence.

Deletion of *rocA* in both serotype M1 and M3 GAS strain backgrounds results in an altered transcriptome that is similar, but not identical, to CovRS mutant strain transcriptomes (164, 165). Analysis of a panel of isogenic *rocA* and *covRS* gene deletion mutants demonstrated that RocA functions through CovRS (164, 166). That is, a functional CovRS TCS is required for RocA gene regulation of CovRS-regulated genes. Deletion of *rocA* decreases CovR phosphorylation by CovS (164, 167), suggesting that RocA functions by altering either CovS kinase or phosphatase activity. Mutagenesis of cytoplasmic histidine residues confirmed that RocA is not a histidine kinase (160, 166). Further studies demonstrated that RocA has a dosage effect, since overexpression of RocA truncation mutants containing at least the N-terminal transmembrane domains can complement a strain with a *rocA* null allele (165). Thus, the C-terminus of RocA appears to be dispensable for regulatory activity, and RocA is a pseudokinase towards CovR (166, 168, 169).

Investigations into the role of supraphysiological levels of Mg²⁺ and subinhibitory levels of LL-37 on RocA gene regulation demonstrated that deletion of *rocA* results in loss of LL-37 regulatory activity toward CovRS (165). Thus, LL-37 may function by interfering with the proposed RocA-CovS protein interaction occurring in the cell membrane. Of note, this observation provides a possible explanation for serotype-specific differences in response

to LL-37 (131). Deletion of *rocA* did not alter the ability of Mg^{2+} to affect gene regulation through CovRS (165). Thus, some *in vitro* stimuli for CovRS are also sensed by RocA.

A few studies have identified GAS clinical isolates (167, 170, 171) and animal passaged strains (172) with nonsense and frameshift mutations in *rocA*, resulting in a *rocA* null phenotype. In serotype M89 GAS clinical isolates, several strains had deletion of one repeat in a variable number tandem repeat (VNTR) upstream of *rocA* (167). The VNTR contains three repeats, and deletion of any number of repeats results in loss of *rocA* translation, due to loss of the presumed ribosomal binding site for *rocA* (167). However, no SNPs that result in amino acid changes in RocA have been studied prior to the research described in this dissertation.

The accumulation of data has led to the development of a model for RocA molecular pathogenesis (165): RocA heterodimerizes with CovS to form a functional unit with high kinase activity and low phosphatase activity, resulting in high levels of CovR phosphorylation and low levels of virulence factor gene expression. Mutation of *rocA* abrogates the interaction, resulting in a CovRS system with either lower kinase activity or higher phosphatase activity, decreased CovR phosphorylation and increased virulence factor gene expression. Although the basic mechanism of RocA gene regulatory activity is understood, a detailed molecular mechanism is still lacking, and the role in which amino acid changes can alter the functionality of this accessory protein and, ultimately, GAS molecular pathogenesis, remains unknown.

1.4. Overarching hypothesis

Recent whole-genome sequence analysis of 2,101 serotype M28 GAS strains recovered from large population-based studies of patients with invasive infections revealed

an unexpectedly high number of missense (amino-acid changing) and nonsense (protein truncating) polymorphisms in *rocA* (14, 173). In total, 48 strains were identified with polymorphisms in *rocA*, resulting in 29 unique alleles (Fig. 1-2). A majority of the polymorphisms occurred in the predicted N-terminal transmembrane domain (Fig. 1-2). The abundance of polymorphisms of *rocA* was unexpected. Population-based studies of serotype M1, M59, and M89 GAS strains did not identify a high number of *rocA* alleles (12, 13, 174), suggesting that RocA may play an important role in the pathogenesis of serotype M28 GAS in invasive infections.

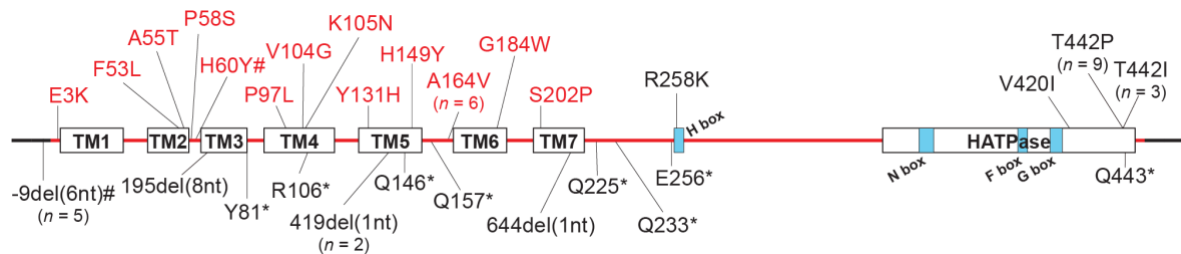


Fig. 1-2 *rocA* polymorphisms in serotype M28 GAS strains.

The affected codon and amino acid change conferred by each polymorphism are shown. For polymorphisms due to nucleotide deletion, the affected nucleotide is identified. Alleles identified in multiple isolates are indicated. Polymorphisms that result in RocA protein truncation or loss of *rocA* mRNA translation are shown below the protein schematic, and polymorphisms that result in amino acid changes are shown above the protein schematic. Missense polymorphisms in the predicted domains sufficient for regulatory activity (165) are colored red. Predicted domains of the RocA protein using Phyre2 are indicated (TM, transmembrane domain; HATPase, histidine kinase ATPase domain) (42). Predicted functional domains of the potential histidine kinase domain (H box, N box, F box, G box) are identified (160). #, one strain has two polymorphisms in *rocA*. Adapted from Bernard et al. (173).

My overarching hypothesis is that polymorphisms in *rocA* result in altered RocA-RocA and RocA-CovS protein interaction, giving rise to an altered global transcriptome and increased virulence in serotype M28 GAS. Results demonstrate: 1) RocA is an important accessory protein involved in virulence in serotype M28 GAS; 2) naturally-occurring polymorphisms in *rocA* alter the global GAS transcriptome and increase strain virulence;

and 3) polymorphisms in *rocA* alter the physical interaction between RocA and CovS. Taken together, the data add important new understanding of the molecular pathogenesis of RocA specifically and accessory proteins in general.

1.5. References

1. Cunningham MW. 2000. Pathogenesis of group A streptococcal infections. *Clin Microbiol Rev* 13:470-511.
2. Walker MJ, Barnett TC, McArthur JD, Cole JN, Gillen CM, Henningham A, Sriprakash KS, Sanderson-Smith ML, Nizet V. 2014. Disease manifestations and pathogenic mechanisms of group A *Streptococcus*. *Clin Microbiol Rev* 27:264-301.
3. Olsen RJ, Musser JM. 2010. Molecular pathogenesis of necrotizing fasciitis. *Annu Rev Pathol Mech Dis* 5:1-31.
4. Carapetis JR, Steer AC, Mulholland EK, Weber M. 2005. The global burden of group A streptococcal diseases. *Lancet Infect Dis* 5:685-694.
5. Kachroo P, Eraso JM, Olsen RJ, Zhu L, Kubiak SL, Pruitt L, Yerramilli P, Cantu CC, Ojeda Saavedra M, Pensar J, Corander J, Jenkins L, Kao L, Granillo A, Porter AR, DeLeo FR, Musser JM. 2020. New pathogenesis mechanisms and translational leads identified by multidimensional analysis of necrotizing myositis in primates. *mBio* 11:e03363-19.
6. Smeesters PR, McMillan DJ, Sriprakash KS. 2010. The streptococcal M protein: a highly versatile molecule. *Trends Microbiol* 18:275-282.
7. Sanderson-Smith M, De Oliveira DM, Guglielmini J, McMillan DJ, Vu T, Holien JK, Henningham A, Steer AC, Bessen DE, Dale JB, Curtis N, Beall BW, Walker

- MJ, Parker MW, Carapetis JR, Van Melder L, Sriprakash KS, Smeesters PR, The M Protein Study Group. 2014. A systematic and functional classification of *Streptococcus pyogenes* that serves as a new tool for molecular typing and vaccine development. *J Infect Dis* 210:1325-1338.
8. Steer AC, Law I, Matatolu L, Beall BW, Carapetis JR. 2009. Global *emm* type distribution of group A streptococci: systematic review and implications for vaccine development. *Lancet Infect Dis* 9:611-616.
 9. Chochua S, Metcalf BJ, Li Z, Rivers J, Mathis S, Jackson D, Gertz RE, Jr., Srinivasan V, Lynfield R, Van Beneden C, McGee L, Beall B. 2017. Population and whole genome sequence based characterization of invasive group A streptococci recovered in the United States during 2015. *mBio* 8:e01422-17.
 10. Beres SB, Richter EW, Nagiec MJ, Sumbly P, Porcella SF, DeLeo FR, Musser JM. 2006. Molecular genetic anatomy of inter- and intraserotype variation in the human bacterial pathogen group A *Streptococcus*. *Proc Natl Acad Sci U S A* 103:7059-7064.
 11. Beres SB, Carroll RK, Shea PR, Sitkiewicz I, Martinez-Gutierrez JC, Low DE, McGeer A, Willey BM, Green K, Tyrrell GJ, Goldman TD, Feldgarden M, Birren BW, Fofanov Y, Boos J, Wheaton WD, Honisch C, Musser JM. 2010. Molecular complexity of successive bacterial epidemics deconvoluted by comparative pathogenomics. *Proc Natl Acad Sci U S A* 107:4371-4376.
 12. Nasser W, Beres SB, Olsen RJ, Dean MA, Rice KA, Long SW, Kristinsson KG, Gottfredsson M, Vuopio J, Raisanen K, Caugant DA, Steinbakk M, Low DE, McGeer A, Darenberg J, Henriques-Normark B, Van Beneden CA, Hoffmann S,

- Musser JM. 2014. Evolutionary pathway to increased virulence and epidemic group A *Streptococcus* disease derived from 3,615 genome sequences. *Proc Natl Acad Sci U S A* 111:E1768-1776.
13. Beres SB, Kachroo P, Nasser W, Olsen RJ, Zhu L, Flores AR, de la Riva I, Paez-Mayorga J, Jimenez FE, Cantu C, Vuopio J, Jalava J, Kristinsson KG, Gottfredsson M, Corander J, Fittipaldi N, Di Luca MC, Petrelli D, Vitali LA, Raiford A, Jenkins L, Musser JM. 2016. Transcriptome remodeling contributes to epidemic disease caused by the human pathogen *Streptococcus pyogenes*. *mBio* 7:e00403-16.
14. Kachroo P, Eraso JM, Beres SB, Olsen RJ, Zhu L, Nasser W, Bernard PE, Cantu CC, Saavedra MO, Arredondo MJ, Strobe B, Do H, Kumaraswami M, Vuopio J, Grondahl-Yli-Hannuksela K, Kristinsson KG, Gottfredsson M, Pesonen M, Pensar J, Davenport ER, Clark AG, Corander J, Caugant DA, Gaini S, Magnussen MD, Kubiak SL, Nguyen HAT, Long SW, Porter AR, DeLeo FR, Musser JM. 2019. Integrated analysis of population genomics, transcriptomics and virulence provides novel insights into *Streptococcus pyogenes* pathogenesis. *Nat Genet* 51:548-559.
15. Zhu L, Olsen RJ, Nasser W, Beres SB, Vuopio J, Kristinsson KG, Gottfredsson M, Porter AR, DeLeo FR, Musser JM. 2015. A molecular trigger for intercontinental epidemics of group A *Streptococcus*. *J Clin Invest* 125:3545-3559.

16. Zhu L, Olsen RJ, Nasser W, de la Riva Morales I, Musser JM. 2015. Trading capsule for increased cytotoxin production: contribution to virulence of a newly emerged clade of *emm89 Streptococcus pyogenes*. *mBio* 6:e01378-15.
17. Eriksson BKG, Norgen M, McGregor K, Spratt BG, Henriques-Normark B. 2003. Group A streptococcal infections in Sweden: a comparative study of invasive and noninvasive infections and analysis of dominant T28 *emm28* isolates. *Clin Infect Dis* 37:1189-1193.
18. Tyrrell GJ, Lovgren M, Forwick B, Hoe NP, Musser JM, Talbot JA. 2002. M types of group A streptococcal isolates submitted to the National Centre for Streptococcus (Canada) from 1993 to 1999. *J Clin Microbiol* 40:4466-4471.
19. Vlamincx B, van Pelt W, Schouls L, van Silfhout A, Elzenaar C, Mascini E, Verhoef J, Schellekens J. 2004. Epidemiological features of invasive and noninvasive group A streptococcal disease in the Netherlands, 1992-1996. *Eur J Clin Microbiol Infect Dis* 23:434-444.
20. Colman G, Tanna A, Efstratiou A, Gaworzewska E. 1993. The serotypes of *Streptococcus pyogenes* present in Britain during 1980-1990 and their association with disease. *J Med Microbiol* 39:165-178.
21. Gaworzewska E, Colman G. 1988. Changes in the pattern of infection caused by *Streptococcus pyogenes*. *Epidem Inf* 100:257-269.
22. Green NM, Zhang S, Porcella SF, Nagiec MJ, Barbian KD, Beres SB, LeFebvre RB, Musser JM. 2005. Genome sequence of a serotype M28 strain of group A *Streptococcus*: potential new insights into puerperal sepsis and bacterial disease specificity. *J Infect Dis* 192:760-770.

23. Chuang I, Van Beneden C, Beall B, Schuchat A, Active Bacterial Core Surveillance/Emerging Infections Network. 2002. Population-based surveillance for postpartum invasive group A streptococcus infection, 1995-2000. *Clin Infect Dis* 35:665-670.
24. Ben Zakour NL, Venturini C, Beatson SA, Walker MJ. 2012. Analysis of a *Streptococcus pyogenes* puerperal sepsis cluster by use of whole-genome sequencing. *J Clin Microbiol* 50:2224-2228.
25. Grondahl-Yli-Hannuksela K, Beres SB, Hyyrylainen HL, Kallonen T, Musser JM, Vuopio J. 2020. Genetic evolution of invasive *emm28 Streptococcus pyogenes* strains and significant association with puerperal infections in young women, Finland. *Clin Microbiol Infect* doi:10.1016/j.cmi.2020.04.004.
26. Jain I, Sarkar P, Danger JL, Medicielo J, Roshika R, Calfee G, Ramalinga A, Burgess C, Sumbly P. 2019. A mobile genetic element promotes the association between serotype M28 group A *Streptococcus* isolates and cases of puerperal sepsis. *J Infect Dis* 220:882-891.
27. Green NM, Beres SB, Graviss EA, Allison JE, McGeer AJ, Vuopio-Varkila J, LeFebvre RB, Musser JM. 2005. Genetic diversity among type *emm28* group A *Streptococcus* strains causing invasive infections and pharyngitis. *J Clin Microbiol* 43:4083-4091.
28. Beres SB, Sylva GL, Sturdevant DE, Granville CN, Liu M, Ricklefs SM, Whitney AR, Parkins LD, Hoe NP, Adams GJ, Low DE, DeLeo FR, McGeer A, Musser JM. 2004. Genome-wide molecular dissection of serotype M3 group A

- Streptococcus* strains causing two epidemics of invasive infections. Proc Natl Acad Sci U S A 101:11833-11838.
29. Rodriguez-Ortega MJ, Norais N, Bensi G, Liberatori S, Capo S, Mora M, Scarselli M, Doro F, Ferrari G, Garaguso I, Maggi T, Neumann A, Covre A, Telford JL, Grandi G. 2006. Characterization and identification of vaccine candidate proteins through analysis of the group A *Streptococcus* surface proteome. Nat Biotechnol 24:191-197.
 30. McNamara C, Zinkernagel AS, Macheboeuf P, Cunningham MW, Nizet V, Ghosh J. 2008. Coiled-coil irregularities and instabilities in group A *Streptococcus* are required for virulence. Science 319:1405-1408.
 31. Macheboeuf P, Buffalo C, Fu C, Zinkernagel AS, Cole JN, Johnson JE, Nizet V, Ghosh P. 2011. Streptococcal M1 protein constructs a pathological host fibrinogen network. Nature 472:64-68.
 32. Cao TN, Liu Z, Cao TH, Pflughoeft KJ, Trevino J, Danger JL, Beres SB, Musser JM, Sumbly P. 2014. Natural disruption of two regulatory networks in serotype M3 group A *Streptococcus* isolates contributes to the virulence factor profile of this hypervirulent serotype. Infect Immun 82:1744-1754.
 33. Stock AM, Robinson VL, Goudreau PN. 2000. Two-component signal transduction. Annu Rev Biochem 69:183-215.
 34. West AH, Stock AM. 2001. Histidine kinases and response regulator proteins in two-component signaling systems. Trends Biochem Sci 26:369-376.
 35. Mascher T, Helmann JD, Uuden G. 2006. Stimulus perception in bacterial signal-transducing histidine kinases. Microbiol Mol Biol Rev 70:910-938.

36. Beier D, Gross R. 2006. Regulation of bacterial virulence by two-component systems. *Curr Opin Microbiol* 9:143-152.
37. Wolanin PM, Thomason PA, Stock JB. 2002. Histidine protein kinases: key signal transducers outside the animal kingdom. *Genome Biol* 3:review3013.1-3013.8.
38. Bem AE, Velikova N, Pellicer MT, Baarlen P, Marina A, Wells JM. 2015. Bacterial histidine kinases as novel antibacterial drug targets. *ACS Chem Biol* 10:213-224.
39. Kim D, Forst S. 2001. Genomic analysis of the histidine kinase family in bacteria and archaea. *Microbiology* 147:1197-1212.
40. Zschiedrich CP, Keidel V, Szurmant H. 2016. Molecular mechanisms of two-component signal transduction. *J Mol Biol* 428:3752-3775.
41. Wang C, Sang J, Wang J, Su M, Downey JS, Wu Q, Wang S, Cai Y, Xu X, Wu J, Senadheera DB, Cvitkovitch DG, Chen L, Goodman SD, Han A. 2013. Mechanistic insights revealed by the crystal structure of a histidine kinase with signal transducer and sensor domains. *PLoS Biol* 11:e1001493.
42. Kelley LA, Mezulis S, Yates CM, Wass MN, Sternberg MJE. 2015. The Phyre2 web portal for protein modeling, prediction and analysis. *Nat Protoc* 10:845-858.
43. Buelow DR, Raivio TL. 2010. Three (and more) component regulatory systems - auxiliary regulators of bacterial histidine kinases. *Mol Microbiol* 75:547-566.
44. Buckley SJ, Timms P, Davies MR, McMillan DJ. 2018. *In silico* characterisation of the two-component system regulators of *Streptococcus pyogenes*. *PLoS One* 13:e0199163.

45. Sitkiewicz I, Musser JM. 2006. Expression microarray and mouse virulence analysis of four conserved two-component gene regulatory systems in group A *Streptococcus*. *Infect Immun* 74:1339-1351.
46. Virtaneva K, Graham MR, Porcella SF, Hoe NP, Su H, Graviss EA, Gardner TJ, Allison JE, Lemon WJ, Bailey JR, Parnell MJ, Musser JM. 2003. Group A *Streptococcus* gene expression in humans and cynomolgus macaques with acute pharyngitis. *Infect Immun* 71:2199-2207.
47. Olsen RJ, Fittipaldi N, Kachroo P, Sanson MA, Long SW, Como-Sabetti KJ, Valson C, Cantu C, Lynfield R, Van Beneden C, Beres SB, Musser JM. 2014. Clinical laboratory response to a mock outbreak of invasive bacterial infections: a preparedness study. *J Clin Microbiol* 52:4210-4216.
48. Fabret C, Hoch JA. 1998. A two-component signal transduction system essential for growth of *Bacillus subtilis*: implications for anti-infective therapy. *J Bacteriol* 180:6375-6383.
49. Throup JP, Koretke KK, Bryant AP, Ingraham KA, Chalker AF, Ge Y, Marra A, Wallis NG, Brown JR, Holmes DJ, Rosenberg M, Burnham MK. 2000. A genomic analysis of two-component signal transduction in *Streptococcus pneumoniae*. *Mol Microbiol* 35:566-576.
50. Senadheera MD, Guggenheim B, Spatafora GA, Huang YC, Choi J, Hung DC, Treglown JS, Goodman SD, Ellen RP, Cvitkovitch DG. 2005. A VicRK signal transduction system in *Streptococcus mutans* affects *gtfBCD*, *gbpB*, and *fff* expression, biofilm formation, and genetic competence development. *J Bacteriol* 187:4064-4076.

51. Zhu L, Charbonneau ARL, Waller AS, Olsen RJ, Beres SB, Musser JM. 2017. Novel genes required for the fitness of *Streptococcus pyogenes* in human saliva. *mSphere* 2:e00460-17.
52. Le Breton Y, Belew AT, Valdes KM, Islam E, Curry P, Tettelin H, Shirtliff ME, El-Sayed NM, McIver KS. 2015. Essential genes in the core genome of the human pathogen *Streptococcus pyogenes*. *Sci Rep* 5:9838.
53. Liu M, Hanks TS, Zhang J, McClure MJ, Siemsen DW, Elser JL, Quinn MT, Lei B. 2006. Defects in *ex vivo* and *in vivo* growth and sensitivity to osmotic stress of group A *Streptococcus* caused by interruption of response regulator gene *vicR*. *Microbiology* 152:967-978.
54. Bouvier J, Borders P, Romeo Y, Fourcans A, Bouvier I, Gutierrez C. 2000. Characterization of OpuA, a glycine-betaine uptake system of *Lactococcus lactis*. *J Mol Microbiol Biotechnol* 2:199-205.
55. Zhu L, Olsen RJ, Beres SB, Ojeda Saavedra M, Kubiak SL, Cantu CC, Jenkins L, Yerramilli P, Pruitt L, Charbonneau ARL, Waller AS, Musser JM. 2020. Genome-wide screens identify group A *Streptococcus* surface proteins promoting female genital tract colonization and virulence. *Am J Pathol* doi:10.1016/j.ajpath.2019.12.003.
56. Paluscio E, Caparon MG. 2015. *Streptococcus pyogenes* malate degradation pathway links pH regulation and virulence. *Infect Immun* 83:1162-1171.
57. Deniskin R, Shah B, Munoz FM, Flores AR. 2019. Clinical manifestations and bacterial genomic analysis of group A *Streptococcus* strains that cause pediatric toxic shock syndrome. *J Pediatric Infect Dis Soc* 8:265-268.

58. Upton M, Tagg JR, Wescombe P, Jenkinson HF. 2001. Intra- and interspecies signaling between *Streptococcus salivarius* and *Streptococcus pyogenes* mediated by SalA and SalA1 lantibiotic peptides. *J Bacteriol* 183:3931-3938.
59. Wescombe PA, Tagg JR. 2003. Purification and characterization of streptin, a type A1 lantibiotic produced by *Streptococcus pyogenes*. *Appl Environ Microb* 69:2737-2747.
60. Kawada-Matsuo M, Tatsuno I, Arie K, Zendo T, Oogai Y, Noguchi K, Hasegawa T, Sonomoto K, Komatsuzawa H. 2016. Two-component systems involved in susceptibility to Nisin A in *Streptococcus pyogenes*. *Appl Environ Microbiol* 82:5930-5939.
61. Wescombe PA, Upton M, Dierksen KP, Ragland NL, Sivabalan S, Wirawan RE, Inglis MA, Moore CJ, Walker GV, Chilcott CN, Jenkinson HF, Tagg JR. 2006. Production of the lantibiotic salivaricin A and its variants by oral streptococci and use of a specific induction assay to detect their presence in human saliva. *Appl Environ Microbiol* 72:1459-1466.
62. Phelps HA, Neely MN. 2007. SalY of the *Streptococcus pyogenes* lantibiotic locus is required for full virulence and intracellular survival in macrophages. *Infect Immun* 75:4541-4551.
63. Namprachan-Frantz P, Rowe HM, Runft DL, Neely MN. 2014. Transcriptional analysis of the *Streptococcus pyogenes* salivaricin locus. *J Bacteriol* 196:604-613.
64. Shelburne SA, 3rd, Sumby P, Sitkiewicz I, Granville C, DeLeo FR, Musser JM. 2005. Central role of a bacterial two-component gene regulatory system of

- previously unknown function in pathogen persistence in human saliva. Proc Natl Acad Sci U S A 102:16037-16042.
65. Voyich JM, Sturdevant DE, Braughton KR, Kobayashi SD, Lei B, Virtaneva K, Dorward DW, Musser JM, DeLeo FR. 2003. Genome-wide protective response used by group A *Streptococcus* to evade destruction by human polymorphonuclear leukocytes. Proc Natl Acad Sci U S A 100:1996-2001.
 66. Voyich JM, Braughton KR, Sturdevant DE, Vuong C, Kobayashi SD, Porcella SF, Otto M, Musser JM, DeLeo FR. 2004. Engagement of the pathogen survival response used by group A *Streptococcus* to avert destruction by innate host defense. J Immunol 173:1194-1201.
 67. Riani C, Standar K, Srimuang S, Lembke C, Kreikemeyer B, Podbielski A. 2007. Transcriptome analyses extend understanding of *Streptococcus pyogenes* regulatory mechanisms and behavior toward immunomodulatory substances. Int J Med Microbiol 297:513-523.
 68. Schnorpfeil A, Kranz M, Kovacs M, Kirsch C, Gartmann J, Brunner I, Bittmann S, Bruckner R. 2013. Target evaluation of the non-coding csRNAs reveals a link of the two-component regulatory system CiaRH to competence control in *Streptococcus pneumoniae* R6. Mol Microbiol 89:334-349.
 69. Marx P, Nuhn M, Kovacs M, Hakenbeck R, Bruckner R. 2010. Identification of genes for small non-coding RNAs that belong to the regulon of the two-component regulatory system CiaRH in *Streptococcus*. BMC Genomics 11:661.

70. Tatsuno I, Isaka M, Okada R, Zhang Y, Hasegawa T. 2014. Relevance of the two-component sensor protein CiaH to acid and oxidative stress responses in *Streptococcus pyogenes*. BMC Research Notes 7:189.
71. Leday TV, Gold KM, Kinkel TL, Roberts SA, Scott JR, McIver KS. 2008. TrxR, a new CovR-repressed response regulator that activates the Mga virulence regulon in group A streptococcus. Infect Immun 76:4659-4668.
72. Ribardo DA, McIver KS. 2006. Defining the Mga regulon: comparative transcriptome analysis reveals both direct and indirect regulation by Mga in the group A streptococcus. Mol Microbiol 62:491-508.
73. Sanson M, Makthal N, Gavagan M, Cantu C, Olsen RJ, Musser JM, Kumaraswami M. 2015. Phosphorylation events in the multiple gene regulator of group A *Streptococcus* significantly influence global gene expression and virulence. Infect Immun 83:2382-2395.
74. Lukomski S, Nakashima K, Abdi I, Cipriano VJ, Ireland RM, Reid SD, Adams GG, Musser JM. 2000. Identification and characterization of the *scl* gene encoding a group A *Streptococcus* extracellular protein virulence factor with similarity to human collagen. Infect Immun 68:6542-6553.
75. Terao Y, Kawabata S, Kunitomo E, Murakami J, Nakagawa I, Hamada S. 2001. Fba, a novel fibronectin-binding protein from *Streptococcus pyogenes*, promotes bacterial entry into epithelial cells, and the *fba* gene is positively transcribed under the Mga regulator. Mol Microbiol 42:75-86.
76. Wexler DE, Chenoweth DE, Cleary PP. 1985. Mechanism of action of the group A streptococcal C5a inactivator. Proc Natl Acad Sci U S A 82:8144-8148.

77. Stenberg L, O'Toole P, Lindahl G. 1992. Many group A streptococcal strains express two different immunoglobulin-binding proteins, encoded by closely linked genes: characterization of the proteins expressed by four strains of different M-type. *Mol Microbiol* 6:1185-1194.
78. Courtney HS, Hasty DL, Dale JB. 2006. Anti-phagocytic mechanisms of *Streptococcus pyogenes*: binding of fibrinogen to M-related protein. *Mol Microbiol* 59:936-947.
79. Jeng A, Sakota V, Li Z, Datta V, Beall B, Nizet V. 2003. Molecular genetic analysis of a group A *Streptococcus* operon encoding serum opacity factor and a novel fibronectin-binding protein, SfbX. *J Bacteriol* 185:1208-1217.
80. Zhu L, Olsen RJ, Musser JM. 2017. Opacification domain of serum opacity factor inhibits beta-hemolysis and contributes to virulence of *Streptococcus pyogenes*. *mSphere* 2:e00147-17.
81. Gold KM. 2011. Characterization of the TrxSR two-component signal transduction system of *Streptococcus pyogenes* and its role in virulence regulation. PhD thesis. University of Maryland, College Park, College Park, MD.
82. Baruch M, Belotserkovsky I, Hertzog BB, Ravins M, Dov E, McIver KS, Le Breton YS, Zhou Y, Cheng CY, Hanski E. 2014. An extracellular bacterial pathogen modulates host metabolism to regulate its own sensing and proliferation. *Cell* 156:97-108.
83. Jordan S, Junker A, Helmann JD, Mascher T. 2006. Regulation of LiaRS-dependent gene expression in *Bacillus subtilis*: identification of inhibitor proteins,

- regulator binding sites, and target genes of a conserved cell envelope stress-sensing two-component system. *J Bacteriol* 188:5153-5166.
84. Schrecke K, Jordan S, Mascher T. 2013. Stoichiometry and perturbation studies of the LiaFSR system of *Bacillus subtilis*. *Mol Microbiol* 87:769-788.
 85. Suntharalingam P, Senadheera MD, Mair RW, Levesque CM, Cvitkovitch DG. 2009. The LiaFSR system regulates the cell envelope stress response in *Streptococcus mutans*. *Journal of Bacteriology* 191:2973-2984.
 86. Ichikawa M, Minami M, Isaka M, Tatsuno I, Hasegawa T. 2011. Analysis of two-component sensor proteins involved in the response to acid stimuli in *Streptococcus pyogenes*. *Microbiology* 157:3187-3194.
 87. Roobthaisong A, Aikawa C, Nozawa T, Maruyama F, Nakagawa I. 2017. YvqE and CovRS of group A *Streptococcus* play a pivotal role in viability and phenotypic adaptations to multiple environmental stresses. *PLoS One* 12:e0170612.
 88. Flores AR, Jewell BE, Yelamanchili D, Olsen RJ, Musser JM. 2015. A single amino acid replacement in the sensor kinase LiaS contributes to a carrier phenotype in group A *Streptococcus*. *Infect Immun* 83:4237-4246.
 89. Port GC, Cusumano ZT, Tumminello PR, Caparon MG. 2017. SpxA1 and SpxA2 act coordinately to fine-tune stress responses and virulence in *Streptococcus pyogenes*. *mBio* 8:e00288-17.
 90. Flores AR, Olsen RJ, Cantu C, Pallister KB, Guerra FE, Voyich JM, Musser JM. 2017. Increased pilus production conferred by a naturally occurring mutation

alters host-pathogen interaction in favor of carriage in *Streptococcus pyogenes*.
Infect Immun 85:e00949-16.

91. Isaka M, Tatsuno I, Maeyama J, Matsui H, Zhang Y, Hasegawa T. 2016. The YvqE two-component system controls biofilm formation and acid production in *Streptococcus pyogenes*. APMIS 124:574-85.
92. Kreikemeyer B, Boyle MDP, Buttaro BA, Heinemann M, Podbielski A. 2001. Group A streptococcal growth phase-associated virulence factor regulation by a novel operon (Fas) with homologues to two-component-type regulators requires a small RNA molecule. Mol Microbiol 39:392-406.
93. Liu Z, Trevino J, Ramirez-Pena E, Sumby P. 2012. The small regulatory RNA FasX controls pilus expression and adherence in the human bacterial pathogen group A *Streptococcus*. Mol Microbiol 86:140-154.
94. Ramirez-Pena E, Trevino J, Liu Z, Perez N, Sumby P. 2010. The group A *Streptococcus* small regulatory RNA FasX enhances streptokinase activity by increasing the stability of the *ska* mRNA transcript. Mol Microbiol 78:1332-1347.
95. Danger JL, Cao TN, Cao TH, Sarkar P, Trevino J, Pflughoeft KJ, Sumby P. 2015. The small regulatory RNA FasX enhances group A *Streptococcus* virulence and inhibits pilus expression via serotype-specific targets. Mol Microbiol 96:249-262.
96. Danger JL, Makthal N, Kumaraswami M, Sumby P. 2015. The FasX small regulatory RNA negatively regulates the expression of two fibronectin-binding proteins in group A *Streptococcus*. J Bacteriol 197:3720-3730.

97. Levin JC, Wessels MR. 1998. Identification of *csrR/csrS*, a genetic locus that regulates hyaluronic acid capsule synthesis in group A *Streptococcus*. *Mol Microbiol* 30:209-219.
98. Bernish B, van de Rijn I. 1999. Characterization of a two-component system in *Streptococcus pyogenes* which is involved in regulation of hyaluronic acid production. *J Biol Chem* 274:4786-4793.
99. Federle MJ, McIver KS, Scott JR. 1999. A response regulator that represses transcription of several virulence operons in the group A *Streptococcus*. *J Bacteriol* 181:3649-3657.
100. Graham MR, Smoot LM, Lux Migiliaccio CA, Virtaneva K, Sturdevant DE, Porcella SF, Federle MJ, Adams GJ, Scott JR, Musser JM. 2002. Virulence control in group A *Streptococcus* by a two-component gene regulatory system: global expression profiling and *in vivo* infection modeling. *Proc Natl Acad Sci U S A* 99:13855-13860.
101. Sumbly P, Whitney AR, Graviss EA, DeLeo FR, Musser JM. 2006. Genome-wide analysis of group A streptococci reveals a mutation that modulates global phenotype and disease specificity. *PLoS Pathog* 2:e5.
102. Shelburne SA, Olsen RJ, Suber B, Sahasrabhojane P, Sumbly P, Brennan RG, Musser JM. 2010. A combination of independent transcriptional regulators shapes bacterial virulence gene expression during infection. *PLoS Pathog* 6:e1000817.
103. Galloway-Pena J, DebRoy S, Brumlow C, Li X, Tran TT, Horstmann N, Yao H, Chen K, Wang F, Pan BF, Hawke DH, Thompson EJ, Arias CA, Fowler VG, Jr., Bhatti MM, Kalia A, Flores AR, Shelburne SA. 2018. Hypervirulent group A

- Streptococcus* emergence in an acapsular background is associated with marked remodeling of the bacterial cell surface. PLoS One 13:e0207897.
104. Flores AR, Jewell BE, Fittipaldi N, Beres SB, Musser JM. 2012. Human disease isolates of serotype M4 and M22 group A streptococcus lack genes required for hyaluronic acid capsule biosynthesis. mBio 3:e00413-12.
 105. Gao J, Gusa AA, Scott JR, Churchward G. 2005. Binding of the global response regulator protein CovR to the *sag* promoter of *Streptococcus pyogenes* reveals a new mode of CovR-DNA interaction. J Biol Chem 280:38948-38956.
 106. Nizet V. 2002. Streptococcal beta-hemolysins: genetics and role in disease pathogenesis. Trends Microbiol 10:575-580.
 107. Heath A, DiRita VJ, Barg NL, Engleberg NC. 1999. A two-component system, CsrR-CsrS, represses expression of three *Streptococcus pyogenes* virulence factors, hyaluronic acid capsule, streptolysin S, and pyrogenic exotoxin B. Infect Immun 67:5298-5305.
 108. Olsen RJ, Raghuram A, Cantu C, Hartman MH, Jimenez FE, Lee S, Ngo A, Rice KA, Saddington D, Spillman H, Valson C, Flores AR, Beres SB, Long SW, Nasser W, Musser JM. 2015. The majority of 9,729 group A streptococcus strains causing disease secrete SpeB cysteine protease: pathogenesis implications. Infect Immun 83:4750-4758.
 109. Churchward G, Bates C, Gusa AA, Stringer V, Scott JR. 2009. Regulation of streptokinase expression by CovR/S in *Streptococcus pyogenes*: CovR acts through a single high-affinity binding site. Microbiology 155:566-575.

110. Huang T-T, Malke H, Ferretti JJ. 1989. Heterogeneity of the streptokinase gene in group A streptococci. *Infect Immun* 57:502-506.
111. Rasmussen M, Muller H-P, Bjorck L. 1999. Protein GRAB of *Streptococcus pyogenes* regulates proteolysis at the bacterial surface by binding alpha2-macroglobulin. *J Biol Chem* 274:15336-15344.
112. Lei B, DeLeo FR, Hoe NP, Graham MR, Mackie SM, Cole RL, Liu M, Hill HR, Low DE, Federle MJ, Scott JR, Musser JM. 2001. Evasion of human innate and acquired immunity by a bacterial homolog of CD11b that inhibits opsonophagocytosis. *Nat Med* 7:1298-1305.
113. von Pawel-Rammingen U, Johansson BP, Bjorck L. 2002. IdeS, a novel streptococcal cysteine proteinase with unique specificity for immunoglobulin G. *EMBO J* 21:1607-1615.
114. Edwards RJ, Taylor GW, Ferguson M, Murray S, Rendell N, Wrigley A, Bai Z, Boyle J, Finney SJ, Jones A, Russell HH, Turner C, Cohen J, Faulkner L, Sriskandan S. 2005. Specific C-terminal cleavage and inactivation of interleukin-8 by invasive disease isolates of *Streptococcus pyogenes*. *J Infect Dis* 192:783-790.
115. Zhu L, Olsen RJ, Lee JD, Porter AR, DeLeo FR, Musser JM. 2017. Contribution of secreted NADase and streptolysin O to the pathogenesis of epidemic serotype M1 *Streptococcus pyogenes* infections. *Am J Pathol* 187:605-613.
116. Horstmann N, Sahasrabhojane P, Suber B, Kumaraswami M, Olsen RJ, Flores A, Musser JM, Brennan RG, Shelburne SA, 3rd. 2011. Distinct single amino acid

- replacements in the control of virulence regulator protein differentially impact streptococcal pathogenesis. *PLoS Pathog* 7:e1002311.
117. Bao YJ, Liang Z, Mayfield JA, Lee SW, Ploplis VA, Castellino FJ. 2015. CovRS-regulated transcriptome analysis of a hypervirulent M23 strain of group A *Streptococcus pyogenes* provides new insights into virulence determinants. *J Bacteriol* 197:3191-3205.
 118. Otsuji K, Fukuda K, Maruoka T, Ogawa M, Saito M. 2020. Acquisition of genetic mutations in Group A Streptococci at infection site and subsequent systemic dissemination of the mutants with lethal mutations in a streptococcal toxic shock syndrome mouse model. *Microb Pathog* 143:104116.
 119. Chiang-Ni C, Tsou CC, Lin YS, Chuang WJ, Lin MT, Liu CC, Wu JJ. 2008. The transcriptional terminator sequences downstream of the *covR* gene terminate *covR/S* operon transcription to generate *covR* monocistronic transcripts in *Streptococcus pyogenes*. *Gene* 427:99-103.
 120. Gusa AA, Scott JR. 2005. The CovR response regulator of group A streptococcus (GAS) acts directly to repress its own promoter. *Mol Microbiol* 56:1195-207.
 121. Miller AA, Engleberg NC, DiRita VJ. 2001. Repression of virulence genes by phosphorylation-dependent oligomerization of CsrR at target promoters in *S. pyogenes*. *Mol Microbiol* 40:976-990.
 122. Federle MJ, Scott JR. 2002. Identification of binding sites for the group A streptococcal global regulator CovR. *Mol Microbiol* 43:1161-1172.

123. Gusa AA, Gao J, Stringer V, Churchward G, Scott JR. 2006. Phosphorylation of the group A streptococcal CovR response regulator causes dimerization and promoter-specific recruitment by RNA polymerase. *J Bacteriol* 188:4620-4626.
124. Gusa AA, Froehlich BJ, Desai D, Stringer V, Scott JR. 2007. CovR activation of the dipeptide permease promoter (*PdppA*) in group A streptococcus. *J Bacteriol* 189:1407-1416.
125. Horstmann N, Sahasrabhojane P, Yao H, Su X, Shelburne SA, Stock AM. 2017. Use of a phosphorylation site mutant to identify distinct modes of gene repression by the control of virulence regulator (CovR) in *Streptococcus pyogenes*. *J Bacteriol* 199:e00835-16.
126. Dalton TL, Scott JR. 2004. CovS inactivates CovR and is required for growth under conditions of general stress in *Streptococcus pyogenes*. *J Bacteriol* 186:3928-3937.
127. Horstmann N, Saldana M, Sahasrabhojane P, Yao H, Su X, Thompson E, Koller A, Shelburne SA, 3rd. 2014. Dual-site phosphorylation of the control of virulence regulator impacts group A streptococcal global gene expression and pathogenesis. *PLoS Pathog* 10:e1004088.
128. Horstmann N, Tran CN, Brumlow C, DebRoy S, Yao H, Noguera Gonzalez G, Makthal N, Kumaraswami M, Shelburne SA. 2018. Phosphatase activity of the control of virulence sensor kinase CovS is critical for the pathogenesis of group A streptococcus. *PLoS Pathog* 14:e1007354.
129. Trevino J, Perez N, Ramirez-Pena E, Liu Z, Shelburne SA, 3rd, Musser JM, Sumbly P. 2009. CovS simultaneously activates and inhibits the CovR-mediated

- repression of distinct subsets of group A *Streptococcus* virulence factor-encoding genes. *Infect Immun* 77:3141-3149.
130. Churchward G. 2007. The two faces of Janus: virulence gene regulation by CovR/S in group A streptococci. *Mol Microbiol* 64:34-41.
 131. Horstmann N, Sahasrabhojane P, Saldana M, Ajami NJ, Flores AR, Sumbly P, Liu CG, Yao H, Su X, Thompson E, Shelburne SA. 2015. Characterization of the effect of the histidine kinase CovS on response regulator phosphorylation in group A *Streptococcus*. *Infect Immun* 83:1068-1077.
 132. Gryllos I, Levin JC, Wessels MR. 2003. The CsrR/CsrS two-component system of group A *Streptococcus* responds to environmental Mg²⁺. *Proc Natl Acad Sci U S A* 100:4227-4232.
 133. Gryllos I, Tran-Winkler HJ, Cheng M, Chung H, Bolcome R, Lu W, Lehrer RI, Wessels MR. 2008. Induction of group A *Streptococcus* virulence by a human antimicrobial peptide. *Proc Natl Acad Sci U S A* 105:16755-16760.
 134. Gryllos I, Grifantini R, Colaprico A, Jiang S, Deforce E, Hakansson A, Telford JL, Grandi G, Wessels MR. 2007. Mg²⁺ signalling defines the group A streptococcal CsrRS (CovRS) regulon. *Mol Microbiol* 65:671-683.
 135. Tran-Winkler HJ, Love JF, Gryllos I, Wessels MR. 2011. Signal transduction through CsrRS confers an invasive phenotype in group A *Streptococcus*. *PLoS Pathog* 7:e1002361.
 136. Velarde JJ, Ashbaugh M, Wessels MR. 2014. The human antimicrobial peptide LL-37 binds directly to CsrS, a sensor histidine kinase of group A *Streptococcus*, to activate expression of virulence factors. *J Biol Chem* 289:36315-36324.

137. Sugareva V, Arlt R, Fiedler T, Riani C, Podbielski A, Kreikemeyer B. 2010. Serotype- and strain- dependent contribution of the sensor kinase CovS of the CovRS two-component system to *Streptococcus pyogenes* pathogenesis. BMC Microbiol 10:34.
138. Chiang-Ni C, Tseng HC, Hung CH, Chiu CH. 2017. Acidic stress enhances CovR/S-dependent gene repression through activation of the *covR/S* promoter in *emm1*-type group A *Streptococcus*. Int J Med Microbiol 307:329-339.
139. Chiang-Ni C, Kao C-Y, Hsu C-Y, Chiu C-H. 2019. Phosphorylation at the D53 but not the T65 residue of CovR determines the repression of *rgg* and *speB* transcription in *emm1*- and *emm49*-type group A streptococci. J Bacteriol 201:e00681-18.
140. Li J, Liu G, Feng W, Zhou Y, Liu M, Wiley JA, Lei B. 2014. Neutrophils select hypervirulent CovRS mutants of M1T1 group A *Streptococcus* during subcutaneous infection of mice. Infect Immun 82:1579-1590.
141. Hollands A, Pence MA, Timmer AM, Osvath SR, Turnbull L, Whitchurch CB, Walker MJ, Nizet V. 2010. Genetic switch to hypervirulence reduces colonization phenotypes of the globally disseminated group A *Streptococcus* M1T1 clone. J Infect Dis 202:11-19.
142. Flores AR, Luna RA, Runge JK, Shelburne SA, 3rd, Baker CJ. 2017. Cluster of fatal group A streptococcal *emm87* infections in a single family: molecular basis for invasion and transmission. J Infect Dis 215:1648-1652.
143. Mitrophanov AY, Groisman EA. 2008. Signal integration in bacterial two-component regulatory systems. Genes Dev 22:2601-2611.

144. Eguchi Y, Utsumi R. 2008. Introduction to bacterial signal transduction networks. *Adv Exp Med Biol* 631:1-6.
145. Eguchi Y, Itou J, Yamane M, Demizu R, Yamato F, Okada A, Mori H, Kato A, Utsumi R. 2007. B1500, a small membrane protein, connects the two-component systems EvgS/EvgA and PhoQ/PhoP in *Escherichia coli*. *Proc Natl Acad Sci U S A* 104:18712-18717.
146. Ishii E, Eguchi Y, Utsumi R. 2013. Mechanism of activation of PhoQ/PhoP two-component signal transduction by SafA, an auxiliary protein of PhoQ histidine kinase in *Escherichia coli*. *Biosci Biotechnol Biochem* 77:814-819.
147. Carlyon RE, Ryther JL, VanYperen RD, Griffitts JS. 2010. FeuN, a novel modulator of two-component signalling identified in *Sinorhizobium meliloti*. *Mol Microbiol* 77:170-182.
148. Szurmant H, Mohan MA, Imus PM, Hoch JA. 2007. YycH and YycI interact to regulate the essential YycFG two-component system in *Bacillus subtilis*. *J Bacteriol* 189:3280-3289.
149. Szurmant H, Bu L, Brooks CL, 3rd, Hoch JA. 2008. An essential sensor histidine kinase controlled by transmembrane helix interactions with its auxiliary proteins. *Proc Natl Acad Sci U S A* 105:5891-5896.
150. Zhou X, Keller R, Volkmer R, Krauss N, Scheerer P, Hunke S. 2011. Structural basis for two-component system inhibition and pilus sensing by the auxiliary CpxP protein. *J Biol Chem* 286:9805-9814.

151. Kilmury SLN, Burrows LL. 2016. Type IV pilins regulate their own expression via direct intramembrane interactions with the sensor kinase PilS. *Proc Natl Acad Sci U S A* 113:6017-6022.
152. Liu Q, Yeo WS, Bae T. 2016. The SaeRS two-component system of *Staphylococcus aureus*. *Genes (Basel)* 7:81.
153. Jeong DW, Cho H, Jones MB, Shatzkes K, Sun F, Ji Q, Liu Q, Peterson SN, He C, Bae T. 2012. The auxiliary protein complex SaePQ activates the phosphatase activity of sensor kinase SaeS in the SaeRS two-component system of *Staphylococcus aureus*. *Mol Microbiol* 86:331-348.
154. Hu Q, Peng H, Rao X. 2016. Molecular events for promotion of vancomycin resistance in vancomycin intermediate *Staphylococcus aureus*. *Front Microbiol* 7:1601.
155. Falord M, Karimova G, Hiron A, Msadek T. 2012. GraXSR proteins interact with the VraFG ABC transporter to form a five-component system required for cationic antimicrobial peptide sensing and resistance in *Staphylococcus aureus*. *Antimicrob Agents Chemother* 56:1047-1058.
156. Dubrac S, Bisicchia P, Devine KM, Msadek T. 2008. A matter of life and death: cell wall homeostasis and the WalkR (YycGF) essential signal transduction pathway. *Mol Microbiol* 70:1307-1322.
157. Poupel O, Proux C, Jagla B, Msadek T, Dubrac S. 2018. SpdC, a novel virulence factor, controls histidine kinase activity in *Staphylococcus aureus*. *PLoS Pathog* 14:e1006917.

158. Firon A, Tazi A, Da Cunha V, Brinster S, Sauvage E, Dramsi S, Golenbock DT, Glaser P, Poyart C, Trieu-Cuot P. 2013. The Abi-domain protein Abx1 interacts with the CovS histidine kinase to control virulence gene expression in group B *Streptococcus*. PLoS Pathog 9:e1003179.
159. Six A, Firon A, Plainvert C, Caplain C, Bouaboud A, Touak G, Dmytruk N, Longo M, Letourneur F, Fouet A, Trieu-Cuot P, Poyart C. 2016. Molecular characterization of nonhemolytic and nonpigmented group B streptococci responsible for human invasive infections. J Clin Microbiol 54:75-82.
160. Biswas I, Scott JR. 2003. Identification of *rocA*, a positive regulator of *covR* expression in the group A streptococcus. J Bacteriol 185:3081-3090.
161. Lynskey NN, Goulding D, Gierula M, Turner CE, Dougan G, Edwards RJ, Sriskandan S. 2013. RocA truncation underpins hyper-encapsulation, carriage longevity and transmissibility of serotype M18 group A streptococci. PLoS Pathog 9:e1003842.
162. Lynskey NN, Turner CE, Heng LS, Sriskandan S. 2015. A truncation in the regulator RocA underlies heightened capsule expression in serotype M3 group A streptococci. Infect Immun 83:1732-1733.
163. Miller EW, Pflughoeft KJ, Sumby P. 2015. Reply to "A truncation in the regulator RocA underlies heightened capsule expression in serotype M3 group A streptococci". Infect Immun 83:1734.
164. Miller EW, Danger JL, Ramalinga AB, Horstmann N, Shelburne SA, Sumby P. 2015. Regulatory rewiring confers serotype-specific hyper-virulence in the human pathogen group A *Streptococcus*. Mol Microbiol 98:473-489.

165. Jain I, Miller EW, Danger JL, Pflughoeft KJ, Sumby P. 2017. RocA is an accessory protein to the virulence-regulating CovRS two-component system in group A *Streptococcus*. *Infect Immun* 85:e00274-17.
166. Paluscio E. 2015. Adaptive mechanisms to niche remodeling in *Streptococcus pyogenes*. PhD thesis. Washington University in St. Louis, St. Louis, MO.
167. Zhu L, Olsen RJ, Horstmann N, Shelburne SA, Fan J, Hu Y, Musser JM. 2016. Intergenic variable-number tandem-repeat polymorphism upstream of rocA alters toxin production and enhances virulence in *Streptococcus pyogenes*. *Infect Immun* 84:2086-2093.
168. Sarkar P, Sumby P. 2017. Regulatory gene mutation: a driving force behind group A *Streptococcus* strain- and serotype-specific variation. *Mol Microbiol* 103:576-589.
169. Reiterer V, Eyers PA, Farhan H. 2014. Day of the dead: pseudokinases and pseudophosphatases in physiology and disease. *Trends Cell Biol* 24:489-505.
170. Yoshida H, Ishigaki Y, Takizawa A, Moro K, Kishi Y, Takahashi T, Matsui H. 2015. Comparative genomics of the mucoid and nonmucoid strains of *Streptococcus pyogenes*, isolated from the same patient with streptococcal meningitis. *Genome Announc* 3:e0021-15.
171. Ikebe T, Matsumura T, Nihonmatsu H, Ohya H, Okuno R, Mitsui C, Kawahara R, Kameyama M, Sasaki M, Shimada N, Ato M, Ohnishi M. 2016. Spontaneous mutations in *Streptococcus pyogenes* isolates from streptococcal toxic shock syndrome patients play roles in virulence. *Sci Rep* 6:28761.

172. Feng W, Minor D, Liu M, Li J, Ishaq SL, Yeoman C, Lei B. 2017. Null mutations of group A *Streptococcus* orphan kinase RocA: selection in mouse infection and comparison with CovS mutations in alteration of *in vitro* and *in vivo* protease SpeB expression and virulence. *Infect Immun* 85:e00790-16.
173. Bernard PE, Kachroo P, Zhu L, Beres SB, Eraso JM, Kajani Z, Long SW, Musser JM, Olsen RJ. 2018. RocA has serotype-specific gene regulatory and pathogenesis activities in serotype M28 group A streptococcus. *Infect Immun* 86:e00467-18.
174. Fittipaldi N, Beres SB, Olsen RJ, Kapur V, Shea PR, Watkins ME, Cantu CC, Laucirica DR, Jenkins L, Flores AR, Lovgren M, Ardanuy C, Linares J, Low DE, Tyrrell GJ, Musser JM. 2012. Full-genome dissection of an epidemic of severe invasive disease caused by a hypervirulent, recently emerged clone of group A *Streptococcus*. *Am J Pathol* 180:1522-1534.

2. ROCA HAS SEROTYPE-SPECIFIC GENE REGULATORY AND PATHOGENESIS ACTIVITIES IN SEROTYPE M28 GROUP A STREPTOCOCCUS*

2.1. Summary

Serotype M28 group A streptococcus (GAS) is a common cause of infections such as pharyngitis (“strep throat”) and necrotizing fasciitis (“flesh-eating” disease). Relatively little is known about the molecular mechanisms underpinning M28 GAS pathogenesis. Whole-genome sequencing studies of M28 GAS strains recovered from patients with invasive infections found an unexpectedly high number of missense (amino acid-changing) and nonsense (protein-truncating) polymorphisms in *rocA* (regulator of Cov), leading us to hypothesize that altered RocA activity contributes to M28 GAS molecular pathogenesis. To test this hypothesis, an isogenic *rocA* deletion mutant strain was created. Transcriptome sequencing (RNA-seq) analysis revealed that RocA inactivation significantly alters the level of transcripts for 427 and 323 genes at mid-exponential and early stationary growth phases, respectively, including genes for 41 transcription regulators and 21 virulence factors. In contrast, RocA transcriptomes from other GAS M protein serotypes are much smaller and include fewer transcription regulators. The *rocA* mutant strain had significantly increased activity of multiple virulence factors and grew to significantly higher colony counts under acid stress *in vitro*. RocA inactivation also significantly increased GAS virulence in a mouse model of necrotizing myositis. Our results demonstrate that RocA is an important regulator

*Reprinted from “RocA has serotype-specific gene regulatory and pathogenesis activities in serotype M28 group A streptococcus” by Bernard PE, Kachroo P, Zhu L, Beres SB, Eraso JM, Kajani Z, Long SW, Musser JM, and Olsen RJ. 2018. *Infect Immun* 86, e00467-18, Copyright © 2018 by American Society for Microbiology.

of transcription regulators and virulence factors in M28 GAS and raise the possibility that naturally occurring polymorphisms in *rocA* in some fashion contribute to human invasive infections caused by M28 GAS strains.

2.2. Introduction

Group A streptococcus (GAS) is a human-specific pathogen that causes diseases ranging in severity from relatively innocuous pharyngitis (“strep throat”) to life-threatening necrotizing fasciitis (“flesh-eating” disease) (1, 2). In addition, GAS is responsible for postinfectious immune sequelae such as rheumatic heart disease and poststreptococcal glomerulonephritis (3). The global disease burden and economic impact of GAS disease are immense. The World Health Organization estimates that GAS causes over 700 million superficial infections, 1.78 invasive infections, and 512,000 deaths annually (4). Despite decades of research, there is no commercially available vaccine to prevent GAS infections.

GAS strains are commonly classified by sequence variation in the *emm* gene, which encodes the highly polymorphic M protein virulence factor (3). Serotype M28 strains are among the more common causes of GAS pharyngitis and invasive infections in the United States and other countries (1, 5-11). Of note, serotype M28 GAS strains are strongly associated with puerperal sepsis (7-9, 12-14). Despite the importance of M28 strains in human disease, relatively little is known about the molecular pathogenesis of M28 GAS (1, 5, 12, 13). Historically, GAS pathogenesis research has focused on the strains of other numerically important serotypes, such as M1 and M3 (2, 15-21).

One gene of increasingly recognized importance to GAS pathogenesis is *rocA* (regulator of Cov), encoding the RocA protein (22). RocA was initially identified as a positive regulator of the CovRS (control of virulence) two-component system, which is a

negative regulator of virulence (22-24). Further study of *rocA* in multiple GAS serotypes identified a naturally occurring nonsense mutation in all serotype M18 strains that results in hyperencapsulation and increases carriage longevity in the mouse nasopharynx (25). Similarly, RocA is inactivated in all serotype M3 strains by a single nucleotide deletion that introduces a frameshift mutation, and restoration of RocA by introduction of the serotype M1 wild-type *rocA* allele decreases M3 GAS virulence in a mouse model of bacteremia (26-28). Deletion of *rocA* in serotype M1, M3, M6, M14, M18, and M89 GAS results in increased expression of virulence factors known to be regulated by the CovRS system (26-32). Although the molecular mechanisms for RocA function has not been determined, RocA increases phosphorylation of the DNA binding response regulator CovR in the presence of its cognate sensor histidine kinase CovS, resulting in CovR activation (28, 30). The N-terminal transmembrane domains of RocA are crucial for the regulatory activity of RocA, suggesting that RocA functions as an accessory protein to the CovRS system (32). However, the role, if any, of RocA in pathogenesis has not been studied in M28 GAS.

Whole-genome sequencing studies of M28 GAS strains recovered from human invasive infections found an unexpectedly high number of missense (amino acid-altering) and nonsense (protein-truncating) polymorphisms in *rocA* (GenBank accession no. MH884522 to MH884551) (Fig. 2-1). Previous studies of *rocA* in strains of other GAS M protein serotypes identified several nonsense mutations and many frameshifting insertions and deletions (indels) that result in protein truncation (25-28, 30-35). However, very few *rocA* missense mutations have been reported in other GAS serotypes, and none have been studied previously (25-28, 30-35). The striking increase in missense mutation frequency in M28 strains led us to speculate that RocA has serotype-specific functions in M28 GAS

strains. We hypothesized that RocA inactivation significantly contributes to the molecular pathogenesis of invasive infections caused by serotype M28 GAS. To test this hypothesis, we created an isogenic *rocA* deletion mutant strain and discovered that RocA regulates a substantial portion of the M28 GAS transcriptome, including many genes encoding transcription regulators and virulence factors. Consistent with the transcriptome data, *in vitro* assays showed that RocA inactivation significantly increases the secreted activity of multiple virulence factors and increases CFU under acid stress. The RocA-inactivated strain was also significantly more virulent in a mouse model of necrotizing myositis.

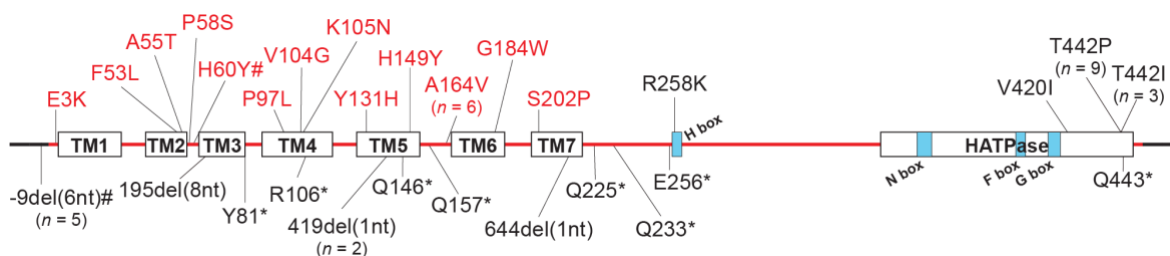


Fig. 2-1 *rocA* is unusually polymorphic in serotype M28 GAS strains.

The affected codon and amino acid change conferred by each polymorphism are shown. For polymorphisms due to nucleotide deletion, the affected nucleotide is identified. Alleles identified in multiple isolates are indicated. Polymorphisms that result in RocA protein truncation or loss of *rocA* mRNA translation are shown below the protein schematic, and polymorphisms that result in amino acid changes are shown above the protein schematic. Missense polymorphisms in the predicted domains sufficient for regulatory activity (32) are colored red. Predicted domains of the RocA protein using Phyre2 are indicated (TM, transmembrane domain; HATPase, histidine kinase ATPase domain) (106). Predicted functional domains of the potential histidine kinase domain (H box, N box, F box, G box) are identified (22). #, one strain has two polymorphisms in *rocA*.

2.3. Results

2.3.1. *rocA* is unusually polymorphic in serotype M28 GAS

Recent whole-genome sequencing studies of serotype M28 GAS strains recovered from human invasive infections revealed an unexpectedly high number of missense and nonsense polymorphisms in *rocA* (GenBank accession no. MH884522 to MH884551) (Fig.

2-1). We identified 29 unique polymorphisms (25 single nucleotide polymorphisms [SNPs] and 4 insertions/deletions [indels]) among 2,101 M28 GAS strains. The frequency of polymorphisms in *rocA* is significantly greater than expected by chance alone ($P < 0.01$, Fisher's exact test). The 29 unique polymorphisms included 17 missense mutations, 11 nonsense mutations, and one six-nucleotide deletion in the upstream noncoding region that affects the presumed ribosomal binding site (30) (Fig. 2-1). Of note, 13/17 (76.5%) of the missense mutations occur in the 5' end of *rocA*, resulting in amino acid changes in the N terminus of RocA that may be crucial for its function as an accessory protein to the CovRS system (32) (Fig. 2-1).

The abundance of *rocA* polymorphisms found in the M28 GAS strains prompted a reevaluation of data from our previously published whole-genome sequencing studies of large, comprehensive, population-based collections of other GAS M protein serotypes (15, 36, 37). We discovered that M1 and M59 GAS strains had a much lower frequency of *rocA* polymorphisms (see Fig. A-1 in the Appendix) (15, 22, 32, 36, 37, 106). Although 29 unique *rocA* polymorphisms were identified among 2,101 M28 GAS strains (13.8 *rocA* alleles per 1,000 M28 strains), only 16 unique *rocA* polymorphisms were identified among 3,443 M1 GAS strains (4.6 alleles per 1,000 strains) (15), and two unique *rocA* polymorphisms were identified among 310 M59 GAS strains (6.5 alleles per 1,000 strains) (37). In contrast, 18 unique *rocA* polymorphisms were found among 1,193 M89 strains (15.1 alleles per 1,000 strains) (36).

The very high number of variants identified in serotype M28 GAS strains suggests that the *rocA* polymorphisms are selected for during human invasive infection to alter the

regulatory activity of RocA. We hypothesize that altered RocA activity contributes to the molecular pathogenesis of M28 GAS.

2.3.2. Creation of an isogenic *rocA* deletion mutant strain

As a first step toward investigating the role of RocA in serotype M28 GAS molecular pathogenesis, we created an isogenic *rocA* deletion mutant strain using allelic exchange (38). Wild-type (WT) strain MGAS28426 was chosen as the parental strain because it is genetically representative of serotype M28 GAS strains that commonly cause human infections, and it has a wild-type allele for all major global transcription regulatory genes, including *covRS*, *ropB*, *mga*, *ccpA*, and *rocA*. Whole-genome sequencing of the isogenic *rocA* deletion ($\Delta rocA$) mutant strain confirmed the absence of spurious mutations. To determine if *rocA* deletion alters the growth phenotype of M28 GAS, the parental WT and isogenic $\Delta rocA$ mutant strains were grown in Todd-Hewitt broth supplemented with yeast extract (THY), a nutrient-rich medium. No significant difference in growth was observed (Fig. 2-2A) ($P =$ not significant [NS], two-way analysis of variance [ANOVA]).

2.3.3. Deletion of *rocA* in M28 GAS strain MGAS28426 results in a substantial transcriptome change

To test the hypothesis that *rocA* deletion results in altered global gene transcript levels in M28 GAS, transcriptome sequencing (RNA-seq) analysis was performed using strains grown to mid-exponential (ME) (optical density at 600 nm [OD₆₀₀] = 0.5) and early stationary (ES) (OD₆₀₀ = 1.65) growth phases (Fig. 2-2A). Principal-component analysis showed that *rocA* deletion markedly alters the global transcriptome of serotype M28 GAS at both growth phases (Fig 2-2B). In total, 427 (25.8%) and 323 (19.5%) genes had significantly altered transcript levels at ME and ES growth phases, respectively (absolute

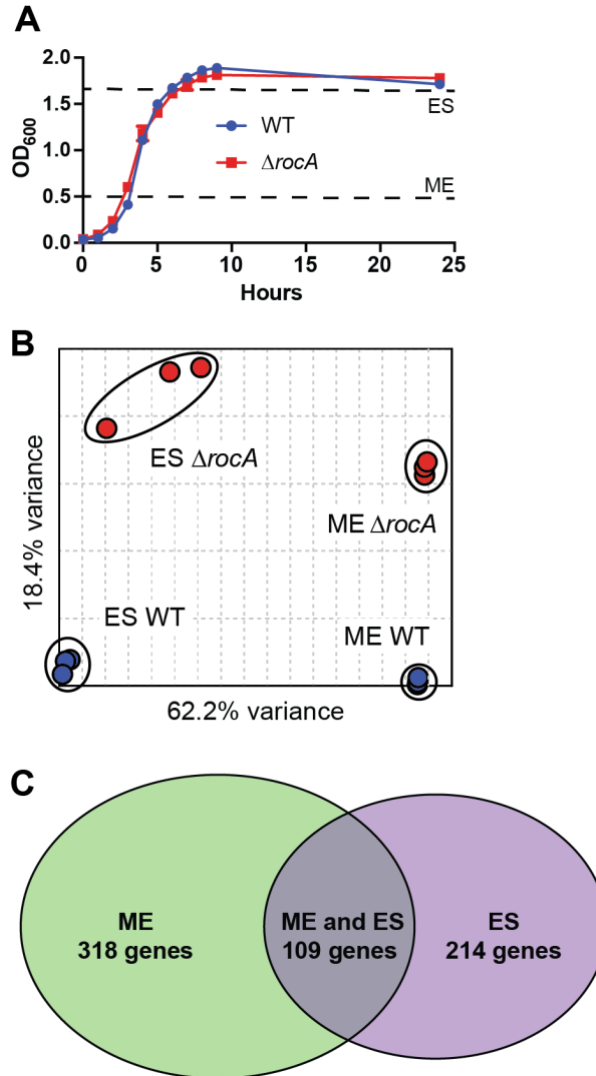


Fig. 2-2 Deletion of *rocA* significantly alters the GAS transcriptome. (A) No significant growth difference in nutrient-rich liquid medium was observed between the parental wild-type (WT) and isogenic $\Delta rocA$ mutant strains. Dashed lines represent the OD₆₀₀ of mid-exponential (ME) and early stationary (ES) growth phases for cultures that were collected for RNA-seq analysis. (B) Principal component analysis of the WT and $\Delta rocA$ strain transcriptomes at the ME and ES growth phases. (C) Number of genes with significantly altered transcript levels at the ME and ES growth phases (107).

transcript fold change, ≥ 1.5 ; $P < 0.05$ after Baggerly's test with Bonferroni's correction for multiple comparisons) (Fig. 2-2C). Of these genes, 109 were common to both growth phases (Fig. 2-2C). Many of the significantly differentially expressed genes encode transcription regulators and proven virulence factors (see below). A complete list of genes with significantly altered transcript levels is provided in Tables B-1 and B-2 in the Appendix.

Table 2-1 GAS transcription regulator genes (proven and inferred) directly or indirectly regulated by RocA at mid-exponential (ME) and early-stationary (ES) growth phases.

Locus Tag ^a	Gene	Known or Putative Function ^b	Fold change relative to WT ^c	
			ME	ES
<i>M28_Spy0034</i>	<i>comR</i> ^{d,e,f}	Competence (39)	-1.7	
<i>M28_Spy0104</i>	<i>rofA</i> ^{d,e,f}	Regulator of fibronectin binding protein (40)	-1.9	
<i>M28_Spy0153</i>	<i>sgaR</i>	Ascorbate utilization (41)	-1.5	
<i>M28_Spy0184</i>	<i>rivR</i> ^{d,e}	Negative regulator of GRAB (42)	2.4	
<i>M28_Spy0189</i>	<i>yjdR</i>	Multidrug resistance transporters (41)	-2.3	
<i>M28_Spy0276</i>	<i>nrdR</i> ^d	Ribonucleotide metabolism (43)		1.8
<i>M28_Spy0522</i>	<i>agaR2</i>	Carbohydrate metabolism (41)	-1.9	
<i>M28_Spy0538</i>	<i>ralp3</i> ^d	RofA-like transcription regulator (44)	-2.3	-1.8
<i>M28_Spy0681</i>	<i>cpsY</i> ^{d,e,f}	Resistance to opsonophagocytic killing (45)	1.6	
<i>M28_Spy0780</i>	<i>srtK</i> ^d	Lantibiotic biosynthesis (46)		1.7
<i>M28_Spy0872</i>	<i>M28_Spy0872</i> ^f	GntR family transcription regulator (41)	-1.8	
<i>M28_Spy0889</i>	<i>nagR</i>	N-acetylglucosamine utilization (41)		2.8
<i>M28_Spy0896</i>	<i>pdxR</i>	Pyridoxin metabolism (41)		1.8
<i>M28_Spy0919</i>	<i>ciaH</i> ^d	Acid and oxidative stress (47)		2.1
<i>M28_Spy0920</i>	<i>ciaR</i> ^e			2.0
<i>M28_Spy0963</i>	<i>M28_Spy0963</i> ^f	Transport (41)	2.0	-1.7
<i>M28_Spy1346</i>	<i>trxR</i> ^{d,e}	Two-component system (48)	-1.9	
<i>M28_Spy1347</i>	<i>trxS</i> ^{d,e}		-2.0	
<i>M28_Spy1373</i>	<i>liaR</i> ^{d,e}	Regulator of pilus proteins (49)		-1.7
<i>M28_Spy1384</i>	<i>atoR</i> ^{d,e,f}	Short chain fatty acid metabolism (50)	1.7	
<i>M28_Spy1420</i>	<i>M28_Spy1420</i>	Mga family transcription regulator (41)		-2.0
<i>M28_Spy1445</i>	<i>lacR.1</i> ^d	Galactose metabolism (51)		-2.3
<i>M28_Spy1449</i>	<i>copY</i> ^{d,f}	Copper toxicity (52)	-2.4	
<i>M28_Spy1501</i>	<i>codY</i> ^d	Pleiotropic transcription regulator (53)	1.5	
<i>M28_Spy1531</i>	<i>scrR</i>	Sucrose utilization (41)		-1.6
<i>M28_Spy1545</i>	<i>M28_Spy1545</i> ^f	XRE family transcription regulator (41)	1.7	
<i>M28_Spy1546</i>	<i>M28_Spy1546</i> ^f	XRE family transcription regulator (41)	1.5	
<i>M28_Spy1564</i>	<i>srv</i> ^{d,e}	Streptococcal regulator of virulence (54)		3.1
<i>M28_Spy1566</i>	<i>M28_Spy1566</i> ^f	XRE family transcription regulator (41)	-2.5	
<i>M28_Spy1569</i>	<i>M28_Spy1569</i>	MerR family transcription regulator (41)	-1.6	
<i>M28_Spy1615</i>	<i>salR</i> ^d	Lantibiotic biosynthesis (55)		1.8
<i>M28_Spy1636</i>	<i>M28_Spy1636</i>	XRE family transcription regulator (41)		-1.9
<i>M28_Spy1704</i>	<i>mga</i> ^{d,e}	Multiple gene regulator (56)	2.2	2.0
<i>M28_Spy1708</i>	<i>ihk</i> ^{d,e,f}	Polymorphonuclear leukocyte evasion (57)	1.5	
<i>M28_Spy1724</i>	<i>ropB</i> ^{d,e}	Regulator of SpeB (58)	-2.3	
<i>M28_Spy1750</i>	<i>ctsR</i> ^f	Stress and heat shock response (59)		2.7
<i>M28_Spy1763</i>	<i>M28_Spy1763</i> ^f	LuxR family transcription regulator (41)	-1.6	
<i>M28_Spy1769</i>	<i>treR</i> ^f	Trehalose utilization (41)	-1.5	
<i>M28_Spy1782</i>	<i>spxA2</i> ^{d,e}	Stress resistance, regulator of SpeB (60)	4.0	
<i>M28_Spy1835</i>	<i>ywzG</i> ^f	Transport (41)	-1.5	-2.0
<i>M28_Spy1839</i>	<i>pipR</i>	Phage infection protein (41)		1.8

^aLocus tag identified in the serotype M28 reference genome MGAS6180.

^bKnown or putative function based on known role in GAS or inferred homology. Selected references are provided.

^cEmpty (blank) cells: the gene does not satisfy the *P* value and/or fold change requirement.

^dTranscription regulators that have been previously studied in GAS.

^eTranscription regulators with a proven role in GAS virulence.

^fTranscription regulators unique to the M28 ME RocA transcriptome compared to the M1 and M3 ME RocA transcriptomes (28, 32).

2.3.4. RocA directly or indirectly regulates transcription regulators involved in virulence in serotype M28 GAS

The RNA-seq data demonstrated that RocA inactivation significantly altered the transcript levels of 41 transcription regulators in serotype M28 strain MGAS28426 (Table 2-1) (39-60). Of the 41 transcription regulators that are directly or indirectly regulated by RocA in M28 GAS, 22 have been previously studied in GAS, 11 have inferred function by homology with transcription regulators in other *Streptococcus* species, and 8 are of unknown function (Table 2-1) (39-60). One particularly interesting regulator whose expression is significantly altered by RocA inactivation in M28 GAS is *mga* (multiple virulence gene regulator of GAS) (56). Mga regulates the expression of multiple genes encoding proven virulence factors, including *sclA* (encoding a collagen binding protein) (61), *fba* (encoding a fibronectin binding protein) (62), *scpA* (encoding C5a peptidase) (63), *enn* (encoding IgA binding protein) (64), *emm* (encoding antiphagocytic M protein) (65), *mrp* (encoding M-related protein) (66), *sfbX* (encoding a fibronectin binding protein) (67), and *sof* (encoding serum opacity factor [SOF]) (68). Compared to the parental WT strain, the isogenic $\Delta rocA$ deletion mutant strain had significantly increased transcript levels for each gene in the Mga regulon at one or both time points (Fig. 2-3A and Tables B-1 and B-2).

To determine if the observed difference in transcript levels of genes in the Mga regulon result in an altered phenotype, SOF activity was assayed *in vitro*. Consistent with the RNA-seq data, the isogenic $\Delta rocA$ deletion mutant strain had significantly increased SOF activity compared to the parental WT strain (Fig. 2-3B).

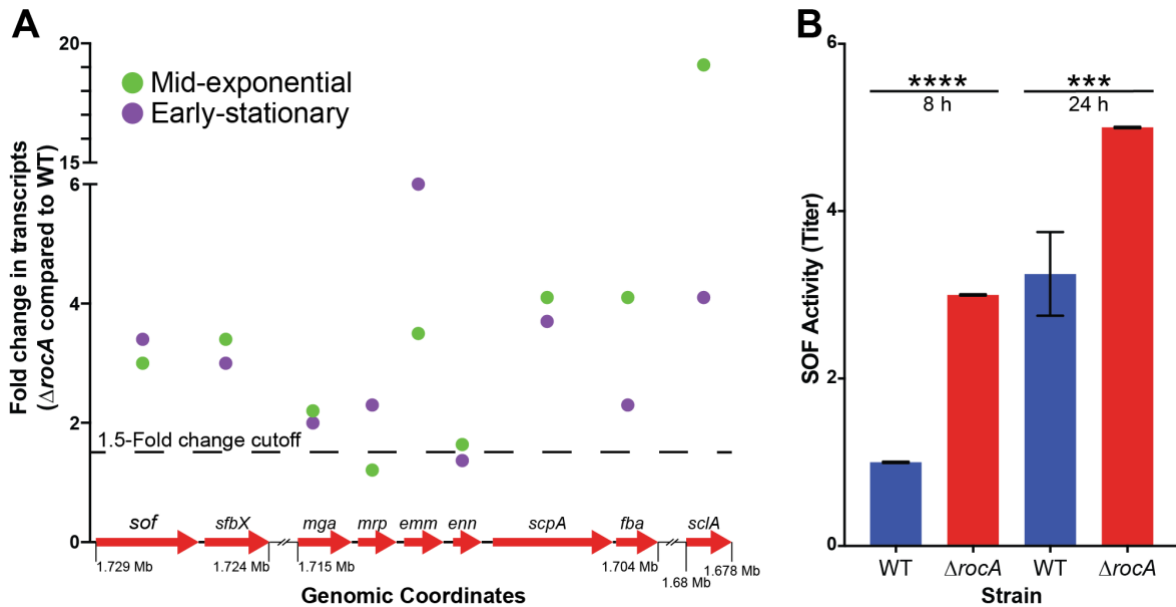


Fig. 2-3 Deletion of *rocA* significantly increases the transcript levels of genes in the Mga regulon.

(A) The transcript levels of *mga* and eight Mga-regulated genes were significantly increased in the $\Delta rocA$ mutant strain compared to the WT strain. Genomic coordinates and fold change in transcripts are shown for each gene at mid-exponential and early stationary growth phases ($P < 0.05$, Baggerly test with Bonferroni correction for multiple comparisons). Points below the 1.5-fold-change cutoff did not reach statistical significance and are included for completeness. (B) Serum opacity factor (SOF) activity assay results. Data are shown as mean \pm standard deviation. ***, $P < 0.001$; ****, $P < 0.0001$ (Student's *t* test).

2.3.5. RocA directly or indirectly regulates transcription regulators and virulence factors involved in the stress response in serotype M28 GAS

During infection, GAS cells are exposed to oxidative and acidic stress in purulent lesions (69-71). Among the 41 transcription regulators that are directly or indirectly regulated by RocA in M28 GAS, 4 are implicated in oxidative and acidic stress responses, including the CiaHR two-component system, NrdR, and SpxA2 (Table 2-1) (43, 47, 60). Additionally, the *arcABCD* operon had significantly increased transcript levels in the $\Delta rocA$ mutant strain (Fig. 2-4A and Table B-1 in the Appendix). The *arcABCD* operon encodes the ArcABCD proteins of the arginine deiminase pathway, which are also involved in the GAS response to acidic environments (72-74).

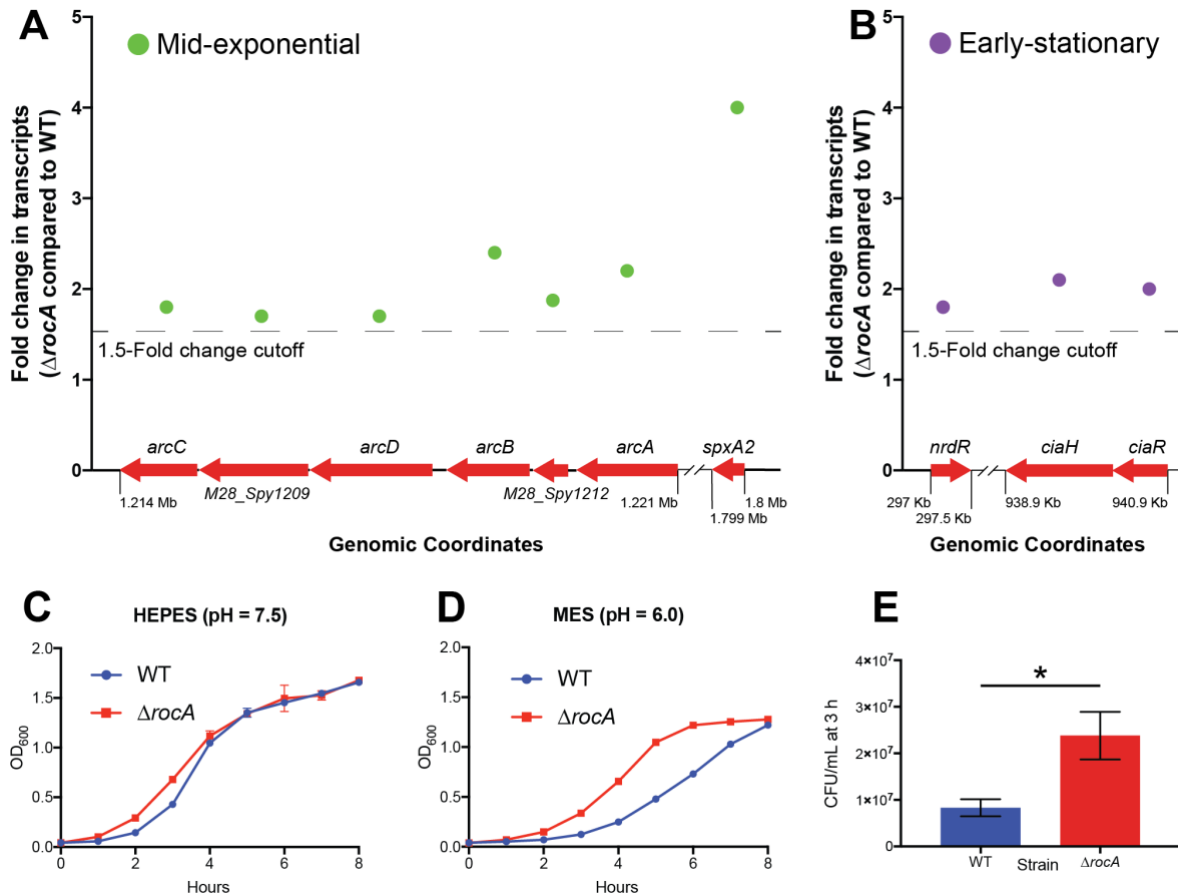


Fig. 2-4 Deletion of *rocA* significantly increases the transcript levels of genes encoding transcription regulators and proteins involved in the stress response.

(A) The transcript levels of *arcABCD* and *spxA2* were significantly increased in the $\Delta rocA$ mutant strain compared to the WT strain at mid-exponential growth phase. *M28_Spy1209* encodes a putative dipeptidase, and *M28_Spy1212* encodes a putative *N*-acetyltransferase. Genomic coordinates and fold change in transcripts are shown for each gene ($P < 0.05$, Baggerly test with Bonferroni correction for multiple comparisons). (B) The transcript levels of *nrdR* and *ciaHR* were significantly increased in the $\Delta rocA$ mutant strain compared to the WT strain at early stationary growth phase. Genomic coordinates and fold change in transcripts are shown for each gene ($P < 0.05$, Baggerly test with Bonferroni correction for multiple comparisons). (C) Growth of strains in THY buffered with HEPES (pH 7.5). (D) Growth of strains in THY buffered with 2-(*N*-morpholino)ethanesulfonic acid (MES) (pH 6.0). (E) CFU counts of strains grown in THY buffered with MES (pH 6.0) at 3 h. Data are shown as mean \pm standard error of the mean (SEM). *, $P < 0.05$ (Mann-Whitney test).

Because *ciaHR*, *nrdR*, *spxA2*, and *arcABCD* had significantly increased transcript levels in the isogenic $\Delta rocA$ deletion mutant strain compared to the parental WT strain (Fig. 2-4A and B), we hypothesized that the isogenic $\Delta rocA$ deletion mutant strain is significantly more resistant to acidic stress. To test this hypothesis, the isogenic $\Delta rocA$ deletion mutant strain and parental WT strains were grown in THY alone, THY buffered to neutral conditions using HEPES (pH 7.5), and THY buffered to acidic conditions using 2-(*N*-

morpholino)ethanesulfonic acid (MES) (pH 6.0) (29). Under neutral conditions (THY alone and HEPES, pH 7.5), the growth curves of the isogenic $\Delta rocA$ mutant and parental WT strain were nearly superimposable (Fig. 2-2A and 2-4C). Consistent with our hypothesis, when grown under acidic conditions (MES, pH 6.0), the isogenic $\Delta rocA$ deletion mutant strain had a shortened lag phase and increased slope of the exponential phase compared to the parental WT strain (Fig. 2-4D). After 3 h of growth under acidic conditions, significantly more CFU were present in cultures of the isogenic $\Delta rocA$ deletion mutant strain than in those of the parental WT strain (Fig. 2-4E).

2.3.6. Deletion of *rocA* results in differential transcript levels of multiple GAS virulence factors

Several proven and putative virulence factors had significantly altered transcript levels in the isogenic $\Delta rocA$ deletion mutant strain compared to the parental WT strain (Table 2-2). Many of the differentially expressed virulence factors are known to be regulated by the CovRS two-component system, as well as RocA, in other GAS serotypes (24, 28, 32). Selected virulence factors genes with increased transcript levels in the isogenic $\Delta rocA$ mutant strain include *nga* (encoding NAD⁺-glycohydrolase [SPN]) (38), *slo* (encoding streptolysin O [SLO]) (38), *spyCEP* (encoding interleukin-8 [IL-8] protease) (75), *mac* (encoding an IgG endopeptidase and an inhibitor of reactive oxygen species generation) (76-78), and *sse* (encoding streptococcal secreted esterase [SSE]) (79). Selected virulence factor genes with decreased transcript levels in the isogenic $\Delta rocA$ strain include *M28_Spy0109* (encoding pilin protein) (49, 80), the *sag* operon (carrying streptolysin S biosynthesis genes) (81), *grab* (encoding protein-G-related α_2 -macroglobulin binding protein) (82), *ska*

(encoding streptokinase [SKA]) (83), and *speB* (encoding streptococcal cysteine protease B) (84).

Table 2-2 Selected proven and putative virulence factors of GAS regulated by *rocA* at mid-exponential (ME) and early-stationary (ES) growth phases.

Locus tag ^a	Gene	Function	Fold change relative to wild-type ^b	
			ME	ES
<i>M28_Spy0109</i>	<i>M28_Spy0109</i>	Pilin protein	-2.8	
<i>M28_Spy0137</i>	<i>nga</i>	NAD ⁺ -glycohydrolase	6.3	7.6
<i>M28_Spy0139</i>	<i>slo</i>	Streptolysin O	6.0	7.2
<i>M28_Spy0329</i>	<i>spyCEP</i>	IL-8 protease	38.0	
<i>M28_Spy0540</i>	<i>sagA</i>	Streptolysin S precursor	-2.7	
<i>M28_Spy0541</i>	<i>sagB</i>	Streptolysin S biosynthesis protein	-3.4	
<i>M28_Spy0542</i>	<i>sagC</i>	Streptolysin S biosynthesis protein	-3.2	
<i>M28_Spy0543</i>	<i>sagD</i>	Streptolysin S biosynthesis protein	-3.5	
<i>M28_Spy0544</i>	<i>sagE</i>	Streptolysin S self-immunity protein	-3.0	
<i>M28_Spy0545</i>	<i>sagF</i>	Streptolysin S biosynthesis protein	-2.5	
<i>M28_Spy0546</i>	<i>sagG</i>	Streptolysin S export ATP-binding protein	-3.1	
<i>M28_Spy0547</i>	<i>sagH</i>	Streptolysin S export transmembrane protein	-2.9	
<i>M28_Spy0548</i>	<i>sagI</i>	Streptolysin S export transmembrane protein	-2.7	
<i>M28_Spy0649</i>	<i>mac</i>	IgG endopeptidase and inhibitor of reactive oxygen species generation	38.1	
<i>M28_Spy1098</i>	<i>grab</i>	Protein-G related α_2 -macroglobulin-binding protein	-5.5	-8.7
<i>M28_Spy1450</i>	<i>sse</i>	Streptococcal secreted esterase	3.6	1.7
<i>M28_Spy1672</i>	<i>ska</i>	Streptokinase	-2.2	-7.4
<i>M28_Spy1675</i>	<i>sclA</i>	Collagen binding protein	19.1	4.1
<i>M28_Spy1699</i>	<i>fba</i>	Fibronectin binding protein	4.1	2.3
<i>M28_Spy1700</i>	<i>scpA</i>	C5a peptidase	4.1	3.7
<i>M28_Spy1701</i>	<i>emm</i>	IgA binding protein	1.6	
<i>M28_Spy1702</i>	<i>emm</i>	Anti-phagocytic M protein	3.5	6.0
<i>M28_Spy1703</i>	<i>mrp</i>	M-related protein		2.3
<i>M28_Spy1715</i>	<i>sfbX</i>	Fibronectin binding protein	3.4	3.0
<i>M28_Spy1716</i>	<i>sof</i>	Serum opacity factor	3.0	3.4
<i>M28_Spy1721</i>	<i>speB</i>	Streptococcal cysteine protease B		-3.2
<i>M28_Spy1884</i>	<i>hasA</i>	Hyaluronan synthase	17.2	
<i>M28_Spy1885</i>	<i>hasB</i>	UDP-glucose 6-dehydrogenase	18.8	
<i>M28_Spy1886</i>	<i>hasC</i>	UTP-glucose-1-phosphate uridylyltransferase	17.7	

^aLocus tag identified in the serotype M28 reference genome MGAS6180.

^bEmpty (blank) cells: the gene does not satisfy the *P* value and/or fold change requirement.

To assess the phenotypic effect of the differential transcript levels for selected virulence factors, a series of *in vitro* assays was performed. Compared to the parental WT strain, the isogenic $\Delta rocA$ deletion mutant strain expressed increased amounts of

immunoreactive SPN and SLO proteins (Fig. 2-5A). Additionally, compared to the parental WT strain, the isogenic $\Delta rocA$ mutant deletion strain had significantly increased SOF, SPN, SLO, and SSE secreted activity (Fig. 2-3B and 2-5B to D) and significantly decreased SKA secreted activity (Fig. 2-5E). The results are consistent with the RNA-seq data and raise the possibility that deletion of *rocA* in M28 GAS increase virulence.

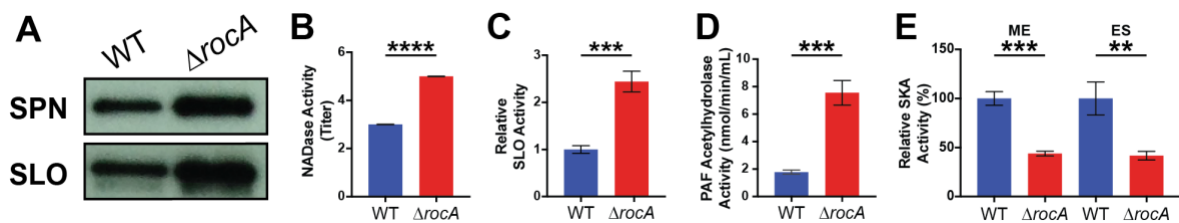


Fig. 2-5 Deletion of *rocA* significantly increases GAS virulence factor levels and activity in the culture supernatant. (A) Western immunoblot analysis of NAD⁺-glycohydrolase (SPN) and streptolysin O (SLO). (B) SPN activity. (C) SLO activity. (D) Platelet activating factor (PAF) acetylhydrolase activity. (E) SKA activity. Data are shown as mean \pm standard deviation. **, $P < 0.01$; ***, $P < 0.001$; ****, $P < 0.0001$ (Student's *t* test).

2.3.7. Deletion of *rocA* results in increased virulence in a mouse model of necrotizing myositis

Next, we hypothesized that deletion of *rocA* significantly increases M28 GAS virulence. To test this hypothesis, the virulences of the isogenic $\Delta rocA$ deletion mutant and parental WT strains were compared using a well-established mouse model of necrotizing myositis (36, 85, 86). Compared to the parental WT strain, the isogenic $\Delta rocA$ deletion mutant strain caused significantly more mortality (Fig. 2-6A) and larger lesions with more tissue destruction (Fig. 2-6B). Also, compared to infection with the parental WT strain, significantly more CFU were recovered from mouse limbs infected with the isogenic $\Delta rocA$ deletion mutant strain (Fig. 2-6C). Together, these data demonstrate that deletion of *rocA* in serotype M28 GAS significantly increases virulence.

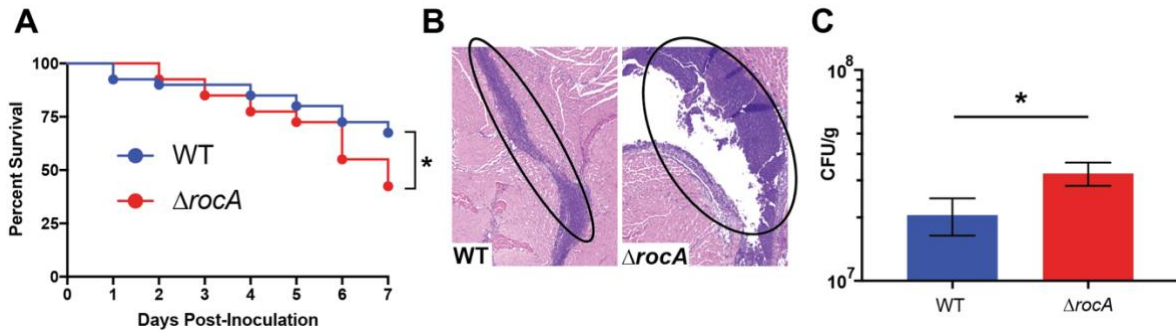


Fig. 2-6 Deletion of *rocA* increases GAS virulence in a mouse model of necrotizing myositis.

(A) Kaplan-Meier survival curve ($n = 40$ mice/strain). *, $P < 0.05$ (log rank test). (B) Representative microscopic lesions from the inoculation site of the right lower hindlimb of mice infected with the WT or $\Delta rocA$ mutant strain on day 1 postinoculation. The necrotic lesions are encompassed by black ovals. Original magnification, $\times 4$. (C) CFU/gram of tissue recovered on day 3 postinoculation ($n = 20$ mice/strain). Data are shown as mean \pm SEM. *, $P < 0.05$ (Mann-Whitney test).

2.4. Discussion

Serotype M28 GAS strains are a common cause of pharyngeal and invasive infections globally (1, 5-11). However, relatively little is known about the molecular pathogenesis of M28 strains. GAS molecular pathogenesis studies have historically used other numerically important serotypes such as M1 and M3 strains as model organisms (2). Recent whole-genome sequence analysis of 2,101 serotype M28 GAS strains recovered from large population-based studies of patients with invasive infections revealed an unexpectedly high number of missense and nonsense polymorphisms in *rocA* (GenBank accession no. MH884522 to MH884551) (Fig. 2-1), a finding that was not observed in our previous studies with M1, M59, and M89 GAS (15, 36, 37). Inactivation of *rocA* in a genetically representative serotype M28 GAS strain resulted in a substantial transcriptome change (38.8% of all GAS genes) (Fig. 2-2), including many genes encoding transcription regulators and proven or putative virulence factors. *In vitro* assays confirmed the RNA-seq results (Fig. 2-3 to 2-5), and the M28 RocA-inactivated strain was significantly more virulent in a mouse

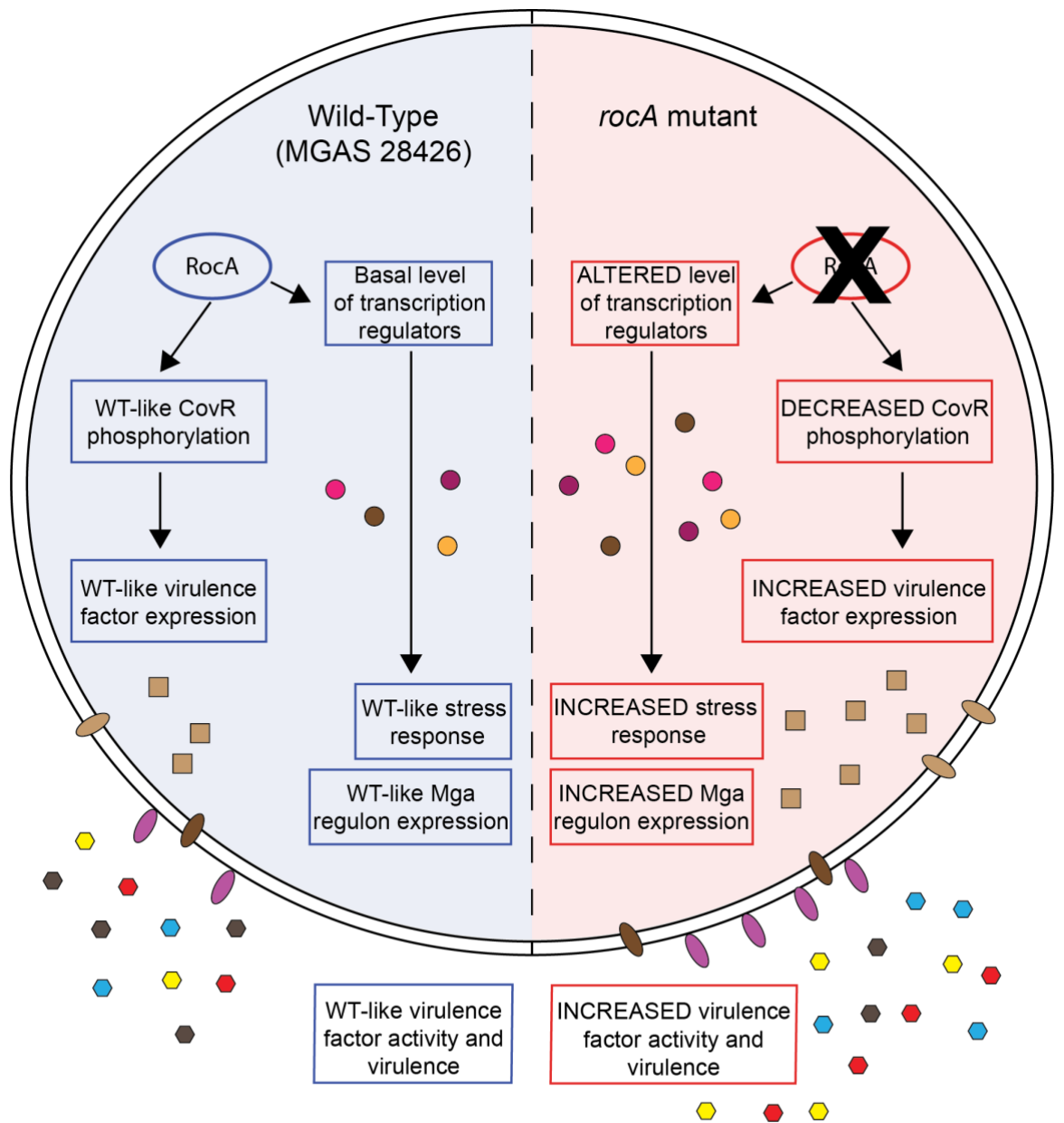


Fig. 2-7 Model of RocA contribution to the molecular pathogenesis of serotype M28 GAS.
 GAS strains with a wild-type *rocA* gene (such as MGAS28426, left panel) have a basal level of *rocA* expression, RocA-regulated genes, and a wild-type virulence phenotype. GAS strains with *rocA* mutations (such as $\Delta rocA$, right panel) have a substantially altered transcriptome that significantly increase virulence factor expression, stress response, and virulence.

model of necrotizing myositis (Fig. 2-6). Taken together, these data suggest that RocA plays a key role in M28 GAS molecular pathogenesis in human invasive infections (Fig. 2-7).

We found that deletion of *rocA* in a genetically representative serotype M28 GAS strain resulted in a very substantial transcriptome change (Fig. 2-2; see Tables B-1 and B-2 in the Appendix). Previous research on RocA has led to the publication of RocA transcriptomes from serotype M1 and M3 GAS strains (28, 32). The time point for collecting GAS cells, the culture media used, and the process of making RNA-seq libraries for the published M1 and M3 studies were very similar to those for our M28 RocA RNA-seq experiment (28, 32). However, the bioinformatic processes used for analysis in each study differed. Thus, to compare the three transcriptomes, we reanalyzed the publicly available M1 (accession number GSE97325) (32) and M3 (accession number GSE68277) (28) RocA RNA-seq data using a bioinformatics process identical to that for our M28 ME RocA RNA-seq data (see Materials and Methods). In contrast to the M1 and M3 RocA transcriptomes, we discovered a much higher number of genes directly or indirectly regulated by RocA in M28 GAS (see Table B-3 and Fig. A-2 in the Appendix) (107). At ME growth, 427 genes have significantly altered transcript levels in the serotype M28 isogenic $\Delta rocA$ deletion mutant strain, whereas only 357 and 224 genes have significantly altered transcript levels in the *rocA* deletion M1 and M3 strains, respectively (Table B-3 and Fig. A-2) (107). The substantially increased size of the M28 RocA regulon compared to those of the M1 and M3 RocA regulons may be due, in part, to the number of genes encoding transcription regulators that were differentially expressed (Fig. A-2) (107). Of the 41 transcription regulators directly or indirectly regulated by RocA in serotype M28 GAS (Table 2-1), 26 had altered transcript levels at mid-exponential growth. In comparison, RocA altered the expression of only 24

and 15 transcription regulators in the M1 and M3 strains, respectively. That is, RocA may regulate the expression of more genes in M28 GAS due to its effect on many different transcription regulators. Another possible explanation for the much smaller RocA transcriptome in M3 GAS is the experimental strategy used. The M1 and M28 RocA transcriptomes were determined by creating isogenic deletion mutant strains lacking the *rocA* gene (32). In contrast, the M3 study compared an M3 GAS strain containing the naturally occurring *rocA* mutation to an isogenic strain carrying the serotype M1 wild-type *rocA* allele (28). The naturally occurring RocA mutant protein in M3 GAS has partial RocA function when overexpressed, suggesting that M3 strains may natively retain some very limited amount of RocA activity (28, 32).

The RocA transcriptome has not been previously studied at early stationary growth phase (28, 32). In most GAS RNA-seq studies, regulators typically alter the expression of more genes at early stationary growth than at mid-exponential growth (24, 87-90). However, in M28 GAS, we discovered that *rocA* deletion significantly altered the transcript levels of fewer genes at early stationary growth phase (323 compared to 427) (Fig. 2-2C). Analysis of *rocA* expression at both growth phases identified significantly more transcripts at mid-exponential growth phase (see Fig. A-3 in the Appendix), suggesting that RocA is expressed at a higher level during early growth. Additionally, more genes encoding transcription regulators had significantly altered transcript levels at mid-exponential growth (26 at mid-exponential growth phase compared to 19 at early stationary growth phase). The two findings may, in part, explain the higher number of genes directly or indirectly regulated by RocA at mid-exponential growth phase compared to early stationary growth phase.

One possible molecular mechanism for RocA inactivation to increase M28 GAS virulence is by decreasing CovR phosphorylation via the CovRS two-component regulatory system. Spontaneous mutations in *covR* and *covS* have been identified in GAS strains recovered from animals with experimental infections and humans with invasive infections (23, 91). In general, mutations in *covR* or *covS* substantially alter the GAS transcriptome and increase strain virulence (23, 24, 92). That is, *covRS* mutations may provide a fitness advantage in some host environments. We speculate that *rocA* mutations may also be selected *in vivo* after the initial infection is established. Although *covR* and *covS* expression was not significantly altered in the M28 isogenic *rocA* deletion mutant strain (Tables B-1 and B-2), RocA increases CovR phosphorylation, which is a key step in CovRS activation (28, 30). In support, approximately 15% of the genes that are differentially expressed in the $\Delta rocA$ M28 strain are known to be regulated by CovRS in other GAS serotypes (Tables B-1 and B-2) (24). For example, RocA inactivation significantly increased *nga* and *slo* expression (Fig. 2-5). CovRS is known to regulate *nga* and *slo* (23, 24). Possibly important to the role of RocA inactivation in M28 GAS virulence, increased expression and activity of SPN and SLO was recently implicated as the central factor underlying the emergence and global spread of epidemic clade 3 M89 strains (36, 93).

Another possible molecular mechanism for RocA inactivation to increase M28 GAS virulence is by significantly altering gene expression independently of CovRS (Table 2-2). That is, RocA may directly or indirectly regulate or act as an accessory protein to additional regulatory systems in GAS. For example, the isogenic $\Delta rocA$ deletion mutant strain had significantly increased transcript levels of *mga* and Mga-regulated genes (Fig. 2-3). Sanson et al. demonstrated that a naturally occurring mutation in *mga* increased the expression of

mga and Mga-regulated genes in M59 GAS to significantly increased virulence in mice, nonhuman primates, and humans (94-96). In the *rocA*-inactivated serotype M1 and M3 GAS strains, *mga* and some genes in the Mga regulon also had increased expression (Table B-3). Possibly important to the serotype-specific effect of RocA on *mga* expression, the genes comprising the Mga regulon differ in each of the three serotypes (57). Similarly, the stress response genes *ciaHR*, *nrdR*, and *spxA2* and the arginine deiminase pathway genes *arcABCD* had significantly increased transcript levels in the $\Delta rocA$ M28 mutant strain (Fig. 2-4) (43, 47, 60,73, 74). Consistent with the RNA-seq data, the isogenic $\Delta rocA$ strain had increased resistance to acidic stress, a condition encountered in purulent lesions (69-71). The expression of *spxA2* was increased in the *rocA*-inactivated serotype M1 and M3 GAS strains (Table B-3). In comparison, the *arcABCD* genes had significantly decreased expression in the *rocA*-inactivated serotype M1 GAS strain, whereas the *arcABCD* genes had significantly increased expression in the *rocA*-inactivated serotype M3 and M28 GAS strains (Table B-3). The molecular basis for the serotype-specific regulatory activity of RocA on *arcABCD* is unknown.

Unexpectedly, the M28 $\Delta rocA$ isogenic deletion mutant had significantly decreased transcript levels of *ska* (Tables B-1 and B-2). The *ska* gene encodes streptokinase (SKA), an important virulence factor that disrupts the host fibrinolytic system (83, 97). SKA also leads to degradation of host extracellular matrix and basement membrane proteins. Whereas *ska* has significantly decreased transcript levels in the M28 $\Delta rocA$ strain, it had significantly increased transcript levels in the M1 and M3 RocA-inactivated strains (Table B-3) (28, 32). Compared to that in the WT strain, SKA activity was significantly decreased in the M28 $\Delta rocA$ strain (Fig. 2-5E). The reason for the observed serotype-specific differences in

regulation of *ska* is uncertain. To date, *ska* is known to be regulated by two different systems, FasBCAX and CovRS (42, 98-100). We detected no significant difference in expression of *fasBCA* or *covRS* in the M28 isogenic $\Delta rocA$ deletion mutant strain under the conditions studied. Our RNA-seq protocol does not capture small RNA transcripts, so *fasX*, a small RNA, could not be measured. One possible explanation for the serotype-specific regulation of *ska* is that one of the 41 differentially expressed transcription regulators, including the 14 regulators that are uniquely regulated by RocA in M28 GAS (Table 2-1 and Fig. A-2) (107), directly or indirectly regulates *ska* expression. Further studies will be needed to better understand the molecular mechanisms underlying altered expression of *ska*.

The difference in *rocA* allele frequency between M28 and other M protein serotype strains may be due to inherent genetic differences that favor a RocA-inactivated phenotype. For example, most serotype M1 and M59 GAS strains are encapsulated (15, 37), but virtually all M28 and epidemic clade 3 M89 GAS are capsule deficient (93, 101). Epidemic clade 3 M89 GAS strains lack the *hasABC* locus, which is required for hyaluronic acid capsule production (93). M28 GAS strains have a one-nucleotide frameshifting insertion in *hasA* that results in a truncated HasA protein without enzymatic activity (GenBank accession no. MH884522 to MH884551) (101). Thus, although the M28 *rocA* isogenic deletion mutant strain demonstrated significantly increased *hasABC* transcript levels (Table 2-2), virtually all M28 strains are incapable of capsule biosynthesis (see Fig. A-4 in the Appendix) (36). Additionally, virtually all serotype M28 GAS strains have a missense mutation in *mac*, the gene encoding Mac, an IgG endopeptidase and inhibitor of reactive oxygen species generation (76-78). The missense mutation results in a loss of Mac IgG endopeptidase activity (77). The two phenotypic characteristics, possibly in combination with other, yet-

unrecognized genomic factors, may predispose serotype M28, and also M89, GAS strains to select for *rocA* polymorphisms that increase fitness in the invasive infection environment. Additionally, the preponderance of missense mutations in the transmembrane domains of RocA in serotype M28 GAS compared to the other serotype is of particular interest (Fig. A-1). As the transmembrane domains are crucial for the regulatory activity of RocA, detailed analyses of the missense mutations located in the transmembrane domains are warranted.

In summary, our study shows that in serotype M28 GAS, RocA directly or indirectly regulates a substantial portion of the GAS transcriptome (38.8% of all GAS genes), including many transcription regulators and proven or putative virulence factors. The number of genes and transcription regulators directly or indirectly regulated by RocA in serotype M28 GAS is greater than that observed in RocA studies performed with serotype M1 and M3 GAS. The M28 RocA-inactivated strain was significantly more virulent in a mouse model of necrotizing myositis. Taken together, these data suggest that RocA plays a key role in M28 GAS molecular pathogenesis and thus may contribute to the high number of naturally occurring polymorphisms found in M28 strains recovered from human invasive infections. Our findings underscore the critical need for molecular pathogenesis research efforts to study many different microbial strains from many different genetic backgrounds (i.e., within the same serotype and across different serotypes).

2.5. Materials and methods

2.5.1. Determination of SNPs in *rocA* in serotype M28 GAS strains

Whole-genome sequence analysis of the 2,101 serotype M28 GAS strains was previously performed (GenBank accession no. MH884522 to MH884551). Six strains are distant outliers and were excluded from further analysis. Among the remaining 2,095 M28

strains, 20,135 single nucleotide polymorphism (SNP) sites were identified across the core genome that spans 1,735,432 bp. Assuming that SNP sites are randomly distributed across the core genome, 1 SNP site is expected to occur every 86 bp. Given a random distribution, approximately 16 SNP sites are expected to occur in the *rocA* coding and upstream regulatory region that spans 1,374 bp. As previously described, Fisher's exact test was used to demonstrate that significantly more SNP sites were identified in *rocA* than would be expected to occur by random chance (17, 36, 58).

2.5.2. Construction of an isogenic *rocA* deletion strain

Strain MGAS28426 was selected as the serotype M28 parental wild-type (WT) strain because it is genetically representative of serotype M28 GAS strains and has a wild-type allele for all major global transcription regulators. The isogenic *rocA* deletion ($\Delta rocA$) mutant strain was constructed by deleting the entire open reading frame of *rocA*, as previously described (38). Sequences for primers used are listed in Table B-4 in the Appendix. Whole-genome sequence analysis of the isogenic $\Delta rocA$ mutant strain confirmed that no spurious mutations were introduced during strain construction.

2.5.3. RNA-seq analysis

The WT and isogenic $\Delta rocA$ mutant strains were grown in triplicate in THY with 5% CO₂ at 37°C to mid-exponential (ME) (OD₆₀₀ = 0.5) and early stationary (ES) (OD₆₀₀ = 1.65) growth phases as previously described (94, 95). RNAprotect Bacteria Reagent (Qiagen Inc., Germantown, MD) was added (2:1), and cells were lysed by ballistic disintegration (FastPrep-96 instrument and lysing matrix B [MP Biomedicals, Santa Ana, CA]). RNA was extracted using standard methods (RNeasy kit [Qiagen Inc., Germantown, MD]), and RNA quality and quantity were assessed (Agilent 2100 Bioanalyzer [Agilent Technologies, Santa

Clara, CA] and Qubit [Invitrogen, Carlsbad, CA]). RNA-seq libraries were prepared using standard methods (ScriptSeq Complete kit [Epicentre, Madison, WI]) and sequenced with an Illumina NextSeq Instrument (Illumina, San Diego, CA) using the default settings.

On average, we obtained 39.5 million reads/sample for the 12 samples (WT and isogenic *ΔrocA* mutant strains grown in triplicate and collected at ME and ES growth phases). Reads were mapped to the genome of serotype M28 GAS reference strain MGAS6180 (12), and differential transcript analysis was performed with CLC Genomics Workbench 10.5 (Qiagen Inc., Germantown, MD) using the default settings. Genes encoding rRNA, tRNA, phage, and mobile genetic elements were excluded from analysis, as there are limitations in read mapping to repetitive sequences found within the aforementioned elements. Genes with an absolute transcript change of ≥ 1.5 -fold and a *P* value of < 0.05 after Baggerly's test with Bonferroni's correction for multiple comparisons were considered to be significantly differentially expressed.

RocA transcriptomes from M1 and M3 GAS strains have been published (28, 32). The time point for collecting the GAS cells at ME growth phase, the culture media used, and the process of making the RNA-seq libraries in the published M1 and M3 studies were very similar to those used in our M28 RocA RNA-seq experiment conducted at ME growth phase. However, the bioinformatics process used for analysis in each study differed. To compare the M1, M3, and M28 RocA transcriptomes, publicly available M1 and M3 RNA-seq sequencing data (28, 32) were reanalyzed with a bioinformatics process identical to that described above. That this, to compare the RocA transcriptomes of the M1, M3, and M28 GAS strains, we used a common bioinformatics process to analyze the three RNA-seq data sets. Briefly, the publicly available RNA-seq reads for the M1 (accession number

GSE97325) (32) and M3 (accession number GSE68277) (28) GAS strains were downloaded and mapped to the serotype M1 MGAS5005 (102) and M3 MGAS315 (103) reference genomes, respectively. Differential transcript analysis was performed with CLC Genomics Workbench 10.5 (Qiagen Inc., Germantown, MD) using the default settings. Genes encoding rRNA, tRNA, phage, and mobile genetic elements were excluded, as there are limitations in the read mapping to repetitive sequences found within the aforementioned elements. Genes not present in the M28 reference strain also were excluded from analysis. Genes with an absolute transcript change of ≥ 1.5 -fold and a P value of < 0.05 after Baggerly's test with Bonferroni's correction for multiple comparisons were considered to be significantly differentially expressed. The differentially expressed genes were then compared across the three strains.

2.5.4. SOF activity assay

Serum opacity factor (SOF) activity in the culture supernatants was assayed as previously described (68), with the modification that samples were serially diluted 2-fold in phosphate-buffered saline (PBS) with 1% sodium dodecyl sulfate (SDS) before incubation with horse serum (1:10 sample-to-horse-serum volume). PBS with 1% SDS was used as a negative control. Dilutions were determined to be positive for serum opacity factor activity at an absorbance at 405 nm of greater than 0.8 (104). Mean titers of four biological replicates were compared using Student's t test (Prism 7 [GraphPad, La Jolla, CA]), with a P value of < 0.05 considered to be statistically significant.

2.5.5. Growth under acidic conditions

For growth under acidic conditions, THY supplemented with 0.1 M 2-(*N*-morpholino)ethanesulfonic acid (MES) (pH 6.0) (Sigma-Aldrich, St. Louis, MO) was used.

THY supplemented with 0.1 M HEPES (pH 7.5) (Sigma-Aldrich, St. Louis, MO) was used to determine the baseline effects of a buffered medium on GAS strain growth (29). For CFU, cultures grown in quadruplicate were harvested at 3 h, serially diluted 10-fold, and plated onto THY agar supplemented with 5% sheep blood. Colonies were counted after incubation overnight. The mean CFU of four biological replicates were compared using the Mann-Whitney test (Prism 7 [GraphPad, La Jolla, CA]), with a *P* value of < 0.05 considered to be statistically significant.

2.5.6. Western immunoblot analysis of SPN and SLO in culture supernatant

GAS strains were grown to mid-exponential growth phase and pelleted by centrifugation, and supernatants were assessed for the presence of immunoreactive NAD⁺-glycohydrolase (SPN) and streptolysin O (SLO) as described previously (38).

2.5.7. SPN and SLO activity assays

GAS strains were grown to mid-exponential growth phase and pelleted by centrifugation, and supernatants were assayed for NAD⁺-glycohydrolase (SPN) and streptolysin O (SLO) activity as previously described (85). The mean titers (SPN) and activities (SLO) of three biological replicates were compared using Student's *t* test (Prism 7 [GraphPad, La Jolla, CA]), with a *P* value of < 0.05 considered to be statistically significant.

2.5.8. PAF acetylhydrolase activity assay

Streptococcal secreted esterase (SSE) is a known secreted GAS virulence factor that hydrolyzes platelet-activating factor (PAF) (79). Thus, SSE activity in culture supernatants collected at mid-exponential growth phase was assayed with the PAF acetylhydrolase assay kit (Cayman Chemical, Ann Arbor, MI), according to the manufacturer's instructions with minor modifications (31). GAS strains were grown in triplicate in THY to mid-exponential

growth phase. Supernatants were collected by centrifugation at 4,000 rpm for 10 min. The supernatant (10 μ l) was added to assay buffer 2 (5 μ l) and incubated with 2-thio-PAF (200 μ l) at room temperature for 30 min. 5,5-Dithiobis(2-nitrobenzoic acid) (10 μ l) was added to each sample, mixed, and incubated for 1 min at room temperature. The absorbance of each sample at 412 nm was measured and used to calculate the PAF acetylhydrolase activity. Fresh THY was used as a negative control. The mean activities of three biological replicates were compared using Student's *t* test (Prism 7 [GraphPad, La Jolla, CA]), with a *P* value of < 0.05 considered to be statistically significant.

2.5.9. SKA activity assay

GAS strains were grown to mid-exponential and early stationary growth phases and pelleted by centrifugation, and cell-free supernatants were assayed for streptokinase (SKA) activity as previously described (99). Activity was determined as the change in absorbance overtime from the initial time point to maximum absorbance at 405 nm. The mean relative activities of three biological replicates were compared using Student's *t* test (Prism 7 [GraphPad, La Jolla, CA]), with a *P* value of < 0.05 considered to be statistically significant.

2.5.10. Mouse model of necrotizing myositis

Mouse necrotizing myositis studies were performed as previously described (36, 85, 86). Immunocompetent 4-week-old female CD1 mice (Envigo Laboratories, Houston, TX) were randomly assigned to treatment groups and inoculated in the right lower hindlimb with 5×10^8 CFU of each bacterial strain in 100 μ l PBS ($n = 40$ mice/strain). Mice were monitored at least once daily, and mortality was determined using internationally recognized criteria (105). Survival was compared using the log rank test (Prism 7 [GraphPad, La Jolla, CA]), with a *P* value of < 0.05 considered statistically significant. For histopathological evaluation,

mice were sacrificed on day 1 postinoculation, and limbs were processed by standard methods (86). For quantitative culture ($n = 20$ mice/strain), mice were sacrificed on day 3 postinoculation. Infected limbs were amputated, placed in tared tubes containing sterile PBS, weighed, and homogenized. Tenfold serial dilutions were grown overnight on THY agar supplemented with 5% sheep blood, and CFU were counted. Mean CFU were compared by the Mann-Whitney test (Prism 7 [GraphPad, La Jolla, CA]), with a P value of < 0.05 considered statistically significant. All animal experiments were approved by the Institutional Animal Care and Use Committee of the Houston Methodist Research Institute. Sample sizes for each experiment were determined using a power calculation.

2.5.11. Hyaluronic acid capsule assay

GAS strains were grown in triplicate in THY to mid-exponential growth phase. Cells were collected from 10 ml of culture by centrifugation at 4,000 rpm for 10 min, and the supernatant was discarded. The cells were resuspended in a 1:1 (vol/vol) mixture of water and chloroform (1 ml) and vortexed for 30 s. The mixture was centrifuged (13,200 rpm, 10 min), and the resulting aqueous phase was used to assay for the presence of hyaluronic acid capsule using the hyaluronic acid quantitative test kit (Corgenix, Broomfield, CO) according to the manufacturer's instructions. MGAS2221, a serotype M1 GAS strain whose capsule production is well documented (38), was used as a positive control.

2.5.12. Accession number(s)

The serotype M28 RNA-seq data have been deposited at the National Center for Biotechnology Information (NCBI) under BioProject no. PRJNA470894.

2.6. References

1. Cunningham MW. 2000. Pathogenesis of group A streptococcal infections. *Clin Microbiol Rev* 13:470-511.
2. Olsen RJ, Musser JM. 2010. Molecular pathogenesis of necrotizing fasciitis. *Annu Rev Pathol Mech Dis* 5:1-31.
3. Walker MJ, Barnett TC, McArthur JD, Cole JN, Gillen CM, et al. 2014. Disease manifestations and pathogenic mechanisms of group A *Streptococcus*. *Clin Microbiol Rev* 27:264-301.
4. Carapetis JR, Steer AC, Mulholland EK, Weber M. 2005. The global burden of group A streptococcal diseases. *Lancet Infect Dis* 5:685-694.
5. Steer AC, Law I, Matatolu L, Beall BW, Carapetis JR. 2009. Global *emm* type distribution of group A streptococci: systematic review and implications for vaccine development. *Lancet Infect Dis* 9:611-616.
6. Chochua S, Metcalf BJ, Li Z, Rivers J, Mathis S, et al. 2017. Population and whole genome sequence based characterization of invasive group A streptococci recovered in the United States during 2015. *mBio* 8:e01422-17.
7. Colman G, Tanna A, Efstratiou A, Gaworzewska E. 1993. The serotypes of *Streptococcus pyogenes* present in Britain during 1980-1990 and their association with disease. *J Med Microbiol* 39:165-178.
8. Eriksson BKG, Norgen M, McGregor K, Spratt BG, Henriques-Normark B. 2003. Group A streptococcal infections in Sweden: a comparative study of invasive and noninvasive infections and analysis of dominant T28 *emm28* isolates. *Clin Infect Dis* 37:1189-1193.

9. Gaworzewska E, Colman G. 1988. Changes in the pattern of infection caused by *Streptococcus pyogenes*. *Epidem Inf* 100:257-269.
10. Tyrrell GJ, Lovgren M, Forwick B, Hoe NP, Musser JM, et al. 2002. M types of group A streptococcal isolates submitted to the national centre for Streptococcus (Canada) from 1993 to 1999. *J Clin Microbiol* 40:4466-4471.
11. Vlamincx B, van Pelt W, Schouls L, van Silfhout A, Elzenaar C, et al. 2004. Epidemiological features of invasive and noninvasive group A streptococcal disease in the Netherlands, 1992-1996. *Eur J Clin Microbiol Infect Dis* 23:434-444.
12. Green NM, Zhang S, Porcella SF, Nagiec MJ, Barbian KD, et al. 2005. Genome sequence of a serotype M28 strain of group A *Streptococcus*: potential new insights into puerperal sepsis and bacterial disease specificity. *J Infect Dis* 192:760-770.
13. Green NM, Beres SB, Graviss EA, Allison JE, McGeer AJ, et al. 2005. Genetic diversity among type *emm28* group A *Streptococcus* strains causing invasive infections and pharyngitis. *J Clin Microbiol* 43:4083-4091.
14. Chuang I, Van Beneden C, Beall B, Schuchat A, Active Bacterial Core Surveillance/Emerging Infections Program Network. 2002. Population-based surveillance for postpartum invasive group A streptococcus infection, 1995-2000. *Clin Infect Dis* 35:665-670.
15. Nasser W, Beres SB, Olsen RJ, Dean MA, Rice KA, et al. 2014. Evolutionary pathway to increased virulence and epidemic group A *Streptococcus* disease derived from 3,615 genome sequences. *Proc Natl Acad Sci U S A* 111:E1768-1776.

16. Virtaneva K, Porcella SF, Graham MR, Ireland RM, Johnson CA, et al. 2005. Longitudinal analysis of the group A *Streptococcus* transcriptome in experimental pharyngitis in cynomolgus macaques. *Proc Natl Acad Sci U S A* 102:9014-9019.
17. Beres SB, Carroll RK, Shea PR, Sitkiewicz I, Martinez-Gutierrez JC, et al. 2010. Molecular complexity of successive bacterial epidemics deconvoluted by comparative pathogenomics. *Proc Natl Acad Sci U S A* 107:4371-4376.
18. Beres SB, Sylva GL, Sturdevant DE, Granville CN, Liu M, et al. 2004. Genome-wide molecular dissection of serotype M3 group A *Streptococcus* strains causing two epidemics of invasive infections. *Proc Natl Acad Sci U S A* 101:11833-11838.
19. Rodriguez-Ortega MJ, Norais N, Bensi G, Liberatori S, Capo S, et al. 2006. Characterization and identification of vaccine candidate proteins through analysis of the group A *Streptococcus* surface proteome. *Nat Biotechnol* 24:191-197.
20. McNamara C, Zinkernagel AS, Macheboeuf P, Cunningham MW, Nizet V, et al. 2008. Coiled-coil irregularities and instabilities in group A *Streptococcus* are required for virulence. *Science* 319:1405-1408.
21. Macheboeuf P, Buffalo C, Fu C, Zinkernagel AS, Cole JN, et al. 2011. Streptococcal M1 protein constructs a pathological host fibrinogen network. *Nature* 472:64-68.
22. Biswas I, Scott JR. 2003. Identification of *rocA*, a positive regulator of *covR* expression in the group A streptococcus. *J Bacteriol* 185:3081-3090.
23. Sumbly P, Whitney AR, Graviss EA, DeLeo FR, Musser JM. 2006. Genome-wide analysis of group A streptococci reveals a mutation that modulates global phenotype and disease specificity. *PLoS Pathog* 2:e5.

24. Shelburne SA, Olsen RJ, Suber B, Sahasrabhojane P, Sumbly P, et al. 2010. A combination of independent transcriptional regulators shapes bacterial virulence gene expression during infection. *PLoS Pathog* 6:e1000817.
25. Lynskey NN, Goulding D, Gierula M, Turner CE, Dougan G, et al. 2013. RocA truncation underpins hyper-encapsulation, carriage longevity and transmissibility of serotype M18 group A streptococci. *PLoS Pathog* 9:e1003842.
26. Lynskey NN, Turner CE, Heng LS, Sriskandan S. 2015. A truncation in the regulator RocA underlies heightened capsule expression in serotype M3 group A streptococci. *Infect Immun* 83:1732-1733.
27. Miller EW, Pflughoeft KJ, Sumbly P. 2015. Reply to "A truncation in the regulator RocA underlies heightened capsule expression in serotype M3 group A streptococci". *Infect Immun* 83:1734.
28. Miller EW, Danger JL, Ramalinga AB, Horstmann N, Shelburne SA, et al. 2015. Regulatory rewiring confers serotype-specific hyper-virulence in the human pathogen group A *Streptococcus*. *Mol Microbiol* 98:473-489.
29. Paluscio E. 2015. Adaptive mechanisms to niche remodeling in *Streptococcus pyogenes*. PhD thesis. Washington University in St. Louis, St. Louis, MO.
30. Zhu L, Olsen RJ, Horstmann N, Shelburne SA, Fan J, et al. 2016. Intergenic variable-number tandem-repeat polymorphism upstream of *rocA* alters toxin production and enhances virulence in *Streptococcus pyogenes*. *Infect Immun* 84:2086-2093.
31. Feng W, Minor D, Liu M, Li J, Ishaq SL, et al. 2017. Null mutations of group A *Streptococcus* orphan kinase RocA: selection in mouse infection and comparison

- with CovS mutations in alteration of *in vitro* and *in vivo* protease SpeB expression and virulence. *Infect Immun* 85:e00790-16.
32. Jain I, Miller EW, Danger JL, Pflughoeft KJ, Sumbly P. 2017. RocA is an accessory protein to the virulence-regulating CovRS two-component system in group A *Streptococcus*. *Infect Immun* 85:e00274-17.
 33. Yoshida H, Ishigaki Y, Takizawa A, Moro K, Kishi Y, et al. 2015. Comparative genomics of the mucoid and nonmucoid strains of *Streptococcus pyogenes*, isolated from the same patient with streptococcal meningitis. *Genome Announc* 3:e0021-15.
 34. Ikebe T, Matsumura T, Nihonmatsu H, Ohya H, Okuno R, et al. 2016. Spontaneous mutations in *Streptococcus pyogenes* isolates from streptococcal toxic shock syndrome patients play roles in virulence. *Sci Rep* 6:28761.
 35. Sarkar P, Sumbly P. 2017. Regulatory gene mutation: a driving force behind group A *Streptococcus* strain- and serotype-specific variation. *Mol Microbiol* 103:576-589.
 36. Beres SB, Kachroo P, Nasser W, Olsen RJ, Zhu L, et al. 2016. Transcriptome remodeling contributes to epidemic disease caused by the human pathogen *Streptococcus pyogenes*. *mBio* 7:e00403-16.
 37. Fittipaldi N, Beres SB, Olsen RJ, Kapur V, Shea PR, et al. 2012. Full-genome dissection of an epidemic of severe invasive disease caused by a hypervirulent, recently emerged clone of group A *Streptococcus*. *Am J Pathol* 180:1522-1534.

38. Zhu L, Olsen RJ, Nasser W, Beres SB, Vuopio J, et al. 2015. A molecular trigger for intercontinental epidemics of group A *Streptococcus*. *J Clin Invest* 125:3545-3559.
39. Mashburn-Warren L, Morrison DA, Federle MJ. 2012. The cryptic competence pathway in *Streptococcus pyogenes* is controlled by a peptide pheromone. *J Bacteriol* 194:4589-4600.
40. Fogg GC, Caparon MG. 1997. Constitutive expression of fibronectin binding in *Streptococcus pyogenes* as a result of anaerobic activation of *rofA*. *J Bacteriol* 179:6172-6180.
41. Ravcheev DA, Best AA, Sernova NV, Kazanov MD, Novichkov PS, et al. 2013. Genomic reconstruction of transcriptional regulatory networks in lactic acid bacteria. *BMC Genomics* 14:94.
42. Cao TN, Liu Z, Cao TH, Pflughoeft KJ, Trevino J, et al. 2014. Natural disruption of two regulatory networks in serotype M3 group A *Streptococcus* isolates contributes to the virulence factor profile of this hypervirulent serotype. *Infect Immun* 82:1744-1754.
43. Zhang Y, Okada R, Isaka M, Tatsuno I, Isobe K-I, et al. 2015. Analysis of the roles of NrdR and DnaB from *Streptococcus pyogenes* in response to host defense. *APMIS* 123:252-259.
44. Siemens N, Fiedler T, Normann J, Klein J, Munch R, et al. 2012. Effects of the ERES pathogenicity region regulator Ralp3 on *Streptococcus pyogenes* serotype M49 virulence factor expression. *J Bacteriol* 194:3618-3626.

45. Vega LA, Valdes KM, Sundar GS, Belew AT, Islam E, et al. 2017. The transcriptional regulator CpsY is important for innate immune evasion in *Streptococcus pyogenes*. *Infect Immun* 85:e00925-16.
46. Wescombe PA, Tagg JR. 2003. Purification and characterization of streptin, a type A1 lantibiotic produced by *Streptococcus pyogenes*. *Appl Environ Microb* 69:2737-2747.
47. Tatsuno I, Isaka M, Okada R, Zhang Y, Hasegawa T. 2014. Relevance of the two-component sensor protein CiaH to acid and oxidative stress responses in *Streptococcus pyogenes*. *BMC Research Notes* 7:189.
48. Leday TV, Gold KM, Kinkel TL, Roberts SA, Scott JR, et al. 2008. TrxR, a new CovR-repressed response regulator that activates the Mga virulence regulon in group A streptococcus. *Infect Immun* 76:4659-4668.
49. Flores AR, Olsen RJ, Cantu C, Pallister KB, Guerra FE, et al. 2017. Increased pilus production conferred by a naturally occurring mutation alters host-pathogen interaction in favor of carriage in *Streptococcus pyogenes*. *Infect Immun* 85:e00949-16.
50. Sitkiewicz I, Musser JM. 2017. Deletion of *atoR* from *Streptococcus pyogenes* results in hypervirulence in a mouse model of sepsis and is LuxS independent. *Pol J Microbiol* 66:17-24.
51. Loughman JA, Caparon MG. 2007. Comparative functional analysis of the *lac* operons in *Streptococcus pyogenes*. *Mol Microbiol* 64:269-280.

52. Young CA, Gordon LD, Fang Z, Holder RC, Reid SD. 2015. Copper tolerance and characterization of a copper-responsive operon, *copYAZ*, in an MIT1 clinical strain of *Streptococcus pyogenes*. *J Bacteriol* 197:2580-2592.
53. Malke H, Steiner K, McShan WM, Ferretti JJ. 2006. Linking the nutritional status of *Streptococcus pyogenes* to alteration of transcriptional gene expression: the action of CodY and RelA. *Int J Med Microbiol* 296:259-275.
54. Reid SD, Chaussee MS, Doern CD, Chaussee MA, Montgomery AG, et al. 2006. Inactivation of the group A *Streptococcus* regulator *srv* results in chromosome wide reduction of transcript levels, and changes in extracellular levels of Sic and SpeB. *FEMS Immunol Med Microbiol* 48:283-292.
55. Namprachan-Frantz P, Rowe HM, Runft DL, Neely MN. 2014. Transcriptional analysis of the *Streptococcus pyogenes* salivaricin locus. *J Bacteriol* 196:604-613.
56. Ribardo DA, McIver KS. 2006. Defining the Mga regulon: comparative transcriptome analysis reveals both direct and indirect regulation by Mga in the group A streptococcus. *Mol Microbiol* 62:491-508.
57. Voyich JM, Sturdevant DE, Braughton KR, Kobayashi SD, Lei B, et al. 2003. Genome-wide protective response used by group A *Streptococcus* to evade destruction by human polymorphonuclear leukocytes. *Proc Natl Acad Sci U S A* 100:1996-2001.
58. Olsen RJ, Laucirica DR, Watkins ME, Feske ML, Garcia-Bustillos JR, et al. 2012. Polymorphisms in regulator of protease B (RopB) alter disease phenotype and strain virulence of serotype M3 group A *Streptococcus*. *J Infect Dis* 204:1719-1729.

59. Derre I, Rapoport G, Msadek T. 1999. CtsR, a novel regulator of stress and heat shock response, controls *clp* and molecular chaperone gene expression in Gram-positive bacteria. *Mol Microbiol* 31:117-131.
60. Port GC, Cusumano ZT, Tumminello PR, Caparon MG. 2017. SpxA1 and SpxA2 act coordinately to fine-tune stress responses and virulence in *Streptococcus pyogenes*. *mBio* 8:e00288-17.
61. Lukomski S, Nakashima K, Abdi I, Cipriano VJ, Ireland RM, et al. 2000. Identification and characterization of the *scl* gene encoding a group A *Streptococcus* extracellular protein virulence factor with similarity to human collagen. *Infect Immun* 68:6542-6553.
62. Terao Y, Kawabata S, Kunitomo E, Murakami J, Nakagawa I, et al. 2001. Fba, a novel fibronectin-binding protein from *Streptococcus pyogenes*, promotes bacterial entry into epithelial cells, and the *fba* gene is positively transcribed under the Mga regulator. *Mol Microbiol* 42:75-86.
63. Wexler DE, Chenoweth DE, Cleary PP. 1985. Mechanism of action of the group A streptococcal C5a inactivator. *Proc Natl Acad Sci U S A* 82:8144-8148.
64. Stenberg L, O'Toole P, Lindahl G. 1992. Many group A streptococcal strains express two different immunoglobulin-binding proteins, encoded by closely linked genes: characterization of the proteins expressed by four strains of different M-type. *Mol Microbiol* 6:1185-1194.
65. Smeesters PR, McMillan DJ, Sriprakash KS. 2010. The streptococcal M protein: a highly versatile molecule. *Trends Microbiol* 18:275-282.

66. Courtney HS, Hasty DL, Dale JB. 2006. Anti-phagocytic mechanisms of *Streptococcus pyogenes*: binding of fibrinogen to M-related protein. *Mol Microbiol* 59:936-947.
67. Jeng A, Sakota V, Li Z, Datta V, Beall B, et al. 2003. Molecular genetic analysis of a group A *Streptococcus* operon encoding serum opacity factor and a novel fibronectin-binding protein, SfbX. *J Bacteriol* 185:1208-1217.
68. Zhu L, Olsen RJ, Musser JM. 2017. Opacification domain of serum opacity factor inhibits beta-hemolysis and contributes to virulence of *Streptococcus pyogenes*. *mSphere* 2:e00147-17.
69. Nekoofar MH, Namazikhah MS, Sheykhrezae MS, Mohammadi MM, Kazemi A, et al. 2009. pH of pus collected from periapical abscesses. *Int Endod J* 42:534-538.
70. Bryant RE, Mazza JA. 1989. Effect of the abscess environment on the antimicrobial activity of ciprofloxacin. *Am J Med* 87:23S-27S.
71. Wiese KG. 1994. Electrolyte concentration, real and osmotic pressure in abscesses. *Zentralbl Chir* 119:54-59.
72. Degnan BA, Fontaine MC, Doebereiner AH, Lee JJ, Mastroeni P, et al. 2000. Characterization of an isogenic mutant of *Streptococcus pyogenes* Manfredo lacking the ability to make streptococcal acid glycoprotein. *Infect Immun* 68:2441-2448.
73. Cusumano ZT, Watson ME, Jr., Caparon MG. 2014. *Streptococcus pyogenes* arginine and citrulline catabolism promotes infection and modulates innate immunity. *Infect Immun* 82:233-242.

74. Cusumano ZT, Caparon MG. 2015. Citrulline protects *Streptococcus pyogenes* from acid stress using the arginine deiminase pathway and the F1Fo-ATPase. *J Bacteriol* 197:1288-1296.
75. Edwards RJ, Taylor GW, Ferguson M, Murray S, Rendell N, et al. 2005. Specific C-terminal cleavage and inactivation of interleukin-8 by invasive disease isolates of *Streptococcus pyogenes*. *J Infect Dis* 192:783-790.
76. von Pawel-Rammingen U, Johansson BP, Bjorck L. 2002. IdeS, a novel streptococcal cysteine proteinase with unique specificity for immunoglobulin G. *EMBO J* 21:1607-1615.
77. Soderberg JJ, Engstrom P, von Pawel-Rammingen U. 2008. The intrinsic immunoglobulin G endopeptidase activity of streptococcal Mac-2 proteins implies a unique role for the enzymatically impaired Mac-2 protein of M28 serotype strains. *Infect Immun* 76:2183-2188.
78. Lei B, DeLeo FR, Reid SD, Voyich JM, Magoun L, et al. 2002. Opsonophagocytosis-inhibiting Mac protein of group A *Streptococcus*: identification and characteristics of two gene complexes. *Infect Immun* 70:6880-6890.
79. Liu M, Zhu H, Li J, Garcia CC, Feng W, et al. 2012. Group A *Streptococcus* secreted esterase hydrolyzes platelet-activating factor to impede neutrophil recruitment and facilitate innate immune evasion. *PLoS Pathog* 8:e1002624.
80. Calfee G, Danger JL, Jain I, Miller EW, Sarkar P, et al. 2018. Identification and characterization of serotype-specific variation in group A *Streptococcus* pilus expression. *Infect Immun* 86:e00792-17.

81. Nizet V. 2002. Streptococcal beta-hemolysins: genetics and role in disease pathogenesis. *Trends Microbiol* 10:575-580.
82. Rasmussen M, Muller H-P, Bjorck L. 1999. Protein GRAB of *Streptococcus pyogenes* regulates proteolysis at the bacterial surface by binding alpha2-macroglobulin. *J Biol Chem* 274:15336-15344.
83. Huang T-T, Malke H, Ferretti JJ. 1989. Heterogeneity of the streptokinase gene in group A streptococci. *Infect Immun* 57:502-506.
84. Olsen RJ, Raghuram A, Cantu C, Hartman MH, Jimenez FE, et al. 2015. The majority of 9,729 group A streptococcus strains causing disease secrete SpeB cysteine protease: pathogenesis implications. *Infect Immun* 83:4750-4758.
85. Zhu L, Olsen RJ, Lee JD, Porter AR, DeLeo FR, et al. 2017. Contribution of secreted NADase and streptolysin O to the pathogenesis of epidemic serotype M1 *Streptococcus pyogenes* infections. *Am J Pathol* 187:605-613.
86. Olsen RJ, Sitkiewicz I, Ayeras AA, Gonulal VE, Cantu C, et al. 2010. Decreased necrotizing fasciitis capacity caused by a single nucleotide mutation that alters a multiple gene virulence axis. *Proc Natl Acad Sci U S A* 107:888-893.
87. Eraso JM, Olsen RJ, Beres SB, Kachroo P, Porter AR, et al. 2016. Genomic landscape of intrahost variation in group A *Streptococcus*: repeated and abundant mutational inactivation of the *fabT* gene encoding a regulator of fatty acid synthesis. *Infect Immun* 84:3268-3281.
88. Flores AR, Jewell BE, Yelamanchili D, Olsen RJ, Musser JM. 2015. A single amino acid replacement in the sensor kinase LiaS contributes to a carrier phenotype in group A *Streptococcus*. *Infect Immun* 83:4237-4246.

89. Graham MR, Smoot LM, Lux Migiliaccio CA, Virtaneva K, Sturdevant DE, et al. 2002. Virulence control in group A *Streptococcus* by a two-component gene regulatory system: global expression profiling and *in vivo* infection modeling. Proc Natl Acad Sci U S A 99:13855-13860.
90. Voyich JM, Braughton KR, Sturdevant DE, Vuong C, Kobayashi SD, et al. 2004. Engagement of the pathogen survival response used by group A *Streptococcus* to avert destruction by innate host defense. J Immunol 173:1194-1201.
91. Li J, Liu G, Feng W, Zhou Y, Liu M, et al. 2014. Neutrophils select hypervirulent CovRS mutants of MIT1 group A *Streptococcus* during subcutaneous infection of mice. Infect Immun 82:1579-1590.
92. Horstmann N, Saldana M, Sahasrabhojane P, Yao H, Su X, et al. 2014. Dual-site phosphorylation of the control of virulence regulator impacts group a streptococcal global gene expression and pathogenesis. PLoS Pathog 10:e1004088.
93. Zhu L, Olsen RJ, Nasser W, de la Riva Morales I, Musser JM. 2015. Trading capsule for increased cytotoxin production: contribution to virulence of a newly emerged clade of *emm89 Streptococcus pyogenes*. mBio 6:e01378-15.
94. Sanson M, O'Neill BE, Kachroo P, Anderson JR, Flores AR, et al. 2015. A naturally occurring single amino acid replacement in multiple gene regulator of group A streptococcus significantly increases virulence. Am J Pathol 185:462-471.
95. Sanson M, Makthal N, Gavagan M, Cantu C, Olsen RJ, et al. 2015. Phosphorylation events in the multiple gene regulator of group A *Streptococcus* significantly influence global gene expression and virulence. Infect Immun 83:2382-2395.

96. Fittipaldi N, Tyrrell GJ, Low DE, Martin I, Lin D, et al. 2013. Integrated whole-genome sequencing and temporospatial analysis of a continuing group A *Streptococcus* epidemic. *Emerg Microbes Infect* 2:e13.
97. Sun H, Xu Y, Sitkiewicz I, Ma Y, Wang X, et al. 2012. Inhibitor of streptokinase gene expression improves survival after group A streptococcus infection in mice. *Proc Natl Acad Sci U S A* 109:3469-3474.
98. Churchward G, Bates C, Gusa AA, Stringer V, Scott JR. 2009. Regulation of streptokinase expression by CovR/S in *Streptococcus pyogenes*: CovR acts through a single high-affinity binding site. *Microbiology* 155:566-575.
99. Ramirez-Pena E, Trevino J, Liu Z, Perez N, Sumbly P. 2010. The group A *Streptococcus* small regulatory RNA FasX enhances streptokinase activity by increasing the stability of the *ska* mRNA transcript. *Mol Microbiol* 78:1332-1347.
100. Danger JL, Cao TN, Cao TH, Sarkar P, Trevino J, et al. 2015. The small regulatory RNA FasX enhances group A *Streptococcus* virulence and inhibits pilus expression via serotype-specific targets. *Mol Microbiol* 96:249-262.
101. Tagini F, Aubert B, Troillet N, Pillonel T, Praz G, et al. 2017. Importance of whole genome sequencing for the assessment of outbreaks in diagnostic laboratories: analysis of a case series of invasive *Streptococcus pyogenes* infections. *Eur J Clin Microbiol Infect Dis* 36:1173-1180.
102. Sumbly P, Porcella SF, Madrigal AG, Barbian KD, Virtaneva K, et al. 2005. Evolutionary origin and emergence of a highly successful clone of serotype M1 group A *Streptococcus* involved multiple horizontal gene transfer events. *J Infect Dis* 192:771-782.

103. Beres SB, Sylva GL, Barbian KD, Lei B, Hoff JS, et al. 2002. Genome sequence of a serotype M3 strain of group A *Streptococcus*: phage-encoded toxins, the high-virulence phenotype, and clone emergence. *Proc Natl Acad Sci U S A* 99:10078-10083.
104. Courtney HS, Zhang Y-M, Frank MW, Rock CO. 2006. Serum opacity factor, a streptococcal virulence factor that binds to apolipoproteins A-I and A-II and disrupts high density lipoprotein structure. *J Biol Chem* 281:5515-5521.
105. National Research Council. 2011. Guide for the care and use of laboratory animals, 8th ed. National Academies Press, Washington, DC.
106. Kelley LA, Mezulis S, Yates CM, Wass MN, Sternberg MJE. 2015. The Phyre2 web portal for protein modeling, prediction and analysis. *Nat Protoc* 10:845-858.
107. Chen H, Boutros PC. 2011. VennDiagram: a package for the generation of highly-customizable Venn and Euler diagrams in R. *BMC Bioinformatics* 12:35.

3. POLYMORPHISMS IN REGULATOR OF COV CONTRIBUTE TO THE MOLECULAR PATHOGENESIS OF SEROTYPE M28 GROUP A *Streptococcus*[†]

3.1. Summary

Two-component systems (TCSs) are signal transduction proteins that enable bacteria to respond to external stimuli by altering the global transcriptome. Accessory proteins interact with TCSs to fine-tune their activity. In group A *Streptococcus* (GAS), regulator of Cov (RocA) is an accessory protein that functions with the control of virulence regulator/sensor TCS, which regulates approximately 15% of the GAS transcriptome. Whole-genome sequencing analysis of serotype M28 GAS strains collected from invasive infections in humans identified a higher number of missense (amino acid-altering) and nonsense (protein-truncating) polymorphisms in *rocA* than expected. We hypothesized that polymorphisms in RocA alter the global transcriptome and virulence of serotype M28 GAS. We used naturally occurring clinical isolates with *rocA* polymorphisms ($n = 48$), an isogenic *rocA* deletion mutant strain, and five isogenic *rocA* polymorphism mutant strains to perform genome-wide transcript analysis (RNA sequencing), *in vitro* virulence factor assays, and mouse and nonhuman primate pathogenesis studies to test this hypothesis. Results demonstrated that polymorphisms in *rocA* result in either a subtle transcriptome change, causing a wild-type-like virulence phenotype, or a substantial transcriptome change, leading to a significantly increased virulence phenotype. Each polymorphism had a unique effect on

[†]Reprinted with permission from “Polymorphisms in regulator of Cov contribute to the molecular pathogenesis of serotype M28 group A *Streptococcus*” by Bernard PE, Kachroo P, Eraso JM, Zhu L, Madry JE, Linson SE, Ojeda Saavedra M, Cantu C, Musser JM, and Olsen RJ. 2019. *Am J Pathol*, 189, 2002-2018, Copyright © 2019 by American Society for Investigative Pathology.

the global GAS transcriptome. Taken together, our data show that naturally occurring polymorphisms in one gene encoding an accessory protein can significantly alter the global transcriptome and virulence phenotype of GAS, an important human pathogen.

3.2. Introduction

Two-component systems (TCSs) are signal transduction proteins that enable bacteria to rapidly adapt to external stimuli by altering gene expression (1). TCSs typically consist of a stimulus-sensing histidine kinase (HK) and a cognate response regulator (2). HKs form homodimers that sense stimuli through their amino-terminal extracellular domains. The signal is propagated through transmembrane domains that result in autophosphorylation of the conserved histidine. Next, the phosphate group is moved to a conserved response regulator aspartic acid residue, resulting in a change in DNA-binding affinity or oligomerization and altered gene expression (2-4). TCSs have been described in virtually all human bacterial pathogens, including *Salmonella enterica*, *Escherichia coli*, *Vibrio cholerae*, *Bordetella pertussis*, *Staphylococcus aureus*, and *Streptococcus pyogenes* (group A *Streptococcus* [GAS]) (1). Inasmuch as TCSs participate in bacterial virulence but are not present in higher eukaryotes, they are potential targets for developing new antibacterial therapies (4,5).

TCSs are signaling modules that alter gene expression in response to one or more external stimuli. The additional regulatory contribution of accessory proteins in fine-tuning TCS activity is becoming increasingly understood (4). Accessory proteins may have different functions, such as sensing external stimuli, signaling through the membrane, or altering the HK-to-response regulator phosphotransfer reaction (4). Accessory proteins may also connect two otherwise independent TCSs to generate a more complex regulatory

network (6). Accessory proteins have been implicated in molecular pathogenesis, including acid stress resistance (7), cell wall metabolism (8), antibiotic resistance (9), and virulence factor expression (10-12). However, many key knowledge gaps bearing on accessory proteins remain, including the effect of naturally occurring polymorphisms on gene expression, molecular pathogenesis, and virulence phenotype.

GAS is a human-specific pathogen that causes human diseases of varying severity, from relatively innocuous pharyngitis (strep throat) to life-threatening necrotizing fasciitis (flesh-eating disease) (13). The global disease burden attributed to GAS is immense (14). The World Health Organization estimates that GAS causes > 700 million infections and 512,000 deaths annually (14). GAS organisms are historically classified by the hypervariable *emm* gene sequence, encoding the M protein virulence factor (15). More than 220 GAS M-types have been identified (16). In the United States and Western Europe, GAS disease is predominantly caused by relatively few M-types, including serotype M28 GAS strains that commonly cause both pharyngitis and invasive infections, such as necrotizing fasciitis (17-19).

Serotype M28 GAS strains have 13 TCSs (20-30). The control of virulence regulator/sensor (CovRS) TCS is a well-characterized signaling system that regulates approximately 15% of the GAS transcriptome (29-34). CovRS in GAS is a negative regulator, and inactivation leads to substantial transcriptome changes and increased strain virulence (29, 30). Although the external stimulus for a CovRS response *in vivo* is unknown, CovS kinase and phosphatase activities can be altered *in vitro* by suprabiological concentrations of Mg²⁺ or subinhibitory concentrations of the human antimicrobial cationic peptide LL-37 (34-37). The regulator of Cov (*rocA*) gene encodes RocA, an accessory

protein to the CovRS TCS (38). RocA protein truncation mutations or whole gene deletions in several GAS serotypes, including serotype M28 strains, result in increased virulence in mouse infection models (39-43). Although its molecular mechanism of action is unknown, RocA increases the activity of CovR by increasing CovR phosphorylation in a CovS-dependent manner (40). Putative functional domains of RocA have been mapped to the amino-terminal transmembrane domains (44), suggesting membrane interactions of RocA and CovS are important for signal modulation (Fig. 3-1A) (45).

Our interest in RocA is based on serotype M28 GAS whole-genome sequencing studies of strains collected from human invasive infections (43, 46). Although previous molecular pathogenesis studies bearing on RocA have investigated strains with laboratory-generated gene deletions and protein truncations (39-44, 47), we discovered that the number of missense (amino acid-altering) and nonsense (protein-truncating) polymorphisms in *rocA* within the M28 population studied was higher than expected (Fig. 3-1A) (43, 46). We hypothesized that naturally occurring polymorphisms in *rocA* result in altered RocA function and contribute to the molecular pathogenesis of serotype M28 GAS invasive infections. To test this hypothesis, clinical isolates and isogenic mutant strains were used to perform genome-wide transcript analysis (RNA sequencing [RNA-seq]), *in vitro* virulence factor assays, and mouse and nonhuman primate (NHP) pathogenesis studies.

3.3. Materials and methods

3.3.1. RNA-seq analysis

3.3.1.1. Clinical isolates grown in duplicate

GAS strains were grown in duplicate at 37°C with 5% CO₂ in Todd-Hewitt broth with 0.2% yeast extract (THY) to mid-exponential (ME; OD₆₀₀ = 0.5) and early-stationary

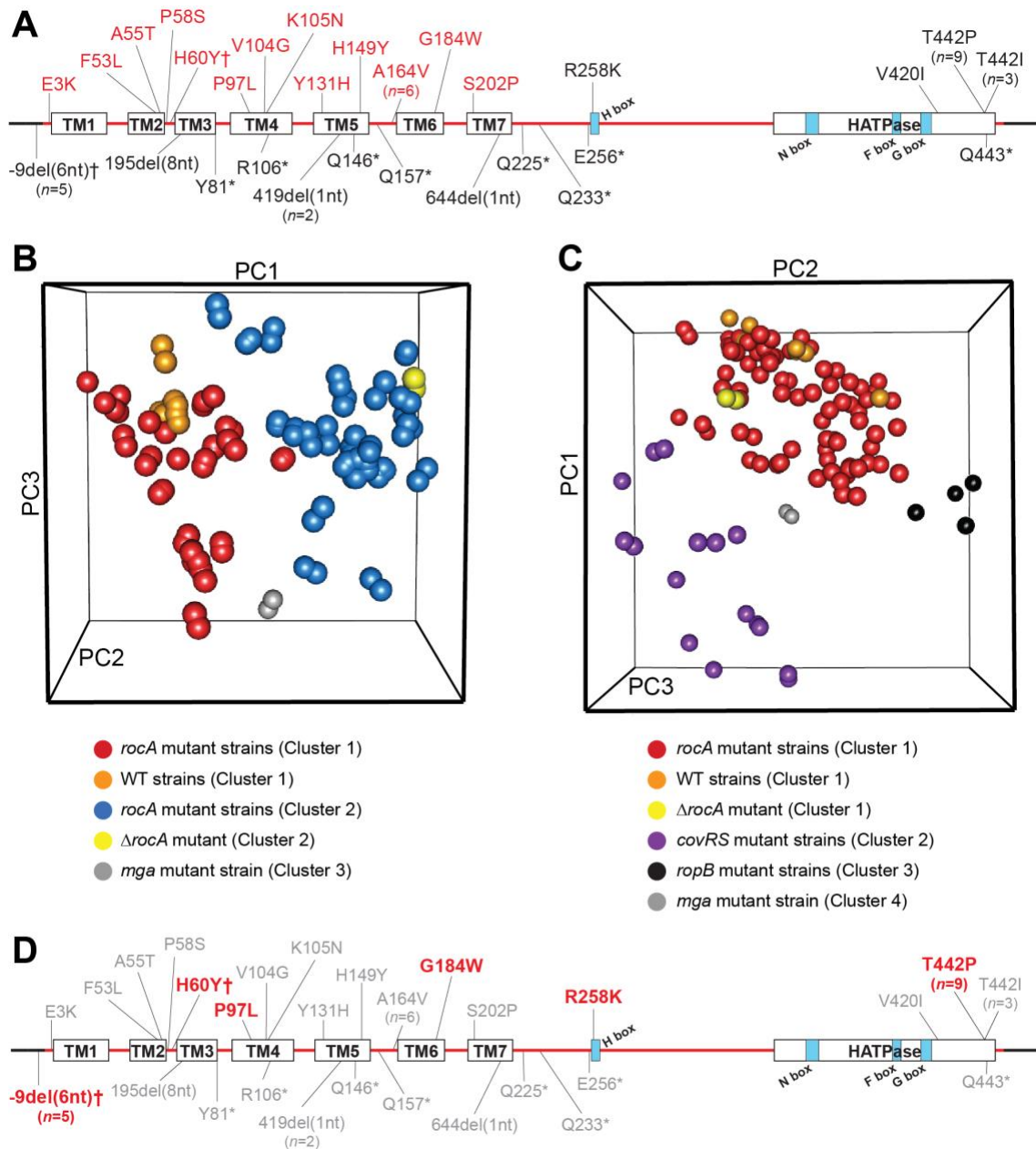


Fig. 3-1 Clinical isolates with naturally occurring *rocA* polymorphisms have altered global transcriptomes.

(A) *rocA* is unusually polymorphic in serotype M28 GAS strains. The affected codon and amino acid change conferred by each polymorphism are shown. For polymorphisms due to nucleotide deletion, the affected nucleotide is identified. Alleles identified in multiple isolates are indicated. Polymorphisms that result in RocA protein truncation or presumed loss of *rocA* mRNA translation (41) are shown below the protein schematic, and polymorphisms that result in amino acid changes are shown above the protein schematic. Missense polymorphisms in the amino-terminal transmembrane domains are red. Predicted domains of the RocA protein are indicated (45). Predicted functional domains of the putative histidine kinase domain (H box, N box, F box, and G box) are identified (38). Adapted from Bernard et al. (43). Copyright © American Society for Microbiology. (B and C) Three-dimensional principal component (PC) analysis of the RNA-sequencing data generated with the clinical isolates with naturally occurring *rocA* polymorphisms, an isogenic *rocA* deletion mutant ($\Delta rocA$) strain, and four phylogenetically matched wild-type (WT) strains at mid-exponential (B) and early stationary (C) growth phases. Clusters were determined by average-linkage hierarchical clustering and keyed by manual inspection of the data to determine common and differentiating features of strains within each cluster. (D) Protein schematic highlighting RocA variants chosen for further study by generation of isogenic mutant strains. Asterisks denote stop codons. Daggers indicate one strain that has two polymorphisms in *rocA*. HATPase, histidine kinase ATPase domain; TM, transmembrane domain.

(ES; OD₆₀₀ = 1.65) growth phases, as previously described (43, 48, 49). RNAprotect Bacteria Reagent (Qiagen Inc., Germantown, MD) was added at a 2:1 ratio, and then cells were lysed by ballistic disintegration (FastPrep-96 instrument and lysing matrix B; MP Biomedicals, Santa Ana, CA). RNA was extracted using standard methods (RNeasy kit; Qiagen Inc.), and then RNA quality and quantity were assessed using an Agilent 2100 Bioanalyzer (Agilent Technologies, Santa Clara, CA) and Qubit (Invitrogen, Carlsbad, CA), respectively. cDNA libraries were prepared using standard procedures (Ribo-Zero rRNA Removal Kit Bacteria [Illumina, San Diego, CA] and ScriptSeq Complete Kit [Epicentre, Madison, WI]). The cDNA libraries were sequenced with an Illumina NextSeq500 instrument using the default settings.

3.3.1.2. Isogenic *rocA* mutant strains grown in triplicate

GAS strains were grown in triplicate at 37°C with 5% CO₂ in THY to ME and ES growth phases, as previously described (43, 48, 49). RNAprotect Bacteria Reagent was added at a 2:1 ratio, and then cells were lysed by ballistic disintegration (FastPrep-96 instrument and lysing matrix B). RNA was extracted using standard methods (RNeasy kit), and then RNA quality and quantity were assessed using an Agilent 2100 Bioanalyzer and Qubit, respectively. Ribosomal RNA was removed with the MicrobExpress Kit (Ambion, Carlsbad, CA). cDNA libraries were prepared using the NEBNext Ultra II Directional RNA Library Prep Kit for Illumina (New England BioLabs, Ipswich, MA), according to the manufacturer's instructions. The cDNA libraries were then sequenced using an Illumina NextSeq500 instrument using the default settings.

3.3.1.3. RNA-seq data analysis

On average, 14.9 million reads/sample were obtained for the phylogenetically matched wild-type (WT) strains, the isogenic *rocA* deletion mutant ($\Delta rocA$) strain, and the clinical isolates with naturally occurring *rocA* polymorphisms (clinical isolate RNA-seq); and 42.6 million reads/sample were obtained for the parental WT strain and isogenic *rocA* mutant strains (isogenic *rocA* mutant RNA-seq). Reads were mapped to the serotype M28 GAS reference strain MGAS6180 genome (19) with EDGE-pro (50), and then differential expression analysis was performed using DESeq2 version 1.14.1 (51). For the clinical isolate RNA-seq data, genes encoding rRNA, tRNA, phage, and mobile genetic elements were excluded from analysis, as these elements are not present in every clinical isolate (46). For the isogenic *rocA* mutant RNA-seq data, genes encoding rRNA and tRNA were excluded from the analysis, along with genes from phage 6180.2 because the parental WT strain lacks this phage (46). Genes with an absolute transcript change of ≥ 1.5 -fold and $P < 0.05$ after Wald test with Bonferroni correction for multiple comparisons were considered as significantly differentially expressed. For principal component analysis, clusters were determined by average-linkage hierarchical clustering and keyed by manual inspection of the data to determine common and differentiating features of strains within each cluster.

3.3.2. Generation of isogenic *rocA* polymorphism strains

Strain MGAS28426 was selected as the serotype M28 parental WT strain because it is genetically representative of serotype M28 GAS strains and because it has a WT allele for the major global transcription regulators (43, 46). In addition, this strain is also used in animal infection studies (43, 46). The isogenic *rocA* deletion mutant strain has been previously described (43). The isogenic *rocA* polymorphism mutant strains were constructed

by allelic exchange (the allele of interest was cloned from a clinical isolate with the naturally occurring *rocA* polymorphism), as previously described (52). Primer sequences are listed in Table 3-1. Whole genome sequence analysis of the isogenic *rocA* mutant strains confirmed the expected *rocA* polymorphism and absence of spurious mutations.

Table 3-1 Primers used in this study.

Primer	Sequence	Remarks
rocA-3F	5' - GCGCTAGCGAATTCATTGGCGAATTGAC - 3'	Sanger sequencing flanking primer
rocA-5F	5' - GCGCGGTTTACCAAGAAGCTCAAGAGTAT - 3'	
rocA-H60Y-1	5' - GCGTGGATCCGACGACTCAAGTCGCTCTAACGGCTT - 3'	Sanger sequencing H60Y mutation Sanger sequencing -9del(6nt) mutation (41)
rocA-H60Y-2	5' - GCGTGGATCCTTCCTCAGGTTAAAACGGTTGCCTT - 3'	
rocA-H60Y-seq	5' - AACCAAATAATAGACACTAGTGGAAAAAAGGC - 3'	
rocA-VNTR-seq	5' - CTGTTAGAATGACAGAACTTATGATA - 5'	
rocA-P97L-1	5' - GCGTGGATCCACAATTTGCCAGCTATTGGCGGGCA - 3'	Sanger sequencing P97L mutation
rocA-P97L-2	5' - GCGTGGATCCAGACTATGGATTTCGCTTATCACCG - 3'	
rocA-P97L-seq	5' - GCTCTATGTATTGAAAATATTGGCGCCAGG - 3'	
rocA-G184W-1	5' - GCGTGGATCCGATGCCACCTTTTGAAGAATCCAA - 3'	Sanger sequencing G184W mutation
rocA-G184W-2	5' - GCGTGGATCCAGGCAGGGAAGGCAGAGGATATTAT - 3'	
rocA-G184W-seq	5' - GCCTCAATAGAGTTTTGTTTTACATAACGC - 3'	
rocA-R258K-1	5' - GCGTGGATCCGTGACATCACAGAACGCCAAGCAAGA - 3'	Sanger sequencing R258K mutation
rocA-R258K-2	5' - GCGTGGATCCTGTAGACATGTTCCCCATACAGCT - 3'	
rocA-R258K-seq	5' - CTAACAAGTTAAATCAAGTCTGTATCTTTTAGC - 3'	
rocA-T442P-1	5' - GCGTGGATCCGACTCTCCCAATCTTTCCAAGTCA - 3'	Sanger sequencing T442P mutation
rocA-T442P-2	5' - GCGTGGATCCAATATAGAAAAGTTACTTAATCAAG - 3'	
rocA-T442P-seq	5' - CCAACTGGCAAAGCTGAAATTTTAACTCTAGC - 3'	
tufA-TaqF	5' - GACACGCGACTACGTTAAA - 3'	<i>tufA</i> TaqMan primers and probes
tufA-TaqR	5' - CACCAACCTGACGTGAAAGA - 3'	
tufA-TaqP	5' - 6FAM-CGCTCAAATGGACGGAGCTATCCTT-TAMRA - 3'	
fasX-TaqF	5' - GATATGATGGCTCGGCAGAC - 3'	<i>fasX</i> TaqMan primers and probes
fasX-TaqR	5' - GCCGGGCTTTGATACTGAT - 3'	
fasX-TaqP	5' - 6FAM-TGACGATGTCAGTTGTCTTTGTTTGA-TAMRA - 3'	

BamHI sites are underlined. Seq, sequencing; VNTR, variable number tandem repeat.

3.3.3. Growth in acidic conditions

GAS strains were grown using THY supplemented with 0.1 mol/L 2-(*N*-morpholino)ethanesulfonic acid (pH 6.0; Sigma Aldrich, St. Louis, MO), as previously described (43).

3.3.4. Western immunoblot analysis of SPN and SLO in culture supernatants

Western immunoblot analysis of NAD⁺-glycohydrolase (SPN) and streptolysin O (SLO) was performed, as previously described, at ME growth phase (52). Total protein, as determined by a bicinchoninic acid assay (Pierce BCA Protein Assay Kit, Thermo Fisher Scientific, Waltham, MA), was used as the loading control.

3.3.5. Activity assays

SPN and SLO activity assay was measured, as previously described, using ME growth phase culture supernatants (53). Serum opacity factor (SOF) activity in overnight culture supernatants was assayed, as previously described (43). Secreted streptococcal pyrogenic exotoxin B (SpeB) protease activity was assayed using the casein hydrolysis (milk plate) assay, as previously described (54). Streptokinase (SKA) activity was measured, as previously described, using ME and ES growth phase cell-free culture supernatants (43, 55).

3.3.6. Quantitative RT-PCR analysis

GAS strains were grown in triplicate at 37°C with 5% CO₂ in THY to ME growth phase, as previously described (41, 46). RNeasy Protect Bacteria Reagent was added at a 2:1 ratio, and then the cells were lysed by ballistic disintegration (FastPrep-96 instrument and lysing matrix B). Standard methods were used to extract RNA (RNeasy kit). The RNA was converted to cDNA using Superscript III Reverse Transcriptase (Invitrogen). Quantitative RT-PCR was conducted using the TaqMan Fast Universal PCR Master Mix (Applied Biosystems, Foster City, CA) and an ABI 7500 Fast System instrument (Life Technologies, Carlsbad, CA). The sequences of the TaqMan primers and probes are listed in Table 3-1. Each experiment was performed with three biological replicates and two technical replicates. Transcript levels were measured relative to the constitutively expressed gene *tufA* (56).

3.3.7. Animal infection models

3.3.7.1. Mouse model of necrotizing myositis

Mouse necrotizing fasciitis/myositis studies were performed, as previously described (43, 53, 57, 58). Immunocompetent 4-week-old female CD1 mice (Envigo Laboratories, Houston, TX) were randomly assigned to treatment groups and inoculated in the right lower hind limb with 5×10^8 colony-forming units of the indicated bacterial strain suspended in 100 μ L phosphate-buffered saline ($n = 40$ mice per strain). Mice were monitored at least once daily, and near-mortality was determined using NIH's Guide for the Care and Use of Laboratory Animals (59). Survival was compared by the log-rank test. For gross and histologic evaluation, mice ($n = 3$ mice per strain) were sacrificed on day 1 after inoculation and the limbs were processed using standard methods (58).

3.3.7.2. NHP model of necrotizing myositis

A well-described NHP model of necrotizing fasciitis/myositis was used (52, 58, 60). Briefly, NHPs ($n = 8$) were sedated and inoculated at a uniform depth with 1×10^9 colony-forming units/kg in the left or right quadriceps muscle ($n = 4$ limbs per strain). Animals were observed and necropsied 24 hours after infection.

All animal experiments were approved by the Institutional Animal Care and Use Committee of the Houston Methodist Research Institute (Houston, TX; AUP-1217-0058 and AUP-0318-0016). Sample sizes for each experiment were determined with a power calculation.

3.3.8. Statistical analysis

All statistical analyses were performed using Prism 7 (GraphPad Software Inc., La Jolla, CA) with three biological replicates, and $P < 0.05$ was considered statistically significant.

3.3.9. Data availability

The serotype M28 RNA-seq sequence data have been deposited at the National Center for Biotechnology Information (<https://www.ncbi.nlm.nih.gov/bioproject>; accession number PRJNA540250).

3.4. Results

3.4.1. Naturally occurring polymorphisms in *rocA* are associated with altered transcriptomes in serotype M28 GAS strains

Whole genome sequence analysis of 2101 serotype M28 GAS strains recovered from large, comprehensive, population-based collections of human invasive infections identified 29 unique polymorphisms in *rocA* in 48 strains (Fig. 3-1A and Table B-5) (43, 46). Unlike other GAS serotypes previously investigated (57, 61, 62), the number of *rocA* allelic variants in serotype M28 GAS was greater than expected by chance ($P < 0.01$, Fisher's exact test) (43). As a first approach to understanding the role of naturally occurring *rocA* polymorphisms in serotype M28 GAS biology, RNA-seq analysis was performed on all 48 clinical isolates with naturally occurring *rocA* polymorphisms, an isogenic *rocA* deletion mutant strain ($\Delta rocA$) (43), and four phylogenetically matched WT strains. The phylogenetically matched WT strains were included in the RNA-seq analysis to normalize for genetic differences (beside *rocA* sequence) among the naturally occurring clinical isolates that, in principle, may alter the transcriptome (Table B-5) (46). Gene expression

analysis was conducted at ME ($OD_{600} = 0.5$) and ES ($OD_{600} = 1.65$) growth phases, as previously described (43).

Principal component analysis revealed that, in general, polymorphisms in *rocA* result in two distinct transcriptomes at ME growth phase (Fig. 3-1B). One *rocA* transcriptome group was allied with the phylogenetically matched WT strains (cluster 1; 21/48 *rocA* polymorphism strains). The second *rocA* transcriptome group had *rocA* mutant strains with substantially altered transcriptomes that are more closely allied with the isogenic $\Delta rocA$ deletion mutant strain (cluster 2; 26/48 *rocA* polymorphism strains). One clinical isolate with a mutation in the *mga* regulatory gene had an outlier transcriptome (cluster 3) (Table B-5) (48, 49, 63). More important, no naturally occurring *rocA* polymorphism strain had a transcriptome identical to its phylogenetically matched WT strain. That is, each *rocA* allele in the clinical isolates resulted in a unique transcriptome at ME growth phase.

At ES growth phase, principal component analysis revealed four different transcriptome clusters (Fig. 3-1C). Unlike with ME growth phase (Fig. A-5), each cluster was heavily influenced by the presence of mutations in global gene regulators other than *rocA* (Fig. 3-1C). Cluster 1 strains were *rocA* polymorphism strains, including the isogenic $\Delta rocA$ deletion mutant strain, that were allied with the WT strains. Cluster 2 strains had mutations in *covRS*, cluster 3 strains had mutations in *ropB*, and cluster 4 had the single strain with a mutation in *mga*. Consistent with the ME growth phase data, no naturally occurring *rocA* polymorphism strain had a transcriptome identical to its phylogenetically matched WT strain.

A list of each strain's *rocA* polymorphism, transcriptome cluster at ME and ES growth phases, and genes with significantly altered transcript levels compared with its

phylogenetically matched WT strain (absolute transcript fold change ≥ 1.5 and $P < 0.05$ after Wald test with Bonferroni correction for multiple comparisons) is provided in Tables B-6 and B-7 in the Appendix.

3.4.2. Selection and construction of isogenic *rocA* polymorphism strains

Because the clinical isolates with naturally occurring *rocA* polymorphisms may have mutations in other genes that also influence the global transcriptome (as evidenced by the ES transcriptome data) (Fig. 3-1C and Table B-5) (46), five *rocA* polymorphisms were selected for further characterization by generating isogenic mutant strains. The alleles were selected using multiple criteria, including the following: i) the nature of the polymorphism, with an emphasis on amino acid alterations (rather than protein truncations) in the predicted functional domains of RocA (Fig. 3-1A) (44); ii) the predicted effect of the RocA polymorphism based on the global transcriptome of the naturally occurring clinical isolates (Fig. 3-1B and C); and iii) the independent recurrence of the same polymorphism in multiple strains or the repeated presence of polymorphisms in the same codon (Fig. 3-1A). Based mainly on these criteria, five RocA variants were selected for analysis: -9del(6nt) + H60Y (hereinafter referred to as variable number tandem repeat [VNTR] + H60Y), P97L, G184W, R258K, and T442P (Fig. 3-1D).

The VNTR + H60Y RocA variant was selected because its respective clinical isolate is the only naturally occurring strain to have two polymorphisms in *rocA* (Fig. 3-1A). The VNTR sequence has been previously studied in serotype M89 GAS (41). In M89 strains, the VNTR deletion results in a lack of RocA protein translation due to a presumed loss of the ribosomal binding site (41). The P97L RocA variant was selected because codon 97 occurs in an inferred transmembrane domain (Fig. 3-1D), and the RocA P97L clinical isolate had a

rocA deletion-like transcriptome at ME growth phase (Table B-6). The G184W RocA variant was selected because codon 184 occurs in a different inferred transmembrane domain (Fig. 3-1D) and is also polymorphic in serotype M89 GAS (Fig. A-6). The R258K RocA variant was selected because codon 258 occurs in the H box of the putative HK domain (Fig. 3-1D) (38). The T442P RocA variant was selected because multiple clinical isolates ($n = 9$) acquired the polymorphism, a second polymorphism also occurs in codon 442 (T442I) (Fig. 3-1A), and the T442P clinical isolates had substantially altered transcriptomes compared with their phylogenetically matched WT strains at ME growth phase (Table B-6). The isogenic *rocA* mutant strains were generated using allelic exchange in parental WT strain MGAS28426, as previously described (52). MGAS28426 was selected as it is genetically representative of serotype M28 GAS strains (46) and contains a WT allele for all major global transcription regulatory genes. It is also the parental strain used for the isogenic *rocA* deletion mutant strain (43) and has been previously used in animal infection studies (43, 46). Whole genome sequencing of each isogenic *rocA* mutant strain confirmed the absence of spurious mutations.

To determine whether *rocA* polymorphisms alter the growth phenotype of serotype M28 GAS, the parental WT strain, isogenic *rocA* deletion mutant strain ($\Delta rocA$), and five isogenic *rocA* mutant strains were grown in nutrient-rich THY. The growth curves of the G184W and R258K isogenic mutant strains were indistinguishable from the parental WT strain (Fig. 3-2A). In comparison, the isogenic $\Delta rocA$ deletion mutant strain and VNTR + H60Y, P97L, and T442P isogenic mutant strains had a decreased lag phase (Fig. 3-2A). However, the slope of the growth curves did not differ significantly.

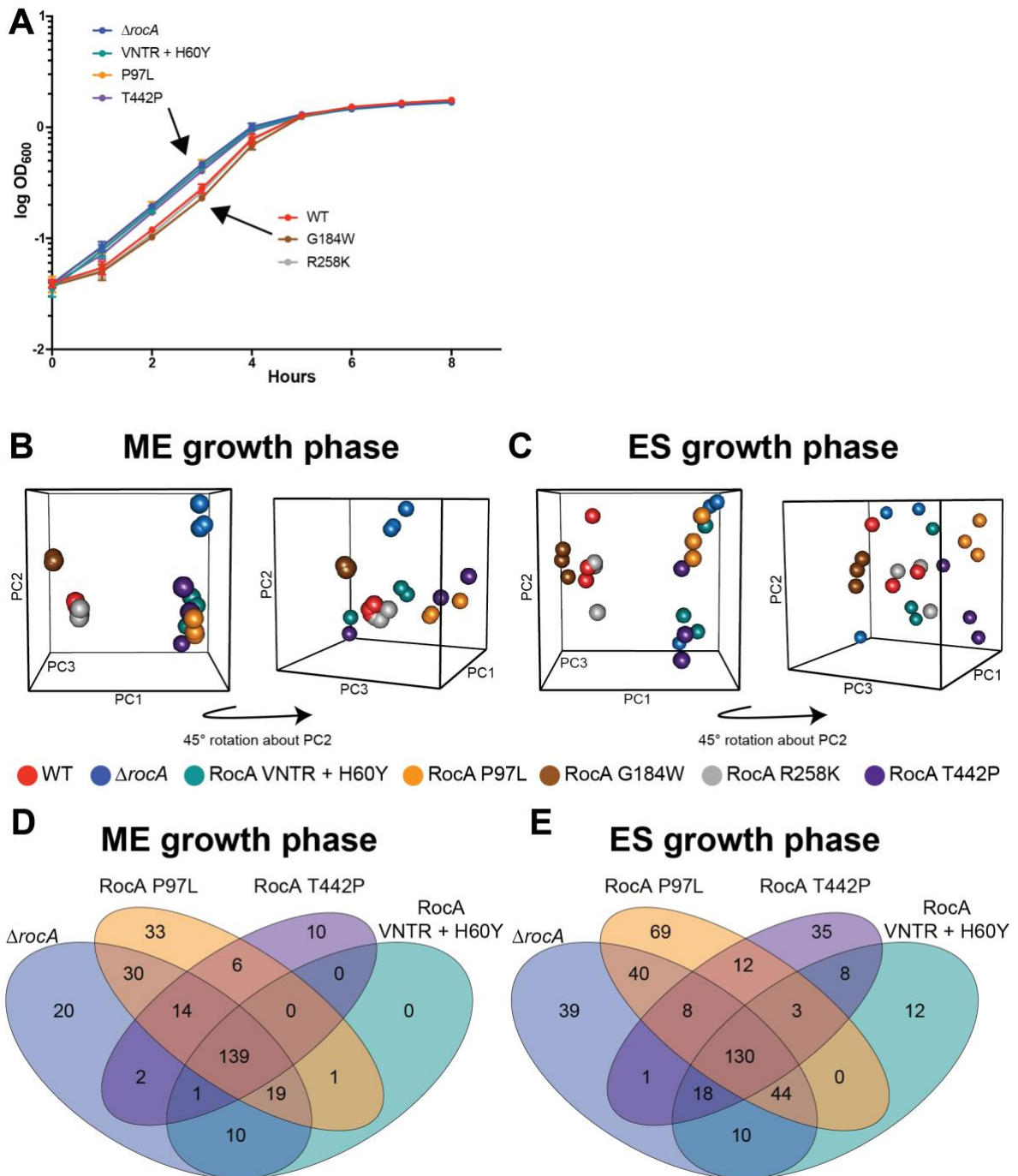


Fig. 3-2 Polymorphisms in *rocA* significantly alter the GAS transcriptome.

(A) Growth curve of the parental wild-type (WT) and isogenic *rocA* mutant strains in nutrient-rich THY. (B and C) Principal component analysis (PCA) of the RNA-sequencing data generated from the parental WT strain and isogenic *rocA* mutant strains at mid-exponential (ME; C) and early stationary (ES; D) growth phases. Each growth phase is represented by two PCA plots that are rotated approximately 45 degrees about the PC2 axis. (D and E) Comparison of differentially expressed genes in the isogenic $\Delta rocA$ deletion mutant strain and the isogenic variable number tandem repeat (VNTR) + H60Y, P97L, and T442P mutant strains at ME (D) and ES (E) (64).

3.4.3. Polymorphisms in *rocA* result in an altered transcriptome in M28 GAS strains

To test the hypothesis that naturally occurring *rocA* polymorphisms alter global gene transcript levels in serotype M28 GAS, RNA-seq analysis was performed using the parental WT strain, isogenic $\Delta rocA$ deletion mutant strain, and five isogenic *rocA* mutant strains grown to ME and ES growth phases. Principal component analysis revealed that each *rocA* polymorphism conferred a unique transcriptome that varied from the WT strain to different extents (Fig. 3-2B and C). Whereas the G184W and R258K isogenic mutant strains had transcriptomes more similar to the parental WT strain, the VNTR + H60Y, P97L, and T442P isogenic mutant strain transcriptomes (hereinafter referred to collectively as the deletion-like strains) were allied with the isogenic $\Delta rocA$ deletion mutant strain at both ME and ES growth phases (Fig. 3-2B and C).

Between 1 and 319 genes (0.05% to 17.48% of GAS genes) per strain were found to have significantly altered transcript levels at both ME and ES growth phases relative to the parental WT strain (absolute fold change ≥ 1.5 and $P < 0.05$ after Wald test with Bonferroni correction for multiple comparisons). The R258K isogenic mutant strain had 1 and 5 significantly altered transcript levels at ME and ES growth phases, respectively. Similarly, the G184W isogenic mutant strain had 22 and 25 significantly altered transcripts at ME and ES growth phases, respectively. In comparison, the isogenic $\Delta rocA$ deletion mutant strain and three deletion-like strains (VNTR + H60Y, P97L, and T442P isogenic mutant strains) had a common set of 130 and 139 genes at ME and ES growth phases, respectively, that were significantly differentially regulated (Fig. 3-2D and E) (64). Additional genes were identified as significantly differentially expressed in some, but not all, of the deletion-like

strains (Fig. 3-2D and E). Genes with significantly altered transcript levels in each strain are listed in Tables B-8 and B-9.

3.4.4. Polymorphisms in *rocA* confer two distinct responses to acid stress in M28 GAS

RNA-seq analysis showed that genes implicated in acidic stress response had altered transcript levels in the isogenic $\Delta rocA$ deletion mutant and isogenic *rocA* mutant strains (Tables B-8 and B-9). For example, the *arcABCD*, *ciaH*, and *spxA2* genes were significantly differentially regulated compared with the parental WT strain (25, 65-67). Increased resistance to acid stress, a physiological condition present in a developing purulent lesion (68-70), is one possible advantage for GAS to inactivating RocA *in vivo*. To test the hypothesis that polymorphisms in *rocA* alter GAS growth when exposed to acidic stress, the parental WT strain, isogenic $\Delta rocA$ deletion mutant strain, and five isogenic *rocA* mutant strains were grown in THY buffered with 2-(*N*-morpholino)ethanesulfonic acid (pH = 6.0). Consistent with our hypothesis, the isogenic $\Delta rocA$ deletion mutant strain and three deletion-like strains (VNTR + H60Y, P97L, and T442P isogenic mutant strains) grown in acidic conditions [2-(*N*-morpholino)ethanesulfonic acid; pH = 6.0] had a shortened lag phase and an increased slope of the exponential phase compared with the parental WT strain (Fig. 3-3A). In contrast, the G184W and R258K isogenic mutant strains did not significantly differ in overall growth from the parental WT strain (Fig. 3-3A). Taken together, the data show that polymorphisms in *rocA* alter the growth phenotype of M28 GAS strains in acidic conditions and suggest they contribute to altered molecular pathogenesis during human invasive infections.

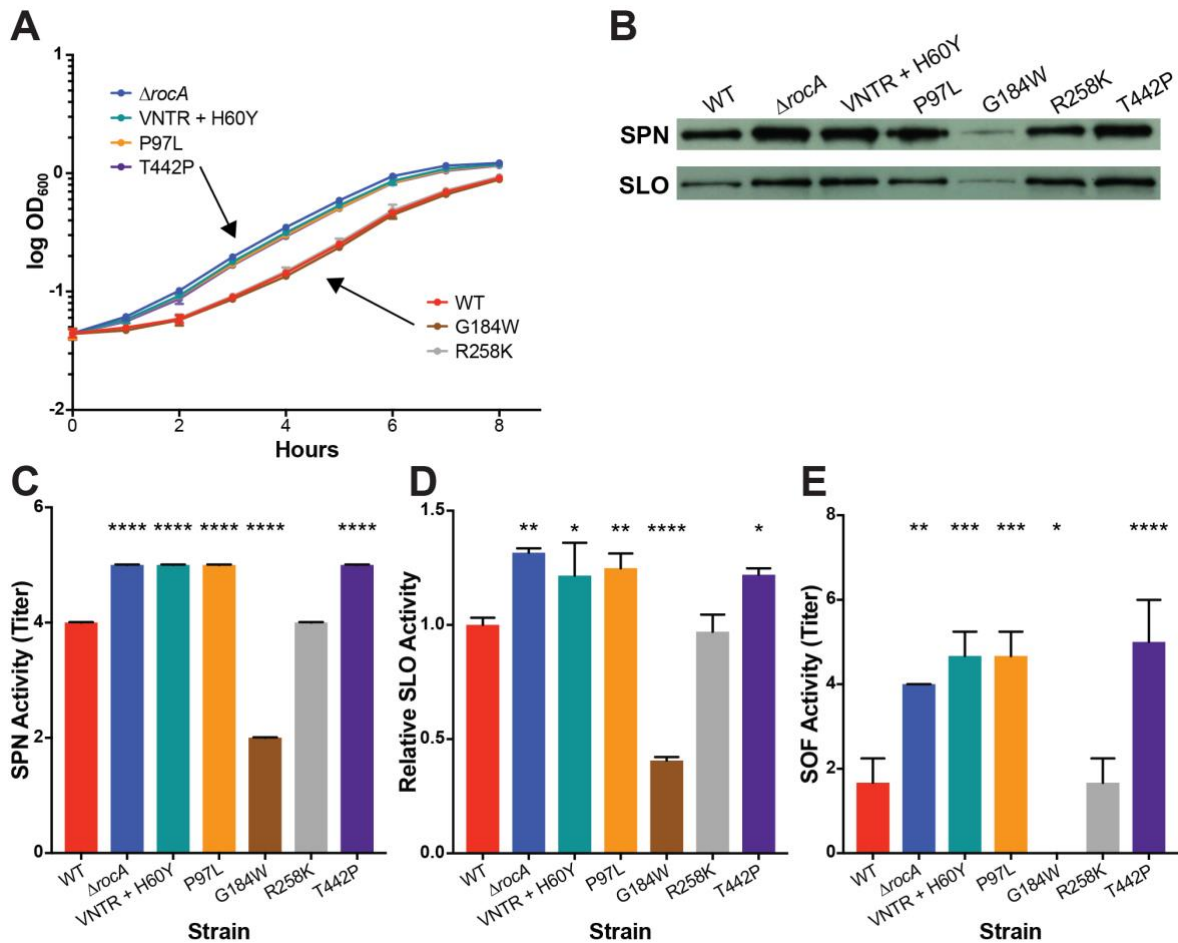


Fig. 3-3 Polymorphisms in *rocA* result in an altered virulence phenotype *in vitro*. (A) Growth curve of the parental wild-type (WT) and isogenic *rocA* polymorphism strains in THY buffered with 0.1 mol/L 2-(*N*-morpholino)ethanesulfonic acid (pH = 6.0). (B) Western immunoblot analysis of NAD⁺-glycohydrolase (SPN) and streptolysin O (SLO). (C) SPN activity. (D) SLO activity. (E) Serum opacity factor (SOF) activity. Data are expressed as means ± SD (C-E). **P* < 0.05, ***P* < 0.01, ****P* < 0.001, and *****P* < 0.0001 versus WT (one-way analysis of variance with Dunnett multiple comparisons test). VNTR, variable number tandem repeat.

3.4.5. Polymorphisms in *rocA* confer different virulence factor expression and enzymatic activity profiles in M28 GAS strains

Consistent with our previously published isogenic *ΔrocA* deletion mutant strain transcriptome data (43), several proven and putative virulence factors had significantly altered transcript levels in the isogenic *rocA* mutant strains (Table B-10). Selected virulence factors include the Mga regulon virulence factors (48, 49, 63): *sclA* (71), *fba* (72, 73), *scpA*, (74), *enn* (75), *emm* (76), *mrp* (77), *sfbX* (78), and *sof* (encoding SOF) (79). Other

differentially expressed genes are CovRS regulated virulence factors (29, 30), such as *nga* (encoding SPN) (52), *slo* (encoding SLO) (52), *spyCEP* (80), *mac* (81-83), *sse* (84), *ska* (encoding SKA) (85), and *speB* (encoding SpeB) (54) (Table B-10). To measure the phenotypic effect of differential transcript levels associated with each *rocA* polymorphism, *in vitro* virulence factor assays were performed. The isogenic $\Delta rocA$ deletion mutant strain and three deletion-like strains (VNTR + H60Y, P97L, and T442P isogenic mutant strains) had increased expression of secreted immunoreactive SPN and SLO (Fig. 3-3B) and significantly increased SPN NAD⁺-glycohydrolase, SLO cytotoxin, and SOF secreted activity (Fig. 3-3C-E), consistent with the RNA-seq data. In comparison, the R258K isogenic mutant strain had WT-like virulence factor expression and activity (Fig. 3-3). In contrast, but also consistent with the RNA-seq data (Table B-10), the G184W isogenic mutant strain had decreased expression of secreted immunoreactive SPN and SLO protein (Fig. 3-3B), and significantly decreased secreted activity of SPN, SLO, and SOF (Fig. 3-3C-E). No difference in secreted SpeB protease activity was observed among the isogenic mutant strains compared with the parental WT strain (Fig. A-7). Thus, different polymorphisms in *rocA* result in different *in vitro* virulence phenotypes.

3.4.6. Polymorphisms in *rocA* confer different secreted streptokinase activities

In addition to the aforementioned virulence factors, *ska*, the gene encoding SKA (85), was differentially regulated in the isogenic *rocA* polymorphisms strains (Table B-10). At ES growth phase, *ska* had the largest range of transcript levels among the common set of genes differentially expressed by the isogenic $\Delta rocA$ deletion mutant and deletion-like strains (VNTR + H60Y, P97L, and T442P isogenic mutant strains) (Table B-9). The *ska* gene was also significantly differentially expressed at ME growth phase only by the T442P

isogenic mutant strain (Table B-8). To determine whether polymorphisms in *rocA* decrease secreted SKA activity, an *in vitro* assay was performed. At ME growth phase, the isogenic $\Delta rocA$ deletion mutant strain and all five isogenic *rocA* mutant strains had significantly decreased secreted SKA activity compared with the parental WT strain (Fig. 3-4A). Whereas the G184W and R258K isogenic mutant strains (WT-like transcriptomes) had secreted SKA activity more similar to the WT strain, the three deletion-like strains (VNTR + H60Y, P97L, and T442P isogenic mutant strains) had markedly lower secreted SKA activity (Fig. 3-4A). Unexpectedly, the P97L isogenic mutant strain had an intermediate level of secreted SKA activity, and the T442P isogenic mutant strain had very low secreted SKA activity (Fig. 3-4A). That is, the P97L and T442P isogenic mutant strains had significantly increased and decreased secreted SKA activity, respectively, compared with the isogenic $\Delta rocA$ deletion mutant strain. Similar data were observed at ES growth phase (Fig. 3-4B).

The *ska* gene is regulated by the CovRS and FasBCA/*fasX* systems (55, 86). We hypothesized that *fasX* may contribute to the unexpectedly low *ska* transcripts and SKA activity in the T442P strain. *fasX* encodes a small RNA that is regulated by FasBCA and enhances *ska* transcript stability (55). Because our RNA-seq protocol cannot reliably measure transcripts of small RNAs, such as *fasX*, quantitative RT-PCR analysis of *fasX* was performed for the parental WT strain, isogenic $\Delta rocA$ deletion mutant strain, and isogenic *rocA* mutant strains at ME growth phase. As expected, the T442P isogenic mutant strain had significantly decreased expression of *fasX* compared with the parental WT strain (Fig. 3-4C). Thus, differences in secreted SKA activity among the *rocA* polymorphism strains may, in part, be explained by altered expression of *fasX*.

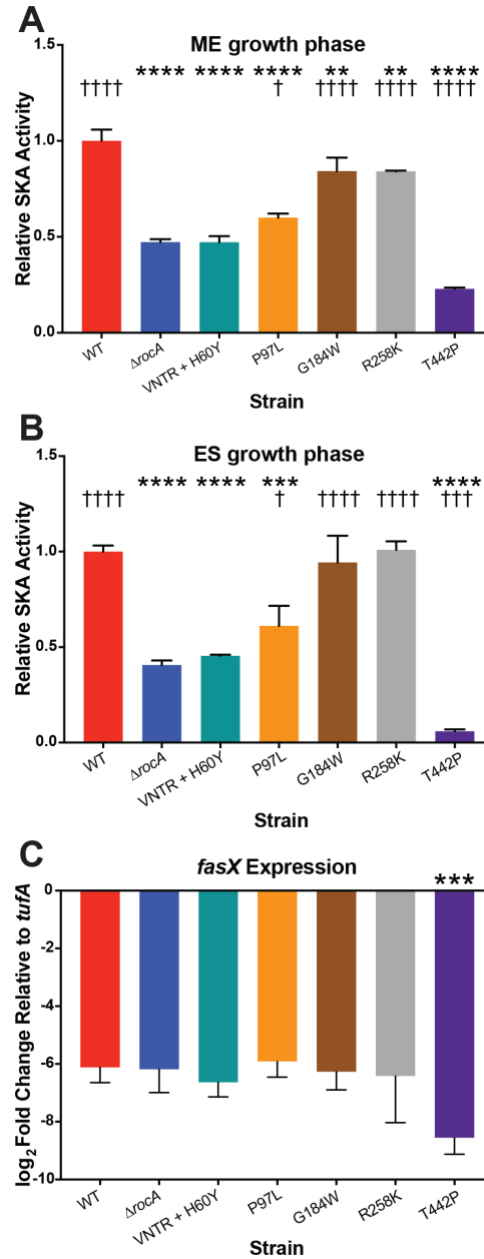


Fig. 3-4 Polymorphisms in *rocA* result in decreased *ska* transcript levels and streptokinase (SKA) activity, in part, due to altered *fasX* regulation.

(A and B) SKA activity at mid-exponential (ME; A) and early stationary (ES; B) growth phases. (C) Quantitative RT-PCR analysis of *fasX* at ME growth phase. The log₂ fold changes relative to *tufA* are shown. Data are expressed as means ± SD (A-C). **P* < 0.05, ****P* < 0.001, and *****P* < 0.0001 versus the parental WT strain (one-way analysis of variance with Tukey multiple comparisons test); †*P* < 0.05, ††*P* < 0.001, †††*P* < 0.0001 versus the isogenic Δ*rocA* deletion mutant strain (one-way analysis of variance with Tukey multiple comparisons test). VNTR, variable number tandem repeat; WT, wild-type.

3.4.7. Polymorphisms in *rocA* confer two distinct virulence phenotypes in a mouse model of necrotizing myositis

To determine whether polymorphisms in *rocA* result in altered virulence, the parental WT strain, isogenic $\Delta rocA$ deletion mutant strain, and five isogenic *rocA* mutant strains were compared using a well-established necrotizing myositis mouse model (43, 46, 57, 58). Compared with the parental WT strain, the $\Delta rocA$, VNTR + H60Y, and T442P isogenic mutant strains caused significantly increased near mortality (Fig. 3-5A) and larger lesions with more tissue destruction (Fig. 3-5B). Isogenic mutant strains containing either the G184W or R258K amino acid replacements (WT-like transcriptomes) did not differ significantly in virulence from the parental WT strain (Fig. 3-5A). Unexpectedly, the mouse virulence of the P97L isogenic mutant strain, which has a *rocA* deletion-like transcriptome, did not significantly differ from the parental WT strain (Fig. 3-5A).

To begin to identify the possible molecular basis of the decreased virulence phenotype of the P97L strain, the RNA-seq data was reexamined. Compared with the other deletion-like transcriptome strains ($\Delta rocA$, VNTR + H60Y, and T442P isogenic mutant strains), the P97L isogenic mutant strain had 10 genes with significantly altered transcript levels (Table B-11). More important, compared with the other deletion-like transcriptome strains, the isogenic mutant with the P97L amino acid change had significantly decreased transcript levels of four genes (*slo*, *prsA*, *mac*, and *sclA*) encoding proven virulence factors (52, 58, 71, 87). Thus, altered expression of *slo*, *prsA*, *mac*, and *sclA* may explain, in part, the unexpectedly lower virulence phenotype of the P97L isogenic mutant strain.

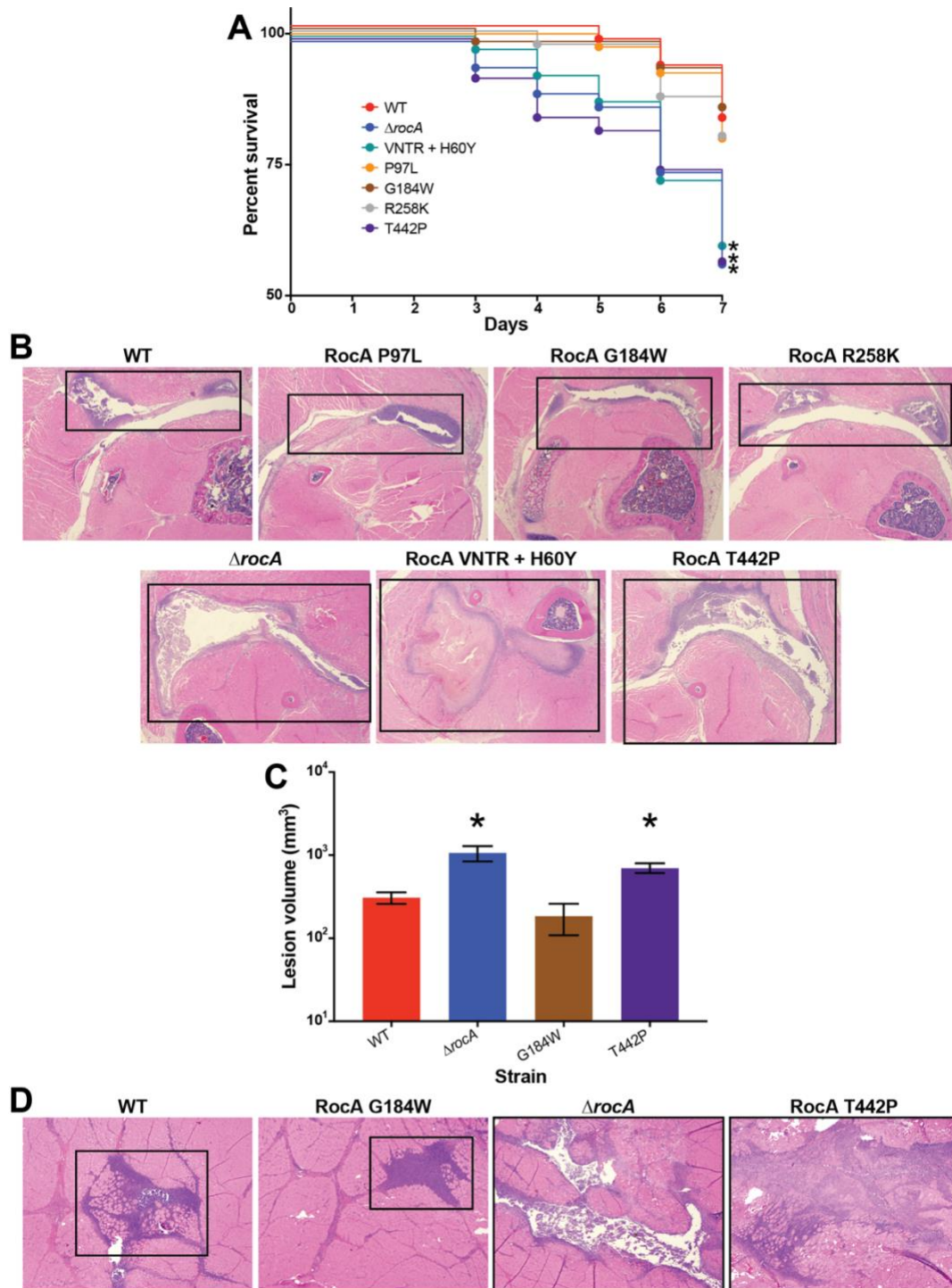


Fig. 3-5 Polymorphisms in *rocA* result in altered virulence in mouse and nonhuman primate (NHP) models of necrotizing myositis.

(A) Kaplan-Meier survival curve for mice infected in the right hindlimb with the indicated strain. Log-rank test was performed. (B) Representative microscopic lesions of the infected limb on postinoculation day 1. The necrotic lesions are encompassed by boxed areas. Hematoxylin and eosin staining was used. (C) Lesion volume of NHPs infected in the quadriceps muscle with the indicated strain. *U*-test was performed. (D) Representative microscopic lesions of the infected muscle. The necrotic lesions are encompassed by boxed areas. Hematoxylin and eosin staining was used. $n = 40$ mice per strain (A); $n = 4$ limbs per strain (C). $*P < 0.05$ versus wild-type (WT). Original magnification, $\times 4$ (B and D). VNTR, variable number tandem repeat.

3.4.8. Polymorphisms in *rocA* result in altered virulence in a NHP model of necrotizing myositis

GAS is a human-specific pathogen, and some virulence factors have specificity for human and NHP molecules (88, 89). To unambiguously demonstrate that polymorphisms in *rocA* contribute to serotype M28 GAS virulence, four strains were compared using an NHP model of necrotizing myositis. We hypothesized that the isogenic $\Delta rocA$ deletion mutant and T442P (deletion-like) isogenic mutant strains are significantly more virulent than the parental WT or G184W (WT-like) isogenic mutant strains. Consistent with our hypothesis, the isogenic $\Delta rocA$ deletion mutant and T442P isogenic mutant strains caused significantly larger lesions (Fig. 3-5C) with more tissue destruction (Fig. 3-5D).

3.5. Discussion

TCSs are used by bacteria to regulate gene expression (1). Depending on the bacterial pathogen species and the TCS studied, regulatory activity can involve a few or many genes. Accessory proteins interact with TCSs to fine-tune TCS regulatory activity, coordinate gene expression across multiple regulatory networks, and contribute to complex cellular phenotypes and virulence (4, 6-12). Across all M protein serotypes studied to date, GAS has 12 conserved TCSs (20, 90), including the well-studied CovRS TCS (29-34, 37, 91-94). RocA is an accessory protein to the CovRS TCS (29, 30, 43). Using several different GAS serotype strains, it has been demonstrated that inactivation of CovRS or RocA leads to significantly increased virulence in mice, NHPS, and human patients (29, 30, 32-34, 39-43, 47, 92, 93, 95-99). Recent whole genome sequence analysis of large, comprehensive, population-based collections of serotype M28 GAS strains demonstrated higher numbers of polymorphisms in *rocA* than expected (43, 46). Herein, we investigated the effect of different

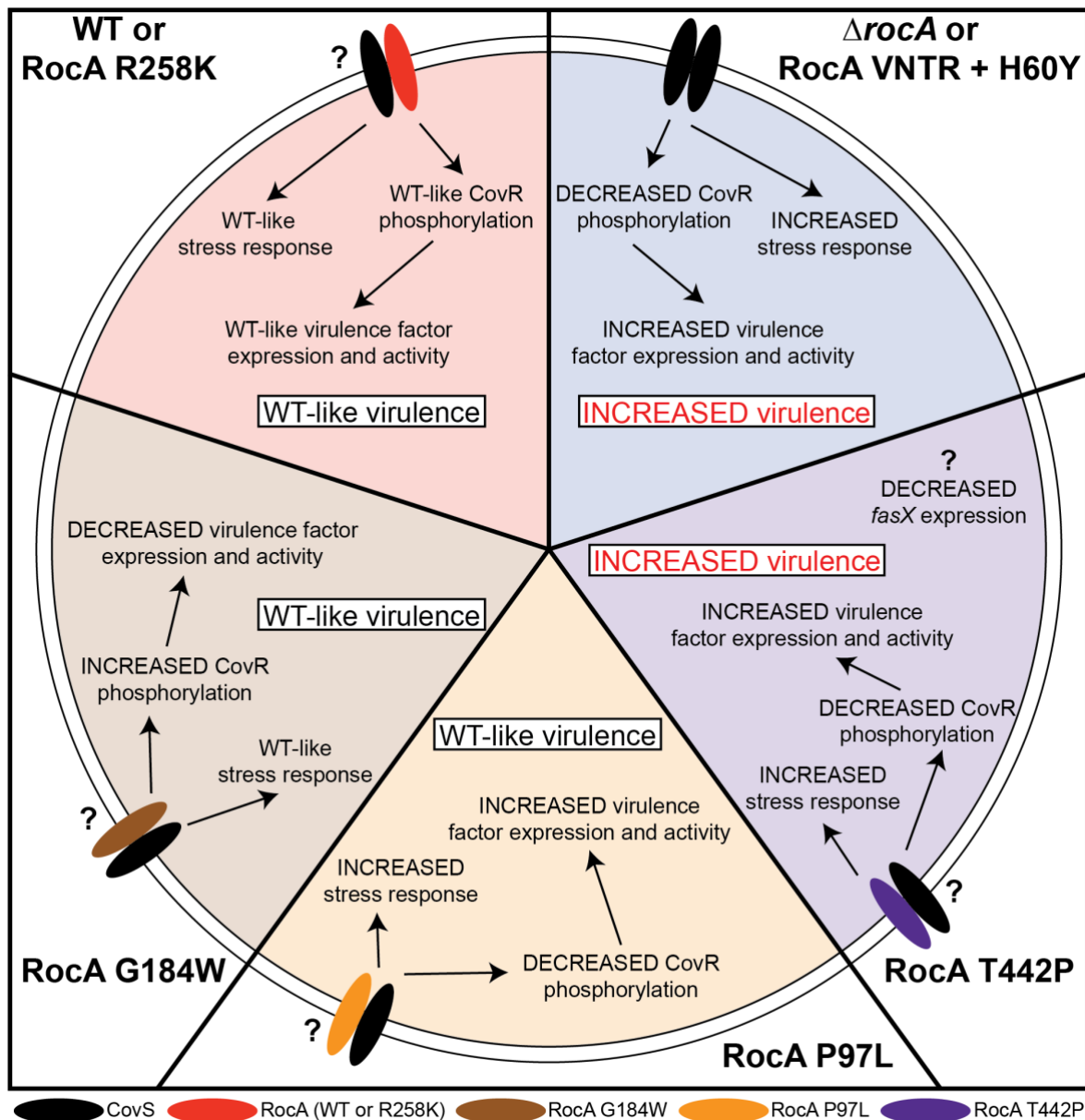


Fig. 3-6 Model of RocA contribution to the molecular pathogenesis of serotype M28 GAS.

M28 GAS strains with a wild-type (WT) *rocA* gene or WT-like variant, such as R258K (red panel), have normal levels of RocA-regulated genes and a normal virulence phenotype. Mutation of RocA at codon 184 (brown panel) results in decreased transcript levels of some virulence factor genes but no change in virulence phenotype. In contrast, M28 GAS strains with a deletion of *rocA* or loss of RocA translation (variable number tandem repeat [VNTR] + H60Y; blue panel) have a substantially altered transcriptome that significantly increases virulence factor expression and virulence in mice and nonhuman primates. Similarly, mutation at codon 442 (purple panel) or codon 97 (orange panel) also results in a *rocA* deletion-like phenotype. CovR, control of virulence regulator; CovS, control of virulence sensor.

naturally occurring polymorphisms in *rocA* on serotype M28 GAS gene expression, virulence factor activity, and virulence in mice and NHPs (Fig. 3-6). We discovered that

each polymorphism resulted in either a subtly altered WT-like transcriptome or a substantially altered *rocA* deletion-like transcriptome (Fig. 3-2). Each polymorphism had a unique effect on the global GAS transcriptome. Taken together, these data suggest that naturally occurring polymorphisms in *rocA* contribute to the molecular pathogenesis of serotype M28 GAS invasive strains.

Our laboratory and others have recently used transposon mutagenesis libraries to identify genes essential for GAS fitness, including serotype M28 GAS strains, in various niches (60, 100-102). Consistent with the data reported herein, transposon mutagenesis studies have shown *rocA* inactivation to significantly increase GAS fitness in mouse s.c. and NHP necrotizing myositis infection models (60, 101). The RNA-seq data demonstrate that *rocA* polymorphisms and *rocA* gene deletion significantly alter expression of many proven and putative virulence factors (Fig. 3-3 and Table B-10) (43). As a result, *rocA* polymorphisms significantly increase M28 GAS virulence (Fig. 3-5). Many RocA regulated genes are also individually predicted by the transposon mutagenesis studies to be essential to GAS fitness (Table B-12) (60, 100-102). For example, several transporters regulated by RocA alter GAS fitness. Deletion of a putative methionine transporter system (encoded by *M28_Spy0263/0264/0265*) and two putative export systems (encoded by *M28_Spy0625/0626/0627* and *M28_Spy1711/1712*) results in decreased fitness in human saliva *ex vivo* and NHP muscle *in vivo* (60, 102). In addition, genes encoding several proven virulence factors regulated by RocA also contribute to GAS fitness in various anatomic niches (Table B-12) (23, 25, 60, 65, 66, 100-108). Furthermore, increased expression of *nga* and *slo* (Fig. 3-3 and Table B-12) was recently implicated in the emergence and global dissemination of epidemic serotype M1 and M89 GAS strains (52, 57, 61, 109, 110).

Regulation of the *ska* gene by RocA in serotype M28 GAS is unique (43). Although *rocA* polymorphisms in other GAS serotype strains result in increased *ska* transcript and SKA protein levels, *rocA* polymorphisms in M28 GAS strains cause decreased *ska* transcript levels and secreted SKA activity (Table B-10 and Fig. 3-4) (40, 43, 44, 47). The *ska* gene is regulated by the FasBCA/*fasX* and CovRS systems (21, 22, 29-31, 33, 37, 55, 86), and decreased *fasX* transcripts in the isogenic RocA T442P mutant strain likely resulted in a more severely decreased SKA activity phenotype (Fig. 3-4). Our data suggest that RocA may interact, either directly or indirectly, with the FasBCA/*fasX* system to alter SKA activity. In addition, M28 GAS strains with a polymorphism in *rocA* have altered expression of *gidA*, a tRNA modifying enzyme that affects transcript levels of genes encoding several virulence factors, including *ska* (Table B-9) (111,112). Interestingly, the transposon mutagenesis library screens found deletion of *fasBCA* to result in increased GAS fitness for serotype M28, but not M1, in NHP necrotizing myositis (60). Thus, the RocA and FasBCA/*fasX* systems may have serotype-specific regulatory functions.

Polymorphisms in RocA or *rocA* gene deletion results in significantly altered transcript levels of *speB* and *hasABC* (Tables B-6, B-7, B-8, and B-9). The *speB* gene encodes a secreted cysteine protease and well-documented virulence factor (54). Although there were differences in *speB* transcript levels, there was no difference in secreted protease activity (Fig. A-7), which may be due to the complex regulation and activation of SpeB (54). The *hasABC* genes encode proteins required for synthesis of the antiphagocytic hyaluronic acid capsule (113). All serotype M28 GAS strains have a naturally occurring nucleotide deletion in *hasA* that results in a nonfunctional HasA protein and loss of hyaluronic capsule production (43).

RocA is hypothesized to heterodimerize with CovS to affect CovR phosphorylation and downstream regulatory activity (34, 40, 41, 44). However, a physical interaction between RocA and CovS (or any other transcription regulator) has not been definitively shown. RocA inactivation alters CovR phosphorylation and transcription of CovRS regulated genes (34, 40, 41). However, the molecular mechanism of the interaction remains unknown. Accessory proteins are often membrane proteins (4, 7, 9-12). Structural models predict that RocA folds similarly to an HK because of the presence of a predicted membrane-spanning region and putative HK domain (Fig. 3-1) (38, 45, 114). However, Paluscio (115) reported that RocA lacks HK activity. Consistent with the putative H-box being dispensable for RocA function, the RocA R258K strain (with an amino acid change in the putative H-box) (Fig. 3-1) retained a WT-like transcriptome and virulence phenotype (Fig. 3-6).

Jain et al. (44) have suggested that the amino-terminal transmembrane domains, but not the carboxy-terminal domain, contribute to RocA regulatory function. The seven predicted transmembrane-spanning domains (45, 114) may enable RocA to heterodimerize with CovS or other TCS sensor proteins. Consistent with the idea that protein-protein interactions are key to wild-type RocA activity, our naturally occurring and isogenic mutant strains with *rocA* polymorphisms occurring in the transmembrane domains have *rocA* deletion-like transcriptomes (Fig. 3-1 and 3-6). Drawing additional attention to the transmembrane domain, the isogenic RocA P97L and G184W mutant strains generated unexpected results relative to the parental WT strain and isogenic $\Delta rocA$ deletion mutant strain (Fig. 3-6). Of note, codon 184 is also polymorphic (G184E) (Fig. A-6) and function altering (Fig. A-8) in serotype M89 GAS strains (57).

In contrast to published studies (44), we also demonstrate that the carboxy-terminal domain is essential to wild-type RocA activity in serotype M28 GAS (Fig. 3-6). Mutations in codon 442, located in the putative nonfunctional HK ATPase domain (Fig. 3-1), independently arose multiple times (T442P and T442I) and were propagated by vertical inheritance ($n = 9$ and 3 strains, respectively) (Fig. 3-1). The isogenic T442P mutant strain had a *rocA* deletion-like transcriptome, virulence factor activity profile, and virulence phenotype in mice and NHPs (Fig. 3-6). The repeated occurrence of polymorphisms at codon 442 strongly suggests selection for variation at this site in invasive strains. Additional studies of RocA are needed to fully elucidate the functional domains of RocA.

In summary, we used transcriptome analysis, isogenic mutant strains, *in vitro* virulence factor assays, and mouse and NHP pathogenesis studies to investigate the effect of RocA amino acid variation on serotype M28 GAS biology, including host-pathogen interactions. Our study has brought novel insight into the role of an accessory protein in bacterial virulence and molecular pathogenesis.

3.6. References

1. Beier D, Gross R. 2006. Regulation of bacterial virulence by two-component systems. *Curr Opin Microbiol* 9:143-152.
2. Kim D, Forst S. 2001. Genomic analysis of the histidine kinase family in bacteria and archaea. *Microbiology* 147:1197-1212.
3. West AH, Stock AM. 2001. Histidine kinases and response regulator proteins in two-component signaling systems. *Trends Biochem Sci* 26:369-376.
4. Buelow DR, Raivio TL. 2010. Three (and more) component regulatory systems - auxiliary regulators of bacterial histidine kinases. *Mol Microbiol* 75:547-566.

5. Bem AE, Velikova N, Pellicer MT, Baarlen P, Marina A, et al. 2015. Bacterial histidine kinases as novel antibacterial drug targets. *ACS Chem Biol* 10:213-224.
6. Mitrophanov AY, Groisman EA. 2008. Signal integration in bacterial two-component regulatory systems. *Genes Dev* 22:2601-2611.
7. Eguchi Y, Itou J, Yamane M, Demizu R, Yamato F, et al. 2007. B1500, a small membrane protein, connects the two-component systems EvgS/EvgA and PhoQ/PhoP in *Escherichia coli*. *Proc Natl Acad Sci U S A* 104:18712-18717.
8. Szurmant H, Bu L, Brooks CL, 3rd, Hoch JA. 2008. An essential sensor histidine kinase controlled by transmembrane helix interactions with its auxiliary proteins. *Proc Natl Acad Sci U S A* 105:5891-5896.
9. Falord M, Karimova G, Hiron A, Msadek T. 2012. GraXSR proteins interact with the VraFG ABC transporter to form a five-component system required for cationic antimicrobial peptide sensing and resistance in *Staphylococcus aureus*. *Antimicrob Agents Chemother* 56:1047-1058.
10. Jeong DW, Cho H, Jones MB, Shatzkes K, Sun F, et al. 2012. The auxiliary protein complex SaePQ activates the phosphatase activity of sensor kinase SaeS in the SaeRS two-component system of *Staphylococcus aureus*. *Mol Microbiol* 86:331-348.
11. Firon A, Tazi A, Da Cunha V, Brinster S, Sauvage E, et al. 2013. The Abi-domain protein Abx1 interacts with the CovS histidine kinase to control virulence gene expression in group B *Streptococcus*. *PLoS Pathog* 9:e1003179.

12. Poupel O, Proux C, Jagla B, Msadek T, Dubrac S. 2018. SpdC, a novel virulence factor, controls histidine kinase activity in *Staphylococcus aureus*. PLoS Pathog 14:e1006917.
13. Cunningham MW. 2000. Pathogenesis of group A streptococcal infections. Clin Microbiol Rev 13:470-511.
14. Carapetis JR, Steer AC, Mulholland EK, Weber M. 2005. The global burden of group A streptococcal diseases. Lancet Infect Dis 5:685-694.
15. Walker MJ, Barnett TC, McArthur JD, Cole JN, Gillen CM, et al. 2014. Disease manifestations and pathogenic mechanisms of group A *Streptococcus*. Clin Microbiol Rev 27:264-301.
16. Sanderson-Smith M, De Oliveira DM, Guglielmini J, McMillan DJ, Vu T, et al. 2014. A systematic and functional classification of *Streptococcus pyogenes* that serves as a new tool for molecular typing and vaccine development. J Infect Dis 210:1325-1338.
17. Steer AC, Law I, Matatolu L, Beall BW, Carapetis JR. 2009. Global *emm* type distribution of group A streptococci: systematic review and implications for vaccine development. Lancet Infect Dis 9:611-616.
18. Chochua S, Metcalf BJ, Li Z, Rivers J, Mathis S, et al. 2017. Population and whole genome sequence based characterization of invasive group A streptococci recovered in the United States during 2015. mBio 8:e01422-17.
19. Green NM, Zhang S, Porcella SF, Nagiec MJ, Barbian KD, et al. 2005. Genome sequence of a serotype M28 strain of group A *Streptococcus*: potential new insights into puerperal sepsis and bacterial disease specificity. J Infect Dis 192:760-770.

20. Sitkiewicz I, Musser JM. 2006. Expression microarray and mouse virulence analysis of four conserved two-component gene regulatory systems in group A *Streptococcus*. *Infect Immun* 74:1339-1351.
21. Kreikemeyer B, Boyle MDP, Buttaro BA, Heinemann M, Podbielski A. 2001. Group A streptococcal growth phase-associated virulence factor regulation by a novel operon (Fas) with homologues to two-component-type regulators requires a small RNA molecule. *Mol Microbiol* 39:392-406.
22. Danger JL, Cao TN, Cao TH, Sarkar P, Trevino J, et al. 2015. The small regulatory RNA FasX enhances group A *Streptococcus* virulence and inhibits pilus expression via serotype-specific targets. *Mol Microbiol* 96:249-262.
23. Flores AR, Olsen RJ, Cantu C, Pallister KB, Guerra FE, et al. 2017. Increased pilus production conferred by a naturally occurring mutation alters host-pathogen interaction in favor of carriage in *Streptococcus pyogenes*. *Infect Immun* 85:e00949-16.
24. Liu M, Hanks TS, Zhang J, McClure MJ, Siemsen DW, et al. 2006. Defects in *ex vivo* and *in vivo* growth and sensitivity to osmotic stress of group A *Streptococcus* caused by interruption of response regulator gene *vicR*. *Microbiology* 152:967-978.
25. Tatsuno I, Isaka M, Okada R, Zhang Y, Hasegawa T. 2014. Relevance of the two-component sensor protein CiaH to acid and oxidative stress responses in *Streptococcus pyogenes*. *BMC Research Notes* 7:189.
26. Shelburne SA, 3rd, Sumby P, Sitkiewicz I, Granville C, DeLeo FR, et al. 2005. Central role of a bacterial two-component gene regulatory system of previously

- unknown function in pathogen persistence in human saliva. Proc Natl Acad Sci U S A 102:16037-16042.
27. Voyich JM, Sturdevant DE, Braughton KR, Kobayashi SD, Lei B, et al. 2003. Genome-wide protective response used by group A *Streptococcus* to evade destruction by human polymorphonuclear leukocytes. Proc Natl Acad Sci U S A 100:1996-2001.
 28. Voyich JM, Braughton KR, Sturdevant DE, Vuong C, Kobayashi SD, et al. 2004. Engagement of the pathogen survival response used by group A *Streptococcus* to avert destruction by innate host defense. J Immunol 173:1194-1201.
 29. Sumby P, Whitney AR, Graviss EA, DeLeo FR, Musser JM. 2006. Genome-wide analysis of group A streptococci reveals a mutation that modulates global phenotype and disease specificity. PLoS Pathog 2:e5.
 30. Shelburne SA, Olsen RJ, Suber B, Sahasrabhojane P, Sumby P, et al. 2010. A combination of independent transcriptional regulators shapes bacterial virulence gene expression during infection. PLoS Pathog 6:e1000817.
 31. Graham MR, Smoot LM, Lux Migiliaccio CA, Virtaneva K, Sturdevant DE, et al. 2002. Virulence control in group A *Streptococcus* by a two-component gene regulatory system: global expression profiling and *in vivo* infection modeling. Proc Natl Acad Sci U S A 99:13855-13860.
 32. Horstmann N, Sahasrabhojane P, Suber B, Kumaraswami M, Olsen RJ, et al. 2011. Distinct single amino acid replacements in the control of virulence regulator protein differentially impact streptococcal pathogenesis. PLoS Pathog 7:e1002311.

33. Horstmann N, Saldana M, Sahasrabhojane P, Yao H, Su X, et al. 2014. Dual-site phosphorylation of the control of virulence regulator impacts group A streptococcal global gene expression and pathogenesis. *PLoS Pathog* 10:e1004088.
34. Horstmann N, Tran CN, Brumlow C, DebRoy S, Yao H, et al. 2018. Phosphatase activity of the control of virulence sensor kinase CovS is critical for the pathogenesis of group A *streptococcus*. *PLoS Pathog* 14:e1007354.
35. Gryllos I, Levin JC, Wessels MR. 2003. The CsrR/CsrS two-component system of group A *Streptococcus* responds to environmental Mg²⁺. *Proc Natl Acad Sci U S A* 100:4227-4232.
36. Gryllos I, Tran-Winkler HJ, Cheng M, Chung H, Bolcome R, et al. 2008. Induction of group A *Streptococcus* virulence by a human antimicrobial peptide. *Proc Natl Acad Sci U S A* 105:16755-16760.
37. Horstmann N, Sahasrabhojane P, Saldana M, Ajami NJ, Flores AR, et al. 2015. Characterization of the effect of the histidine kinase CovS on response regulator phosphorylation in group A *Streptococcus*. *Infect Immun* 83:1068-1077.
38. Biswas I, Scott JR. 2003. Identification of *rocA*, a positive regulator of *covR* expression in the group A streptococcus. *J Bacteriol* 185:3081-3090.
39. Lynskey NN, Goulding D, Gierula M, Turner CE, Dougan G, et al. 2013. RocA truncation underpins hyper-encapsulation, carriage longevity and transmissibility of serotype M18 group A streptococci. *PLoS Pathog* 9:e1003842.
40. Miller EW, Danger JL, Ramalinga AB, Horstmann N, Shelburne SA, et al. 2015. Regulatory rewiring confers serotype-specific hyper-virulence in the human pathogen group A *Streptococcus*. *Mol Microbiol* 98:473-489.

41. Zhu L, Olsen RJ, Horstmann N, Shelburne SA, Fan J, et al. 2016. Intergenic variable-number tandem-repeat polymorphism upstream of *rocA* alters toxin production and enhances virulence in *Streptococcus pyogenes*. *Infect Immun* 84:2086-2093.
42. Feng W, Minor D, Liu M, Li J, Ishaq SL, et al. 2017. Null mutations of group A *Streptococcus* orphan kinase RocA: selection in mouse infection and comparison with CovS mutations in alteration of *in vitro* and *in vivo* protease SpeB expression and virulence. *Infect Immun* 85:e00790-16.
43. Bernard PE, Kachroo P, Zhu L, Beres SB, Eraso JM, et al. 2018. RocA has serotype-specific gene regulatory and pathogenesis activities in serotype M28 group A streptococcus. *Infect Immun* 86:e00467-18.
44. Jain I, Miller EW, Danger JL, Pflughoeft KJ, Sumbly P. 2017. RocA is an accessory protein to the virulence-regulating CovRS two-component system in group A *Streptococcus*. *Infect Immun* 85:e00274-17.
45. Kelley LA, Mezulis S, Yates CM, Wass MN, Sternberg MJE. 2015. The Phyre2 web portal for protein modeling, prediction and analysis. *Nat Protoc* 10:845-858.
46. Kachroo P, Eraso JM, Beres SB, Olsen RJ, Zhu L, et al. 2019. Integrated analysis of population genomics, transcriptomics and virulence provides novel insights into *Streptococcus pyogenes* pathogenesis. *Nat Genet* 51:548-559.
47. Sarkar P, Danger JL, Jain I, Meadows LA, Beam C, et al. 2018. Phenotypic variation in the group A *Streptococcus* due to natural mutation in the accessory protein-encoding gene *rocA*. *mSphere* 3:e00519-18.

48. Sanson M, O'Neill BE, Kachroo P, Anderson JR, Flores AR, et al. 2015. A naturally occurring single amino acid replacement in multiple gene regulator of group A streptococcus significantly increases virulence. *Am J Pathol* 185:462-471.
49. Sanson M, Makthal N, Gavagan M, Cantu C, Olsen RJ, et al. 2015. Phosphorylation events in the multiple gene regulator of group A *Streptococcus* significantly influence global gene expression and virulence. *Infect Immun* 83:2382-2395.
50. Magoc T, Wood D, Salzberg SL. 2013. EDGE-pro: estimated degree of gene expression in prokaryotic genomes. *Evol Bioinform Online* 9:127-136.
51. Love MI, Huber W, Anders S. 2014. Moderated estimation of fold change and dispersion for RNA-seq data with DESeq2. *Genome Biol* 15:550.
52. Zhu L, Olsen RJ, Nasser W, Beres SB, Vuopio J, et al. 2015. A molecular trigger for intercontinental epidemics of group A *Streptococcus*. *J Clin Invest* 125:3545-3559.
53. Zhu L, Olsen RJ, Lee JD, Porter AR, DeLeo FR, et al. 2017. Contribution of secreted NADase and streptolysin O to the pathogenesis of epidemic serotype M1 *Streptococcus pyogenes* infections. *Am J Pathol* 187:605-613.
54. Olsen RJ, Raghuram A, Cantu C, Hartman MH, Jimenez FE, et al. 2015. The majority of 9,729 group A streptococcus strains causing disease secrete SpeB cysteine protease: pathogenesis implications. *Infect Immun* 83:4750-4758.
55. Ramirez-Pena E, Trevino J, Liu Z, Perez N, Sumbly P. 2010. The group A *Streptococcus* small regulatory RNA FasX enhances streptokinase activity by increasing the stability of the *ska* mRNA transcript. *Mol Microbiol* 78:1332-1347.

56. Sanson M, Makthal N, Flores AR, Olsen RJ, Musser JM, et al. 2015. Adhesin competence repressor (AdcR) from *Streptococcus pyogenes* controls adaptive responses to zinc limitation and contributes to virulence. *Nucleic Acids Res* 43:418-432.
57. Beres SB, Kachroo P, Nasser W, Olsen RJ, Zhu L, et al. 2016. Transcriptome remodeling contributes to epidemic disease caused by the human pathogen *Streptococcus pyogenes*. *mBio* 7:e00403-16.
58. Olsen RJ, Sitkiewicz I, Ayeras AA, Gonulal VE, Cantu C, et al. 2010. Decreased necrotizing fasciitis capacity caused by a single nucleotide mutation that alters a multiple gene virulence axis. *Proc Natl Acad Sci U S A* 107:888-893.
59. National Research Council. 2011. Guide for the care and use of laboratory animals, 8th ed. National Academies Press, Washington, DC.
60. Zhu L, Olsen RJ, Beres SB, Eraso JM, Saavedra MO, et al. 2019. Gene fitness landscape of group A streptococcus during necrotizing myositis. *J Clin Invest* 129:887-901.
61. Nasser W, Beres SB, Olsen RJ, Dean MA, Rice KA, et al. 2014. Evolutionary pathway to increased virulence and epidemic group A *Streptococcus* disease derived from 3,615 genome sequences. *Proc Natl Acad Sci U S A* 111:E1768-1776.
62. Fittipaldi N, Beres SB, Olsen RJ, Kapur V, Shea PR, et al. 2012. Full-genome dissection of an epidemic of severe invasive disease caused by a hypervirulent, recently emerged clone of group A *Streptococcus*. *Am J Pathol* 180:1522-1534.

63. Ribardo DA, McIver KS. 2006. Defining the Mga regulon: comparative transcriptome analysis reveals both direct and indirect regulation by Mga in the group A streptococcus. *Mol Microbiol* 62:491-508.
64. Chen H, Boutros PC. 2011. VennDiagram: a package for the generation of highly-customizable Venn and Euler diagrams in R. *BMC Bioinformatics* 12:35.
65. Cusumano ZT, Watson ME, Jr., Caparon MG. 2014. *Streptococcus pyogenes* arginine and citrulline catabolism promotes infection and modulates innate immunity. *Infect Immun* 82:233-242.
66. Cusumano ZT, Caparon MG. 2015. Citrulline protects *Streptococcus pyogenes* from acid stress using the arginine deiminase pathway and the F1Fo-ATPase. *J Bacteriol* 197:1288-1296.
67. Port GC, Cusumano ZT, Tumminello PR, Caparon MG. 2017. SpxA1 and SpxA2 act coordinately to fine-tune stress responses and virulence in *Streptococcus pyogenes*. *mBio* 8:e00288-17.
68. Nekoofar MH, Namazikhah MS, Sheykhrezae MS, Mohammadi MM, Kazemi A, et al. 2009. pH of pus collected from periapical abscesses. *Int Endod J* 42:534-538.
69. Bryant RE, Mazza JA. 1989. Effect of the abscess environment on the antimicrobial activity of ciprofloxacin. *Am J Med* 87:23S-27S.
70. Wiese KG. 1994. Electrolyte concentration, real and osmotic pressure in abscesses. *Zentralbl Chir* 119:54-59.
71. Lukomski S, Nakashima K, Abdi I, Cipriano VJ, Ireland RM, et al. 2000. Identification and characterization of the *scl* gene encoding a group A

- Streptococcus* extracellular protein virulence factor with similarity to human collagen. Infect Immun 68:6542-6553.
72. Terao Y, Kawabata S, Kunitomo E, Murakami J, Nakagawa I, et al. 2001. Fba, a novel fibronectin-binding protein from *Streptococcus pyogenes*, promotes bacterial entry into epithelial cells, and the *fba* gene is positively transcribed under the Mga regulator. Mol Microbiol 42:75-86.
 73. Rouchon CN, Ly AT, Noto JP, Luo F, Lizano S, et al. 2017. Incremental contributions of FbaA and other impetigo-associated surface proteins to fitness and virulence of a classical group A streptococcal skin strain. Infect Immun 85:e00374-17.
 74. Wexler DE, Chenoweth DE, Cleary PP. 1985. Mechanism of action of the group A streptococcal C5a inactivator. Proc Natl Acad Sci U S A 82:8144-8148.
 75. Stenberg L, O'Toole P, Lindahl G. 1992. Many group A streptococcal strains express two different immunoglobulin-binding proteins, encoded by closely linked genes: characterization of the proteins expressed by four strains of different M-type. Mol Microbiol 6:1185-1194.
 76. Smeesters PR, McMillan DJ, Sriprakash KS. 2010. The streptococcal M protein: a highly versatile molecule. Trends Microbiol 18:275-282.
 77. Courtney HS, Hasty DL, Dale JB. 2006. Anti-phagocytic mechanisms of *Streptococcus pyogenes*: binding of fibrinogen to M-related protein. Mol Microbiol 59:936-947.

78. Jeng A, Sakota V, Li Z, Datta V, Beall B, et al. 2003. Molecular genetic analysis of a group A *Streptococcus* operon encoding serum opacity factor and a novel fibronectin-binding protein, SfbX. *J Bacteriol* 185:1208-1217.
79. Zhu L, Olsen RJ, Musser JM. 2017. Opacification domain of serum opacity factor inhibits beta-hemolysis and contributes to virulence of *Streptococcus pyogenes*. *mSphere* 2:e00147-17.
80. Edwards RJ, Taylor GW, Ferguson M, Murray S, Rendell N, et al. 2005. Specific C-terminal cleavage and inactivation of interleukin-8 by invasive disease isolates of *Streptococcus pyogenes*. *J Infect Dis* 192:783-790.
81. von Pawel-Rammingen U, Johansson BP, Bjorck L. 2002. IdeS, a novel streptococcal cysteine proteinase with unique specificity for immunoglobulin G. *EMBO J* 21:1607-1615.
82. Soderberg JJ, Engstrom P, von Pawel-Rammingen U. 2008. The intrinsic immunoglobulin G endopeptidase activity of streptococcal Mac-2 proteins implies a unique role for the enzymatically impaired Mac-2 protein of M28 serotype strains. *Infect Immun* 76:2183-2188.
83. Lei B, DeLeo FR, Reid SD, Voyich JM, Magoun L, et al. 2002. Opsonophagocytosis-inhibiting Mac protein of group A *Streptococcus*: identification and characteristics of two gene complexes. *Infect Immun* 70:6880-6890.
84. Liu M, Zhu H, Li J, Garcia CC, Feng W, et al. 2012. Group A *Streptococcus* secreted esterase hydrolyzes platelet-activating factor to impede neutrophil recruitment and facilitate innate immune evasion. *PLoS Pathog* 8:e1002624.

85. Huang T-T, Malke H, Ferretti JJ. 1989. Heterogeneity of the streptokinase gene in group A streptococci. *Infect Immun* 57:502-506.
86. Churchward G, Bates C, Gusa AA, Stringer V, Scott JR. 2009. Regulation of streptokinase expression by CovR/S in *Streptococcus pyogenes*: CovR acts through a single high-affinity binding site. *Microbiology* 155:566-575.
87. Nandakumar KS, Johansson BP, Bjorck L, Holmdahl R. 2007. Blocking of experimental arthritis by cleavage of IgG antibodies in vivo. *Arthritis Rheum* 56:3253-3260.
88. Sun H, Ringdahl U, Homeister JW, Fay WP, Engleberg NC, et al. 2004. Plasminogen is a critical host pathogenicity factor for group A streptococcal infection. *Science* 305:1283-1286.
89. Gladysheva IP, Turner RB, Sazonova IY, Liu L, Reed GL. 2003. Coevolutionary patterns in plasminogen activation. *Proc Natl Acad Sci U S A* 100:9168-9172.
90. Buckley SJ, Timms P, Davies MR, McMillan DJ. 2018. *In silico* characterisation of the two-component system regulators of *Streptococcus pyogenes*. *PLoS One* 13:e0199163.
91. Churchward G. 2007. The two faces of Janus: virulence gene regulation by CovR/S in group A streptococci. *Mol Microbiol* 64:34-41.
92. Sugareva V, Arlt R, Fiedler T, Riani C, Podbielski A, et al. 2010. Serotype- and strain- dependent contribution of the sensor kinase CovS of the CovRS two-component system to *Streptococcus pyogenes* pathogenesis. *BMC Microbiol* 10:34.

93. Bao YJ, Liang Z, Mayfield JA, Lee SW, Ploplis VA, et al. 2015. CovRS-regulated transcriptome analysis of a hypervirulent M23 strain of group A *Streptococcus pyogenes* provides new insights into virulence determinants. *J Bacteriol* 197:3191-3205.
94. Horstmann N, Sahasrabhojane P, Yao H, Su X, Shelburne SA, et al. 2017. Use of a phosphorylation site mutant to identify distinct modes of gene repression by the control of virulence regulator (CovR) in *Streptococcus pyogenes*. *J Bacteriol* 199:e00835-16.
95. Levin JC, Wessels MR. 1998. Identification of *csrR/csrS*, a genetic locus that regulates hyaluronic acid capsule synthesis in group A *Streptococcus*. *Mol Microbiol* 30:209-219.
96. Tatsuno I, Okada R, Zhang Y, Isaka M, Hasegawa T. 2013. Partial loss of CovS function in *Streptococcus pyogenes* causes severe invasive disease. *BMC Research Notes* 6:126.
97. Flores AR, Sahasrabhojane P, Saldana M, Galloway-Pena J, Olsen RJ, et al. 2014. Molecular characterization of an invasive phenotype of group A *Streptococcus* arising during human infection using whole genome sequencing of multiple isolates from the same patient. *J Infect Dis* 209:1520-1523.
98. Yoshida H, Ishigaki Y, Takizawa A, Moro K, Kishi Y, et al. 2015. Comparative genomics of the mucoid and nonmucoid strains of *Streptococcus pyogenes*, isolated from the same patient with streptococcal meningitis. *Genome Announc* 3:e0021-15.

99. Ikebe T, Matsumura T, Nihonmatsu H, Ohya H, Okuno R, et al. 2016. Spontaneous mutations in *Streptococcus pyogenes* isolates from streptococcal toxic shock syndrome patients play roles in virulence. *Sci Rep* 6:28761.
100. Le Breton Y, Mistry P, Valdes KM, Quigley J, Kumar N, et al. 2013. Genome-wide identification of genes required for fitness of group A streptococcus in human blood. *Infect Immun* 81:862-875.
101. Le Breton Y, Belew AT, Freiberg JA, Sundar GS, Islam E, et al. 2017. Genome-wide discovery of novel MIT1 group A streptococcal determinants important for fitness and virulence during soft-tissue infection. *PLoS Pathog* 13:e1006584.
102. Zhu L, Charbonneau ARL, Waller AS, Olsen RJ, Beres SB, et al. 2017. Novel genes required for the fitness of *Streptococcus pyogenes* in human saliva. *mSphere* 2:e00460-17.
103. Crotty Alexander LE, Maisey HC, Timmer AM, Rooijackers SH, Gallo RL, et al. 2010. MIT1 group A streptococcal pili promote epithelial colonization but diminish systemic virulence through neutrophil extracellular entrapment. *J Mol Med (Berl)* 88:371-381.
104. Calfee G, Danger JL, Jain I, Miller EW, Sarkar P, et al. 2018. Identification and characterization of serotype-specific variation in group A *Streptococcus* pilus expression. *Infect Immun* 86:e00792-17.
105. Kristian SA, Datta V, Weidenmaier C, Kansal R, Fedtke I, et al. 2005. D-alanylation of teichoic acids promotes group A *Streptococcus* antimicrobial peptide resistance, neutrophil survival, and epithelial cell invasion. *J Bacteriol* 187:6719-6725.

106. Cox KH, Ruiz-Bustos E, Courtney HS, Dale JB, Pence MA, et al. 2009. Inactivation of DltA modulates virulence factor expression in *Streptococcus pyogenes*. PLoS One 4:e5366.
107. Kloosterman TG, Hendriksen WT, Bijlsma JJE, Bootsma HJ, van Hijum SAFT, et al. 2006. Regulation of glutamine and glutamate metabolism by GlnR and GlnA in *Streptococcus pneumoniae*. J Biol Chem 281:25097-25109.
108. Si Y, Yuan F, Chang H, Liu X, Li H, et al. 2009. Contribution of glutamine synthetase to the virulence of *Streptococcus suis* serotype 2. Vet Microbiol 139:80-88.
109. Sumbly P, Porcella SF, Madrigal AG, Barbian KD, Virtaneva K, et al. 2005. Evolutionary origin and emergence of a highly successful clone of serotype M1 group A *Streptococcus* involved multiple horizontal gene transfer events. J Infect Dis 192:771-782.
110. Zhu L, Olsen RJ, Nasser W, de la Riva Morales I, Musser JM. 2015. Trading capsule for increased cytotoxin production: contribution to virulence of a newly emerged clade of *emm89 Streptococcus pyogenes*. mBio 6:e01378-15.
111. Cho KH, Caparon MG. 2008. tRNA modification by GidA/MnmE is necessary for *Streptococcus pyogenes* virulence: a new strategy to make live attenuated strains. Infect Immun 76:3176-3186.
112. Shea PR, Virtaneva K, Kupko JJ, 3rd, Porcella SF, Barry WT, et al. 2010. Interactome analysis of longitudinal pharyngeal infection of cynomolgus macaques by group A *Streptococcus*. Proc Natl Acad Sci U S A 107:4693-4698.

113. Ashbaugh CD, Alberti S, Wessels MR. 1998. Molecular analysis of the capsule gene region of group A *Streptococcus*: the *hasAB* genes are sufficient for capsule expression. *J Bacteriol* 180:4955-4959.
114. Omasits U, Ahrens CH, Muller S, Wollscheid B. 2014. Protter: interactive protein feature visualization and integration with experimental proteomic data. *Bioinformatics* 30:884-886.
115. Paluscio E. 2015. Adaptive mechanisms to niche remodeling in *Streptococcus pyogenes*. PhD thesis. Washington University in St. Louis, St. Louis, MO.

4. SINGLE AMINO ACID REPLACEMENTS IN ROCA DISRUPT PROTEIN-
PROTEIN INTERACTIONS TO ALTER THE MOLECULAR PATHOGENESIS OF
GROUP A *Streptococcus*[‡]

4.1. Summary

Group A *Streptococcus* (GAS) is a human-specific pathogen and major cause of disease worldwide. The molecular pathogenesis of GAS, like many pathogens, is dependent on the coordinated expression of genes encoding different virulence factors. The CovRS (control of virulence regulator/sensor) two-component system is a major virulence regulator of GAS that has been extensively studied. More recent investigations have also involved RocA (regulator of Cov), a regulatory accessory protein to CovRS. RocA interacts, in some manner, with CovRS; however, the precise molecular mechanism is unknown. Herein, we demonstrate that RocA is a membrane protein containing seven transmembrane helices with an extracellularly located N-terminus and intracellularly located C-terminus. For the first time, we demonstrate that RocA directly interacts with itself (RocA) and CovS, but not CovR, in intact cells. Single amino acid replacements along the entire length of RocA disrupt RocA-RocA and RocA-CovS interactions to significantly alter the GAS virulence phenotype as defined by global transcriptome, secreted virulence activity *in vitro*, and tissue destruction and mortality *in vivo*. In summary, we show that amino acid replacements in a regulatory accessory protein can affect protein-protein interactions to significantly alter the virulence of a major human pathogen.

[‡] Bernard PE, Duarte A, Bogdanov M, Musser JM, Olsen RJ. Functional consequences of amino acid changes in an accessory protein: the molecular mechanism for RocA-mediated virulence in group A *Streptococcus*. Mol Microbiol, submitted.

4.2. Introduction

Group A *Streptococcus* (GAS) is a human-specific pathogen that causes a number of diseases ranging in severity from relatively innocuous bacterial pharyngitis (“strep throat”) to life-threatening necrotizing fasciitis (“flesh eating” disease) (1, 2). Despite over a century of efforts by many investigators, no licensed GAS vaccine is available (2, 3), which may, in part, be due to the complex regulation of its many putative and proven virulence factors and surface exposed proteins (3-27).

One major virulence regulator of GAS is the CovRS (control of virulence regulator/sensor) two-component system. CovRS is a negative regulator of virulence, regulating approximately 10-15% of the GAS transcriptome (27-31). That is, when activated, CovRS decreases expression of many GAS genes and decreases virulence. In turn, CovRS inactivation significantly increases virulence (27, 29, 31-36). Since its identification over 20 years ago (32, 37, 38), the molecular mechanism of CovRS regulation has been extensively studied. Although the *in vivo* stimulus for CovRS activation remains unknown, CovR activation *in vitro* via phosphorylation by CovS can be modulated by cationic magnesium (Mg²⁺) and the human antimicrobial peptide LL-37 (39-41). Many studies have investigated the effect of single nucleotide polymorphisms and amino acid changes in CovRS, identifying key residues and protein domains important for virulence factor gene regulation (27, 33, 35, 41-45).

More recent study of virulence regulation in GAS has involved RocA (regulator of Cov), a regulatory accessory protein to the CovRS two-component system (25, 46-61). RocA is a positive regulator of CovRS (46). That is, RocA activates CovRS, which in turn, decreases virulence factor gene expression and strain virulence. Inactivation of RocA by

gene deletion or truncation increases virulence factor expression and strain virulence (25, 47, 51-54, 56-59, 61). In contrast to truncation and deletion mutations that can have substantial effects on protein structure, we have recently investigated the effect of single amino acid replacements in RocA on GAS molecular pathogenesis (25). We discovered that many different naturally-occurring amino acid replacements result in a significantly altered global transcriptome, secreted virulence factor activity *in vitro*, and virulence *in vivo* (25). However, the molecular basis of RocA-CovRS interactions remains unknown.

While some aspects of RocA molecular pathogenesis have been discovered (25, 53, 56, 59, 61), many key knowledge gaps remain. First, the physical interaction between RocA and CovS is hypothesized to occur through their N-terminal transmembrane domains (56, 59, 61); however, mutations, including truncation, to the C-terminus unexpectedly result in a RocA deletion-like virulence phenotype (25, 51). That is, the C-terminal cytoplasmic domain has a yet undefined function. Second, a direct physical interaction between RocA and CovS has not been proven in intact cells. Third, the number, location, and boundaries of the N-terminal transmembrane helices are unknown. Whereas some published studies predict six transmembrane helices (55, 56, 58, 61), others predict seven (25, 46, 57, 59). A detailed understanding of RocA topology is necessary for downstream mechanistic and translational studies bearing on RocA-CovRS protein interactions. Fourth, although many different amino acid replacements in RocA are proven to alter GAS virulence (25, 57), none result in identical effects on genome-wide transcriptomes, virulence factor activities *in vitro*, and virulence phenotypes in mice and nonhuman primates (25). The molecular basis for different amino acid replacements conferring different virulence phenotypes is crucial to

understanding the RocA-CovRS interaction specifically and accessory protein-regulatory protein interactions in general.

To begin determining the potential role of single amino acid replacements in altering RocA-CovRS molecular interactions, we addressed the aforementioned knowledge gaps. Our topology studies demonstrate that RocA is a membrane protein with seven N-terminal transmembrane helices. Additionally, using a bacterial adenylate cyclase-based two-hybrid (BACTH) experimental methodology, and in contrast to previous reports (61), we demonstrate that RocA directly interacts with itself and CovS, but not CovR, in intact cells. Finally, we developed a model to explain how single amino acid replacements in RocA alter its interaction with itself and CovS to significantly affect gene expression, secreted virulence factor activity *in vitro*, and strain virulence *in vivo*.

4.3. Results

4.3.1. Multiple *in silico* membrane topology algorithms predict a consensus RocA membrane topology

RocA is composed of two major predicted domains: a functionally important transmembrane domain in the N-terminus and a putative histidine kinase ATPase domain in the C-terminus (Fig. 4-1) (25, 46, 52, 56, 57, 59). Previous investigators have speculated that either six (55, 56, 58, 61) or seven (25, 46, 57, 59) transmembrane helices exist, but the exact number has not been experimentally determined. Furthermore, the overall topology of the N-terminal transmembrane domain of RocA has not been experimentally determined. To understand the mechanism by which single amino acid replacements alter the functionality of RocA, knowledge of the precise protein topology is needed.

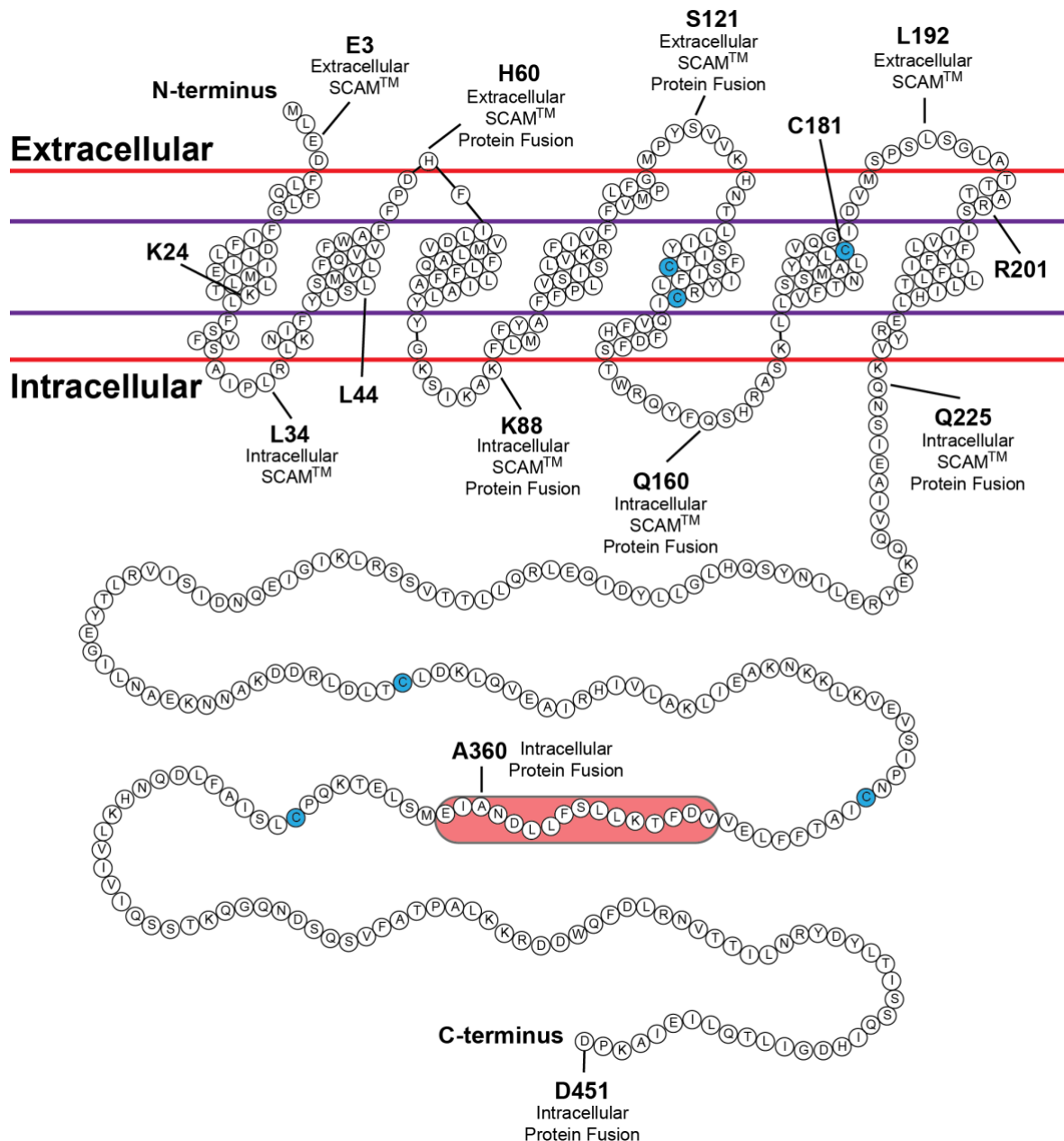


Fig. 4-1 The predicted membrane topology model of RocA has a seven transmembrane helical architecture.

A composite of eight different *in silico* algorithms was used (see Fig. A-9 for details). The N- and C-termini are identified. Residues between the purple lines are predicted to be in transmembrane helices by all algorithms, whereas residues between a red and purple line are predicted to be in transmembrane helices in at least one, but not all, algorithms. Residues in the red shaded box were predicted to be an eighth transmembrane helix by one *in silico* algorithm (Fig. A-9), but the prediction was not supported by experimental evidence. Native cysteine residues are colored blue. Residues used in membrane topology experiments are identified. Relevant results of SCAM™ and protein fusion assays are indicated.

We used multiple *in silico* protein topology algorithms to predict the membrane topology of RocA. The algorithms included Phobius (62), Philius (63), OCTOPUS (64),

PolyPhobius (65), SPOCTOPUS (66), SCAMPI (67), MEMSAT-SVM (68), and Phyre2 (69). These algorithms use a combination of hidden Markov models, artificial neural networks, physical data parameters, and support vector machine-based approaches on well-defined training sets to predict transmembrane segments in proteins based on amino acid sequence and context and protein homology. The consensus topology predicts that RocA has seven transmembrane helices in the N-terminal half of the protein, the N-terminus is located extracellularly, and the C-terminus is located intracellularly (Fig. 4-1). Although none of the protein topology algorithms predicted identical transmembrane helical boundaries (Fig. A-9), each was generally consistent with respect to transmembrane helical boundaries. The one outlier was MEMSAT-SVM, which predicted an eighth transmembrane helix in the C-terminal half of RocA (Fig. 4-1 and A-9). Next, we used the modeled data, predicting a seven transmembrane helical architecture, to guide experiments seeking to precisely determine the membrane topology of RocA.

4.3.2. SCAMTM recapitulates the predicted *in silico* topology of RocA

We applied the substituted-cysteine accessibility method as applied to transmembrane orientation (SCAMTM) methodology as a first approach to determine the membrane topology of the N-terminal transmembrane domain of RocA (70). In this methodology, naturally-occurring or strategically engineered cysteine residues in membrane proteins are differentially labeled based on their cellular localization and accessibility to the water-soluble, thiol-specific labeling reagent 3-(*N*-maleimido-propionyl)biocytin (MPB). Accessible extracellular cysteine residues can be labeled by treating intact cells with MPB. Accessible intracellular cysteine residues can be labeled by first treating cells with non-detectable, water-soluble 4-acetamido-4'-maleimidylstilbene-2,2'-disulfonic acid (AMS) to

block extracellular cysteine residues, followed by treatment of AMS-blocked sonicated cells with MPB. Importantly, SCAMTM uses the full-length protein expressed in GAS, allowing for topological analysis in the native host environment without disrupting the normal protein conformation.

First, we determined the location of the six naturally-occurring cysteine residues in RocA (C135, C144, C181, C304, C338, and C371; Fig. 4-1). Since the *in silico* algorithms predicted that each is located in a transmembrane helix (C135, C144, and C181) or the cytoplasm (C304, C338, and C371), we hypothesized that wild-type RocA would only be labeled under conditions that allowed MPB to access the cytoplasm. We used a wild-type *rocA* allele containing a FLAG-tag epitope at the C-terminus (59, 61). Whole genome sequencing confirmed the absence of spurious mutations in this isogenic clone. No difference in GAS growth in nutrient rich broth or secreted NAD⁺-glycohydrolase (SPN) activity was observed due to the addition of the FLAG-tag epitope (Fig. A-10) (53, 56). As seen in Table 4-1 and Figure A-11A, both of the labeling agent treatment samples contained RocA-FLAG protein, and RocA-FLAG was only labeled with MPB under conditions that allowed the labeling reagent to access intracellular cysteine residues. Based on these data, we conclude that all naturally-occurring accessible cysteine residues in the wild-type RocA-FLAG protein are located in the cytoplasm. Thus, SCAMTM can be used to differentiate between strategically engineered intracellular and extracellular cysteine residues in RocA to subsequently map its membrane topology.

Table 4-1 Experimentally determined cellular location for RocA residues, as determined by SCAM™.

RocA Variant ^a	MPB Labeling		RocA-FLAG ^d		Interpretation ^e
	Extracellular ^b	Intracellular ^c	Extracellular	Intracellular	
WT	No	Yes	Yes	Yes	Int
E3C	Yes	Yes	Yes	Yes	Ext
L34C	No	Yes	Yes	Yes	Int
H60C	Yes	Yes	Yes	Yes	Ext
K88C	No	Yes	Yes	Yes	Int
S121C	Yes	Yes	Yes	Yes	Ext
Q160C	No	Yes	Yes	Yes	Int
L192C	Yes	Yes	Yes	Yes	Ext
Q225C	No	Yes	Yes	Yes	Int

^aRocA allele assayed. All variants had a C-terminal FLAG-tag. WT, wild-type RocA variant.

^bDefined as band present for avidin labeling by MPB without sonication.

^cDefined as band present for avidin labeling by MPB when pretreated with AMS and sonication.

^dPresence of RocA-FLAG protein in indicated sample, as determined by an anti-FLAG-tag antibody.

^eLocation of engineered cysteine residue, as defined in “RocA Variant” column. For WT, location of native cysteine residues that were labeled by MPB. Ext, extracellular; Int, intracellular.

Based on the *in silico* predictions, we engineered eight cysteine residue mutants in RocA-FLAG to determine the number and localization of the N-terminal transmembrane helical boundaries: E3C, L34C, H60C, K88C, S121C, Q160C, L192C, and Q225C. The first mutant (E3C) was created to determine the N-terminus locale, the next 6 mutants (L34C, H60C, K88C, S121C, Q160C, L192C) were designed to define the intervening loops, and the final mutant (Q225C) was created at the boundary between the N-terminal transmembrane and C-terminal cytoplasmic domains (56, 59). Whole genome sequencing confirmed the absence of spurious mutations in each cysteine engineered mutant strain. No difference in GAS growth in nutrient rich broth or secreted SPN activity was observed due to the introduction of the engineered cysteine residues (Fig. A-12). As seen in Table 4-1 and Figure A-11B, RocA-FLAG mutants E3C, H60C, S121C, and L192C had labeling profiles suggestive of an extracellular localization. The RocA-FLAG mutants L34C, K88C, Q160C, and Q225C had labeling profiles suggestive of an intracellular localization (Table 4-1 and Figure A-11B).

4.3.3. RocA-PhoA-LacZ α protein fusions are consistent with the *in silico* algorithm predictions and SCAMTM results

As a second complementary method to experimentally determine RocA topology, we used a PhoA-LacZ α protein fusion system in *Escherichia coli* (71-78). We designed an expression construct to fuse RocA to PhoA-LacZ α at selected amino acids based on the *in silico* algorithm consensus topology predicting an intracellular or extracellular location. Using this experimental strategy, extracellular fusions result in a protein fusion with high alkaline phosphatase activity and low β -galactosidase activity, whereas cytoplasmic (intracellular) fusions result in a protein fusion with low alkaline phosphatase activity and high β -galactosidase activity. Additionally, β -galactosidase and alkaline phosphatase activities can be measured simultaneously using this protein fusion approach, allowing for normalization of the resulting activities and accurate localization determination (71). RocA protein fusions were designed to occur within the six predicted intervening loops (L34, H60, K88, S121, Q160, L192; Fig. 4-1). To determine if an eighth transmembrane helix exists and to identify the location of the C-terminus, we also designed RocA protein fusions to occur at A360 and D451, respectively (Fig. 4-1).

We constructed RocA protein fusions in plasmid pKTop, transformed them into *E. coli* strain DH5 α , and performed β -galactosidase and alkaline phosphatase assays (77, 78). Sanger sequencing confirmed the correct protein fusions were generated with no spurious mutations. Results are shown in Table 4-2 and Figure A-13A. In general, the RocA-PhoA-LacZ α data supported the *in silico* prediction model (Fig. 4-1). Our results indicated that residues H60 and S121 are located extracellularly, and residues K88, Q160, A360, and D451 are located intracellularly, as predicted. However, assays using residues L34 and L192

Table 4-2 Normalized activity ratios (NARs) and experimentally determined cellular location for RocA residues.

RocA Residue ^a	Initial Experimental Design		Additional Experimental Design	
	NAR ^b	Location ^c	NAR	Location
K24	-	-	0.03	Int
L34	0.77	Ind	0.98	Ind
L44	-	-	0.03	Int
H60	7.74	Ext	5.96	Ext
K88	0.01	Int	0.02	Int
S121	4.03	Ext	2.12	Ext
Q160	0.02	Int	0.02	Int
C181	-	-	0.09	Int
L192	0.55	Ind	0.85	Ind
R201	-	-	0.28	Int
Q225	-	-	0.22	Int
A360	0.09	Int	0.13	Int
D451	0.04	Int	0.06	Int

^aTerminal residue of RocA followed by PhoA-LacZ α reporter.

^bNAR calculated as relative alkaline phosphatase activity/relative β -galactosidase activity (78).

^cLocation determined by NAR. Ext, extracellular; Ind, indeterminate; Int, intracellular.

indicated an indeterminate localization for these residues (Table 4-2 and Fig. A-13A). That is, we could not determine whether L34 and L192 were extracellular or intracellular with high certainty with this methodology. To better define the loops containing amino acids L34 and L192, four additional neighboring residues were chosen to create new protein fusions (K24, L44, C181, R201; Fig. 4-1). A protein fusion at Q225 was also created to determine the end boundary of the seventh transmembrane helix. Our results demonstrated that K24, L44, C181, R201, and Q225 are located intracellularly (Table 4-2 and Fig. A-13B).

4.3.4. Summary of the RocA protein topology experiments

Taken together, the *in silico* algorithm predictions, SCAMTM data, and RocA-PhoA-LacZ α protein fusion data demonstrate that RocA has a seven transmembrane helical architecture with an extracellularly located N-terminus and an intracellularly located C-terminus (Fig. 4-1). The seven transmembrane helices span between: 1) residues 3-34 extracellular to intracellular, 2) residues 34-60 intracellular to extracellular, 3) residues 60-88 extracellular to intracellular, 4) residues 88-121 intracellular to extracellular, 5) residues 121-160 extracellular to intracellular, 6) residues 160-192 intracellular to extracellular, and 7) residues 192-225 extracellular to intracellular (Fig. 4-1). In summary, for the first time,

we have experimentally determined the membrane topology of RocA, which will facilitate investigation into the effect of specific amino acid changes on RocA protein-protein interactions.

4.3.5. RocA interacts with RocA and CovS, but not CovR

After experimentally determining the membrane topological architecture of RocA, we next investigated whether specific amino acid changes could alter RocA protein-protein interactions. Previous attempts to demonstrate a direct interaction between RocA and CovRS have had variable success depending on the experimental methodology used (59, 61). While RocA-RocA and RocA-CovS interactions have been demonstrated by co-immunoprecipitation using cell membrane preparations (59, 61), no direct interaction between RocA and RocA, CovS, or CovR in intact cells has been demonstrated. We used bacterial adenylate cyclase-based two-hybrid (BACTH) assays to first assess wild-type RocA, CovS, and CovR protein-protein interactions (79-81). Briefly, RocA, CovS, and CovR were fused to either T18 or T25, two complementary fragments of the catalytic domain of the *Bordetella pertussis* adenylate cyclase. In this assay, interaction between two proteins in *E. coli* brings T18 and T25 into close proximity, leading to a functional adenylate cyclase that generates cAMP. Interactions are then quantitated by β -galactosidase activity. Sanger sequencing confirmed the correct protein fusions were generated with no spurious mutations.

Since the BACTH constructs used in a previous study only included one set of T18/T25 protein fusions (61), we sought to reassess the usefulness of BACTH for testing RocA-CovRS interactions using all possible combinations of T18/T25-RocA/CovS/CovR fusions (Table B-13 and Fig. A-14). In agreement with previously published data, we observed direct interactions of CovS and CovS, CovR and CovR, and CovR and CovS

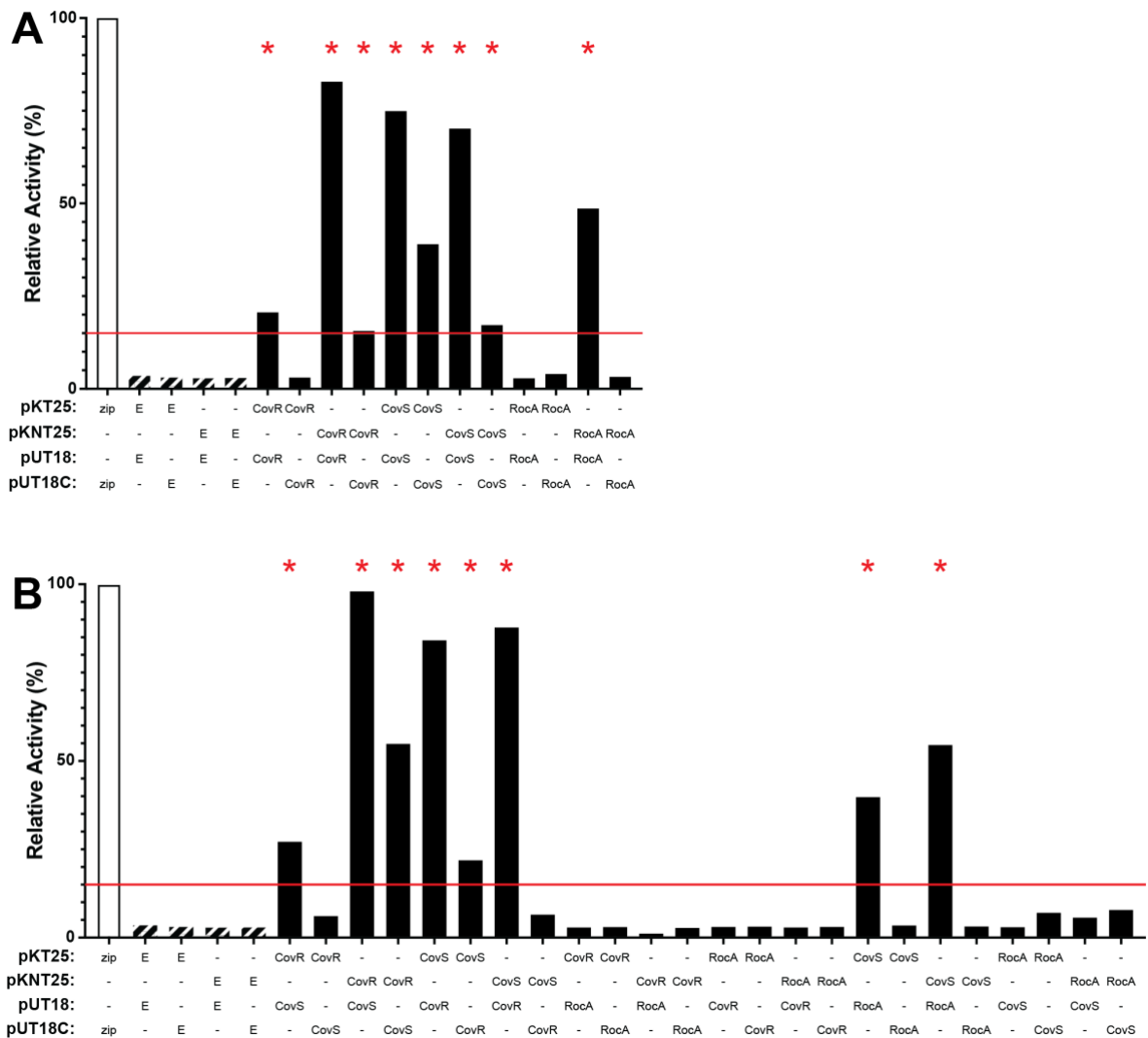


Fig. 4-2 RocA interacts with itself and CovS, but not CovR.

(A-B) Representative BACTH assays performed in *E. coli* strain DHM1 for wild-type RocA, CovS, and CovR homodimers (A) and heterodimers (B). White bar represents the positive control (zip = GCN4 leucine zipper motif), and striped bars represent the negative controls (E = empty plasmid). The red line indicates the positive interaction threshold. A red asterisk indicates a positive interaction between the two assayed proteins.

(Fig. 4-2 and A-15) (61). Additionally, our results demonstrated that RocA interacted with itself (RocA) and CovS but not CovR (Fig. 4-2). Interaction between RocA and RocA or RocA and CovS was only observed when T18/T25 was fused to the C-terminus of RocA (Fig. 4-2 and A-14). That is, consistent with the experimentally determined topology of RocA, only RocA fusions with intracellular T18/T25 (fused at the C-terminus) demonstrated

direct protein-protein interactions. We reproduced these results using a second strain of *E. coli* (Fig. A-15).

4.3.6. Amino acid changes in RocA differentially alter the interaction of RocA with itself and CovS

After demonstrating a direct interaction between the wild-type RocA and CovS proteins, we next tested the hypothesis that single amino acid replacements in RocA can differentially alter its interaction with itself and CovS. We first chose to investigate the RocA P97L, G184W, R258K, and T442P amino acid replacements. The amino acid replacements were selected because they have very well-known effects on the GAS global transcriptome and virulence in mice and nonhuman primates (25). Our results demonstrated that amino acid changes P97L, G184W, and T442P disrupted RocA-RocA interactions, whereas amino acid change R258K did not disrupt RocA-RocA interaction (Fig. 4-3A). RocA with amino acid change T442P disrupted interaction with CovS, whereas RocA with amino acid changes G184W and R258K did not (Fig. 4-3B). RocA with amino acid change P97L had an intermediate RocA-CovS interaction phenotype (Fig. 4-3B). Taken together, the BACTH data suggest that specific amino acid changes in RocA have different effects on RocA functionality by altering the RocA-RocA and/or RocA-CovS physical interaction.

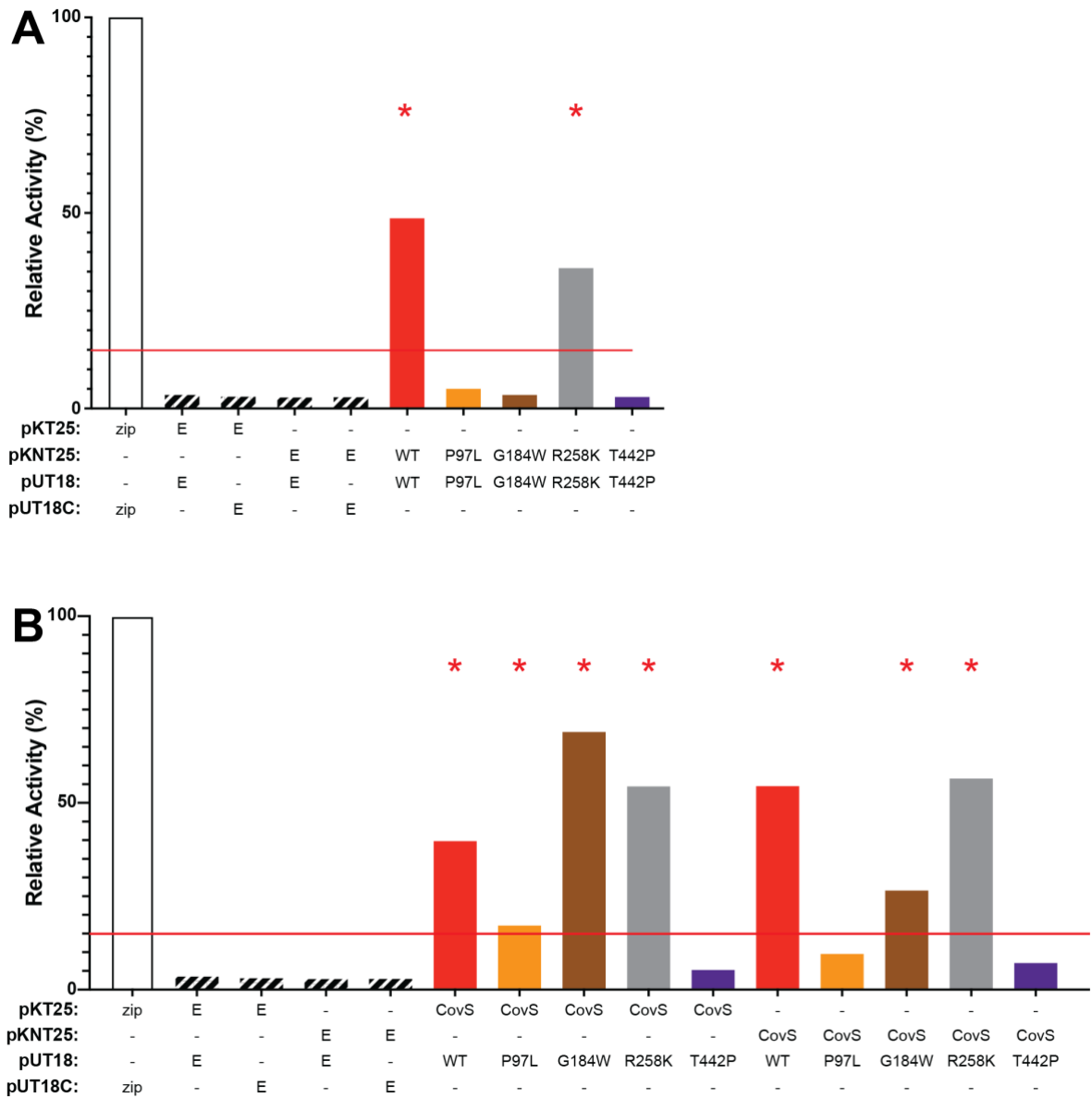


Fig. 4-3 Single amino acid replacements in RocA alter the interaction between RocA and itself and CovS.

(A-B) Representative BACTH assays performed in *E. coli* strain DHM1 for RocA homodimers (A) and RocA-CovS heterodimers (B). The RocA amino acid replacements assayed are indicated (WT = wild-type RocA). White bar represents the positive control (zip = GCN4 leucine zipper motif), and striped bars represent the negative controls (E = empty plasmid). The red line indicates the positive interaction threshold. A red asterisk indicates a positive interaction between the two assayed proteins.

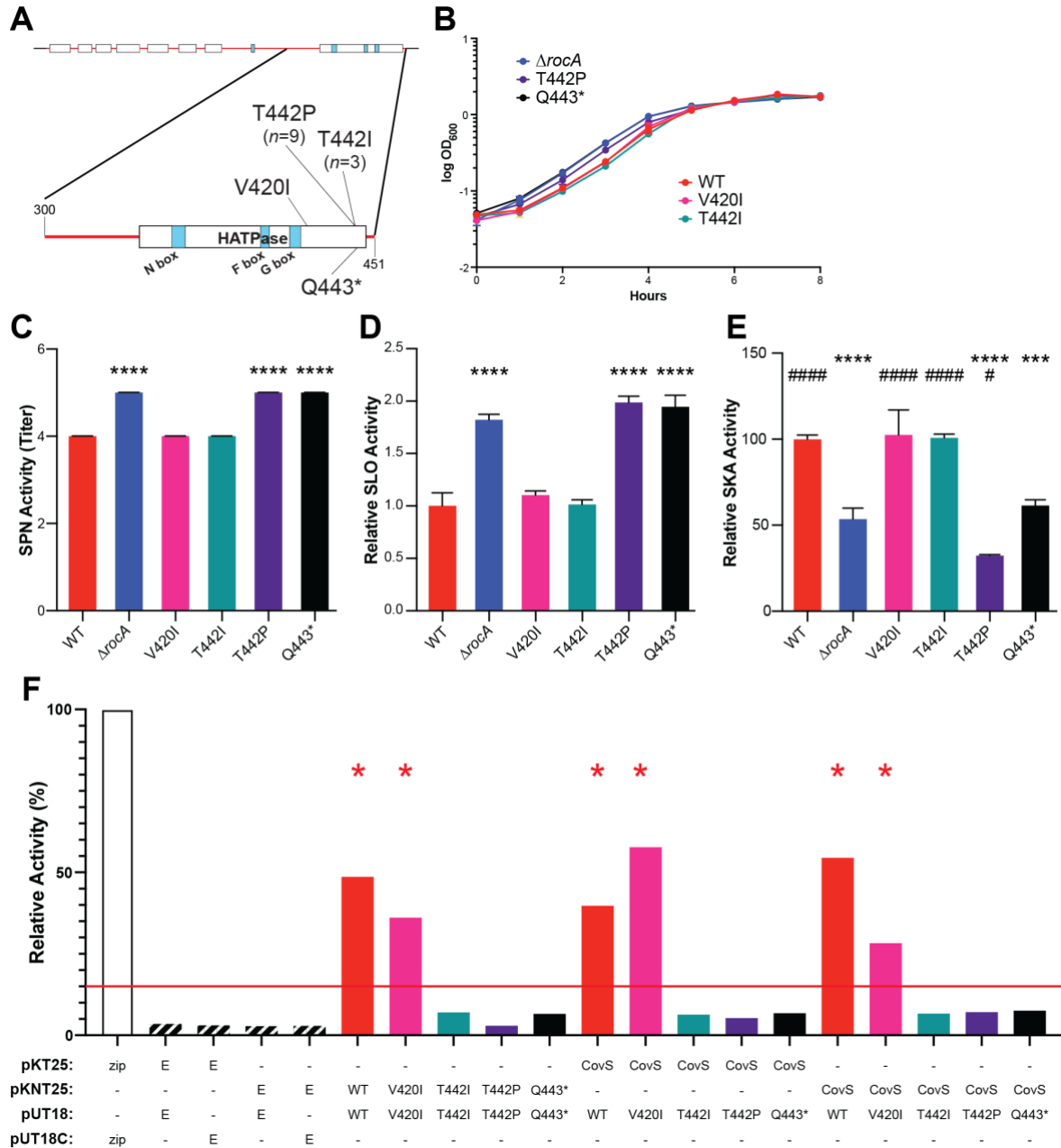


Fig. 4-4 Polymorphisms in the C-terminus of RocA are function-altering.

(A) Protein map of RocA highlighting C-terminus polymorphisms (inset, amino acids 300-451). Predicted domains of the RocA protein are indicated (HATPase, histidine kinase ATPase domain). Predicted functional domains of the putative histidine kinase domain (N box, F box, G box) are identified (42). (B) Growth curve in nutrient-rich THY broth. (C) SPN activity assay. (D) SLO activity assay. (E) SKA activity assay. Data are shown as mean \pm standard deviation ($n = 3$). $***P < 0.001$, $****P < 0.0001$, One-way ANOVA with Tukey's multiple comparisons test compared to the parental wild-type (WT) strain; $*P < 0.05$, $####P < 0.0001$, One-way ANOVA with Tukey's multiple comparisons test compared to the isogenic $\Delta rocA$ deletion mutant strain. (F) Representative BACTH assays performed in *E. coli* strain DHM1 for RocA homodimers and RocA-CovS heterodimers. The RocA amino acid replacements assayed are indicated (WT = wild-type RocA). White bar represents the positive control (zip = GCN4 leucine zipper motif), and striped bars represent the negative controls (E = empty plasmid). The red line indicates the positive interaction threshold. A red asterisk indicates a positive interaction between the two assayed proteins.

4.3.7. Polymorphisms in the C-terminus of RocA are function-altering

A previous study of isogenic *rocA* polymorphism mutants found that mutation of the RocA C-terminus resulted in a *rocA* deletion-like phenotype (25). The results were unexpected, since the C-terminus of RocA had not been previously implicated in RocA functionality (56, 59). We therefore sought to further characterize the role of the RocA C-terminus in GAS molecular pathogenesis. In addition to the previously studied T442P mutation, we identified three other naturally-occurring mutations of interest in the C-terminus of RocA, including V420I, T442I, and Q443* (glutamine 443 replaced with a stop codon; Fig. 4-4A) (25, 57). We constructed isogenic mutant strains, and whole genome sequencing confirmed the absence of spurious mutations. To determine if C-terminal RocA amino acid changes alter the growth phenotype, we grew the parental wild-type strain, isogenic $\Delta rocA$ deletion mutant strain, and four C-terminal *rocA* mutant strains in nutrient-rich Todd-Hewitt broth with yeast extract (THY). While the growth curves of the RocA V420I and T442I mutant strains were similar to the parental wild-type strain, the RocA T442P and Q443* mutant strain growth curves were more similar to the isogenic $\Delta rocA$ strain that has a shortened lag phase (Fig. 4-4B) (25).

Next, to test the hypothesis that amino acid changes in the RocA C-terminus result in altered virulence, we performed *in vitro* virulence factor activity assays. The RocA V420I and T442I isogenic mutant strains had wild-type-like secreted SPN, streptolysin O (SLO), and streptokinase (SKA) activities (Fig. 4-4C-E). In contrast, the $\Delta rocA$ and RocA T442P and Q443* isogenic mutant strains had significantly increased SPN and SLO activity, and significantly decreased SKA activity, compared to the parental wild-type strain (Fig. 4-4C-E). As previously observed (25), the RocA T442P isogenic mutant strain had significantly

decreased SKA activity compared to the isogenic $\Delta rocA$ deletion mutant strain (Fig. 4-4E). The SKA activity of the RocA Q443* isogenic mutant strain did not significantly differ from the secreted SKA activity of the isogenic $\Delta rocA$ deletion mutant strain (Fig. 4-4E). These results are consistent with the BACTH analysis that demonstrated RocA T442P and Q443* variant proteins do not directly interact with themselves or CovS (that is, they behave like *rocA* deletion mutants), whereas RocA V420I interacts with itself and CovS, similar to the wild-type RocA protein (Fig. 4-4F). Interestingly, RocA T442I did not directly interact with itself or CovS (Fig. 4-4F).

Based on the *in vitro* virulence factor assay data, we hypothesized that RocA amino acid replacements T442P and Q443* increase strain virulence. To test this hypothesis, we compared the virulence of the parental wild-type strain, the isogenic $\Delta rocA$ deletion mutant strain, and four C-terminal *rocA* mutant strains in a mouse model of necrotizing myositis (13, 25, 57, 82, 83). Consistent with our hypothesis, the isogenic $\Delta rocA$ deletion and RocA T442P and Q443* mutant strains caused significantly increased mortality and larger lesions with more tissue destruction compared with the parental wild-type strain and wild-type-like RocA V420I and T442I mutant strains (Fig. 4-5).

Altogether, the data demonstrate that the C-terminus of RocA, in addition to the N-terminal transmembrane domain, is important for RocA protein-protein interactions and molecular pathogenesis.

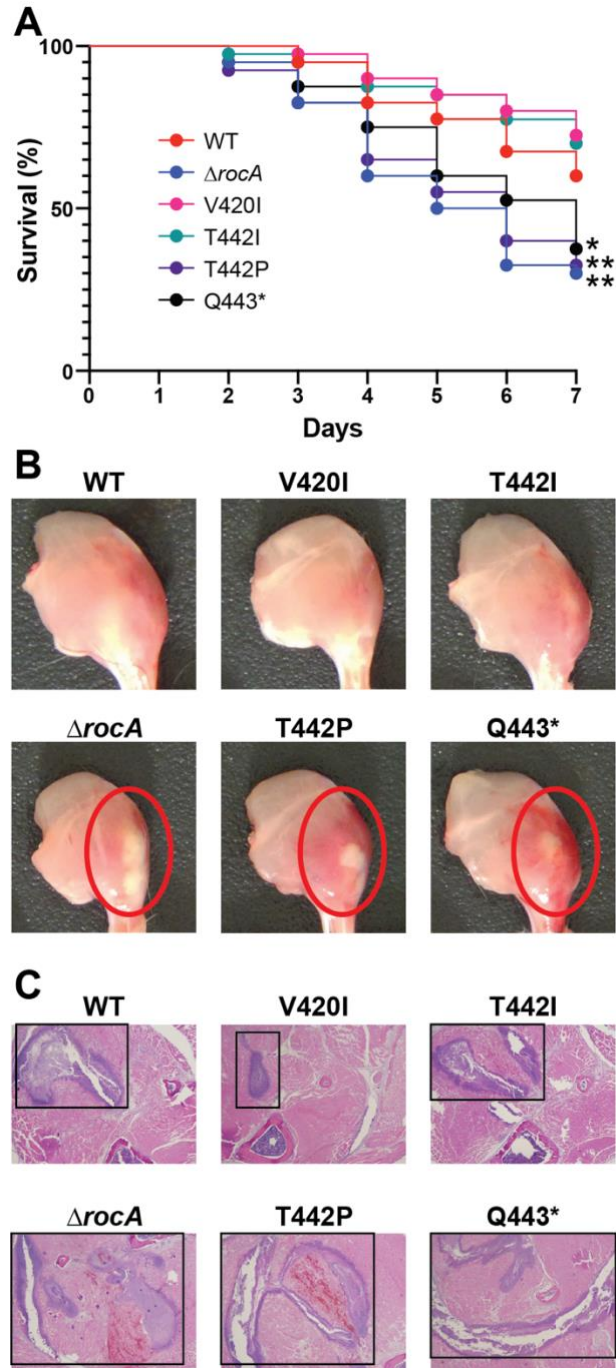


Fig. 4-5 Polymorphisms in the C-terminus of RocA result in altered virulence in a mouse model of necrotizing myositis.

(A) Kaplan-Meier survival curve for mice infected in the right hindlimb with the indicated strain ($n = 40$ mice/strain). $*P < 0.05$, $**P < 0.01$, log rank test compared to the parental wild-type (WT) strain. (B) Representative gross lesions of the infected limb on post-inoculation day 2 ($n = 4$ mice/strain). Abscesses are encompassed by red circles. (C) Representative microscopic lesions of the infected limb on post-inoculation day 1 ($n = 4$ mice/strain). The necrotic lesions are encompassed by black boxes. Hematoxylin and eosin staining was used. Original magnification, 4X.

4.4. Discussion

In recent years, virulence regulation in GAS has focused on transcription regulators such as the CovRS two-component system and its regulatory accessory protein RocA (25, 46-61). Two key knowledge gaps bearing on the molecular pathogenesis of RocA, and accessory proteins in general, are 1) how accessory proteins interact with two-component system proteins, and 2) how naturally-occurring amino acid replacements alter this interaction. Herein, we demonstrate that RocA is a seven transmembrane helix regulatory accessory protein (Fig. 4-1) that interacts with itself (RocA) and CovS, but not CovR (Fig. 4-2). Different amino acid replacements in RocA had different effects on RocA-RocA and RocA-CovS interactions (Fig. 4-3 and 4-4). The disrupted protein-protein interactions lead to significant changes in gene expression, secreted virulence factor activity *in vitro*, and virulence *in vivo* (Fig. 4-5 and 4-6) (25).

We confirmed *in silico* algorithm predictions of RocA membrane topology using two independent experimental methodologies. Some previous published studies predicted six transmembrane helices (55, 56, 58, 61). Herein, results from our topology analyses using two independent methodologies demonstrate that RocA has seven transmembrane helices (Fig. 4-1 and Tables 4-1 and 4-2). SCAMTM assays demonstrated that the N-terminal half of RocA has seven transmembrane helices and the N-terminus is located extracellularly (Fig. 4-1 and Table 4-1). The SCAMTM results were confirmed with RocA-PhoA-LacZ α protein fusions. For the most part, the RocA-PhoA-LacZ α protein fusions expressed in *E. coli* recapitulated the SCAMTM data, with a few indeterminate results, and determined the C-terminus of RocA is located intracellularly (Table 4-2 and Fig. A-13). However, two major limitations to the RocA-PhoA-LacZ α protein fusion methodology are 1) it does not use the

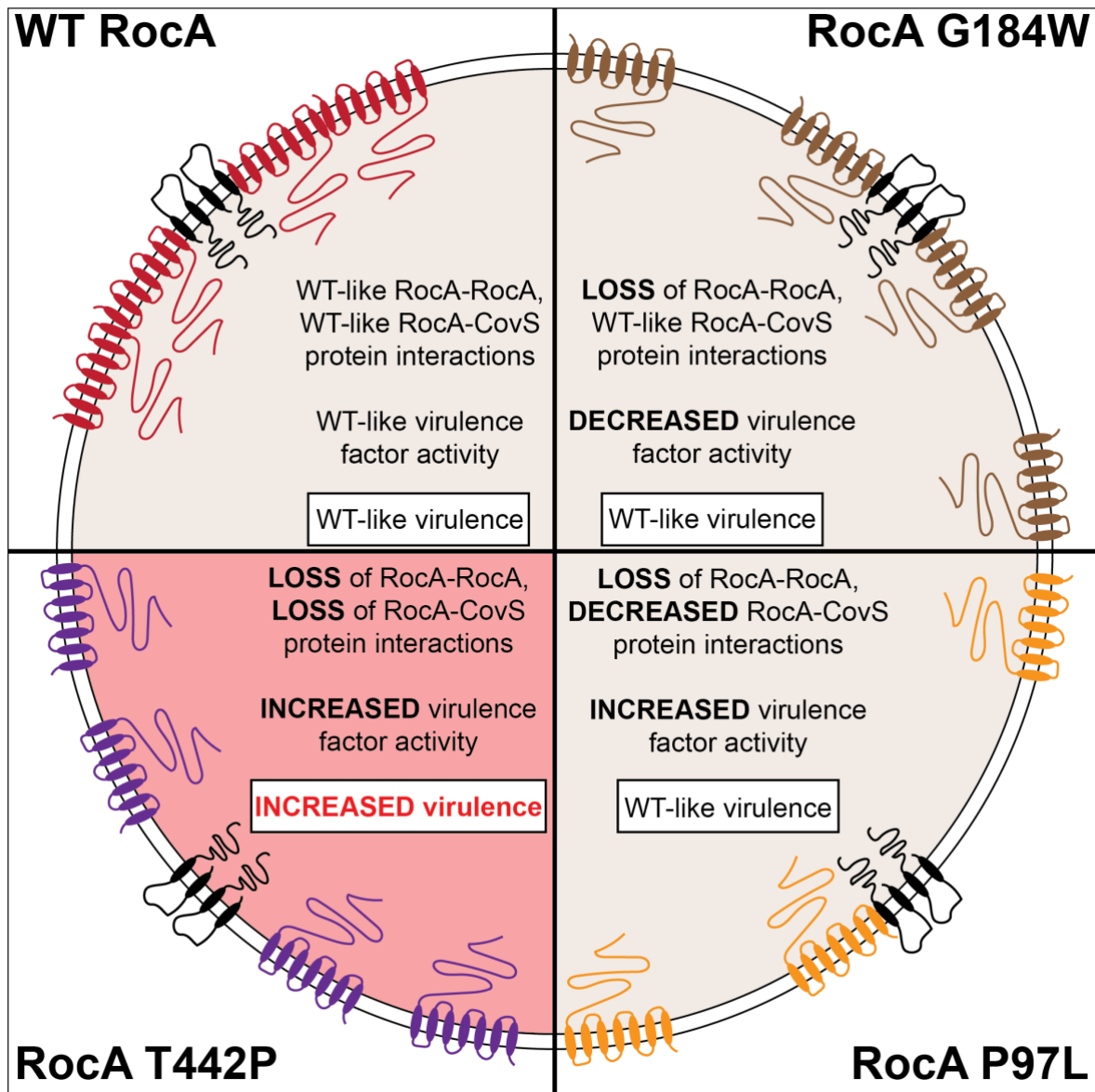


Fig. 4-6 Single amino acid replacements in RocA alter RocA-RocA and RocA-CovS interactions, leading to altered gene expression and virulence.

Under normal conditions (wild-type (WT) RocA, upper left), RocA (blue) interacts with itself and CovS (black), resulting in WT virulence factor expression and secreted activity *in vitro*, and virulence *in vivo*. The RocA G184W amino acid change (brown, upper right) causes a loss of RocA dimerization, but retention of the RocA-CovS interaction, resulting in decreased virulence factor expression and activity *in vitro* but WT-like virulence *in vivo*. The RocA P97L amino acid change (orange, lower right) causes a loss of the RocA-RocA interaction and a transient RocA-CovS interaction, resulting in increased virulence factor expression and activity *in vitro* but WT-like virulence *in vivo*. The RocA T442P (purple, lower left) causes a loss of RocA-RocA and RocA-CovS interactions, resulting in increased virulence factor expression and activity *in vitro* and increased virulence *in vivo*.

full-length protein to determine residue locations, and 2) it is not performed in the native host bacterium. Numerous factors, beyond amino acid sequence, may determine the

membrane topology of transmembrane helices (84-92). Nevertheless, our SCAMTM and protein fusion studies suggest that factors outside of the transmembrane domain amino acid composition may participate in membrane insertion of some RocA transmembrane domains, particularly transmembrane domains 1 and 6.

Two recent studies have demonstrated an interaction between RocA and CovS proteins using co-immunoprecipitation methodologies with cell membrane preparations (59, 61). However, there is no experimental evidence demonstrating direct RocA-RocA or RocA-CovS interaction in intact cells (61). Herein, using a BACTH assay, we unambiguously demonstrated that RocA interacts with itself and CovS in intact cells (Fig. 4-2). In the previous study, Jain, et al. were unable to demonstrate a direct RocA-RocA or RocA-CovS interaction in a BACTH assay. One possible reason is due to the use of N-terminal protein fusions (61). Given that the N-terminus of RocA is extracellularly located (Fig. 4-1), the N-terminal RocA-T18/T25 protein fusion would also be located extracellularly, rendering a negative result regardless of any protein-protein interaction. Consistent with the membrane topology of RocA (Fig. 4-1), the C-terminal RocA-T18/T25 protein fusions used in our study demonstrated direct RocA-RocA and RocA-CovS interactions (Fig. 4-2). Understanding the topological architecture was crucial to making these discoveries and guiding downstream experiments using RocA variants with single amino acid replacements.

A majority of the CovR/CovS-T18/T25 protein fusion construct pairs demonstrated a positive interaction between CovS and CovS, CovR and CovR, and CovR and CovS (Fig. 4-2 and A-15). However, only a C-terminal RocA-T18 protein fusion construct was able to directly interact with CovS (Fig. 4-2, A-15, and A-16). The two plasmid backbones used for the assay differ in their replication origins and copy numbers (81). pUT18 and pUT18C have

a ColE1 high copy number replication origin, whereas pKT25 and pKNT25 have a p15A low copy number replication origin (81). Direct interaction between RocA and CovS was observed only when RocA was expressed from a high copy number plasmid (pUT18) and CovS was expressed from a low copy number plasmid (pKT25/pKNT25; Fig. 4-2). Thus, we speculate that the RocA-CovS interaction only occurs when RocA is present in an excess of CovS, suggesting that RocA and CovS do not merely heterodimerize. That is, under normal conditions, RocA-CovS complexes form only when the stoichiometry of RocA to CovS favors RocA. This discovery can explain the apparent dosage effect of RocA observed in our study and others (Fig. A-4.2 and A-12) (56). A well-defined dosage effect is observed in other regulatory systems, such as the LiaFSR two-component system from *Bacillus subtilis*, where the accessory protein LiaF is present in excess of the histidine kinase LiaS (93), and in GAS, where the MtsR-PrsA-SpeB virulence axis depends on relative amounts of each protein present (13).

Different amino acid changes in RocA resulted in differentially altered RocA-RocA and RocA-CovS physical interactions. The RocA P97L and G184W single amino acid replacements are located in transmembrane helices and generated different protein interaction profiles that corresponded to different virulence phenotypes as defined by secreted virulence factor activity and mortality in mice (Fig. 4-3 and 4-6) (25). The RocA G184W amino acid replacement resulted in a loss of interaction between RocA and RocA, but not between RocA and CovS (Fig. 4-3). A loss of RocA interaction with itself could increase the relative number of RocA G184W protein units available in the membrane to interact with CovS, resulting in decrease virulence factor gene expression and secreted activity *in vitro* (Fig. 4-6) (25). In comparison, the RocA P97L amino acid replacement

resulted in a loss of interaction between RocA and RocA, and interaction between RocA P97L and CovS was only observed for one of the two plasmid construct pairs (Fig. 4-3). A possible explanation for an intermediate phenotype is that the RocA P97L-CovS interaction is more transient than that for the wild-type RocA protein. A transient interaction with CovS could explain the observed discrepant virulence phenotype of an isogenic GAS strain with the RocA P97L variant (25), resulting in increased virulence factor gene expression and secreted activity *in vitro*, but wild-type-like virulence *in vivo*. In support of this idea, a recent dual transcriptome sequencing study of GAS infected nonhuman primate muscle found *rocA* transcripts to be significantly increased *in vivo* compared to *in vitro* conditions (3). Further investigation is warranted to define the host factor(s) that possibly lead to increased *rocA* expression and/or stabilize the RocA-CovS physical interaction *in vivo*.

Previous research has suggested that the RocA cytoplasmic domain is dispensable for RocA-mediated CovRS regulatory functions (56, 59). Our previous study of the RocA T442P variant demonstrated that mutation to the supposed non-functional cytoplasmic domain results in a *rocA* deletion-like phenotype (25). Here, we studied naturally-occurring amino acid changes in the C-terminus of RocA (Fig. 4-4). We demonstrated that loss of the last nine amino acids (RocA Q443*) is sufficient to elicit a RocA deletion-like phenotype (Fig. 4-4 and 4-5), further suggesting a regulatory role for the RocA cytoplasmic domain. BACTH assays demonstrated that the RocA T442P and Q443* variant proteins could not interact with themselves (RocA) or CovS (Fig. 4-4). Interestingly, the RocA T442I amino acid replacement also resulted in a loss of RocA-RocA and RocA-CovS interactions despite having a wild-type-like virulence phenotype (Fig. 4-4). Taken together, the data suggest that threonine 442, both the residue itself (T442P and T442I) and the relative positioning of this

amino acid (T442I and Q443*), is crucial for a wild-type RocA-CovRS regulatory pathway. The molecular basis for these observations is currently under investigation.

In summary, we demonstrate that RocA, an regulatory accessory protein to the virulence regulatory CovRS two-component system, is a seven transmembrane helix protein that directly interacts with itself (RocA) and CovS. Single amino acid replacements in both the transmembrane and cytoplasmic domains result in altered RocA-RocA and/or RocA-CovS interactions that affect downstream gene expression, secreted virulence factor activity *in vitro*, and virulence *in vivo* (Fig. 4-6) (25). In total, our study provides evidence that, under normal conditions, a full-length, wild-type RocA protein is needed to interact with CovS at a tightly regulated stoichiometry for wild-type gene regulation, and single amino acid replacements in an regulatory accessory protein can drastically alter the virulence of a major human pathogen.

4.5. Experimental procedures

4.5.1. Strains and culture conditions

We used serotype M28 GAS strain MGAS28426 because it is genetically representative of serotype M28 GAS strains circulating globally (27), it has a wild-type allele for all major virulence factors and transcription regulators, including *rocA* and *covRS*, and it has been used in multiple animal virulence models (25, 27, 57). Information about this strain and its derivatives is provided in Table B-13 (25, 57, 77, 94). GAS strains were grown in Todd-Hewitt broth supplemented with 0.2% yeast extract (THY), with chloramphenicol (10 $\mu\text{g mL}^{-1}$) as needed. For standard cloning and PhoA-LacZ α reporter fusion studies, we used *E. coli* strain DH5 α . For bacterial adenylate cyclase-based two-hybrid (BACTH) assays, we

used *E. coli* strains DHM1 and BTH101. *E. coli* strains were grown in LB broth at 37 °C with agitation, with ampicillin (100 µg mL⁻¹) and/or kanamycin (50 µg mL⁻¹) as needed.

4.5.2. *In silico* modeling and prediction of RocA membrane topology

The wild-type RocA protein sequence (GenBank AAX72469.1) was used to model and predict the membrane topology of RocA. Multiple algorithms were used to determine a consensus topology (Fig. 4-1 and A-9) that was used for codon selection in membrane topology experiments. The algorithms used included: Phobius (<http://phobius.sbc.su.se/>) (62); Philius (<http://www.yeastrc.org/philius/pages/philius/runPhilius.jsp>) (63); OCTOPUS (<http://octopus.cbr.su.se/>) (64); PolyPhobius (<http://phobius.sbc.su.se/poly.html>) (65); SPOCTOPUS (<http://octopus.cbr.su.se/index.php>) (66); SCAMPI (<http://topcons.cbr.su.se/>) (67); MEMSAT-SVM (<http://bioinf.cs.ucl.ac.uk/psipred/>) (68); and Phyre2 (<http://www.sbg.bio.ic.ac.uk/phyre2/html/page.cgi?id=index>) (69). All membrane topology predictions were accessed on January 17, 2020.

4.5.3. Construction of cysteine-engineered RocA-FLAG-tag plasmids and strains

Based on the predicted membrane topology of RocA (Fig. 4-1), cysteine residue codons were engineered into a wild-type *rocA* gene allele with a C-terminal FLAG-tag epitope on plasmid pDC123 expressed in the serotype M28 GAS isogenic $\Delta rocA$ deletion mutant strain (25, 57). Briefly, we introduced the FLAG-tag epitope and engineered cysteine residues into the wild-type *rocA* allele by PCR using primers FLAGRocA-F and the corresponding cysteine primer-R, and FLAGRocA-R and the corresponding cysteine primer-F (Table B-14) (25, 53). The two resulting fragments were fused together by combinatorial PCR using primers RocA-FLAG_fwd and RocA-FLAG_rev1. Plasmid pDC123 was amplified using primers pDC123_fwd1 and pDC123_rev, and the two resulting

products were circularized using the NEBuilder HiFi DNA Assembly kit (New England BioLabs, Ipswich, MA). The resulting plasmid was transformed into the serotype M28 GAS isogenic $\Delta rocA$ deletion mutant strain (25, 57). The genomes of all transformants were sequenced to verify correct insertion of the engineered cysteine residues and FLAG-tag epitope and absence of spurious mutations.

To ensure that the engineered cysteine residues and FLAG-tag epitope did not result in an altered growth or secreted NAD⁺-glycohydrolase (SPN) activity phenotype, we generated two additional plasmids as described above: pDC123 expressing a wild-type *rocA* allele, and pDC123 expressing a wild-type *rocA* allele with a C-terminal FLAG-tag epitope. These plasmids were transformed into the isogenic $\Delta rocA$ deletion mutant, and resulting transformants were sequenced to verify correct plasmid and genome sequences.

4.5.4. Membrane topology studies: Substituted-cysteine accessibility method as applied to transmembrane orientation (SCAMTM)

The membrane topology of the N-terminal transmembrane helices of RocA was determined using SCAMTM as previously described (70), with minor modifications. Strains carrying plasmids with the engineered cysteine residues and FLAG-tag epitope in *rocA* were grown to the mid-exponential growth phase, pelleted by centrifugation, washed with phosphate-buffered saline (PBS), and resuspended in Buffer A (100 mM HEPES-KOH pH 8.1, 250 mM sucrose, 25 mM MgCl₂, 0.1 mM KCl). For labeling of accessible extracellular cysteine residues, cells were treated with 3-(*N*-maleimido-propionyl)biocytin (MPB; 100 μ M) for five minutes, followed by quenching with 20 mM β -mercaptoethanol. Samples were then sonicated at an amplitude of 15% for one minute. For labeling of accessible intracellular cysteine residues, cells were pre-treated with non-detectable, water-soluble 4-acetamido-4'-

maleimidylstilbene-2,2'-disulfonic acid (AMS; 5 mM) for 30 minutes in the dark with end-over-end rotation to block accessible extracellular cysteine residues. Cells were pelleted and washed twice with Buffer A to remove excess AMS, then resuspended in Buffer A. AMS-pretreated samples were then treated with MPB (100 μ M) for five minutes in total: one minute with sonication at an amplitude of 15%, and four minutes without sonication. Samples were quenched with 20 mM β -mercaptoethanol.

All samples were centrifuged (65,000 X g, 10 minutes, 4 $^{\circ}$ C), and the resulting membranes were resuspended in Buffer A with 20 mM β -mercaptoethanol. Solubilization buffer (50 mM Tris-HCl, pH 8.1, 2% SDS, 0.1 mM EDTA) was added, and the samples were vortexed for 15 minutes at room temperature, incubated at 37 $^{\circ}$ C for 15 minutes, and vortexed again for 15 minutes at room temperature. Samples were diluted with IP1 (50 mM Tris-HCl, pH 8.1, 0.15 M NaCl, 0.1 mM EDTA, 2% nonaethylene glycol monododecyl ether, 0.4% SDS) and pelleted. The resulting supernatant was transferred to a spin column and incubated overnight with anti-FLAG-tag antibody (Abcam, Cambridge, MA, catalog # ab2493; 1:100) with rocking at 4 $^{\circ}$ C.

Protein A/G-agarose affinity resin was added to the samples for a 90 minute incubation at 4 $^{\circ}$ C. The resin was washed with IP1, IP2 (50 mM Tris-HCl, pH 8.1, 1 M NaCl, 0.1 mM EDTA, 2% nonaethylene glycol monododecyl ether, 0.4% SDS), and 10 mM Tris-HCl, pH 8.1. Protein from the samples was extracted in 2X SDS sample buffer (vortexed for 15 minutes at room temperature, incubated at 37 $^{\circ}$ C for 15 minutes, and vortexed again for 15 minutes at room temperature, followed by elution via centrifugation). Samples were subjected to SDS-PAGE, transferred to nitrocellulose membranes, and visualized with avidin-HRP as described below. Since conclusions are only made by comparing sample

pairs, differences in expression and/or labeling efficiency between different engineered cysteine mutant proteins were not determined and are not important.

4.5.5. Western immunoblot analysis

For determination of RocA-FLAG protein expression, whole cell lysates prepared from cells at the mid-exponential growth phase were subjected to SDS-PAGE and transferred to nitrocellulose membranes. Membranes were blocked with 5% milk in PBS with 0.1% Tween™ 20 (PBS-T) for 1 hour before incubation with anti-FLAG-tag antibody (Abcam, Cambridge, MA, catalog # ab2493; 1:5000) for 2 hours. Membranes were washed with PBS-T three times before detection using SuperSignal™ West Pico Plus Chemiluminescent Substrate (ThermoFisher Scientific, Waltham, MA). For determination of MPB labeling, samples were subjected to SDS-PAGE and transferred to nitrocellulose membranes. Membranes were blocked with 5% bovine serum albumin (BSA) in Tris-buffered saline (TBS) overnight before incubation with avidin-HRP (1:5000 in 0.3% BSA in TBS) for 2 hours. Membranes were washed with 0.3% BSA in TBS twice, 0.5% IgePal CA-630 in TBS twice, and TBS once before detection using SuperSignal™ West Femto Maximum Sensitivity Substrate (ThermoFisher Scientific, Waltham, MA).

4.5.6. Membrane topology studies: PhoA-LacZ α protein fusions

The membrane topology of RocA was determined using a PhoA-LacZ α reporter system (78). Reporter plasmid pKTop was used (77) to create RocA fragment PhoA-LacZ α protein fusions after selected RocA amino acids (Fig. 4-1). The *rocA* fragments were PCR amplified from genomic DNA of strain MGAS28426 using the appropriate primers (Table B-14), and pKTop was cleaved using BamHI. Both the linearized vector and PCR amplified fragment were transformed into *E. coli* DH5 α cells as previously described (95). Plasmids

(Table B-13) were verified for the correct insert sequence by Sanger sequencing (Table B-14).

β -galactosidase and phosphatase assays were conducted using *E. coli* DH5 α cells containing pKTop-RocA protein fusion plasmids as previously described (78), with minor modifications. Briefly, a single colony from an LB agar plate with kanamycin and 0.1% glucose was inoculated into LB broth with kanamycin and 0.1% glucose overnight. The overnight culture was diluted 1:100 into fresh LB broth with kanamycin and 0.1% glucose and grown to the mid-exponential growth phase. Isopropyl- β -D-1-thiogalactopyranoside (IPTG; 1 mM) was added, and cultures were incubated for one hour.

For the β -galactosidase assay, cells were resuspended in M63 medium (100 mM potassium phosphate monobasic, 15 mM ammonium sulfate, 1.7 μ M ferrous sulfate, 1 mM magnesium sulfate, pH 7.0) and permeabilized with chloroform and 0.05% sodium dodecyl sulfate (SDS). Permeabilized cells were incubated with 0.15% *o*-nitrophenyl- β -galactoside (ONPG) in PM2 buffer (70 mM sodium phosphate dibasic, 30 mM sodium phosphate monobasic, 1 mM magnesium sulfate, 0.2 mM manganese sulfate, 100 mM β -mercaptoethanol, pH 7.0) at 37 °C for one hour. Absorbance was measured, and β -galactosidase enzymatic activity was determined as previously described (78).

For the phosphatase assay, cells were washed with wash buffer (10 mM Tris-HCl, pH 8.0, 10 mM magnesium sulfate), resuspended in PM1 buffer (1 M Tris-HCl, pH 8.0, 0.1 mM zinc chloride, 1 mM iodoacetamide) and permeabilized with chloroform and 0.05% SDS. Permeabilized cells were incubated with 0.15% *p*-nitrophenyl phosphate (pNPP) in 1 M Tris-HCl, pH 8.0, at 37 °C for one hour. Absorbance was measured, and phosphatase enzymatic activity was determined as previously described (78).

To determine the localization of each protein fusion, the normalized activity ratio (NAR) was calculated as previously described (78). An NAR > 2 was considered highly likely to be extracellular, an NAR < 0.5 was considered highly likely to be intracellular, and an NAR between 0.5 and 2 was considered to be indeterminate.

4.5.7. Bacterial adenylate cyclase-based two-hybrid (BACTH) assays

Interactions between RocA, CovR, and CovS were assessed using BACTH assays (79-81). Plasmids pKNT25, pKT25, pUT18, and pUT18C (Euromedex) were used for constructing T25 and T18 fusions, respectively. The *rocA*, *covR*, and *covS* alleles were PCR amplified from genomic DNA of serotype M28 GAS strain MGAS28426 or the respective isogenic *rocA* mutant strain (Table B-13) using the appropriate primers (Table B-14), and plasmids were cleaved using BamHI. Both the linearized vector and PCR amplified fragment were transformed into *E. coli* DH5 α cells as previously described (95). Plasmids (Table B-13) were verified for the correct insert sequence by Sanger sequencing (Table B-14). Once verified, plasmids were transformed into either DHM1 or BTH101 cells for the assay. PCR analysis was used to verify the correct plasmid backbones and inserts after transformation.

For quantification of the interaction between protein fusions, a β -galactosidase assay was performed as previously described (81). Briefly, a single colony from an LB agar plate with kanamycin, ampicillin, and 0.1% glucose was inoculated into LB broth with ampicillin, kanamycin, and 0.5 mM IPTG and grown overnight. Cultures were diluted fivefold with M63 medium and permeabilized with chloroform and 0.05% SDS. Permeabilized cells were added to PM2 buffer containing 0.1% ONPG. The reaction was incubated at 37 °C for 30 minutes, absorbance was measured, and β -galactosidase enzymatic activity was determined as previously described (81). Plasmids containing GCN4 leucine zipper motifs (Euromedex)

were used as a positive control, and empty plasmids were used as a negative control. Proteins were considered to have a positive interaction if the resulting β -galactosidase activity was at least five times higher than the negative controls (81).

4.5.8. Generation of isogenic C-terminal *rocA* polymorphism strains

Isogenic strains containing C-terminal *rocA* polymorphisms (25, 57) were generated in the serotype M28 parental wild-type strain MGAS28426. The isogenic RocA T442P mutant strain has been previously described (25). The additional isogenic C-terminal *rocA* polymorphism strains (RocA V420I, T442I and Q443*) were constructed by allelic exchange (the allele of interest was cloned from a clinical isolate with the naturally-occurring *rocA* polymorphism) as previously described (22, 25). Primer sequences are listed in Table B-14. Whole genome sequence analysis of the isogenic C-terminal *rocA* mutant strains confirmed the expected *rocA* polymorphism and absence of spurious mutations.

4.5.9. *In vitro* virulence factor activity assays

SPN and streptolysin O (SLO) activity was measured as previously described using mid-exponential growth phase culture supernatants (83). Streptokinase (SKA) activity was measured as previously described using mid-exponential growth phase cell-free culture supernatants (15, 25, 57).

4.5.10. Mouse model of necrotizing myositis

Mouse necrotizing fasciitis/myositis studies were performed as previously described (13, 25, 57, 82, 83). Immunocompetent 4-week-old female CD1 mice (Envigo Laboratories, Houston, TX) were randomly assigned to treatment groups and inoculated in the right lower hind limb with 5×10^8 colony-forming units of the indicated bacterial strain suspended in PBS ($n = 40$ mice per strain). Mice were monitored at least once daily, and mortality was

determined using the NIH Guide for the Care and Use of Laboratory Animals (96). Survival comparisons were made using the log-rank test. For gross and histologic evaluation, mice ($n = 4$ mice per strain per time point) were sacrificed on day 1 or day 2 post-inoculation, and the limbs were processed using standard methods (13). All animal experiments were approved by the Institutional Animal Care and Use Committee of the Houston Methodist Research Institute (Houston, TX; AUP-0318-0016). Sample sizes were determined with a power calculation.

4.5.11. Statistical analyses

All statistical analyses were performed using Prism 8 (GraphPad Software Inc., La Jolla, CA) with three biological replicates, and $P < 0.05$ was considered statistically significant.

4.6. References

1. Cunningham MW. 2000. Pathogenesis of group A streptococcal infections. *Clin Microbiol Rev* 13:470-511.
2. Walker MJ, Barnett TC, McArthur JD, Cole JN, Gillen CM, Henningham A, Sriprakash KS, Sanderson-Smith ML, Nizet V. 2014. Disease manifestations and pathogenic mechanisms of group A *Streptococcus*. *Clin Microbiol Rev* 27:264-301.
3. Kachroo P, Eraso JM, Olsen RJ, Zhu L, Kubiak SL, Pruitt L, Yerramilli P, Cantu CC, Ojeda Saavedra M, Pensar J, Corander J, Jenkins L, Kao L, Granillo A, Porter AR, DeLeo FR, Musser JM. 2020. New pathogenesis mechanisms and translational leads identified by multidimensional analysis of necrotizing myositis in primates. *mBio* 11:e03363-19.

4. Voyich JM, Sturdevant DE, Braughton KR, Kobayashi SD, Lei B, Virtaneva K, Dorward DW, Musser JM, DeLeo FR. 2003. Genome-wide protective response used by group A *Streptococcus* to evade destruction by human polymorphonuclear leukocytes. *Proc Natl Acad Sci U S A* 100:1996-2001.
5. Shelburne SA, 3rd, Sumby P, Sitkiewicz I, Granville C, DeLeo FR, Musser JM. 2005. Central role of a bacterial two-component gene regulatory system of previously unknown function in pathogen persistence in human saliva. *Proc Natl Acad Sci U S A* 102:16037-16042.
6. Liu M, Hanks TS, Zhang J, McClure MJ, Siemsen DW, Elser JL, Quinn MT, Lei B. 2006. Defects in *ex vivo* and *in vivo* growth and sensitivity to osmotic stress of group A *Streptococcus* caused by interruption of response regulator gene *vicR*. *Microbiology* 152:967-978.
7. Loughman JA, Caparon MG. 2006. A novel adaptation of aldolase regulates virulence in *Streptococcus pyogenes*. *EMBO J* 25:5414-5422.
8. Sitkiewicz I, Musser JM. 2006. Expression microarray and mouse virulence analysis of four conserved two-component gene regulatory systems in group A *Streptococcus*. *Infect Immun* 74:1339-1351.
9. Churchward G. 2007. The two faces of Janus: virulence gene regulation by CovR/S in group A streptococci. *Mol Microbiol* 64:34-41.
10. Hondorp ER, McIver KS. 2007. The Mga virulence regulon: infection where the grass is greener. *Mol Microbiol* 66:1056-1065.

11. Leday TV, Gold KM, Kinkel TL, Roberts SA, Scott JR, McIver KS. 2008. TrxR, a new CovR-repressed response regulator that activates the Mga virulence regulon in group A streptococcus. *Infect Immun* 76:4659-4668.
12. Shelburne SA, Keith D, Horstmann N, Sumbly P, Davenport MT, Graviss EA, Brennan RG, Musser JM. 2008. A direct link between carbohydrate utilization and virulence in the major human pathogen group A *Streptococcus*. *Proc Natl Acad Sci U S A* 105:1698-1703.
13. Olsen RJ, Sitkiewicz I, Ayeras AA, Gonulal VE, Cantu C, Beres SB, Green NM, Lei B, Humbird T, Greaver J, Chang E, Ragasa WP, Montgomery CA, Cartwright J, Jr., McGeer A, Low DE, Whitney AR, Cagle PT, Blasdel TL, DeLeo FR, Musser JM. 2010. Decreased necrotizing fasciitis capacity caused by a single nucleotide mutation that alters a multiple gene virulence axis. *Proc Natl Acad Sci U S A* 107:888-893.
14. Olsen RJ, Musser JM. 2010. Molecular pathogenesis of necrotizing fasciitis. *Annu Rev Pathol Mech Dis* 5:1-31.
15. Ramirez-Pena E, Trevino J, Liu Z, Perez N, Sumbly P. 2010. The group A *Streptococcus* small regulatory RNA FasX enhances streptokinase activity by increasing the stability of the ska mRNA transcript. *Mol Microbiol* 78:1332-1347.
16. Shelburne SA, 3rd, Sahasrobhrajane P, Suber B, Keith DB, Davenport MT, Horstmann N, Kumaraswami M, Olsen RJ, Brennan RG, Musser JM. 2011. Niche-specific contribution to streptococcal virulence of a MalR-regulated carbohydrate binding protein. *Mol Microbiol* 81:500-514.

17. Cao TN, Liu Z, Cao TH, Pflughoeft KJ, Trevino J, Danger JL, Beres SB, Musser JM, Sumbly P. 2014. Natural disruption of two regulatory networks in serotype M3 group A *Streptococcus* isolates contributes to the virulence factor profile of this hypervirulent serotype. *Infect Immun* 82:1744-1754.
18. Tatsuno I, Isaka M, Okada R, Zhang Y, Hasegawa T. 2014. Relevance of the two-component sensor protein CiaH to acid and oxidative stress responses in *Streptococcus pyogenes*. *BMC Research Notes* 7:189.
19. Flores AR, Jewell BE, Yelamanchili D, Olsen RJ, Musser JM. 2015. A single amino acid replacement in the sensor kinase LiaS contributes to a carrier phenotype in group A *Streptococcus*. *Infect Immun* 83:4237-4246.
20. Paluscio E, Caparon MG. 2015. *Streptococcus pyogenes* malate degradation pathway links pH regulation and virulence. *Infect Immun* 83:1162-1171.
21. Sanson M, Makthal N, Gavagan M, Cantu C, Olsen RJ, Musser JM, Kumaraswami M. 2015. Phosphorylation events in the multiple gene regulator of group A *Streptococcus* significantly influence global gene expression and virulence. *Infect Immun* 83:2382-2395.
22. Zhu L, Olsen RJ, Nasser W, Beres SB, Vuopio J, Kristinsson KG, Gottfredsson M, Porter AR, DeLeo FR, Musser JM. 2015. A molecular trigger for intercontinental epidemics of group A *Streptococcus*. *J Clin Invest* 125:3545-3559.
23. Zhu L, Olsen RJ, Nasser W, de la Riva Morales I, Musser JM. 2015. Trading capsule for increased cytotoxin production: contribution to virulence of a newly emerged clade of *emm89 Streptococcus pyogenes*. *mBio* 6:e01378-15.

24. Do H, Makthal N, VanderWal AR, Rettel M, Savitski MM, Peschek N, Papenfort K, Olsen RJ, Musser JM, Kumaraswami M. 2017. Leaderless secreted peptide signaling molecule alters global gene expression and increases virulence of a human bacterial pathogen. *Proc Natl Acad Sci U S A* 114:E8498-E8507.
25. Bernard PE, Kachroo P, Eraso JM, Zhu L, Madry JE, Linson SE, Ojeda Saavedra M, Cantu C, Musser JM, Olsen RJ. 2019. Polymorphisms in regulator of Cov contribute to the molecular pathogenesis of serotype M28 group A *Streptococcus*. *Am J Pathol* 189:2002-2018.
26. Do H, Makthal N, VanderWal AR, Saavedra MO, Olsen RJ, Musser JM, Kumaraswami M. 2019. Environmental pH and peptide signaling control virulence of *Streptococcus pyogenes* via a quorum-sensing pathway. *Nat Commun* 10:2586.
27. Kachroo P, Eraso JM, Beres SB, Olsen RJ, Zhu L, Nasser W, Bernard PE, Cantu CC, Saavedra MO, Arredondo MJ, Strobe B, Do H, Kumaraswami M, Vuopio J, Grondahl-Yli-Hannuksela K, Kristinsson KG, Gottfredsson M, Pesonen M, Pensar J, Davenport ER, Clark AG, Corander J, Caugant DA, Gaini S, Magnussen MD, Kubiak SL, Nguyen HAT, Long SW, Porter AR, DeLeo FR, Musser JM. 2019. Integrated analysis of population genomics, transcriptomics and virulence provides novel insights into *Streptococcus pyogenes* pathogenesis. *Nat Genet* 51:548-559.
28. Graham MR, Smoot LM, Lux Migiliaccio CA, Virtaneva K, Sturdevant DE, Porcella SF, Federle MJ, Adams GJ, Scott JR, Musser JM. 2002. Virulence control in group A *Streptococcus* by a two-component gene regulatory system: global expression profiling and *in vivo* infection modeling. *Proc Natl Acad Sci U S A* 99:13855-13860.

29. Sumby P, Whitney AR, Graviss EA, DeLeo FR, Musser JM. 2006. Genome-wide analysis of group A streptococci reveals a mutation that modulates global phenotype and disease specificity. *PLoS Pathog* 2:e5.
30. Shelburne SA, Olsen RJ, Suber B, Sahasrabhojane P, Sumby P, Brennan RG, Musser JM. 2010. A combination of independent transcriptional regulators shapes bacterial virulence gene expression during infection. *PLoS Pathog* 6:e1000817.
31. Galloway-Pena J, DebRoy S, Brumlow C, Li X, Tran TT, Horstmann N, Yao H, Chen K, Wang F, Pan BF, Hawke DH, Thompson EJ, Arias CA, Fowler VG, Jr., Bhatti MM, Kalia A, Flores AR, Shelburne SA. 2018. Hypervirulent group A *Streptococcus* emergence in an acapsular background is associated with marked remodeling of the bacterial cell surface. *PLoS One* 13:e0207897.
32. Heath A, DiRita VJ, Barg NL, Engleberg NC. 1999. A two-component system, CsrR-CsrS, represses expression of three *Streptococcus pyogenes* virulence factors, hyaluronic acid capsule, streptolysin S, and pyrogenic exotoxin B. *Infect Immun* 67:5298-5305.
33. Horstmann N, Sahasrabhojane P, Suber B, Kumaraswami M, Olsen RJ, Flores A, Musser JM, Brennan RG, Shelburne SA, 3rd. 2011. Distinct single amino acid replacements in the control of virulence regulator protein differentially impact streptococcal pathogenesis. *PLoS Pathog* 7:e1002311.
34. Bao YJ, Liang Z, Mayfield JA, Lee SW, Ploplis VA, Castellino FJ. 2015. CovRS-regulated transcriptome analysis of a hypervirulent M23 strain of group A *Streptococcus pyogenes* provides new insights into virulence determinants. *J Bacteriol* 197:3191-205.

35. Horstmann N, Tran CN, Brumlow C, DebRoy S, Yao H, Nogueras Gonzalez G, Makthal N, Kumaraswami M, Shelburne SA. 2018. Phosphatase activity of the control of virulence sensor kinase CovS is critical for the pathogenesis of group A *streptococcus*. PLoS Pathog 14:e1007354.
36. Otsuji K, Fukuda K, Maruoka T, Ogawa M, Saito M. 2020. Acquisition of genetic mutations in Group A Streptococci at infection site and subsequent systemic dissemination of the mutants with lethal mutations in a streptococcal toxic shock syndrome mouse model. Microb Pathog 143:104116.
37. Levin JC, Wessels MR. 1998. Identification of *csrR/csrS*, a genetic locus that regulates hyaluronic acid capsule synthesis in group A *Streptococcus*. Mol Microbiol 30:209-219.
38. Federle MJ, McIver KS, Scott JR. 1999. A response regulator that represses transcription of several virulence operons in the group A Streptococcus. J Bacteriol 181:3649-3657.
39. Gryllos I, Levin JC, Wessels MR. 2003. The CsrR/CsrS two-component system of group A *Streptococcus* responds to environmental Mg²⁺. Proc Natl Acad Sci U S A 100:4227-4232.
40. Gryllos I, Tran-Winkler HJ, Cheng M, Chung H, Bolcome R, Lu W, Lehrer RI, Wessels MR. 2008. Induction of group A *Streptococcus* virulence by a human antimicrobial peptide. Proc Natl Acad Sci U S A 105:16755-16760.
41. Velarde JJ, Ashbaugh M, Wessels MR. 2014. The human antimicrobial peptide LL-37 binds directly to CsrS, a sensor histidine kinase of group A Streptococcus, to activate expression of virulence factors. J Biol Chem 289:36315-36324.

42. Tran-Winkler HJ, Love JF, Gryllos I, Wessels MR. 2011. Signal transduction through CsrRS confers an invasive phenotype in group A *Streptococcus*. PLoS Pathog 7:e1002361.
43. Horstmann N, Saldana M, Sahasrabhojane P, Yao H, Su X, Thompson E, Koller A, Shelburne SA, 3rd. 2014. Dual-site phosphorylation of the control of virulence regulator impacts group A streptococcal global gene expression and pathogenesis. PLoS Pathog 10:e1004088.
44. Horstmann N, Sahasrabhojane P, Saldana M, Ajami NJ, Flores AR, Sumbly P, Liu CG, Yao H, Su X, Thompson E, Shelburne SA. 2015. Characterization of the effect of the histidine kinase CovS on response regulator phosphorylation in group A *Streptococcus*. Infect Immun 83:1068-1077.
45. Horstmann N, Sahasrabhojane P, Yao H, Su X, Shelburne SA, Stock AM. 2017. Use of a phosphorylation site mutant to identify distinct modes of gene repression by the control of virulence regulator (CovR) in *Streptococcus pyogenes*. J Bacteriol 199:e00835-16.
46. Biswas I, Scott JR. 2003. Identification of *rocA*, a positive regulator of *covR* expression in the group A streptococcus. J Bacteriol 185:3081-3090.
47. Lynskey NN, Goulding D, Gierula M, Turner CE, Dougan G, Edwards RJ, Sriskandan S. 2013. RocA truncation underpins hyper-encapsulation, carriage longevity and transmissibility of serotype M18 group A streptococci. PLoS Pathog 9:e1003842.

48. Lynskey NN, Turner CE, Heng LS, Sriskandan S. 2015. A truncation in the regulator RocA underlies heightened capsule expression in serotype M3 group A streptococci. *Infect Immun* 83:1732-1733.
49. Miller EW, Pflughoeft KJ, Sumbly P. 2015. Reply to "A truncation in the regulator RocA underlies heightened capsule expression in serotype M3 group A streptococci". *Infect Immun* 83:1734.
50. Yoshida H, Ishigaki Y, Takizawa A, Moro K, Kishi Y, Takahashi T, Matsui H. 2015. Comparative genomics of the mucoid and nonmucoid strains of *Streptococcus pyogenes*, isolated from the same patient with streptococcal meningitis. *Genome Announc* 3:e0021-15.
51. Miller EW, Danger JL, Ramalinga AB, Horstmann N, Shelburne SA, Sumbly P. 2015. Regulatory rewiring confers serotype-specific hyper-virulence in the human pathogen group A *Streptococcus*. *Mol Microbiol* 98:473-489.
52. Paluscio E. 2015. Adaptive mechanisms to niche remodeling in *Streptococcus pyogenes*. PhD thesis. Washington University in St. Louis, St. Louis, MO.
53. Zhu L, Olsen RJ, Horstmann N, Shelburne SA, Fan J, Hu Y, Musser JM. 2016. Intergenic variable-number tandem-repeat polymorphism upstream of *rocA* alters toxin production and enhances virulence in *Streptococcus pyogenes*. *Infect Immun* 84:2086-2093.
54. Feng W, Minor D, Liu M, Li J, Ishaq SL, Yeoman C, Lei B. 2017. Null mutations of group A *Streptococcus* orphan kinase RocA: selection in mouse infection and comparison with CovS mutations in alteration of *in vitro* and *in vivo* protease SpeB expression and virulence. *Infect Immun* 85:e00790-16.

55. Sarkar P, Sumby P. 2017. Regulatory gene mutation: a driving force behind group A *Streptococcus* strain- and serotype-specific variation. *Mol Microbiol* 103:576-589.
56. Jain I, Miller EW, Danger JL, Pflughoeft KJ, Sumby P. 2017. RocA is an accessory protein to the virulence-regulating CovRS two-component system in group A *Streptococcus*. *Infect Immun* 85:e00274-17.
57. Bernard PE, Kachroo P, Zhu L, Beres SB, Eraso JM, Kajani Z, Long SW, Musser JM, Olsen RJ. 2018. RocA has serotype-specific gene regulatory and pathogenesis activities in serotype M28 group A streptococcus. *Infect Immun* 86:e00467-18.
58. Sarkar P, Danger JL, Jain I, Meadows LA, Beam C, Medicielo J, Burgess C, Musser JM, Sumby P. 2018. Phenotypic variation in the group A *Streptococcus* due to natural mutation in the accessory protein-encoding gene *rocA*. *mSphere* 3:e00519-18.
59. Lynskey NN, Velarde JJ, Finn MB, Dove SL, Wessels MR, McDaniel LS. 2019. RocA binds CsrS to modulate CsrRS-mediated gene regulation in group A *Streptococcus*. *mBio* 10:e01495-19.
60. Brouwer S, Walker MJ. 2019. The serotype-specific role of regulator of Cov polymorphisms in the pathogenesis of invasive group A streptococcal infections. *Am J Pathol* 189:1913-1915.
61. Jain I, Danger JL, Burgess C, Uppal T, Sumby P. 2020. The group A *Streptococcus* accessory protein RocA: regulatory activity, interacting partners and influence on disease potential. *Mol Microbiol* 113:190-207.

62. Kall L, Krogh A, Sonnhammer EL. 2007. Advantages of combined transmembrane topology and signal peptide prediction--the Phobius web server. *Nucleic Acids Res* 35:W429-W432.
63. Reynolds SM, Kall L, Riffle ME, Bilmes JA, Noble WS. 2008. Transmembrane topology and signal peptide prediction using dynamic Bayesian networks. *PLoS Comput Biol* 4:e1000213.
64. Viklund H, Elofsson A. 2008. OCTOPUS: improving topology prediction by two-track ANN-based preference scores and an extended topological grammar. *Bioinformatics* 24:1662-1668.
65. Kall L, Krogh A, Sonnhammer EL. 2005. An HMM posterior decoder for sequence feature prediction that includes homology information. *Bioinformatics* 21 Suppl 1:i251-i257.
66. Viklund H, Bernsel A, Skwark M, Elofsson A. 2008. SPOCTOPUS: a combined predictor of signal peptides and membrane protein topology. *Bioinformatics* 24:2928-2929.
67. Bernsel A, Viklund H, Falk J, Lindahl E, von Heijne G, Elofsson A. 2008. Prediction of membrane-protein topology from first principles. *Proc Natl Acad Sci U S A* 105:7177-7181.
68. Nugent T, Jones DT. 2009. Transmembrane protein topology prediction using support vector machines. *BMC Bioinformatics* 10:159.
69. Kelley LA, Mezulis S, Yates CM, Wass MN, Sternberg MJE. 2015. The Phyre2 web portal for protein modeling, prediction and analysis. *Nat Protoc* 10:845-858.

70. Bogdanov M. 2017. Mapping of membrane protein topology by substituted cysteine accessibility method (SCAM™). *Methods Mol Biol* 1615:105-128.
71. Alexeyev MF, Winkler HH. 1999. Membrane topology of the *Rickettsia prowazekii* ATP/ADP translocase revealed by novel dual *pho-lac* reporters. *J Mol Biol* 285:1503-1513.
72. Piazza F, Tortosa P, Dubnau D. 1999. Mutational analysis and membrane topology of ComP, a quorum-sensing histidine kinase of *Bacillus subtilis* controlling competence development. *J Bacteriol* 181:4540-4548.
73. Ethier J, Boyd JM. 2000. Topological analysis and role of the transmembrane domain in polar targeting of PilS, a *Pseudomonas aeruginosa* sensor kinase. *Mol Microbiol* 38:891-903.
74. Heldermon C, DeAngelis PL, Weigel PH. 2001. Topological organization of the hyaluronan synthase from *Streptococcus pyogenes*. *J Biol Chem* 276:2037-2046.
75. Johnsborg O, Diep DB, Nes IF. 2003. Structural analysis of the peptide pheromone receptor PlnB, a histidine protein kinase from *Lactobacillus plantarum*. *J Bacteriol* 185:6913-6920.
76. Smirnova AV, Ullrich MS. 2004. Topological and deletion analysis of CorS, a *Pseudomonas syringae* sensor kinase. *Microbiology* 150:2715-2726.
77. Karimova G, Robichon C, Ladant D. 2009. Characterization of YmgF, a 72-residue inner membrane protein that associates with the *Escherichia coli* cell division machinery. *J Bacteriol* 191:333-346.
78. Karimova G, Ladant D. 2017. Defining membrane protein topology using *pho-lac* reporter fusions. *Methods Mol Biol* 1615:129-142.

79. Karimova G, Pidoux J, Ullmann A, Ladant D. 1998. A bacterial two-hybrid system based on a reconstituted signal transduction pathway. *Proc Natl Acad Sci U S A* 95:5752-5756.
80. Karimova G, Dautin N, Ladant D. 2005. Interaction network among *Escherichia coli* membrane proteins involved in cell division as revealed by bacterial two-hybrid analysis. *J Bacteriol* 187:2233-2243.
81. Karimova G, Gaudiard E, Davi M, Ouellette SP, Ladant D. 2017. Protein-protein interaction: bacterial two-hybrid. *Methods Mol Biol* 1615:159-176.
82. Beres SB, Kachroo P, Nasser W, Olsen RJ, Zhu L, Flores AR, de la Riva I, Paez-Mayorga J, Jimenez FE, Cantu C, Vuopio J, Jalava J, Kristinsson KG, Gottfredsson M, Corander J, Fittipaldi N, Di Luca MC, Petrelli D, Vitali LA, Raiford A, Jenkins L, Musser JM. 2016. Transcriptome remodeling contributes to epidemic disease caused by the human pathogen *Streptococcus pyogenes*. *mBio* 7:e00403-16.
83. Zhu L, Olsen RJ, Lee JD, Porter AR, DeLeo FR, Musser JM. 2017. Contribution of secreted NADase and streptolysin O to the pathogenesis of epidemic serotype M1 *Streptococcus pyogenes* infections. *Am J Pathol* 187:605-613.
84. von Heijne G. 1986. The distribution of positively charged residues in bacterial inner membrane proteins correlates with the trans-membrane topology. *EMBO J* 5:3021-3027.
85. Bibi E, Verner G, Chang C-Y. 1991. Organization and stability of a polytopic membrane protein: deletion analysis of the lactose permease of *Escherichia coli*. *Proc Natl Acad Sci U S A* 88:7271-7275.

86. Ehrmann M, Beckwith J. 1991. Proper insertion of a complex membrane protein in the absence of its amino-terminal export signal. *J Biol Chem* 266:16530-16533.
87. McGovern K, Ehrmann M, Beckwith J. 1991. Decoding signals for membrane protein assembly using alkaline phosphatase fusions. *EMBO J* 10:2773-2782.
88. Calamia J, Manoil C. 1992. Membrane protein spanning segments as export signals. *J Mol Biol* 224:539-543.
89. Bogdanov M, Xie J, Heacock P, Dowhan W. 2008. To flip or not to flip: lipid-protein charge interactions are a determinant of final membrane protein topology. *J Cell Biol* 182:925-935.
90. Dowhan W, Bogdanov M. 2009. Lipid-dependent membrane protein topogenesis. *Annu Rev Biochem* 78:515-540.
91. Bogdanov M, Dowhan W, Vitrac H. 2014. Lipids and topological rules governing membrane protein assembly. *Biochim Biophys Acta* 1843:1475-1488.
92. Baker JA, Wong WC, Eisenhaber B, Warwicker J, Eisenhaber F. 2017. Charged residues next to transmembrane regions revisited: "positive-inside rule" is complemented by the "negative inside depletion/outside enrichment rule". *BMC Biol* 15:66.
93. Schrecke K, Jordan S, Mascher T. 2013. Stoichiometry and perturbation studies of the LiaFSR system of *Bacillus subtilis*. *Mol Microbiol* 87:769-788.
94. Reid SD, Green NM, Sylva GL, Voyich JM, Stenseth ET, DeLeo FR, Palzkill T, Low DE, Hill HR, Musser JM. 2002. Postgenomic analysis of four novel antigens of group A *Streptococcus*: growth phase-dependent gene transcription and human serologic response. *J Bacteriol* 184:6316-6324.

95. Jeong JY, Yim HS, Ryu JY, Lee HS, Lee JH, Seen DS, Kang SG. 2012. One-step sequence- and ligation-independent cloning as a rapid and versatile cloning method for functional genomics studies. *Appl Environ Microbiol* 78:5440-5443.
96. National Research Council. 2011. *Guide for the care and use of laboratory animals*, 8th ed. National Academies Press, Washington, DC.

5. CONCLUSIONS

5.1. RocA: An important virulence regulator in the molecular pathogenesis of GAS

RocA is an accessory protein to the CovRS two-component system, a major regulator of virulence in GAS. In the research presented in this dissertation, RocA was demonstrated to be an important regulator of virulence in serotype M28 GAS (Chapter 2) (1). As a whole, polymorphisms in *rocA* resulting in amino acid changes significantly increased GAS virulence, as assessed by global transcriptome analysis, virulence factor activity and necrotizing myositis infection models (Chapter 3) (2). Amino acid changes in RocA, both in the N-terminal transmembrane domains and in the C-terminal cytoplasmic domain, result in alteration of physical interaction between RocA and CovS (Chapter 4) (Fig. 5-1).

5.2. Polymorphisms in *rocA* differentially effect molecular pathogenesis

Most studies of accessory proteins have focused on the protein as a whole unit through either gene deletions or protein truncations (3-12). A few studies have utilized mutagenesis strategies to identify key residues in either the accessory protein or the two-component system (TCS) proteins (5, 6, 10). Similarly, previous study of RocA in GAS has focused on gene deletions or protein truncations (13-21). While some protein truncations are naturally-occurring in clinical isolates or animal passaged strains (14, 15, 17, 19), no naturally-occurring amino acid changes in RocA, or other well-described accessory proteins, had been studied previous to the research described herein. We demonstrated that naturally-occurring amino acid changes in RocA significantly alter the molecular pathogenesis of serotype M28 GAS. Importantly, not all polymorphisms resulted in identical virulence

phenotypes, as defined by transcriptome, virulence factor activity, and animal infection models. Selected amino acid changes will be discussed in detail in the following sections.

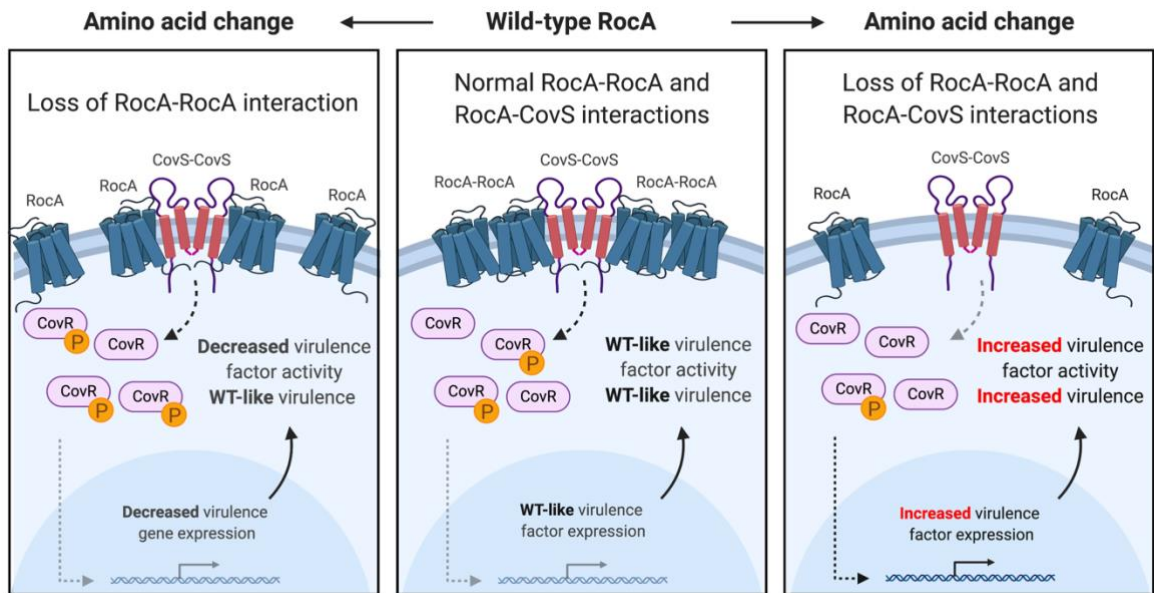


Fig. 5-1 RocA is an accessory protein to the CovRS two-component system in group A *Streptococcus*. In the wild-type condition, RocA physically interacts in the membrane with itself and CovS to affect CovR phosphorylation, gene expression and strain virulence (middle). Some amino acid changes in RocA alter RocA-RocA interactions (left). Other amino acid changes alter both RocA-RocA and RocA-CovS interactions to significantly increase expression and secreted activity of virulence factors and significantly increase strain virulence (right). Created with BioRender.com.

5.2.1. RocA R258K and V420I

The RocA R258K amino acid change was chosen for further study because codon 258 is located in the H box of the putative histidine kinase ATPase domain (Chapter 3) (2). The RocA V420I amino acid change was chosen because it is located in the C-terminus of RocA (Chapter 4). Isogenic mutant strains with RocA amino acid changes R258K and V420I did not significantly differ from the parental WT GAS strain in terms of global transcriptome, interaction with CovS, virulence factor activity *in vitro*, or virulence in

necrotizing myositis infection models (Chapter 3 and 4) (2). The two amino acid changes are conservative in nature, with one being a positively-charged residue replacing another positively-charged residue (R258K; guanidino group replaced by an amino group) and the other a small hydrophobic residue for another small hydrophobic residue (V420I; *iso*-propyl group replaced by a *sec*-butyl group). While it might be assumed that conservative changes would result in a very slight change, if any in tested phenotypes, conservative changes have been observed to cause striking changes in virulence phenotypes. For example, the Ebola virus glycoprotein A82V amino acid change, which occurred early during the 2013-2016 epidemic in West Africa, resulted in increased infectivity (22, 23). Transcriptome analysis of GAS clinical isolates with naturally-occurring polymorphisms in *rocA* demonstrated that many had transcriptome profiles similar to clade-matched WT strains (Chapter 3) (2). Thus, not all polymorphisms in *rocA* result in a significant molecular pathogenesis phenotype. This has been observed for other major virulence regulators in GAS, including *covRS* and *ropB* (24-28).

5.2.2. RocA P97L

The RocA P97L amino acid change was chosen for further study because codon 97 is located in an N-terminal transmembrane domain, and the clinical isolate with this mutation had a *rocA* deletion-like transcriptome (Chapter 3) (2). An isogenic mutant strain with the RocA P97L amino acid change had a *rocA* deletion-like global transcriptome profile and significantly increased virulence factor activity *in vitro*, but a WT-like virulence phenotype in a mouse model of necrotizing myositis (Chapter 3) (2). Further study demonstrated that RocA P97L had a transient-like interaction with CovS (Chapter 4). Thus, the RocA amino

acid change P97L results in an intermediate molecular pathogenesis phenotype between the WT RocA and *rocA* deletion virulence phenotypes.

As *rocA* transcript levels are increased *in vivo* in invasive infection compared to *in vitro* conditions (29), the RocA P97L amino acid change likely confers a minute structural or conformational change that can be overcome with increased RocA protein levels in the cell membrane. Amino acid P97 is predicted to be located at the N-terminus of transmembrane domain 4, which is oriented intracellular to extracellular based on experimental data (Chapter 4). Proline is the only natural amino acid that is actually an imino acid. As no amide proton is present to participate in hydrogen bonding in secondary structures such as α -helices, proline is considered a classical helix breaker and is not commonly found in α -helices in globular proteins (30). In contrast, proline is found at a significantly higher rate in transmembrane α -helices, typically at the ends or center of the helix (31, 32). A proline residue in the center of an α -helix is typically associated with a kink in the helix (32, 33), allowing for greater flexibility in the α -helix. For example, several helical antimicrobial peptides have a central proline that produces a kinked helix, which, when compared to a non-kinked helix, has increased antimicrobial properties and increased selectivity to interact with negatively charged membranes (34, 35).

Due to the observed bias of proline residues in transmembrane α -helices, proline residues in transmembrane domains have been extensively studied to elucidate their potential structural and functional roles. In transport protein, proline residues in transmembrane domains have demonstrated roles in transport ligand selectivity, transporter pore size, and transporter gating mechanisms (36-40). Additionally, proline residues in

transmembrane domains have demonstrated roles in membrane protein localization, folding, and global conformation, as well as intra- and inter-protein transmembrane helix interactions (32, 33, 41-44).

Several studies have demonstrated distinct phenotypes due to proline-to-leucine or leucine-to-proline mutations in α -helices. The Fis protein from *Escherichia coli* is a DNA inversion protein that contains a kinked helix centered near a proline residue (45). Mutation of the proline to leucine (P61L) resulted in a Fis protein that retained the ability to bind DNA but had no DNA inversion activity (45). Analysis of other Fis-P61 mutants suggest that the leucine residue disrupts helical interactions in Fis due to the larger side chain of leucine (*iso*-butyl side chain versus pyrrolidine side chain of proline) (45). Mutations in human glycine transporter 2 (GlyT2) lead to the neurological disease hyperekplexia, also known as startle disorder (40). A proline-to-leucine mutation localized to a transmembrane helix (P429L) results in poor protein trafficking to the cell membrane and a non-functional protein (40). The loss of function may be due to the loss of mobility of adjacent helices that are important for the transporter's gating mechanism (40). The human erythrocyte sialoglycoprotein Glycophorin A (GpA) is a membrane protein with one transmembrane α -helix that has a well described homodimerization motif (46, 47). Proline mutagenesis of the transmembrane domain residues identified leucine 57 (L57), located at the N-terminus of the transmembrane domain, as a site of mutagenesis that retained dimerization potential (46, 47). Further study of the L57P mutant demonstrated that proline extended the N-terminal end of the helix without disrupting the rest of the helix or dimerization motif (47). In an additional study, a synthetic peptide mimicking a transmembrane helix (*t*-Boc-AAALPF-OH) was synthesized due to the identification of a leucine-proline-phenylalanine (LPF) motif in transmembrane

domains of membrane proteins (30). When inserted into lipid micelles, the motif formed a stable γ -turn, a common secondary structure that includes proline residues (30). In RocA, P97 is located in a similar motif (FPL).

Based on studies of proline residues in transmembrane domains, several hypotheses bearing on the potential roles for P97 in RocA can be postulated. The RocA P97L amino acid change may alter the global conformation of RocA, due to a change in transmembrane domain length or loss of important transmembrane domain interactions, resulting in altered RocA-RocA and RocA-CovS interactions. Alternatively, the FPL motif in RocA may fold into a γ -turn that becomes destabilized due to the P97L amino acid change. Regardless of the molecular change that occurs, it is minute compared to other amino acid changes in RocA, as it can be overcome in the *in vivo* condition (Chapter 3) (2).

5.2.3. RocA G184W and G184E

The RocA G184W amino acid change was chosen for further study because codon 184 is located in an N-terminal transmembrane domain and is polymorphic in serotype M89 GAS (G184E; Chapter 3) (2, 48). An isogenic mutant strain with the RocA G184W amino acid change had a global transcriptome and virulence factor activity *in vitro* suggestive of increased RocA activity (Chapter 3) (2). That is, the isogenic RocA G184W mutant strain had significantly decreased virulence factor activity compared to the parental WT GAS strain, although this did not result in decreased virulence in either a mouse or NHP model of necrotizing myositis (Chapter 3) (2). As the pathogenesis of GAS is multifactorial, a loss one or more specific virulence determinants may not result in decreased virulence under the conditions tested. The RocA G184W amino acid change led to loss of RocA homodimerization but retention of interaction with CovS, suggesting that the G184W

mutation may lead to a relative increase of monomeric RocA to interact with CovS (Chapter 4).

RocA has limited sequence homology with histidine kinases of the HPK10 family (13, 49). Histidine kinases of the HPK10 family have five to eight transmembrane domains and demonstrated roles in cell-to-cell communication, such as quorum sensing (49). Topological and functional domain studies of two HPK10 family histidine kinases, AgrC from *Staphylococcus aureus* and PlnB from *Lactobacillus plantarum*, demonstrated a role for the last extracytoplasmic loop and transmembrane domain in inhibiting kinase activity (50, 51). That is, positioning of the last transmembrane domain is important for normal signaling in these two HPK10 family histidine kinases.

The sequence similarity between RocA and HPK10 family members suggests that RocA evolved from an ancient HPK10-like histidine kinase, and, as such, may have retained some functional aspects that have been demonstrated in HPK10 family histidine kinases. RocA amino acid G184 is predicted to be located at the C-terminal end of transmembrane domain 6, which is oriented intracellular to extracellular based on experimental data (Chapter 4). Thus, amino acid G184 is located close to the last extracellular loop and, theoretically, the last transmembrane domain. Glycine is known to be important for helix-helix packing interactions in transmembrane helices (44). Therefore, the replacement of a small residue (glycine; hydrogen side chain) with a larger residue (tryptophan; indole side chain) may destroy interactions between RocA transmembrane domains required for RocA dimerization, but may further stabilize the RocA-CovS interaction. Such a change in interaction may result in increased CovR phosphorylation by CovS. This hypothesis is supported by the RocA G184E amino acid change occurring in serotype M89 GAS. The

small residue glycine (hydrogen side chain) is replaced with a different large residue (glutamate; ethyl carboxylic acid side chain) (48), resulting in a similar virulence factor activity profile as the RocA G184W amino acid change (Chapter 3) (2).

5.2.4. RocA T442I, T442P, and Q443*

The RocA T442P amino acid change was chosen for further study because multiple clinical isolates acquired polymorphisms at codon 442, and clinical isolates with this mutation had a significantly altered transcriptome compared to their phylogenetically-matched wild-type strain (Chapter 3) (2). An isogenic mutant strain with the RocA T442P amino acid change had a *rocA* deletion-like global transcriptome profile and increased virulence factor activity and virulence in animal infection models (Chapter 3) (2). As the C-terminus of RocA had been thought to be dispensable for CovRS regulatory activity, additional study of polymorphisms in the C-terminus of RocA (V420I, T442I, Q443*) were undertaken. Results demonstrated that the RocA Q443* polymorphism increased virulence factor activity *in vitro* and virulence *in vivo* similar to the RocA T442P amino acid change (Chapter 4). Both RocA variants lost the ability to interact with itself and CovS (Chapter 4), demonstrating the importance of not only the C-terminus but the last 10 amino acids in RocA-mediated CovRS interaction and regulation.

Previous studies of RocA functional domains utilized truncation mutants and overexpression systems (18, 20). As RocA has a well demonstrated dosage effect in GAS gene regulation (Chapter 4) (18), the characterization of the N-terminal transmembrane domains as the regulatory domain of RocA (18, 20) may have been premature. The serotype M3 *rocA* allele is truncated from 451 to 416 amino acids, containing an intact N-terminus, and yet does not differ in any measured phenotype when compared to complete deletion of

the *rocA* gene (15). Conversely, some serotype M28 GAS clinical isolates with naturally-occurring truncation polymorphisms in *rocA* have transcriptomes that are more similar to a clade-matched WT strain than a strain lacking the *rocA* gene (2). Taken together, the data suggest that the major regulatory functionality of RocA most likely resides in the N-terminal transmembrane domains that can compensate for loss of the C-terminal cytoplasmic domain functionality when overexpressed.

The C-terminus of RocA is predicted to fold similarly to a histidine kinase ATPase domain, although the key residues for kinase activity and ATP binding are not present, and RocA does not have histidine kinase activity toward CovR (13, 21, 52). However, no crystal structure of RocA has been determined, and thus the *in silico* prediction remains only a prediction. As RocA is predicted to not bind ATP, the C-terminus of RocA has likely evolved from the prototypical histidine kinase ATPase-like fold into a similar structure that allows for a high affinity interaction with CovS. Such a structure may have a requirement of the very last C-terminal amino acids for either stabilization of the global conformation, direct interaction with CovS, or some other mechanism. Interestingly, an isogenic mutant strain with the RocA T442I amino acid change had a WT-like phenotype, but this RocA variant was unable to interact with itself or CovS in a bacterial adenylate cyclase-based two hybrid assay (Chapter 4). The molecular basis for this observation is unknown.

Taken together, further study of the structure of RocA, both the WT protein and amino acid variants, is warranted to better understand how RocA interacts with itself and CovS and how amino acid changes alter RocA molecular pathogenesis.

5.3. Polymorphisms in *covS* that result in altered RocA-CovS interaction

The work presented in this dissertation focused on the role of polymorphisms in *rocA* in the molecular pathogenesis of serotype M28 GAS, and identified several RocA amino acid changes that alter RocA-CovS protein interactions (Chapter 4). Thus, it is likely that polymorphisms in *covS* can alter RocA-CovS protein interaction as well. Most studies of mutant CovS proteins have focused on naturally-occurring frameshifting insertion and deletion polymorphisms rather than amino acid altering polymorphisms (53-57). As *covS* is among the most polymorphic genes in population-based studies of GAS clinical isolates (28, 58, 59), some *covS* mutations may function primarily by altering interaction with RocA to decrease CovR phosphorylation and increase strain virulence.

The serotype M89 GAS strains that were studied in Chapter 3 have the same polymorphism in *rocA* (G184E), but have additional polymorphisms in *covS* and *rocA* (2). The clinical isolates are of the same genetic clade and were isolated in the same geographic region and year (48). Whole genome sequencing analysis identified only 24 polymorphisms differing between the four serotype M89 GAS strains, providing strong evidence that the four strains are phylogenetically related (48). As such, it is likely that the additional *covS* polymorphisms were acquired after the initial *rocA* polymorphism (G184E) to further alter the physical interaction between RocA and CovS. In a similar manner, of the 48 serotype M28 GAS clinical isolates that have naturally-occurring polymorphisms in *rocA*, 27 (56%) have mutations in other major global regulators, including 11 (23%) with polymorphisms in *covRS* (2). Further investigation of CovS amino acid changes that alter the physical interaction of RocA and CovS will provide insight into the precise domain(s) that interact between the two proteins.

5.4. RocA as a global accessory protein: Potential interactions with other TCSs

Comparison of the serotype M28 RocA regulon to a published serotype M1 CovR regulon demonstrated an approximately 15% overlap in differentially expressed genes (Chapter 2) (1, 60). Comparing the serotype M28 RocA regulon to eight published CovRS regulons from serotype M1, M3, and M4 GAS only increases the differentially expressed gene overlap to approximately 57% (1, 27, 55, 60-65). Thus, almost half of the genes regulated by RocA in serotype M28 GAS may be regulated independently of CovRS. As the CovRS regulon for serotype M28 GAS has not been determined, and serotype-specific differences in gene regulation for major global regulators of GAS have been documented, including CovRS (55, 60, 63, 66, 67), the actual overlap may be slightly higher.

RocA is a membrane protein and may interact with other TCSs and other membrane regulatory proteins to exert an effect on gene regulation. In *S. aureus*, SpdC was initially identified as an accessory to the WalkR TCS, but can also directly interact with histidine kinases of nine other TCSs (9). Several TCS genes are regulated by RocA in serotype M28 GAS (Chapter 2) (1), and many TCSs are known to regulate their own expression (68-70). Additionally, 86% of differentially expressed genes in the serotype M28 RocA regulon are regulated by another TCS in GAS (27, 55, 60-65, 69, 71-76).

An isogenic mutant strain with the RocA T442P amino acid change had significantly decreased secreted streptokinase (SKA) activity compared to not only the parental WT strain but also the isogenic *rocA* deletion mutant (Chapter 3) (2). Differential expression of *fasX* may, in part, explain the very low SKA activity of the RocA T442P mutant strain (Chapter 3) (2). *fasX* expression is dependent on a functional FasBCA system (77), although no difference in expression for *fasBCA* was observed in any of the isogenic *rocA* deletion and

polymorphism strains (Chapter 3) (2). The RocA T442P variant may be able to interact with either FasB or FasC to modulate phosphorylation of FasA and, therefore, expression of *fasX*. A recent study demonstrated that the WT RocA protein from serotype M1 GAS does not interact with the WT FasB protein (21). This finding does not preclude the possibility that mutant RocA proteins could still interact with FasB, as mutant RocA proteins have altered interactions with another histidine kinase, CovS (Chapter 4).

Taken together, the current data suggest that RocA, and mutant RocA variants, may interact with other histidine kinases of TCSs or membrane regulatory proteins to alter gene expression. Further study of multiple TCS regulons in the same GAS strain will greatly aid our understanding of how TCS and accessory protein regulatory pathways interact and overlap. Additional protein-protein interaction studies based on these TCS regulons are warranted to confirm any potential interaction observed.

5.5. Streptokinase regulation in serotype M28 GAS

One RocA regulated virulence factor warranting further investigation is streptokinase (SKA). Deletion of *rocA*, and several polymorphisms in *rocA*, in serotype M28 GAS resulted in significantly decreased *ska* transcript levels and significantly decreased secreted SKA activity (Chapters 2-4) (1, 2). This is in stark contrast to study of RocA in other GAS serotypes, where deletion or truncation of *rocA* resulted in significantly increased *ska* transcript levels, increased immunoreactive SKA protein expression, and significantly increased secreted SKA activity (15, 18, 19, 21). This suggests regulation of *ska* in serotype M28 GAS is unique.

Two major regulatory pathways have been described for *ska*. The FasBCA/*fasX* system positively regulates *ska*. FasBCA regulate the small RNA *fasX*, which binds to the

5'-UTR of *ska* to increase the stability of the *ska* transcript (78). This regulatory mechanism has been demonstrated in multiple GAS serotypes, including M28 (77-80). Deletion of *rocA* in serotype M28 GAS did not result in differential expression of *fasBCAX* (Chapters 2 & 3) (1, 2), suggesting that the WT RocA protein does not influence *ska* expression by regulating the FasBCA/*fasX* system.

In contrast to the FasBCA/*fasX* systems, the CovRS TCS negatively regulates *ska*. Both phosphorylated and non-phosphorylated CovR can bind to the *ska* promoter to inhibit *ska* transcription, though phosphorylated CovR binds with a higher affinity (81). Significantly increased *ska* transcript levels have been observed in *covRS* deletion mutant strains in multiple GAS serotypes (27, 55, 56, 60-63, 65, 82, 83), although the effect of *covRS* deletion on *ska* expression in serotype M28 GAS has not been defined. Serotype-specific differences in gene regulation for major global regulators of GAS have been documented, including CovRS (55, 60, 63, 66, 67). A recent population transcriptomic study of serotype M28 GAS demonstrated two clusters of GAS strain transcriptomes, with one cluster having exclusively *covRS* mutant strains (28). *covRS* mutant strains in the exclusive *covRS* mutant cluster had significantly decreased *ska* transcript levels compared to the other cluster (28), suggesting that, in contrast to other GAS serotypes, CovRS either directly or indirectly positively regulates *ska* in serotype M28 GAS.

5.6. Conclusions

In summary, the major discoveries in this dissertation include: 1) RocA is an important accessory protein involved in virulence in serotype M28 GAS; 2) naturally-occurring polymorphisms in *rocA* alter the global GAS transcriptome and secreted virulence factor activity to increase strain virulence; and 3) amino acids in RocA alter the physical

interaction between RocA and CovS. Taken together, the data create important new understanding of the molecular pathogenesis of RocA in GAS specifically and accessory proteins in general. Further structural studies of RocA and CovS will provide insight into the molecular interactions important for interaction of an accessory protein and TCS in a major human pathogen.

5.7. References

1. Bernard PE, Kachroo P, Zhu L, Beres SB, Eraso JM, Kajani Z, Long SW, Musser JM, Olsen RJ. 2018. RocA has serotype-specific gene regulatory and pathogenesis activities in serotype M28 group A streptococcus. *Infect Immun* 86:e00467-18.
2. Bernard PE, Kachroo P, Eraso JM, Zhu L, Madry JE, Linson SE, Ojeda Saavedra M, Cantu C, Musser JM, Olsen RJ. 2019. Polymorphisms in regulator of Cov contribute to the molecular pathogenesis of serotype M28 group A *Streptococcus*. *Am J Pathol* 189:2002-2018.
3. Eguchi Y, Itou J, Yamane M, Demizu R, Yamato F, Okada A, Mori H, Kato A, Utsumi R. 2007. B1500, a small membrane protein, connects the two-component systems EvgS/EvgA and PhoQ/PhoP in *Escherichia coli*. *Proc Natl Acad Sci U S A* 104:18712-18717.
4. Ishii E, Eguchi Y, Utsumi R. 2013. Mechanism of activation of PhoQ/PhoP two-component signal transduction by SafA, an auxiliary protein of PhoQ histidine kinase in *Escherichia coli*. *Biosci Biotechnol Biochem* 77:814-819.
5. Carlyon RE, Ryther JL, VanYperen RD, Griffiths JS. 2010. FeuN, a novel modulator of two-component signalling identified in *Sinorhizobium meliloti*. *Mol Microbiol* 77:170-182.

6. Szurmant H, Bu L, Brooks CL, 3rd, Hoch JA. 2008. An essential sensor histidine kinase controlled by transmembrane helix interactions with its auxiliary proteins. *Proc Natl Acad Sci U S A* 105:5891-5896.
7. Jeong DW, Cho H, Jones MB, Shatzkes K, Sun F, Ji Q, Liu Q, Peterson SN, He C, Bae T. 2012. The auxiliary protein complex SaePQ activates the phosphatase activity of sensor kinase SaeS in the SaeRS two-component system of *Staphylococcus aureus*. *Mol Microbiol* 86:331-348.
8. Falord M, Karimova G, Hiron A, Msadek T. 2012. GraXSR proteins interact with the VraFG ABC transporter to form a five-component system required for cationic antimicrobial peptide sensing and resistance in *Staphylococcus aureus*. *Antimicrob Agents Chemother* 56:1047-1058.
9. Poupel O, Proux C, Jagla B, Msadek T, Dubrac S. 2018. SpdC, a novel virulence factor, controls histidine kinase activity in *Staphylococcus aureus*. *PLoS Pathog* 14:e1006917.
10. Kilmury SLN, Burrows LL. 2016. Type IV pilins regulate their own expression via direct intramembrane interactions with the sensor kinase PilS. *Proc Natl Acad Sci U S A* 113:6017-6022.
11. Mitchell SL, Ismail AM, Kenrick SA, Camilli A. 2015. The VieB auxiliary protein negatively regulates the VieSA signal transduction system in *Vibrio cholerae*. *BMC Microbiol* 15:59.
12. Zhou X, Keller R, Volkmer R, Krauss N, Scheerer P, Hunke S. 2011. Structural basis for two-component system inhibition and pilus sensing by the auxiliary CpxP protein. *J Biol Chem* 286:9805-9814.

13. Biswas I, Scott JR. 2003. Identification of *rocA*, a positive regulator of *covR* expression in the group A streptococcus. *J Bacteriol* 185:3081-3090.
14. Lynskey NN, Goulding D, Gierula M, Turner CE, Dougan G, Edwards RJ, Sriskandan S. 2013. RocA truncation underpins hyper-encapsulation, carriage longevity and transmissibility of serotype M18 group A streptococci. *PLoS Pathog* 9:e1003842.
15. Miller EW, Danger JL, Ramalinga AB, Horstmann N, Shelburne SA, Sumbly P. 2015. Regulatory rewiring confers serotype-specific hyper-virulence in the human pathogen group A *Streptococcus*. *Mol Microbiol* 98:473-489.
16. Zhu L, Olsen RJ, Horstmann N, Shelburne SA, Fan J, Hu Y, Musser JM. 2016. Intergenic variable-number tandem-repeat polymorphism upstream of *rocA* alters toxin production and enhances virulence in *Streptococcus pyogenes*. *Infect Immun* 84:2086-2093.
17. Feng W, Minor D, Liu M, Li J, Ishaq SL, Yeoman C, Lei B. 2017. Null mutations of group A *Streptococcus* orphan kinase RocA: selection in mouse infection and comparison with CovS mutations in alteration of *in vitro* and *in vivo* protease SpeB expression and virulence. *Infect Immun* 85:e00790-16.
18. Jain I, Miller EW, Danger JL, Pflughoeft KJ, Sumbly P. 2017. RocA is an accessory protein to the virulence-regulating CovRS two-component system in group A *Streptococcus*. *Infect Immun* 85:e00274-17.
19. Sarkar P, Danger JL, Jain I, Meadows LA, Beam C, Medicielo J, Burgess C, Musser JM, Sumbly P. 2018. Phenotypic variation in the group A *Streptococcus*

- due to natural mutation in the accessory protein-encoding gene *rocA*. *mSphere* 3:e00519-18.
20. Lynskey NN, Velarde JJ, Finn MB, Dove SL, Wessels MR, McDaniel LS. 2019. RocA binds CsrS to modulate CsrRS-mediated gene regulation in group A *Streptococcus*. *mBio* 10:e01495-19.
 21. Jain I, Danger JL, Burgess C, Uppal T, Sumby P. 2020. The group A *Streptococcus* accessory protein RocA: regulatory activity, interacting partners and influence on disease potential. *Mol Microbiol* 113:190-207.
 22. Diehl WE, Lin AE, Grubaugh ND, Carvalho LM, Kim K, Kyawe PP, McCauley SM, Donnard E, Kucukural A, McDonel P, Schaffner SF, Garber M, Rambaut A, Andersen KG, Sabeti PC, Luban J. 2016. Ebola virus glycoprotein with increased infectivity dominated the 2013-2016 epidemic. *Cell* 167:1088-1098.
 23. Urbanowicz RA, McClure CP, Sakuntabhai A, Sall AA, Kobinger G, Muller MA, Holmes EC, Rey FA, Simon-Loriere E, Ball JK. 2016. Human adaptation of Ebola virus during the West African outbreak. *Cell* 167:1079-1087.
 24. Carroll RK, Beres SB, Sitkiewicz I, Peterson L, Matsunami RK, Engler DA, Flores AR, Sumby P, Musser JM. 2011. Evolution of diversity in epidemics revealed by analysis of the human bacterial pathogen group A *Streptococcus*. *Epidemics* 3:159-170.
 25. Carroll RK, Shelburne SA, 3rd, Olsen RJ, Suber B, Sahasrabhojane P, Kumaraswami M, Beres SB, Shea PR, Flores AR, Musser JM. 2011. Naturally occurring single amino acid replacements in a regulatory protein alter streptococcal gene expression and virulence in mice. *J Clin Invest* 121:1956-1968.

26. Friaes A, Pato C, Melo-Cristino J, Ramirez M. 2015. Consequences of the variability of the CovRS and RopB regulators among *Streptococcus pyogenes* causing human infections. *Sci Rep* 5:12057.
27. Horstmann N, Sahasrabhojane P, Saldana M, Ajami NJ, Flores AR, Sumbly P, Liu CG, Yao H, Su X, Thompson E, Shelburne SA. 2015. Characterization of the effect of the histidine kinase CovS on response regulator phosphorylation in group A *Streptococcus*. *Infect Immun* 83:1068-1077.
28. Kachroo P, Eraso JM, Beres SB, Olsen RJ, Zhu L, Nasser W, Bernard PE, Cantu CC, Saavedra MO, Arredondo MJ, Strobe B, Do H, Kumaraswami M, Vuopio J, Grondahl-Yli-Hannuksela K, Kristinsson KG, Gottfredsson M, Pesonen M, Pensar J, Davenport ER, Clark AG, Corander J, Caugant DA, Gaini S, Magnussen MD, Kubiak SL, Nguyen HAT, Long SW, Porter AR, DeLeo FR, Musser JM. 2019. Integrated analysis of population genomics, transcriptomics and virulence provides novel insights into *Streptococcus pyogenes* pathogenesis. *Nat Genet* 51:548-559.
29. Kachroo P, Eraso JM, Olsen RJ, Zhu L, Kubiak SL, Pruitt L, Yerramilli P, Cantu CC, Ojeda Saavedra M, Pensar J, Corander J, Jenkins L, Kao L, Granillo A, Porter AR, DeLeo FR, Musser JM. 2020. New pathogenesis mechanisms and translational leads identified by multidimensional analysis of necrotizing myositis in primates. *mBio* 11:e03363-19.
30. Deber CM, Glibowicka M, Woolley GA. 1990. Conformations of proline residues in membrane environments. *Biopolymers* 29:149-157.

31. von Heijne G. 1986. The distribution of positively charged residues in bacterial inner membrane proteins correlates with the trans-membrane topology. *EMBO J* 5:3021-3027.
32. von Heijne G. 1991. Proline kinks in transmembrane alpha-helices. *J Mol Biol* 218:499-503.
33. Cordes FS, Bright JN, Sansom MSP. 2002. Proline-induced distortions of transmembrane helices. *J Mol Biol* 323:951-960.
34. Yang ST, Lee JY, Kim HJ, Eu YJ, Shin SY, Hahm KS, Kim JI. 2006. Contribution of a central proline in model amphipathic alpha-helical peptides to self-association, interaction with phospholipids, and antimicrobial mode of action. *FEBS J* 273:4040-4054.
35. Park S-H, Kim H-E, Kim C-M, Yun H-J, Choi E-C, Lee B-J. 2002. Role of proline, cysteine and a disulphide bridge in the structure and activity of the anti-microbial peptide gaegurin 5. *Biochem J* 368:171-182.
36. Consler TG, Tsolas O, Kaback HR. 1991. Role of proline residues in the structure and function of a membrane transport protein. *Biochemistry-US* 30:1291-1298.
37. Yazyu H, Shiota S, Futai M, Tsuchiya T. 1985. Alteration in cation specificity of the melibiose transport carrier of *Escherichia coli* due to replacement of proline 122 with serine. *J Bacteriol* 162:933-937.
38. Lee DJ-S, Keramidas A, Moorhouse AJ, Schofield PR, Barry PH. 2003. The contribution of proline 250 (P-2') to pore diameter and ion selectivity in the human glycine receptor channel. *Neurosci Lett* 351:196-200.

39. Winn MP, Conlon PJ, Lynn KL, Farrington MK, Creazzo T, Hawkins AF, Daskalakis N, Kwan SY, Ebersviller S, Burchette JL, Pericak-Vance MA, Howell DN, Vance JM, Rosenberg PB. 2005. A mutation in the *TRPC6* cation channel cause familial focal segmental glomerulosclerosis. *Science* 308:1801-1804.
40. Kitzenmaier A, Schaefer N, Kasaragod VB, Polster T, Hantschmann R, Schindelin H, Villmann C. 2019. The P429L loss of function mutation of the human glycine transporter 2 associated with hyperekplexia. *Eur J Neurosci* 50:3906-3920.
41. Hardy JA, Nelson HCM. 2000. Proline in alpha-helical kink is required for folding kinetics but not for kinked structure, function, or stability of heat shock transcription factor. *Protein Sci* 9:2128-2141.
42. Wigley WC, Corboy MJ, Cutler TD, Thibodeau PH, Oldan J, Lee MG, Rizo J, Hunt JF, Thomas PJ. 2002. A protein sequence that can encode native structure by disfavoring alternate conformations. *Nat Struct Biol* 9:381-388.
43. Hong S, Ryu K-S, Oh M-S, Ji I, Ji TH. 1997. Roles of transmembrane prolines and proline-induced kinks of the lutropin/choriogonadotropin receptor. *J Biol Chem* 272:4166-4171.
44. Lu H, Marti T, Booth PJ. 2001. Proline residues in transmembrane alpha helices affect the folding of bacteriorhodopsin. *J Mol Biol* 308:437-446.
45. Yuan HS, Wnag SS, Yang W-Z. 1994. The structure of Fis mutant Pro61Ala illustrates that the kink within the long alpha-helix is not due to the presence of the proline residue. *J Biol Chem* 269:28947-28954.

46. Engelman DM, Adair BD, Brunger A, Flanagan JM, Lemmon MA, Treutlein H, Zhang J. 1992. Dimerization of Glycophorin A transmembrane helices: mutagenesis and modeling. *Jerus Sym Q* 25:115-125.
47. Orzaez M, Salgado J, Gimenez-Giner A, Perez-Paya E, Mingarro I. 2004. Influence of proline residues in transmembrane helix packing. *J Mol Biol* 335:631-640.
48. Beres SB, Kachroo P, Nasser W, Olsen RJ, Zhu L, Flores AR, de la Riva I, Paez-Mayorga J, Jimenez FE, Cantu C, Vuopio J, Jalava J, Kristinsson KG, Gottfredsson M, Corander J, Fittipaldi N, Di Luca MC, Petrelli D, Vitali LA, Raiford A, Jenkins L, Musser JM. 2016. Transcriptome remodeling contributes to epidemic disease caused by the human pathogen *Streptococcus pyogenes*. *mBio* 7:e00403-16.
49. Wolanin PM, Thomason PA, Stock JB. 2002. Histidine protein kinases: key signal transducers outside the animal kingdom. *Genome Biol* 3:review3013.1-3013.8.
50. Lina G, Jarraud S, Ji G, Greenland T, Pedraza A, Etienne J, Novick RP, Vandenesch F. 1998. Transmembrane topology and histidine protein kinase activity of AgrC, the *agr* signal receptor in *Staphylococcus aureus*. *Mol Microbiol* 28:655-662.
51. Johnsborg O, Diep DB, Nes IF. 2003. Structural analysis of the peptide Pheromone receptor PlnB, a histidine protein kinase from *Lactobacillus plantarum*. *J Bacteriol* 185:6913-6920.
52. Paluscio E. 2015. Adaptive mechanisms to niche remodeling in *Streptococcus pyogenes*. PhD thesis. Washington University in St. Louis, St. Louis, MO.
53. Bao YJ, Liang Z, Mayfield JA, Lee SW, Ploplis VA, Castellino FJ. 2015. CovRS-regulated transcriptome analysis of a hypervirulent M23 strain of group A

- Streptococcus pyogenes* provides new insights into virulence determinants. J Bacteriol 197:3191-3205.
54. Flores AR, Sahasrabhojane P, Saldana M, Galloway-Pena J, Olsen RJ, Musser JM, Shelburne SA. 2014. Molecular characterization of an invasive phenotype of group A *Streptococcus* arising during human infection using whole genome sequencing of multiple isolates from the same patient. J Infect Dis 209:1520-1523.
 55. Galloway-Pena J, DebRoy S, Brumlow C, Li X, Tran TT, Horstmann N, Yao H, Chen K, Wang F, Pan BF, Hawke DH, Thompson EJ, Arias CA, Fowler VG, Jr., Bhatti MM, Kalia A, Flores AR, Shelburne SA. 2018. Hypervirulent group A *Streptococcus* emergence in an acapsular background is associated with marked remodeling of the bacterial cell surface. PLoS One 13:e0207897.
 56. Sumbly P, Whitney AR, Graviss EA, DeLeo FR, Musser JM. 2006. Genome-wide analysis of group A streptococci reveals a mutation that modulates global phenotype and disease specificity. PLoS Pathog 2:e5.
 57. Tatsuno I, Okada R, Zhang Y, Isaka M, Hasegawa T. 2013. Partial loss of CovS function in *Streptococcus pyogenes* causes severe invasive disease. BMC Research Notes 6:126.
 58. Beres SB, Carroll RK, Shea PR, Sitkiewicz I, Martinez-Gutierrez JC, Low DE, McGeer A, Willey BM, Green K, Tyrrell GJ, Goldman TD, Feldgarden M, Birren BW, Fofanov Y, Boos J, Wheaton WD, Honisch C, Musser JM. 2010. Molecular complexity of successive bacterial epidemics deconvoluted by comparative pathogenomics. Proc Natl Acad Sci U S A 107:4371-4376.

59. Nasser W, Beres SB, Olsen RJ, Dean MA, Rice KA, Long SW, Kristinsson KG, Gottfredsson M, Vuopio J, Raisanen K, Caugant DA, Steinbakk M, Low DE, McGeer A, Darenberg J, Henriques-Normark B, Van Beneden CA, Hoffmann S, Musser JM. 2014. Evolutionary pathway to increased virulence and epidemic group A *Streptococcus* disease derived from 3,615 genome sequences. *Proc Natl Acad Sci U S A* 111:E1768-1776.
60. Shelburne SA, Olsen RJ, Suber B, Sahasrabhojane P, Sumby P, Brennan RG, Musser JM. 2010. A combination of independent transcriptional regulators shapes bacterial virulence gene expression during infection. *PLoS Pathog* 6:e1000817.
61. Graham MR, Smoot LM, Lux Migiliaccio CA, Virtaneva K, Sturdevant DE, Porcella SF, Federle MJ, Adams GJ, Scott JR, Musser JM. 2002. Virulence control in group A *Streptococcus* by a two-component gene regulatory system: global expression profiling and *in vivo* infection modeling. *Proc Natl Acad Sci U S A* 99:13855-13860.
62. Horstmann N, Sahasrabhojane P, Suber B, Kumaraswami M, Olsen RJ, Flores A, Musser JM, Brennan RG, Shelburne SA, 3rd. 2011. Distinct single amino acid replacements in the control of virulence regulator protein differentially impact streptococcal pathogenesis. *PLoS Pathog* 7:e1002311.
63. Horstmann N, Saldana M, Sahasrabhojane P, Yao H, Su X, Thompson E, Koller A, Shelburne SA, 3rd. 2014. Dual-site phosphorylation of the control of virulence regulator impacts group A streptococcal global gene expression and pathogenesis. *PLoS Pathog* 10:e1004088.

64. Horstmann N, Sahasrabhojane P, Yao H, Su X, Shelburne SA, Stock AM. 2017. Use of a phosphorylation site mutant to identify distinct modes of gene repression by the control of virulence regulator (CovR) in *Streptococcus pyogenes*. *J Bacteriol* 199:e00835-16.
65. Horstmann N, Tran CN, Brumlow C, DebRoy S, Yao H, Noguera Gonzalez G, Makthal N, Kumaraswami M, Shelburne SA. 2018. Phosphatase activity of the control of virulence sensor kinase CovS is critical for the pathogenesis of group A *streptococcus*. *PLoS Pathog* 14:e1007354.
66. Sugareva V, Arlt R, Fiedler T, Riani C, Podbielski A, Kreikemeyer B. 2010. Serotype- and strain- dependent contribution of the sensor kinase CovS of the CovRS two-component system to *Streptococcus pyogenes* pathogenesis. *BMC Microbiol* 10:34.
67. Chiang-Ni C, Tseng HC, Hung CH, Chiu CH. 2017. Acidic stress enhances CovR/S-dependent gene repression through activation of the *covR/S* promoter in *emm1*-type group A *Streptococcus*. *Int J Med Microbiol* 307:329-339.
68. Gusa AA, Scott JR. 2005. The CovR response regulator of group A streptococcus (GAS) acts directly to repress its own promoter. *Mol Microbiol* 56:1195-207.
69. Sitkiewicz I, Musser JM. 2006. Expression microarray and mouse virulence analysis of four conserved two-component gene regulatory systems in group A *Streptococcus*. *Infect Immun* 74:1339-1351.
70. Namprachan-Frantz P, Rowe HM, Runft DL, Neely MN. 2014. Transcriptional analysis of the *Streptococcus pyogenes* salivaricin locus. *J Bacteriol* 196:604-613.

71. Shelburne SA, 3rd, Sumbly P, Sitkiewicz I, Granville C, DeLeo FR, Musser JM. 2005. Central role of a bacterial two-component gene regulatory system of previously unknown function in pathogen persistence in human saliva. *Proc Natl Acad Sci U S A* 102:16037-16042.
72. Leday TV, Gold KM, Kinkel TL, Roberts SA, Scott JR, McIver KS. 2008. TrxR, a new CovR-repressed response regulator that activates the Mga virulence regulon in group A streptococcus. *Infect Immun* 76:4659-4668.
73. Liu M, Hanks TS, Zhang J, McClure MJ, Siemsen DW, Elser JL, Quinn MT, Lei B. 2006. Defects in *ex vivo* and *in vivo* growth and sensitivity to osmotic stress of group A *Streptococcus* caused by interruption of response regulator gene *vicR*. *Microbiology* 152:967-978.
74. Flores AR, Jewell BE, Yelamanchili D, Olsen RJ, Musser JM. 2015. A single amino acid replacement in the sensor kinase LiaS contributes to a carrier phenotype in group A *Streptococcus*. *Infect Immun* 83:4237-4246.
75. Voyich JM, Braughton KR, Sturdevant DE, Vuong C, Kobayashi SD, Porcella SF, Otto M, Musser JM, DeLeo FR. 2004. Engagement of the pathogen survival response used by group A *Streptococcus* to avert destruction by innate host defense. *J Immunol* 173:1194-1201.
76. Riani C, Standar K, Srimuang S, Lembke C, Kreikemeyer B, Podbielski A. 2007. Transcriptome analyses extend understanding of *Streptococcus pyogenes* regulatory mechanisms and behavior toward immunomodulatory substances. *Int J Med Microbiol* 297:513-523.

77. Kreikemeyer B, Boyle MDP, Buttaro BA, Heinemann M, Podbielski A. 2001. Group A streptococcal growth phase-associated virulence factor regulation by a novel operon (Fas) with homologues to two-component-type regulators requires a small RNA molecule. *Mol Microbiol* 39:392-406.
78. Ramirez-Pena E, Trevino J, Liu Z, Perez N, Sumbly P. 2010. The group A *Streptococcus* small regulatory RNA FasX enhances streptokinase activity by increasing the stability of the *ska* mRNA transcript. *Mol Microbiol* 78:1332-1347.
79. Danger JL, Cao TN, Cao TH, Sarkar P, Trevino J, Pflughoeft KJ, Sumbly P. 2015. The small regulatory RNA FasX enhances group A *Streptococcus* virulence and inhibits pilus expression via serotype-specific targets. *Mol Microbiol* 96:249-262.
80. Danger JL, Makthal N, Kumaraswami M, Sumbly P. 2015. The FasX small regulatory RNA negatively regulates the expression of two fibronectin-binding proteins in group A *Streptococcus*. *J Bacteriol* 197:3720-3730.
81. Churchward G, Bates C, Gusa AA, Stringer V, Scott JR. 2009. Regulation of streptokinase expression by CovR/S in *Streptococcus pyogenes*: CovR acts through a single high-affinity binding site. *Microbiology* 155:566-575.
82. Federle MJ, McIver KS, Scott JR. 1999. A response regulator that represses transcription of several virulence operons in the group A *Streptococcus*. *J Bacteriol* 181:3649-3657.
83. Miller AA, Engleberg NC, DiRita VJ. 2001. Repression of virulence genes by phosphorylation-dependent oligomerization of CsrR at target promoters in *S. pyogenes*. *Mol Microbiol* 40:976-990.

APPENDIX A
FIGURES

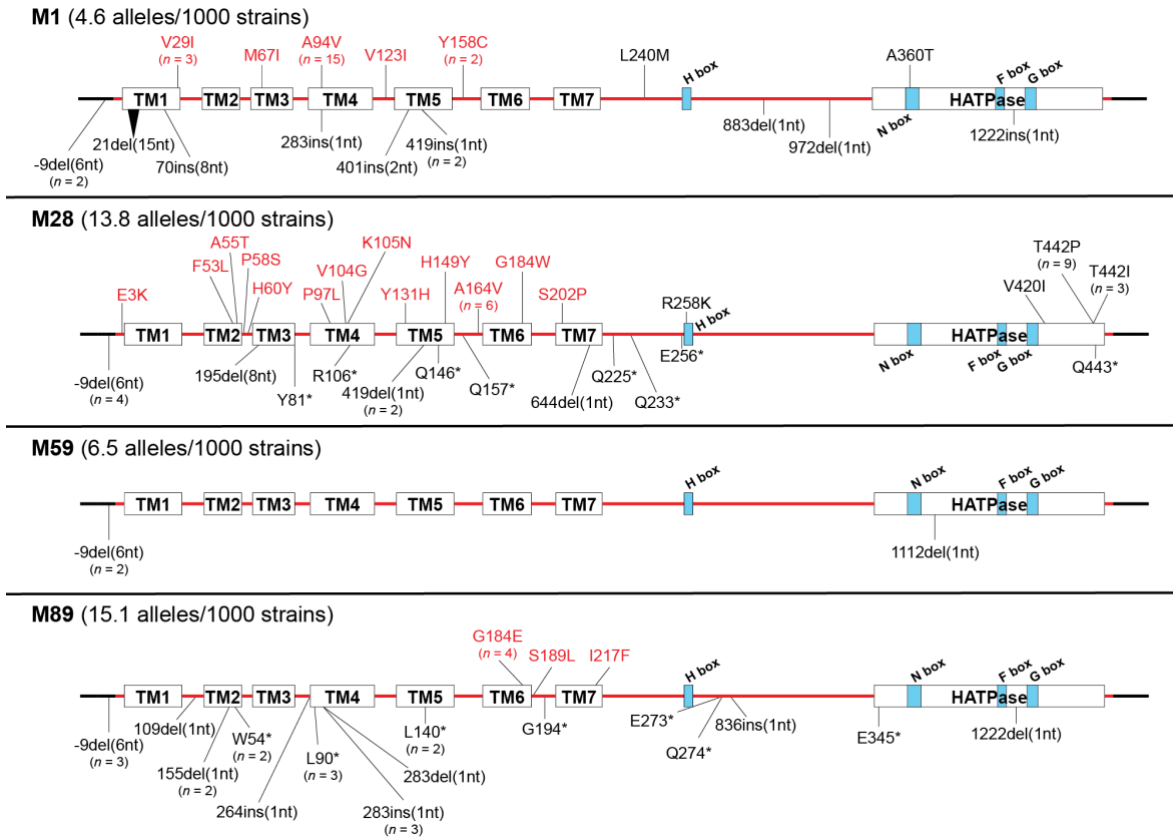


Fig. A-1 *rocA* polymorphisms identified by population-based, whole genome sequencing studies of M1, M28, M59, and M89 GAS strains. The affected codon and amino acid change conferred by each polymorphism are shown. For polymorphisms due to nucleotide deletion, the affected nucleotide is identified. Alleles identified in multiple isolates are indicated. Polymorphisms that result in *RocA* protein truncation or loss of *rocA* translation are shown below the protein schematic, and polymorphisms that result in amino acid changes are shown above the protein schematic. Missense polymorphisms in the predicted domains sufficient for regulatory activity (32) are colored red. Predicted domains of the *RocA* protein using Phyre2 are indicated (TM = transmembrane domain, HATPase = histidine kinase ATPase domain) (106). Predicted functional domains of the potential histidine kinase domain (H box, N box, F box, and G box) are identified (22). # One strain has two polymorphisms in *rocA*.

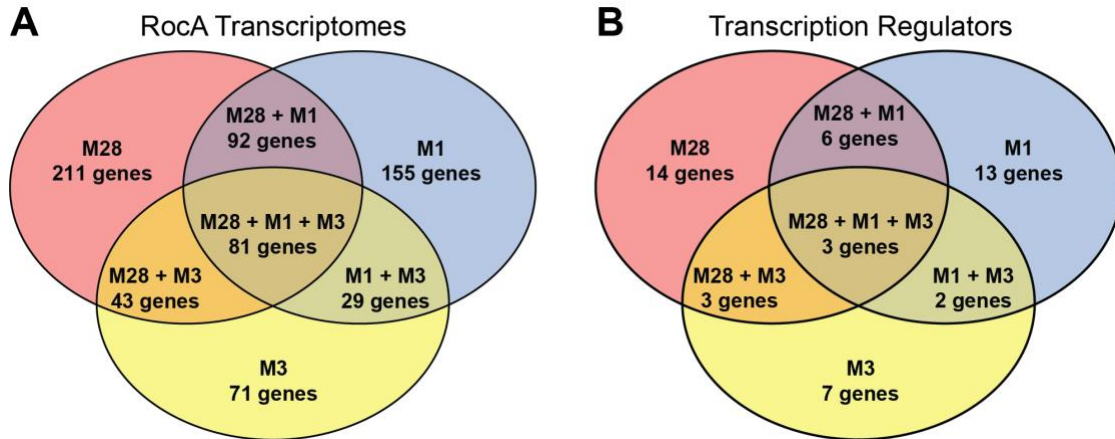


Fig. A-2 Comparison of the reported RocA transcriptomes in various M protein serotypes of GAS (A) and the number of transcription regulator genes directly or indirectly regulated by RocA (B) in serotype M1, M3, and M28 GAS (absolute fold change ≥ 1.5 , $P < 0.05$, Baggerly test with Bonferroni correction for multiple comparisons) (107).

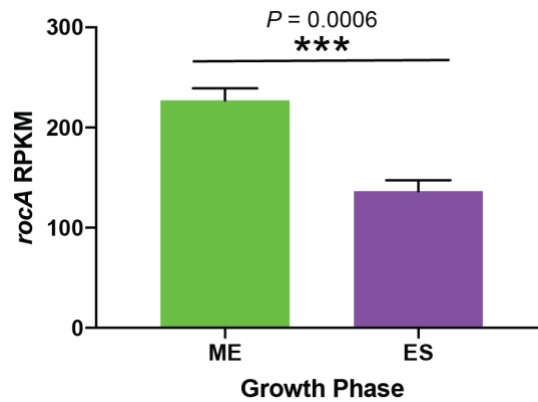


Fig. A-3 Reads per kilobase per million mapped reads (RPKM) for *rocA* in the WT strain at mid-exponential (ME) and early-stationary (ES) growth phases. Data shown as mean \pm standard deviation. *** $P < 0.001$, Student's t-test.

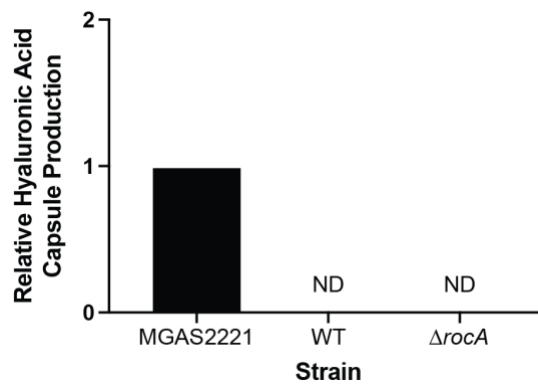


Fig. A-4 Hyaluronic acid capsule production for the parental wild-type (WT) and isogenic $\Delta rocA$ mutant strains. MGAS2221 is a serotype M1 GAS strain that is known to produce capsule (36). ND = not detected.

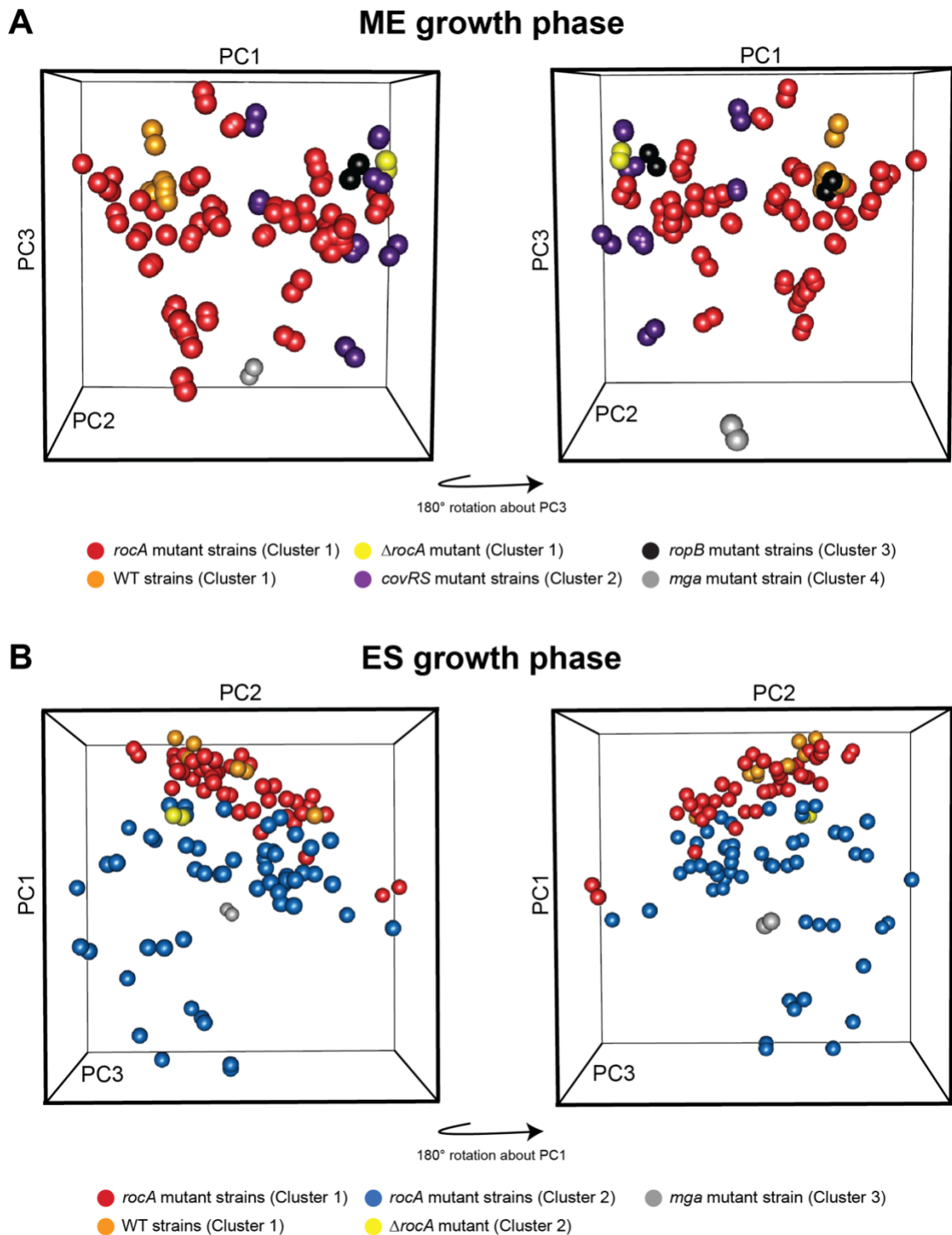


Fig. A-5 Clustering of clinical isolates with naturally occurring *rocA* polymorphisms is growth phase dependent. Three-dimensional principal component analysis (PCA) of the RNA-sequencing data generated with the clinical isolates with naturally occurring *rocA* polymorphisms, an isogenic *rocA* deletion mutant ($\Delta rocA$) strain, and four phylogenetically matched wild-type (WT) strains at mid-exponential (ME; A) and early-stationary (ES; B) growth phases. Each growth phase is represented by two PCA plots that are rotated approximately 180 degrees about the PC3 axis (ME) or the PC1 axis (ES). Clinical isolates are colored by clusters of the opposite growth phase, as determined by average-linkage hierarchical clustering. No obvious clustering is observed with this scheme.

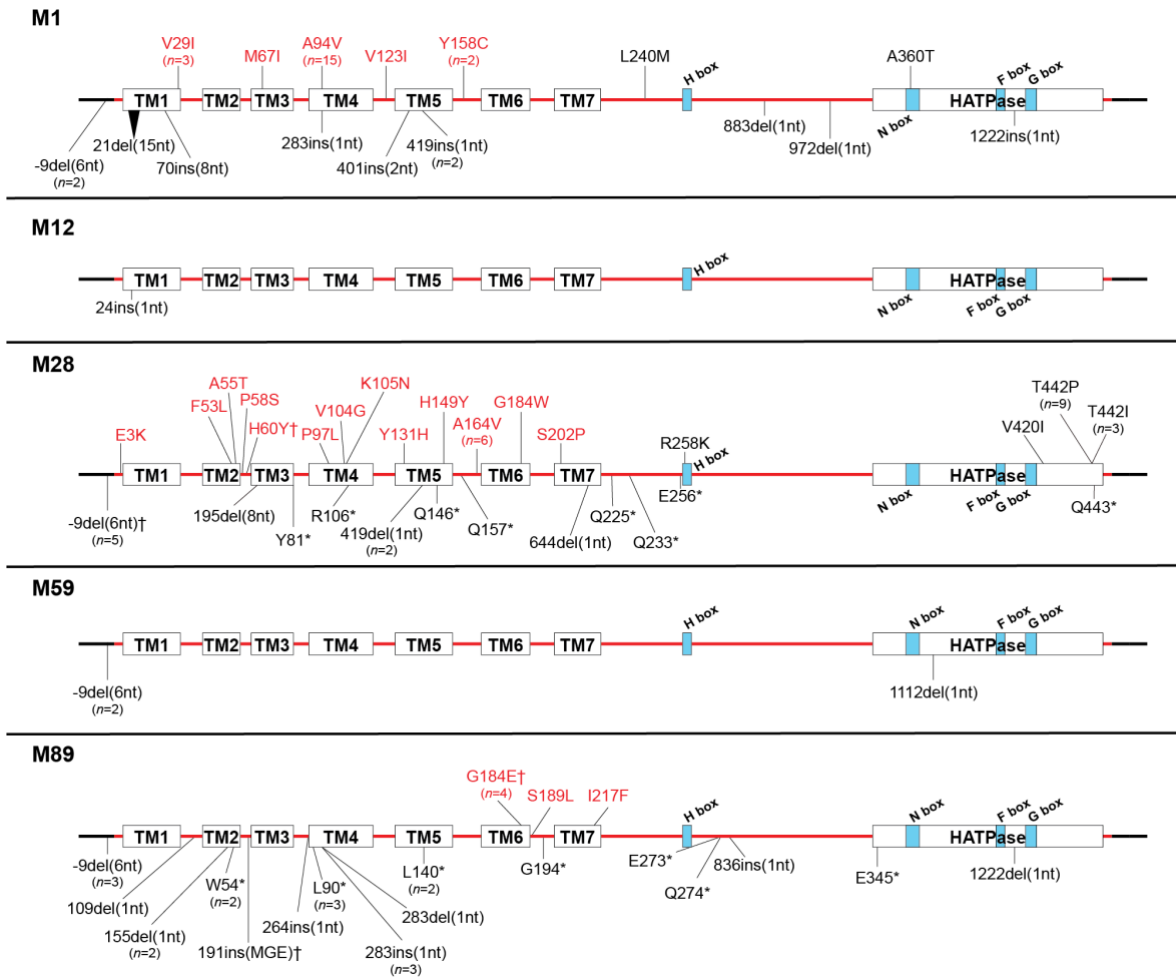


Fig. A-6 *rocA* polymorphisms identified by population-based, whole genome sequencing studies of serotype M1, M12, M28, M59, and M89 GAS strains. The affected codon and amino acid change conferred by each polymorphism are shown. For polymorphisms due to nucleotide deletion or insertion, the affected nucleotide is identified. Alleles identified in multiple isolates are indicated. Polymorphisms that result in RocA protein truncation or presumed loss of *rocA* mRNA translation are shown below the protein schematic, and polymorphisms that result in amino acid changes are shown above the protein schematic. Missense polymorphisms in the amino-terminal transmembrane domains are red. Predicted domains of the RocA protein are indicated. Predicted functional domains of the putative histidine kinase domain (H box, N box, F box, and G box) are identified. Asterisks denote stop codons. Daggers indicate strains that have two polymorphisms in *rocA*. Adapted from Bernard et al. Copyright © American Society for Microbiology. HATPase, histidine kinase ATPase domain; MGE, mobile genetic element; TM, transmembrane domain.

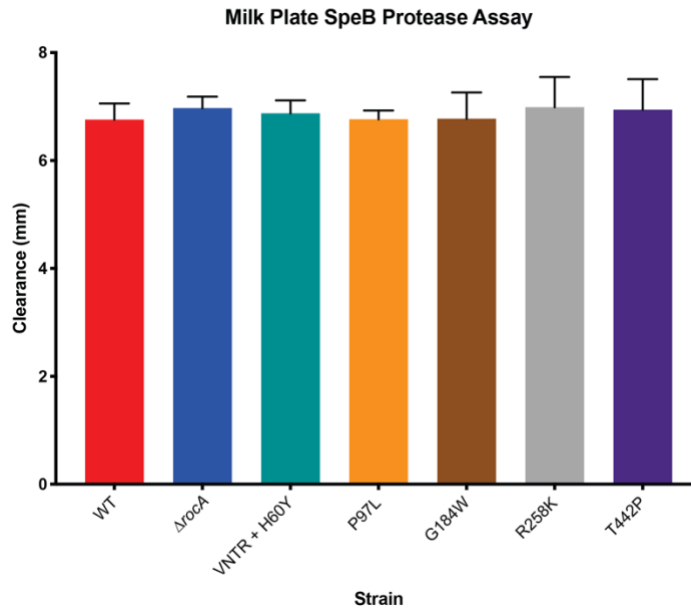


Fig. A-7 Polymorphisms in RocA do not alter secreted streptococcal pyrogenic exotoxin B (SpeB) protease activity in a casein hydrolysis (milk plate) assay. $P = 0.9710$ (one-way analysis of variance with Dunn multiple comparisons test). Data are expressed as means \pm SD. VNTR, variable number tandem repeat; WT, wild type.

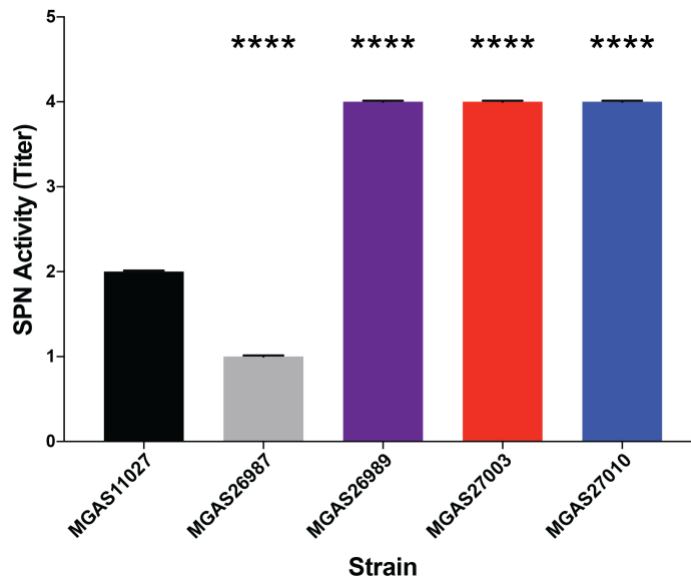


Fig. A-8 The RocA G184E polymorphism in serotype M89 GAS results in decreased secreted NAD^+ -glycohydrolase (SPN) activity *in vitro*. Data are expressed as means \pm SD. **** $P < 0.0001$ (one-way analysis of variance with Dunnett multiple comparisons test). MGAS11027, serotype M89 parental wild-type strain; MGAS26987, serotype M89 RocA G184E mutant; MGAS26989, serotype M89 RocA G184E and control of virulence sensor (CovS) R444I mutant; MGAS27003, serotype M89 RocA G184E and CovS F31I/E50G mutant; MGAS27010, serotype M89 RocA G184E mutant with an additional mobile genetic element disrupting the *rocA* gene.

10	20	30	40	50	60	70	80	90	100	
MLEDFLQFLG	FIFLDIIEIM	LTLKLFSPVS	AIPRLRKNIF	YLSLSMVLFO	VVFWAFPPDH	FILDVVMLAQ	FLFFALIALY	YGKSIKAKFL	MFYAFFPLVS	(1)
MLEDFLQFLG	FIFLDIIEIM	LTLKLFSPVS	AIPRLRKNIF	YLSLSMVLFO	VVFWAFPPDH	FILDVVMLAQ	FLFFALIALY	YGKSIKAKFL	MFYAFFPLVS	(2)
MLEDFLQFLG	FIFLDIIEIM	LTLKLFSPVS	AIPRLRKNIF	YLSLSMVLFO	VVFWAFPPDH	FILDVVMLAQ	FLFFALIALY	YGKSIKAKFL	MFYAFFPLVS	(3)
MLEDFLQFLG	FIFLDIIEIM	LTLKLFSPVS	AIPRLRKNIF	YLSLSMVLFO	VVFWAFPPDH	FILDVVMLAQ	FLFFALIALY	YGKSIKAKFL	MFYAFFPLVS	(4)
MLEDFLQFLG	FIFLDIIEIM	LTLKLFSPVS	AIPRLRKNIF	YLSLSMVLFO	VVFWAFPPDH	FILDVVMLAQ	FLFFALIALY	YGKSIKAKFL	MFYAFFPLVS	(5)
MLEDFLQFLG	FIFLDIIEIM	LTLKLFSPVS	AIPRLRKNIF	YLSLSMVLFO	VVFWAFPPDH	FILDVVMLAQ	FLFFALIALY	YGKSIKAKFL	MFYAFFPLVS	(6)
MLEDFLQFLG	FIFLDIIEIM	LTLKLFSPVS	AIPRLRKNIF	YLSLSMVLFO	VVFWAFPPDH	FILDVVMLAQ	FLFFALIALY	YGKSIKAKFL	MFYAFFPLVS	(7)
MLEDFLQFLG	FIFLDIIEIM	LTLKLFSPVS	AIPRLRKNIF	YLSLSMVLFO	VVFWAFPPDH	FILDVVMLAQ	FLFFALIALY	YGKSIKAKFL	MFYAFFPLVS	(8)
110	120	130	140	150	160	170	180	190	200	
ISLVRKRFIV	FVMPLFGMPY	SVVKHNTLLI	YSITCFSIFL	IYRCIQVPHF	DFSTWRQYFQ	SHRASKLLVF	TNSSMALYYL	CVQGIDVMSF	SLSGLATTATTA	(1)
ISLVRKRFIV	FVMPLFGMPY	SVVKHNTLLI	YSITCFSIFL	IYRCIQVPHF	DFSTWRQYFQ	SHRASKLLVF	TNSSMALYYL	CVQGIDVMSF	SLSGLATTATTA	(2)
ISLVRKRFIV	FVMPLFGMPY	SVVKHNTLLI	YSITCFSIFL	IYRCIQVPHF	DFSTWRQYFQ	SHRASKLLVF	TNSSMALYYL	CVQGIDVMSF	SLSGLATTATTA	(3)
ISLVRKRFIV	FVMPLFGMPY	SVVKHNTLLI	YSITCFSIFL	IYRCIQVPHF	DFSTWRQYFQ	SHRASKLLVF	TNSSMALYYL	CVQGIDVMSF	SLSGLATTATTA	(4)
ISLVRKRFIV	FVMPLFGMPY	SVVKHNTLLI	YSITCFSIFL	IYRCIQVPHF	DFSTWRQYFQ	SHRASKLLVF	TNSSMALYYL	CVQGIDVMSF	SLSGLATTATTA	(5)
ISLVRKRFIV	FVMPLFGMPY	SVVKHNTLLI	YSITCFSIFL	IYRCIQVPHF	DFSTWRQYFQ	SHRASKLLVF	TNSSMALYYL	CVQGIDVMSF	SLSGLATTATTA	(6)
ISLVRKRFIV	FVMPLFGMPY	SVVKHNTLLI	YSITCFSIFL	IYRCIQVPHF	DFSTWRQYFQ	SHRASKLLVF	TNSSMALYYL	CVQGIDVMSF	SLSGLATTATTA	(7)
ISLVRKRFIV	FVMPLFGMPY	SVVKHNTLLI	YSITCFSIFL	IYRCIQVPHF	DFSTWRQYFQ	SHRASKLLVF	TNSSMALYYL	CVQGIDVMSF	SLSGLATTATTA	(8)
210	220	230	240	250	260	270	280	290	300	
RSIIVLFYFI	LFLELLIHLE	RYVKQNSIEA	IVQOKEYREL	INYSQHLGLL	YQDIQELRQL	LTTVSSRLKI	GIEQNDISIV	RLTYEGILNA	EKNNAKDDRL	(1)
RSIIVLFYFI	LFLELLIHLE	RYVKQNSIEA	IVQOKEYREL	INYSQHLGLL	YQDIQELRQL	LTTVSSRLKI	GIEQNDISIV	RLTYEGILNA	EKNNAKDDRL	(2)
RSIIVLFYFI	LFLELLIHLE	RYVKQNSIEA	IVQOKEYREL	INYSQHLGLL	YQDIQELRQL	LTTVSSRLKI	GIEQNDISIV	RLTYEGILNA	EKNNAKDDRL	(3)
RSIIVLFYFI	LFLELLIHLE	RYVKQNSIEA	IVQOKEYREL	INYSQHLGLL	YQDIQELRQL	LTTVSSRLKI	GIEQNDISIV	RLTYEGILNA	EKNNAKDDRL	(4)
RSIIVLFYFI	LFLELLIHLE	RYVKQNSIEA	IVQOKEYREL	INYSQHLGLL	YQDIQELRQL	LTTVSSRLKI	GIEQNDISIV	RLTYEGILNA	EKNNAKDDRL	(5)
RSIIVLFYFI	LFLELLIHLE	RYVKQNSIEA	IVQOKEYREL	INYSQHLGLL	YQDIQELRQL	LTTVSSRLKI	GIEQNDISIV	RLTYEGILNA	EKNNAKDDRL	(6)
RSIIVLFYFI	LFLELLIHLE	RYVKQNSIEA	IVQOKEYREL	INYSQHLGLL	YQDIQELRQL	LTTVSSRLKI	GIEQNDISIV	RLTYEGILNA	EKNNAKDDRL	(7)
RSIIVLFYFI	LFLELLIHLE	RYVKQNSIEA	IVQOKEYREL	INYSQHLGLL	YQDIQELRQL	LTTVSSRLKI	GIEQNDISIV	RLTYEGILNA	EKNNAKDDRL	(8)
310	320	330	340	350	360	370	380	390	400	
DLTCLDKLQV	EAIRHIVLAK	LIEAKNKKLK	VEVSIPNCIA	TFPLEVVDFT	KLLSFLLDNA	IEMSLETKQP	CLSI AFLDQN	HKLVIIVIQSS	TRQGGNDSQS	(1)
DLTCLDKLQV	EAIRHIVLAK	LIEAKNKKLK	VEVSIPNCIA	TFPLEVVDFT	KLLSFLLDNA	IEMSLETKQP	CLSI AFLDQN	HKLVIIVIQSS	TRQGGNDSQS	(2)
DLTCLDKLQV	EAIRHIVLAK	LIEAKNKKLK	VEVSIPNCIA	TFPLEVVDFT	KLLSFLLDNA	IEMSLETKQP	CLSI AFLDQN	HKLVIIVIQSS	TRQGGNDSQS	(3)
DLTCLDKLQV	EAIRHIVLAK	LIEAKNKKLK	VEVSIPNCIA	TFPLEVVDFT	KLLSFLLDNA	IEMSLETKQP	CLSI AFLDQN	HKLVIIVIQSS	TRQGGNDSQS	(4)
DLTCLDKLQV	EAIRHIVLAK	LIEAKNKKLK	VEVSIPNCIA	TFPLEVVDFT	KLLSFLLDNA	IEMSLETKQP	CLSI AFLDQN	HKLVIIVIQSS	TRQGGNDSQS	(5)
DLTCLDKLQV	EAIRHIVLAK	LIEAKNKKLK	VEVSIPNCIA	TFPLEVVDFT	KLLSFLLDNA	IEMSLETKQP	CLSI AFLDQN	HKLVIIVIQSS	TRQGGNDSQS	(6)
DLTCLDKLQV	EAIRHIVLAK	LIEAKNKKLK	VEVSIPNCIA	TFPLEVVDFT	KLLSFLLDNA	IEMSLETKQP	CLSI AFLDQN	HKLVIIVIQSS	TRQGGNDSQS	(7)
DLTCLDKLQV	EAIRHIVLAK	LIEAKNKKLK	VEVSIPNCIA	TFPLEVVDFT	KLLSFLLDNA	IEMSLETKQP	CLSI AFLDQN	HKLVIIVIQSS	TRQGGNDSQS	(8)
410	420	430	440	450						
VFATPALKKR	DDWQFDLRNV	TTILNRYDYL	TISSQIHDGI	LTQLIEIAKP	D					(1)
VFATPALKKR	DDWQFDLRNV	TTILNRYDYL	TISSQIHDGI	LTQLIEIAKP	D					(2)
VFATPALKKR	DDWQFDLRNV	TTILNRYDYL	TISSQIHDGI	LTQLIEIAKP	D					(3)
VFATPALKKR	DDWQFDLRNV	TTILNRYDYL	TISSQIHDGI	LTQLIEIAKP	D					(4)
VFATPALKKR	DDWQFDLRNV	TTILNRYDYL	TISSQIHDGI	LTQLIEIAKP	D					(5)
VFATPALKKR	DDWQFDLRNV	TTILNRYDYL	TISSQIHDGI	LTQLIEIAKP	D					(6)
VFATPALKKR	DDWQFDLRNV	TTILNRYDYL	TISSQIHDGI	LTQLIEIAKP	D					(7)
VFATPALKKR	DDWQFDLRNV	TTILNRYDYL	TISSQIHDGI	LTQLIEIAKP	D					(8)

Fig. A-9 *In silico* algorithm predictions of RocA membrane topology. Blue residues are predicted to be extracellular, red residues are predicted to be intracellular, and black residues are predicted to be in a transmembrane helix. Each line, from top to bottom, represents a different *in silico* prediction algorithm: 1) Phobius (62), 2) Philius (63), 3) OCTOPUS (64), 4) PolyPhobius (65), 5) SPOCTOPUS (66), 6) SCAMPI (67), 7) MEMSAT-SVM (68), 8) Phyre2 (69).

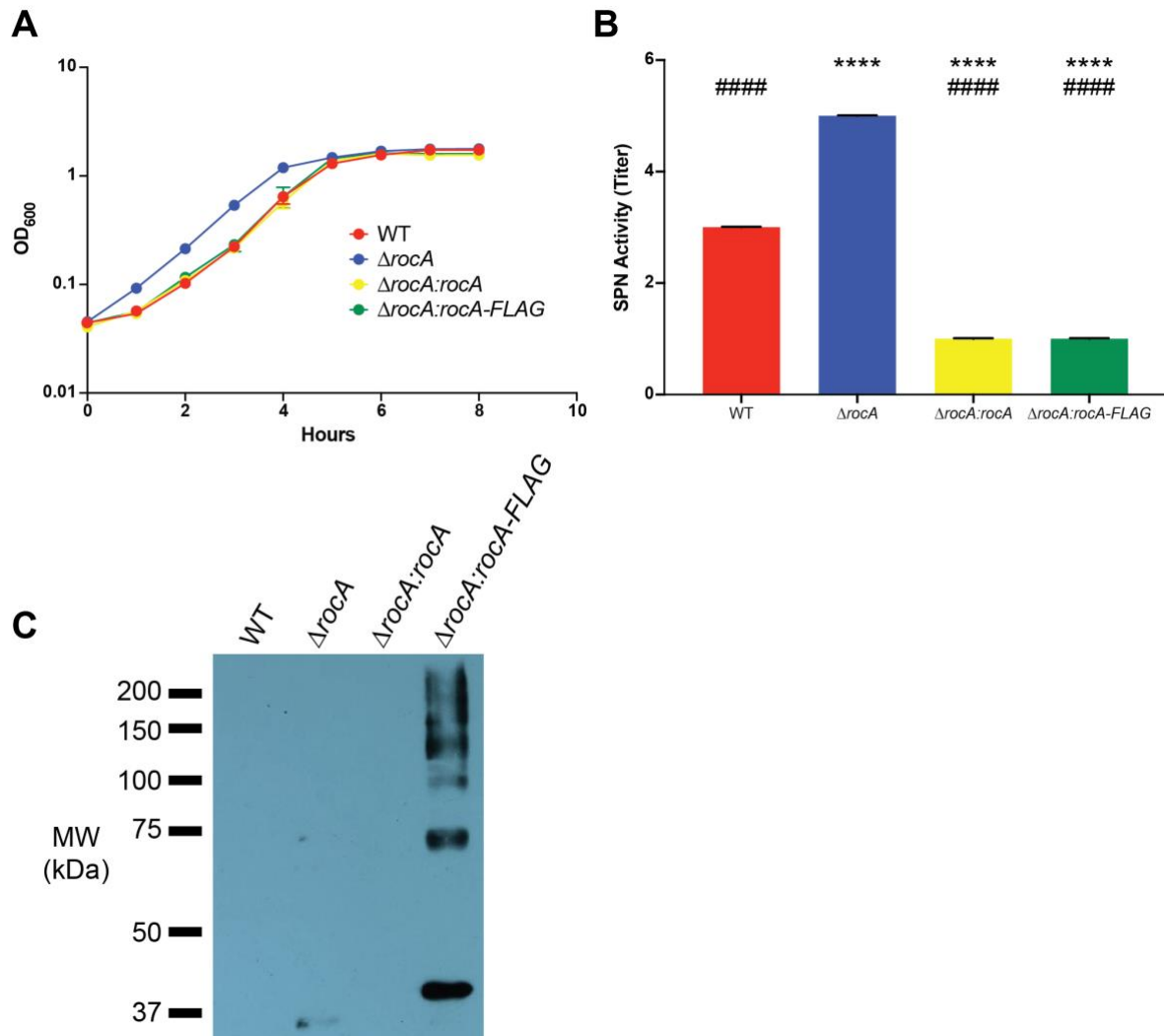


Fig. A-10 Addition of a FLAG-tag epitope to the C-terminus of RocA does not result in an altered cellular phenotype. (A) Growth curve in nutrient-rich THY broth ($n = 3$). (B) SPN activity assay ($n = 3$). Decreased activity is expected for strains carrying *rocA* on pDC123 due to a dosage effect of RocA (56). Data are shown as mean \pm standard deviation. **** $P < 0.0001$, One-way ANOVA with Tukey's multiple comparisons test compared to the parental wild-type (WT) strain; #### $P < 0.0001$, One-way ANOVA with Tukey's multiple comparisons test compared to the isogenic $\Delta rocA$ deletion mutant strain. (C) Representative Western immunoblot using anti-FLAG-tag antibody. Equivalent amounts of whole cell lysates were loaded. RocA has a molecular weight of ~ 50 kDa, but appears at approximately 40 kDa on a SDS-PAGE polyacrylamide gel (53).

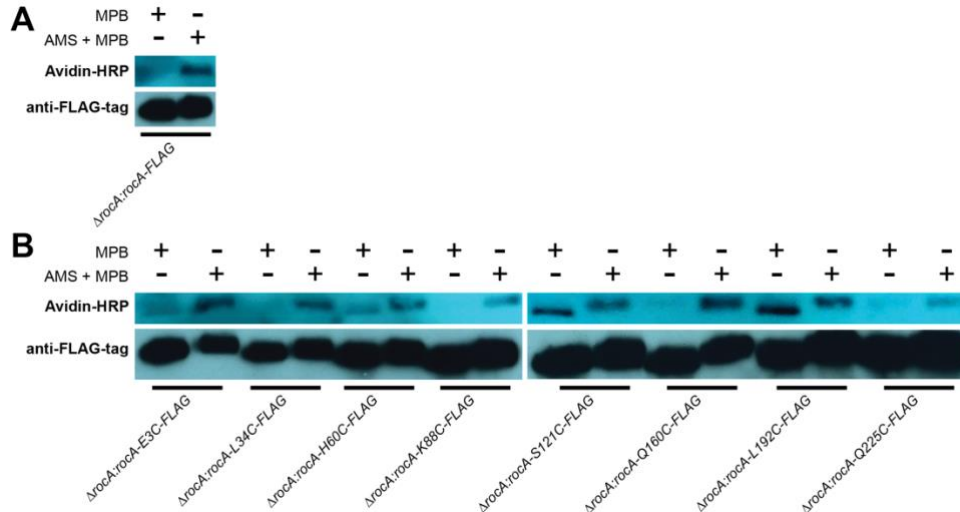


Fig. A-11 SCAM™ recapitulates the predicted in silico membrane topology of RocA in GAS. (A) Representative Western immunoblot for the wild-type RocA-FLAG allele using avidin-HRP (top) and anti-FLAG-tag (bottom). (B) Representative Western immunoblot for the engineered cysteine mutant RocA-FLAG alleles using avidin-HRP (top) and anti-FLAG-tag (bottom). Equivalent volumes for each sample were loaded. MPB: sample was treated with 3-(*N*-maleimido-propionyl)biocytin (MPB) without sonication (labeling of extracellular cysteine residues); AMS: sample was pretreated with 4-acetamido-4'-maleimidylstilbene-2,2'-disulfonic acid (AMS) prior to treatment with MPB with sonication (labeling of intracellular cysteine residues). The shift in band size is due to binding of MPB (molecular weight ~0.5 kDa) to multiple native cysteine residues in RocA.

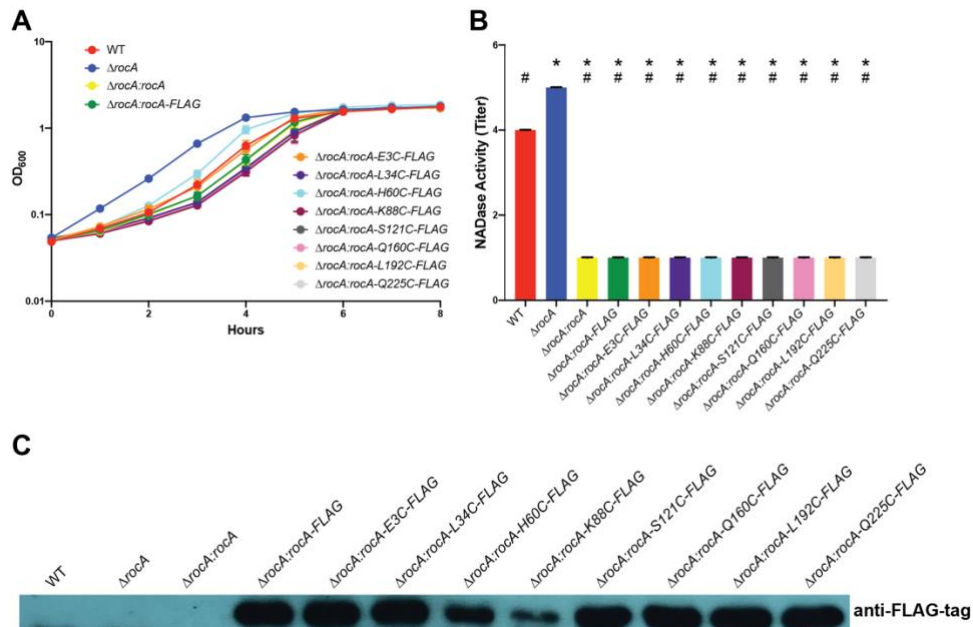


Fig. A-12 Introduction of engineered cysteine residues into RocA does not result in an altered cellular phenotype. (A) Growth curve in nutrient-rich THY broth ($n = 3$). (B) SPN activity assay ($n = 3$). Decreased activity is expected for strains carrying *rocA* on pDC123 due to a dosage effect of RocA (56). Data are shown as mean \pm standard deviation. **** $P < 0.0001$, One-way ANOVA with Tukey's multiple comparisons test compared to the parental wild-type (WT) strain; ##### $P < 0.0001$, One-way ANOVA with Tukey's multiple comparisons test compared to the isogenic $\Delta rocA$ deletion mutant strain. (C) Representative Western immunoblot using anti-FLAG-tag antibody. Equivalent amounts of whole cell lysates were loaded.

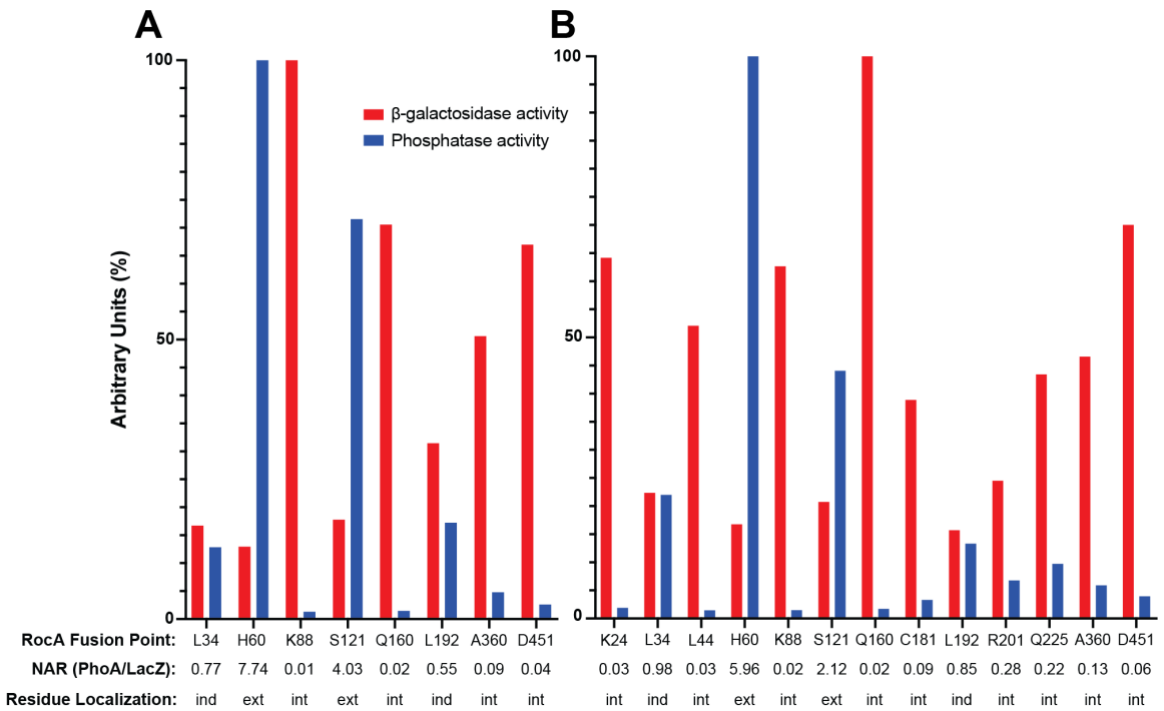


Fig. A-13 Representative β -galactosidase and phosphatase assay results for the initial (A) and additional (B) RocA-PhoA-LacZ α protein fusion experiments. Results are shown as percentage of highest activity level detected in the experimental design. NAR, normalized activity ratio; ext, predicted extracellular localization; int, predicted intracellular localization; ind, indeterminate (unable to definitively provide localization).

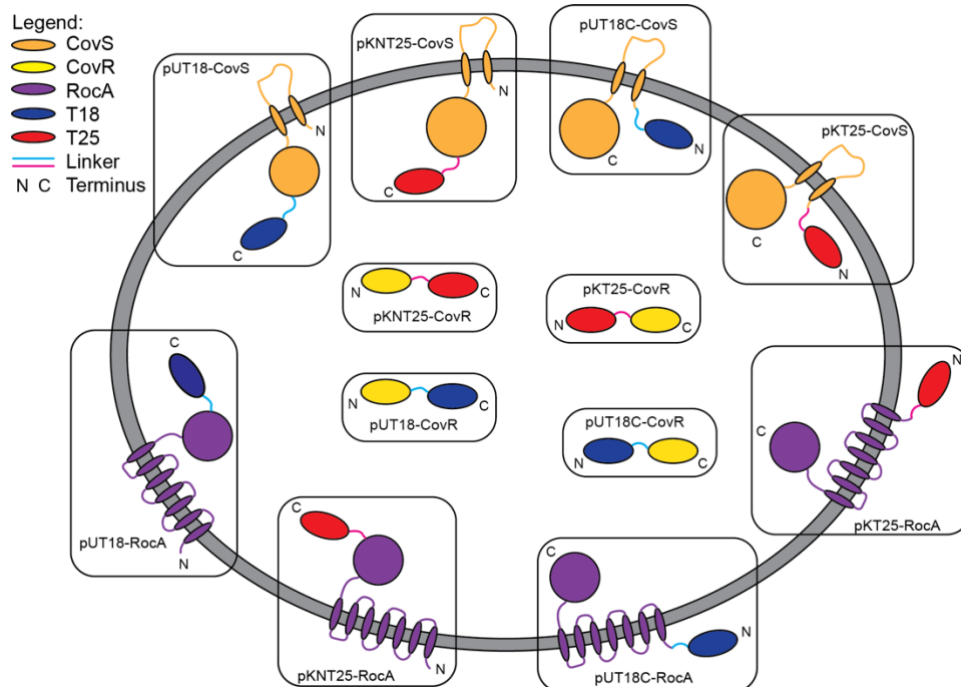


Fig. A-14 Illustration of T18/T25-RocA/CovS/CovR fusions for plasmids used in BACTH assays. The predicted topology of the fusions are depicted, and termini are labeled (N, N-terminus; C, C-terminus).

APPENDIX B

TABLES

Table B-1 Differentially expressed genes in the *ΔrocA* mutant strain compared to the wild-type (WT) strain at mid-exponential growth phase.

Locus tag^a	Gene	Fold change relative to WT	P value^b
<i>M28_Spy0011</i>	<i>tilS</i>	1.7	< 1.10E-16
<i>M28_Spy0012</i>	<i>hpt</i>	1.7	< 1.10E-16
<i>M28_Spy0013</i>	<i>ftsH</i>	2.1	< 1.10E-16
<i>M28_Spy0014</i>	<i>M28_Spy0014</i>	-1.9	< 1.10E-16
<i>M28_Spy0019</i>	<i>recO</i>	1.5	1.97E-12
<i>M28_Spy0022</i>	<i>purC</i>	-2.5	< 1.10E-16
<i>M28_Spy0023</i>	<i>purL</i>	-2.0	< 1.10E-16
<i>M28_Spy0024</i>	<i>purF</i>	-1.8	< 1.10E-16
<i>M28_Spy0025</i>	<i>purM</i>	-1.9	< 1.10E-16
<i>M28_Spy0026</i>	<i>purN</i>	-1.9	2.41E-12
<i>M28_Spy0027</i>	<i>purH</i>	-1.7	5.92E-10
<i>M28_Spy0028</i>	<i>M28_Spy0028</i>	-2.0	6.96E-08
<i>M28_Spy0029</i>	<i>purD</i>	-2.6	< 1.10E-16
<i>M28_Spy0030</i>	<i>purE</i>	-2.3	< 1.10E-16
<i>M28_Spy0031</i>	<i>purK</i>	-2.3	1.71E-11
<i>M28_Spy0032</i>	<i>M28_Spy0032</i>	-1.9	< 1.10E-16
<i>M28_Spy0034</i>	<i>comR</i>	-1.7	< 1.10E-16
<i>M28_Spy0037</i>	<i>M28_Spy0037</i>	-1.5	4.39E-13
<i>M28_Spy0039</i>	<i>M28_Spy0039</i>	2.6	< 1.10E-16
<i>M28_Spy0072</i>	<i>M28_Spy0072</i>	-2.0	5.69E-06
<i>M28_Spy0080</i>	<i>pbp1b</i>	1.5	< 1.10E-16
<i>M28_Spy0104</i>	<i>rofA</i>	-1.9	< 1.10E-16
<i>M28_Spy0105</i>	<i>sfb1</i>	-2.5	< 1.10E-16
<i>M28_Spy0107</i>	<i>cpa</i>	-2.7	< 1.10E-16
<i>M28_Spy0108</i>	<i>lepA</i>	-2.4	< 1.10E-16
<i>M28_Spy0109</i>	<i>M28_Spy0109</i>	-2.8	< 1.10E-16
<i>M28_Spy0110</i>	<i>eftLSL.B</i>	-1.9	< 1.10E-16
<i>M28_Spy0111</i>	<i>M28_Spy0111</i>	-1.8	< 1.10E-16
<i>M28_Spy0114</i>	<i>M28_Spy0114</i>	7.7	< 1.10E-16
<i>M28_Spy0117</i>	<i>atoB.2</i>	-1.5	2.17E-03
<i>M28_Spy0132</i>	<i>M28_Spy0132</i>	1.7	< 1.10E-16
<i>M28_Spy0133</i>	<i>M28_Spy0133</i>	1.5	8.77E-13
<i>M28_Spy0137</i>	<i>nga</i>	6.3	< 1.10E-16
<i>M28_Spy0138</i>	<i>ifs</i>	6.4	< 1.10E-16
<i>M28_Spy0139</i>	<i>slo</i>	6.0	< 1.10E-16
<i>M28_Spy0140</i>	<i>M28_Spy0140</i>	6.4	< 1.10E-16
<i>M28_Spy0141</i>	<i>M28_Spy0141</i>	20.4	< 1.10E-16
<i>M28_Spy0142</i>	<i>M28_Spy0142</i>	3.1	4.17E-12
<i>M28_Spy0143</i>	<i>M28_Spy0143</i>	2.7	< 1.10E-16
<i>M28_Spy0144</i>	<i>metB</i>	-3.0	< 1.10E-16
<i>M28_Spy0146</i>	<i>M28_Spy0146</i>	-2.8	< 1.10E-16

Table B-1 Continued.

Locus tag^a	Gene	Fold change relative to WT	P value^b
<i>M28_Spy0147</i>	<i>M28_Spy0147</i>	-3.3	1.15E-02
<i>M28_Spy0148</i>	<i>M28_Spy0148</i>	-2.6	1.64E-03
<i>M28_Spy0149</i>	<i>M28_Spy0149</i>	-4.0	< 1.10E-16
<i>M28_Spy0150</i>	<i>M28_Spy0150</i>	-3.4	< 1.10E-16
<i>M28_Spy0151</i>	<i>araD</i>	-3.3	< 1.10E-16
<i>M28_Spy0153</i>	<i>sgaR</i>	-1.5	2.63E-12
<i>M28_Spy0155</i>	<i>opuAA</i>	-2.1	< 1.10E-16
<i>M28_Spy0156</i>	<i>opuABC</i>	-1.7	< 1.10E-16
<i>M28_Spy0157</i>	<i>polA</i>	1.5	< 1.10E-16
<i>M28_Spy0167</i>	<i>M28_Spy0167</i>	-1.7	2.45E-03
<i>M28_Spy0172</i>	<i>M28_Spy0172</i>	-1.8	2.66E-04
<i>M28_Spy0174</i>	<i>M28_Spy0174</i>	-1.6	2.19E-05
<i>M28_Spy0178</i>	<i>M28_Spy0178</i>	1.9	< 1.10E-16
<i>M28_Spy0184</i>	<i>rivR</i>	2.4	< 1.10E-16
<i>M28_Spy0187</i>	<i>hasC.2</i>	1.6	< 1.10E-16
<i>M28_Spy0188</i>	<i>gpsA</i>	1.6	< 1.10E-16
<i>M28_Spy0189</i>	<i>yjdR</i>	-2.3	< 1.10E-16
<i>M28_Spy0190</i>	<i>M28_Spy0190</i>	-2.0	< 1.10E-16
<i>M28_Spy0191</i>	<i>M28_Spy0191</i>	-2.0	< 1.10E-16
<i>M28_Spy0196</i>	<i>M28_Spy0196</i>	1.6	< 1.10E-16
<i>M28_Spy0197</i>	<i>glxX</i>	1.5	< 1.10E-16
<i>M28_Spy0206</i>	<i>M28_Spy0206</i>	-2.1	7.89E-12
<i>M28_Spy0207</i>	<i>M28_Spy0207</i>	-1.7	2.34E-06
<i>M28_Spy0208</i>	<i>M28_Spy0208</i>	-1.9	6.29E-11
<i>M28_Spy0209</i>	<i>M28_Spy0209</i>	-2.0	< 1.10E-16
<i>M28_Spy0210</i>	<i>M28_Spy0210</i>	-1.6	8.55E-06
<i>M28_Spy0211</i>	<i>nanH</i>	-1.8	1.81E-10
<i>M28_Spy0212</i>	<i>M28_Spy0212</i>	-1.6	6.13E-06
<i>M28_Spy0233</i>	<i>bacA</i>	1.5	3.18E-06
<i>M28_Spy0266</i>	<i>braB</i>	-2.6	< 1.10E-16
<i>M28_Spy0267</i>	<i>M28_Spy0267</i>	-1.5	< 1.10E-16
<i>M28_Spy0273</i>	<i>M28_Spy0273</i>	1.9	< 1.10E-16
<i>M28_Spy0286</i>	<i>M28_Spy0286</i>	1.8	< 1.10E-16
<i>M28_Spy0302</i>	<i>M28_Spy0302</i>	-1.8	< 1.10E-16
<i>M28_Spy0310</i>	<i>fhuG</i>	-1.7	< 1.10E-16
<i>M28_Spy0311</i>	<i>fhuB</i>	-1.8	< 1.10E-16
<i>M28_Spy0312</i>	<i>fhuD</i>	-1.8	< 1.10E-16
<i>M28_Spy0313</i>	<i>fhuA</i>	-1.9	< 1.10E-16
<i>M28_Spy0315</i>	<i>M28_Spy0315</i>	1.8	< 1.10E-16
<i>M28_Spy0327</i>	<i>exoA</i>	1.8	< 1.10E-16
<i>M28_Spy0329</i>	<i>spyCEP</i>	38.0	< 1.10E-16
<i>M28_Spy0330</i>	<i>M28_Spy0330</i>	-1.7	4.70E-04
<i>M28_Spy0331</i>	<i>M28_Spy0331</i>	-2.0	< 1.10E-16
<i>M28_Spy0335</i>	<i>nrdI</i>	-1.5	9.03E-06
<i>M28_Spy0338</i>	<i>M28_Spy0338</i>	13.3	< 1.10E-16
<i>M28_Spy0341</i>	<i>M28_Spy0341</i>	13.0	< 1.10E-16
<i>M28_Spy0342</i>	<i>M28_Spy0342</i>	2.2	< 1.10E-16
<i>M28_Spy0343</i>	<i>M28_Spy0343</i>	2.8	< 1.10E-16
<i>M28_Spy0346</i>	<i>M28_Spy0346</i>	3.0	< 1.10E-16

Table B-1 Continued.

Locus tag^a	Gene	Fold change relative to WT	P value^b
<i>M28_Spy0355</i>	<i>M28_Spy0355</i>	1.5	< 1.10E-16
<i>M28_Spy0371</i>	<i>M28_Spy0371</i>	2.0	< 1.10E-16
<i>M28_Spy0372</i>	<i>phoH</i>	1.6	< 1.10E-16
<i>M28_Spy0373</i>	<i>M28_Spy0373</i>	1.8	< 1.10E-16
<i>M28_Spy0377</i>	<i>M28_Spy0377</i>	1.6	< 1.10E-16
<i>M28_Spy0390</i>	<i>M28_Spy0390</i>	1.5	1.99E-02
<i>M28_Spy0396</i>	<i>fpg</i>	1.5	2.24E-11
<i>M28_Spy0397</i>	<i>M28_Spy0397</i>	1.7	< 1.10E-16
<i>M28_Spy0398</i>	<i>M28_Spy0398</i>	1.7	< 1.10E-16
<i>M28_Spy0409</i>	<i>gloA</i>	1.8	< 1.10E-16
<i>M28_Spy0410</i>	<i>M28_Spy0410</i>	1.6	< 1.10E-16
<i>M28_Spy0411</i>	<i>pepQ</i>	1.8	< 1.10E-16
<i>M28_Spy0413</i>	<i>M28_Spy0413</i>	2.7	< 1.10E-16
<i>M28_Spy0414</i>	<i>M28_Spy0414</i>	3.1	< 1.10E-16
<i>M28_Spy0426</i>	<i>acpA</i>	1.6	< 1.10E-16
<i>M28_Spy0427</i>	<i>smc</i>	1.6	< 1.10E-16
<i>M28_Spy0448</i>	<i>M28_Spy0448</i>	1.5	7.35E-05
<i>M28_Spy0449</i>	<i>M28_Spy0449</i>	1.5	1.26E-04
<i>M28_Spy0454</i>	<i>M28_Spy0454</i>	-1.8	< 1.10E-16
<i>M28_Spy0458</i>	<i>M28_Spy0458</i>	2.3	< 1.10E-16
<i>M28_Spy0459</i>	<i>M28_Spy0459</i>	2.0	< 1.10E-16
<i>M28_Spy0460</i>	<i>M28_Spy0460</i>	1.8	8.49E-05
<i>M28_Spy0464</i>	<i>M28_Spy0464</i>	4.2	< 1.10E-16
<i>M28_Spy0476</i>	<i>M28_Spy0476</i>	-1.5	6.36E-12
<i>M28_Spy0477</i>	<i>M28_Spy0477</i>	-1.7	< 1.10E-16
<i>M28_Spy0479</i>	<i>M28_Spy0479</i>	1.5	4.39E-13
<i>M28_Spy0480</i>	<i>M28_Spy0480</i>	1.5	< 1.10E-16
<i>M28_Spy0481</i>	<i>M28_Spy0481</i>	1.7	< 1.10E-16
<i>M28_Spy0482</i>	<i>gpoA</i>	1.6	< 1.10E-16
<i>M28_Spy0483</i>	<i>pepF</i>	1.7	< 1.10E-16
<i>M28_Spy0501</i>	<i>M28_Spy0501</i>	-1.6	2.91E-03
<i>M28_Spy0507</i>	<i>M28_Spy0507</i>	1.5	1.55E-10
<i>M28_Spy0513</i>	<i>M28_Spy0513</i>	1.8	< 1.10E-16
<i>M28_Spy0517</i>	<i>M28_Spy0517</i>	1.6	< 1.10E-16
<i>M28_Spy0519</i>	<i>M28_Spy0519</i>	1.6	< 1.10E-16
<i>M28_Spy0520</i>	<i>pepD</i>	1.5	6.58E-13
<i>M28_Spy0521</i>	<i>adcA</i>	1.6	< 1.10E-16
<i>M28_Spy0522</i>	<i>agaR2</i>	-1.9	< 1.10E-16
<i>M28_Spy0523</i>	<i>agaS</i>	-1.8	< 1.10E-16
<i>M28_Spy0536</i>	<i>M28_Spy536</i>	-2.4	< 1.10E-16
<i>M28_Spy0537</i>	<i>M28_Spy0537</i>	-2.3	2.85E-04
<i>M28_Spy0538</i>	<i>ralp3</i>	-2.3	< 1.10E-16
<i>M28_Spy0539</i>	<i>epf</i>	-2.2	< 1.10E-16
<i>M28_Spy0540</i>	<i>sagA</i>	-2.7	< 1.10E-16
<i>M28_Spy0541</i>	<i>sagB</i>	-3.4	< 1.10E-16
<i>M28_Spy0542</i>	<i>sagC</i>	-3.2	< 1.10E-16
<i>M28_Spy0543</i>	<i>sagD</i>	-3.5	< 1.10E-16
<i>M28_Spy0544</i>	<i>sagE</i>	-3.0	< 1.10E-16
<i>M28_Spy0545</i>	<i>sagF</i>	-2.5	< 1.10E-16

Table B-1 Continued.

Locus tag^a	Gene	Fold change relative to WT	P value^b
M28_Spy0546	<i>sagG</i>	-3.1	< 1.10E-16
M28_Spy0547	<i>sagH</i>	-2.9	< 1.10E-16
M28_Spy0548	<i>sagI</i>	-2.7	< 1.10E-16
M28_Spy0549	<i>spnA</i>	-2.2	< 1.10E-16
M28_Spy0572	<i>M28_Spy0572</i>	1.5	< 1.10E-16
M28_Spy0573	<i>rexB</i>	1.9	< 1.10E-16
M28_Spy0574	<i>rexA</i>	1.9	< 1.10E-16
M28_Spy0575	<i>M28_Spy0575</i>	1.6	< 1.10E-16
M28_Spy0595	<i>M28_Spy0595</i>	-1.5	3.02E-04
M28_Spy0608	<i>folC.2</i>	1.6	< 1.10E-16
M28_Spy0609	<i>M28_Spy0609</i>	1.6	< 1.10E-16
M28_Spy0623	<i>M28_Spy0623</i>	-2.0	6.22E-07
M28_Spy0625	<i>M28_Spy0625</i>	1.8	< 1.10E-16
M28_Spy0626	<i>M28_Spy0626</i>	2.0	< 1.10E-16
M28_Spy0627	<i>M28_Spy0627</i>	1.9	< 1.10E-16
M28_Spy0628	<i>M28_Spy0628</i>	1.9	< 1.10E-16
M28_Spy0632	<i>M28_Spy0632</i>	-2.1	< 1.10E-16
M28_Spy0633	<i>M28_Spy0633</i>	-1.7	< 1.10E-16
M28_Spy0645	<i>murI.2</i>	-1.5	< 1.10E-16
M28_Spy0647	<i>M28_Spy0647</i>	13.3	< 1.10E-16
M28_Spy0648	<i>M28_Spy0648</i>	63.8	< 1.10E-16
M28_Spy0649	<i>mac</i>	38.1	< 1.10E-16
M28_Spy0656	<i>M28_Spy0656</i>	-2.2	2.19E-13
M28_Spy0657	<i>fms</i>	-1.7	3.95E-07
M28_Spy0658	<i>s5nA</i>	-2.9	< 1.10E-16
M28_Spy0666	<i>M28_Spy0666</i>	1.6	< 1.10E-16
M28_Spy0667	<i>mvaS.1</i>	1.6	< 1.10E-16
M28_Spy0669	<i>dyr</i>	1.6	< 1.10E-16
M28_Spy0671	<i>clpX</i>	1.6	< 1.10E-16
M28_Spy0672	<i>M28_Spy0672</i>	1.6	< 1.10E-16
M28_Spy0681	<i>cpsY</i>	1.6	< 1.10E-16
M28_Spy0682	<i>M28_Spy0682</i>	-1.5	7.67E-12
M28_Spy0683	<i>pyrF</i>	-1.6	< 1.10E-16
M28_Spy0684	<i>pyrE</i>	-1.6	< 1.10E-16
M28_Spy0686	<i>M28_Spy0686</i>	1.9	< 1.10E-16
M28_Spy0687	<i>M28_Spy0687</i>	1.9	< 1.10E-16
M28_Spy0701	<i>M28_Spy0701</i>	2.1	< 1.10E-16
M28_Spy0715	<i>cpsFP</i>	1.6	< 1.10E-16
M28_Spy0716	<i>cpsFQ</i>	1.5	< 1.10E-16
M28_Spy0719	<i>M28_Spy0719</i>	1.5	< 1.10E-16
M28_Spy0724	<i>M28_Spy0724</i>	-1.5	6.58E-13
M28_Spy0730	<i>acoA</i>	1.5	< 1.10E-16
M28_Spy0731	<i>acoB</i>	1.7	< 1.10E-16
M28_Spy0732	<i>acoC</i>	1.6	< 1.10E-16
M28_Spy0733	<i>M28_Spy0733</i>	1.5	2.63E-12
M28_Spy0734	<i>acoL</i>	1.6	< 1.10E-16
M28_Spy0748	<i>cas9</i>	-1.6	< 1.10E-16
M28_Spy0749	<i>casI</i>	-1.5	< 1.10E-16
M28_Spy0752	<i>M28_Spy0752</i>	-1.6	< 1.10E-16

Table B-1 Continued.

Locus tag^a	Gene	Fold change relative to WT	P value^b
<i>M28_Spy0754</i>	<i>sclB</i>	2.4	< 1.10E-16
<i>M28_Spy0757</i>	<i>ptsA</i>	1.8	< 1.10E-16
<i>M28_Spy0758</i>	<i>ptsB</i>	2.1	< 1.10E-16
<i>M28_Spy0759</i>	<i>ptsC</i>	2.1	< 1.10E-16
<i>M28_Spy0760</i>	<i>ptsD</i>	2.2	< 1.10E-16
<i>M28_Spy0764</i>	<i>gabD</i>	1.7	< 1.10E-16
<i>M28_Spy0765</i>	<i>uvrC</i>	2.1	< 1.10E-16
<i>M28_Spy0766</i>	<i>M28_Spy0766</i>	1.9	< 1.10E-16
<i>M28_Spy0767</i>	<i>M28_Spy0767</i>	1.9	< 1.10E-16
<i>M28_Spy0768</i>	<i>thdF</i>	-1.6	< 1.10E-16
<i>M28_Spy0771</i>	<i>M28_Spy0771</i>	-1.6	5.93E-08
<i>M28_Spy0772</i>	<i>M28_Spy0772</i>	-1.7	< 1.10E-16
<i>M28_Spy0773</i>	<i>M28_Spy0773</i>	-1.6	2.27E-04
<i>M28_Spy0774</i>	<i>M28_Spy0774</i>	-2.3	8.79E-05
<i>M28_Spy0778</i>	<i>srl</i>	-1.7	1.95E-02
<i>M28_Spy0797</i>	<i>folC.1</i>	2.1	< 1.10E-16
<i>M28_Spy0798</i>	<i>folE</i>	1.8	< 1.10E-16
<i>M28_Spy0799</i>	<i>folP</i>	1.9	< 1.10E-16
<i>M28_Spy0800</i>	<i>folQ</i>	1.9	< 1.10E-16
<i>M28_Spy0801</i>	<i>folK</i>	2.0	< 1.10E-16
<i>M28_Spy0811</i>	<i>M28_Spy0811</i>	-1.6	1.96E-03
<i>M28_Spy0833</i>	<i>M28_Spy0833</i>	-1.5	2.19E-13
<i>M28_Spy0835</i>	<i>M28_Spy0835</i>	-1.5	7.32E-04
<i>M28_Spy0846</i>	<i>nox</i>	1.7	< 1.10E-16
<i>M28_Spy0852</i>	<i>M28_Spy0852</i>	1.5	< 1.10E-16
<i>M28_Spy0853</i>	<i>M28_Spy0853</i>	1.6	< 1.10E-16
<i>M28_Spy0858</i>	<i>smf</i>	-1.8	1.78E-07
<i>M28_Spy0862</i>	<i>M28_Spy0862</i>	-1.6	1.51E-03
<i>M28_Spy0863</i>	<i>ddh</i>	-1.7	2.56E-04
<i>M28_Spy0871</i>	<i>citG</i>	-1.5	< 1.10E-16
<i>M28_Spy0872</i>	<i>M28_Spy0872</i>	-1.8	3.95E-12
<i>M28_Spy0882</i>	<i>oadA1</i>	1.5	9.94E-05
<i>M28_Spy0883</i>	<i>citC</i>	1.7	< 1.10E-16
<i>M28_Spy0884</i>	<i>M28_Spy0884</i>	1.6	< 1.10E-16
<i>M28_Spy0885</i>	<i>xerD</i>	-1.7	< 1.10E-16
<i>M28_Spy0903</i>	<i>M28_Spy0903</i>	1.5	1.05E-05
<i>M28_Spy0916</i>	<i>M28_Spy0916</i>	-1.8	< 1.10E-16
<i>M28_Spy0917</i>	<i>coaA</i>	2.4	< 1.10E-16
<i>M28_Spy0923</i>	<i>phoU</i>	-1.6	< 1.10E-16
<i>M28_Spy0924</i>	<i>pstB</i>	-1.6	< 1.10E-16
<i>M28_Spy0925</i>	<i>pstB2</i>	-1.5	< 1.10E-16
<i>M28_Spy0926</i>	<i>pstA</i>	-1.5	8.77E-13
<i>M28_Spy0927</i>	<i>pstC</i>	-1.6	< 1.10E-16
<i>M28_Spy0928</i>	<i>pstS</i>	-1.5	2.63E-12
<i>M28_Spy0933</i>	<i>mreA</i>	1.5	2.19E-13
<i>M28_Spy0934</i>	<i>truB</i>	1.5	< 1.10E-16
<i>M28_Spy0935</i>	<i>M28_Spy0935</i>	1.5	< 1.10E-16
<i>M28_Spy0943</i>	<i>M28_Spy0943</i>	1.8	< 1.10E-16
<i>M28_Spy0944</i>	<i>M28_Spy0944</i>	1.6	3.42E-07

Table B-1 Continued.

Locus tag ^a	Gene	Fold change relative to WT	P value ^b
M28_Spy0945	M28_Spy0945	1.7	< 1.10E-16
M28_Spy0946	M28_Spy0946	1.6	< 1.10E-16
M28_Spy0947	M28_Spy0947	1.6	< 1.10E-16
M28_Spy0948	M28_Spy0948	1.7	9.12E-10
M28_Spy0951	M28_Spy0951	-1.5	1.08E-03
M28_Spy0953	<i>cfa</i>	-1.6	< 1.10E-16
M28_Spy0963	M28_Spy0963	2.0	< 1.10E-16
M28_Spy0964	M28_Spy0964	2.1	< 1.10E-16
M28_Spy0965	M28_Spy0965	2.2	< 1.10E-16
M28_Spy0966	M28_Spy0966	1.7	< 1.10E-16
M28_Spy1050	M28_Spy1050	2.4	< 1.10E-16
M28_Spy1051	<i>dltD</i>	2.2	< 1.10E-16
M28_Spy1052	<i>dltC</i>	2.0	< 1.10E-16
M28_Spy1053	<i>dltB</i>	2.4	< 1.10E-16
M28_Spy1054	<i>dltA</i>	2.2	< 1.10E-16
M28_Spy1055	M28_Spy1055	2.0	< 1.10E-16
M28_Spy1056	<i>uvrB</i>	1.6	< 1.10E-16
M28_Spy1067	M28_Spy1067	-1.9	< 1.10E-16
M28_Spy1074	M28_Spy1074	2.0	< 1.10E-16
M28_Spy1075	M28_Spy1075	-1.9	< 1.10E-16
M28_Spy1098	<i>grab</i>	-5.5	< 1.10E-16
M28_Spy1106	M28_Spy1106	1.5	1.52E-04
M28_Spy1107	M28_Spy1107	1.6	< 1.10E-16
M28_Spy1112	<i>gapN</i>	1.5	< 1.10E-16
M28_Spy1115	<i>nrdH</i>	1.5	6.99E-06
M28_Spy1116	<i>nrdE.2</i>	1.7	< 1.10E-16
M28_Spy1118	<i>nrdF.2</i>	1.6	< 1.10E-16
M28_Spy1127	<i>surA</i>	1.8	< 1.10E-16
M28_Spy1136	M28_Spy1136	-1.7	5.40E-03
M28_Spy1138	M28_Spy1138	-1.7	9.04E-05
M28_Spy1147	<i>kup</i>	-3.4	< 1.10E-16
M28_Spy1150	M28_Spy1150	1.7	< 1.10E-16
M28_Spy1155	M28_Spy1155	-1.6	< 1.10E-16
M28_Spy1162	M28_Spy1162	1.7	1.75E-12
M28_Spy1176	<i>artP</i>	-1.9	< 1.10E-16
M28_Spy1177	<i>artQ</i>	-1.6	< 1.10E-16
M28_Spy1179	<i>clpE</i>	1.8	< 1.10E-16
M28_Spy1193	M28_Spy1193	1.5	1.79E-04
M28_Spy1198	<i>dpr</i>	1.9	< 1.10E-16
M28_Spy1207	<i>asnA</i>	-3.3	< 1.10E-16
M28_Spy1208	<i>arcC</i>	1.8	7.25E-05
M28_Spy1209	M28_Spy1209	1.7	4.58E-10
M28_Spy1210	<i>arcD</i>	1.7	< 1.10E-16
M28_Spy1211	<i>arcB</i>	2.4	< 1.10E-16
M28_Spy1212	M28_Spy1212	1.9	< 1.10E-16
M28_Spy1213	<i>arcA</i>	2.2	< 1.10E-16
M28_Spy1289	<i>cas2</i>	2.0	< 1.10E-16
M28_Spy1290	<i>cas1</i>	1.8	< 1.10E-16
M28_Spy1291	<i>cas4</i>	2.0	< 1.10E-16

Table B-1 Continued.

Locus tag ^a	Gene	Fold change relative to WT	P value ^b
<i>M28_Spy1292</i>	<i>cas7</i>	2.1	< 1.10E-16
<i>M28_Spy1293</i>	<i>cas8</i>	1.8	< 1.10E-16
<i>M28_Spy1294</i>	<i>cas5</i>	1.7	1.48E-08
<i>M28_Spy1295</i>	<i>cas3</i>	1.8	< 1.10E-16
<i>M28_Spy1341</i>	<i>M28_Spy1341</i>	1.5	< 1.10E-16
<i>M28_Spy1342</i>	<i>M28_Spy1342</i>	1.5	2.19E-13
<i>M28_Spy1345</i>	<i>lacZ</i>	-1.8	< 1.10E-16
<i>M28_Spy1346</i>	<i>trxR</i>	-1.9	< 1.10E-16
<i>M28_Spy1347</i>	<i>trxS</i>	-2.0	< 1.10E-16
<i>M28_Spy1359</i>	<i>rocA</i>	-551.0	< 1.10E-16
<i>M28_Spy1361</i>	<i>recX</i>	1.9	< 1.10E-16
<i>M28_Spy1366</i>	<i>M28_Spy1366</i>	1.7	< 1.10E-16
<i>M28_Spy1367</i>	<i>comFC</i>	-1.5	4.03E-03
<i>M28_Spy1384</i>	<i>atoR</i>	1.7	< 1.10E-16
<i>M28_Spy1385</i>	<i>atoB</i>	2.0	< 1.10E-16
<i>M28_Spy1386</i>	<i>atoD.1</i>	1.8	7.91E-05
<i>M28_Spy1387</i>	<i>atoA</i>	1.6	< 1.10E-16
<i>M28_Spy1388</i>	<i>M28_Spy1388</i>	1.8	6.18E-05
<i>M28_Spy1397</i>	<i>pepC</i>	2.0	< 1.10E-16
<i>M28_Spy1415</i>	<i>M28_Spy1415</i>	1.6	< 1.10E-16
<i>M28_Spy1417</i>	<i>M28_Spy1417</i>	1.5	3.07E-12
<i>M28_Spy1429</i>	<i>M28_Spy1429</i>	1.8	< 1.10E-16
<i>M28_Spy1434</i>	<i>M28_Spy1434</i>	4.1	< 1.10E-16
<i>M28_Spy1440</i>	<i>lacB.1</i>	-1.6	3.18E-05
<i>M28_Spy1442</i>	<i>M28_Spy1442</i>	-2.0	< 1.10E-16
<i>M28_Spy1443</i>	<i>M28_Spy1443</i>	-1.6	8.73E-03
<i>M28_Spy1444</i>	<i>M28_Spy1444</i>	-1.8	2.43E-07
<i>M28_Spy1448</i>	<i>copA</i>	-1.8	< 1.10E-16
<i>M28_Spy1449</i>	<i>copY</i>	-2.4	< 1.10E-16
<i>M28_Spy1450</i>	<i>sse</i>	3.6	< 1.10E-16
<i>M28_Spy1461</i>	<i>hit</i>	1.6	< 1.10E-16
<i>M28_Spy1462</i>	<i>M28_Spy1462</i>	1.5	< 1.10E-16
<i>M28_Spy1466</i>	<i>M28_Spy1466</i>	-1.9	< 1.10E-16
<i>M28_Spy1493</i>	<i>M28_Spy1493</i>	-1.6	5.44E-05
<i>M28_Spy1498</i>	<i>M28_Spy1498</i>	-2.9	2.10E-02
<i>M28_Spy1499</i>	<i>M28_Spy1499</i>	-3.8	9.29E-03
<i>M28_Spy1500</i>	<i>M28_Spy1500</i>	-2.8	< 1.10E-16
<i>M28_Spy1501</i>	<i>codY</i>	1.5	2.19E-13
<i>M28_Spy1505</i>	<i>asnB</i>	1.6	< 1.10E-16
<i>M28_Spy1506</i>	<i>M28_Spy1506</i>	4.3	< 1.10E-16
<i>M28_Spy1507</i>	<i>M28_Spy1507</i>	4.3	< 1.10E-16
<i>M28_Spy1525</i>	<i>pmi</i>	2.3	< 1.10E-16
<i>M28_Spy1526</i>	<i>scrK</i>	-2.1	2.41E-12
<i>M28_Spy1537</i>	<i>uvrA</i>	1.7	< 1.10E-16
<i>M28_Spy1543</i>	<i>M28_Spy1543</i>	3.4	< 1.10E-16
<i>M28_Spy1544</i>	<i>mutY</i>	2.2	< 1.10E-16
<i>M28_Spy1545</i>	<i>M28_Spy1545</i>	1.7	1.64E-03
<i>M28_Spy1546</i>	<i>M28_Spy1546</i>	1.5	4.39E-13
<i>M28_Spy1547</i>	<i>trx.2</i>	1.6	1.60E-08

Table B-1 Continued.

Locus tag^a	Gene	Fold change relative to WT	P value^b
M28_Spy1556	<i>dinP</i>	2.0	< 1.10E-16
M28_Spy1562	<i>M28_Spy1562</i>	-2.7	6.33E-05
M28_Spy1563	<i>norA</i>	-2.8	< 1.10E-16
M28_Spy1566	<i>M28_Spy1566</i>	-2.5	1.10E-03
M28_Spy1568	<i>M28_Spy1568</i>	1.5	7.07E-05
M28_Spy1569	<i>M28_Spy1569</i>	-1.6	< 1.10E-16
M28_Spy1570	<i>dnaQ</i>	-1.8	< 1.10E-16
M28_Spy1572	<i>M28_Spy1572</i>	2.1	< 1.10E-16
M28_Spy1574	<i>M28_Spy1574</i>	1.8	7.75E-03
M28_Spy1575	<i>M28_Spy1575</i>	1.9	1.87E-07
M28_Spy1576	<i>M28_Spy1576</i>	2.3	4.17E-12
M28_Spy1580	<i>udp</i>	-1.5	1.75E-12
M28_Spy1593	<i>M28_Spy1593</i>	1.6	< 1.10E-16
M28_Spy1618	<i>salX</i>	-1.5	4.22E-02
M28_Spy1620	<i>salM</i>	-1.6	2.63E-04
M28_Spy1626	<i>lacC.2</i>	-1.6	3.51E-02
M28_Spy1627	<i>lacB.2</i>	-1.6	6.43E-04
M28_Spy1631	<i>M28_Spy1631</i>	1.7	< 1.10E-16
M28_Spy1660	<i>polC</i>	1.5	6.58E-13
M28_Spy1671	<i>lrp</i>	-1.5	1.59E-10
M28_Spy1672	<i>ska</i>	-2.2	< 1.10E-16
M28_Spy1673	<i>M28_Spy1673</i>	1.5	< 1.10E-16
M28_Spy1674	<i>relA</i>	1.5	< 1.10E-16
M28_Spy1675	<i>sclA</i>	19.1	< 1.10E-16
M28_Spy1677	<i>M28_Spy1677</i>	-1.5	3.25E-03
M28_Spy1682	<i>M28_Spy1682</i>	1.6	< 1.10E-16
M28_Spy1683	<i>trpG</i>	1.5	2.19E-13
M28_Spy1684	<i>M28_Spy1684</i>	1.7	< 1.10E-16
M28_Spy1686	<i>flaR</i>	-1.6	< 1.10E-16
M28_Spy1689	<i>dppA</i>	2.0	< 1.10E-16
M28_Spy1690	<i>dppB</i>	2.1	< 1.10E-16
M28_Spy1691	<i>dppC</i>	2.1	< 1.10E-16
M28_Spy1692	<i>dppD</i>	2.0	< 1.10E-16
M28_Spy1693	<i>dppE</i>	2.0	< 1.10E-16
M28_Spy1694	<i>M28_Spy1694</i>	1.5	3.98E-05
M28_Spy1695	<i>htpA</i>	-1.6	< 1.10E-16
M28_Spy1696	<i>lmb</i>	-1.7	3.56E-03
M28_Spy1699	<i>fba</i>	4.1	< 1.10E-16
M28_Spy1700	<i>scpA</i>	4.1	< 1.10E-16
M28_Spy1701	<i>enn</i>	1.6	1.13E-07
M28_Spy1702	<i>emm</i>	3.5	< 1.10E-16
M28_Spy1704	<i>mga</i>	2.2	< 1.10E-16
M28_Spy1706	<i>M28_Spy1706</i>	1.7	3.00E-07
M28_Spy1707	<i>isp</i>	1.5	2.19E-13
M28_Spy1708	<i>ihk</i>	1.5	4.39E-13
M28_Spy1710	<i>M28_Spy1710</i>	1.8	< 1.10E-16
M28_Spy1711	<i>M28_Spy1711</i>	1.6	< 1.10E-16
M28_Spy1712	<i>M28_Spy1712</i>	1.7	< 1.10E-16
M28_Spy1713	<i>M28_Spy1713</i>	1.8	< 1.10E-16

Table B-1 Continued.

Locus tag^a	Gene	Fold change relative to WT	P value^b
<i>M28_Spy1714</i>	<i>M28_Spy1714</i>	1.7	1.45E-11
<i>M28_Spy1715</i>	<i>sfbX</i>	3.4	< 1.10E-16
<i>M28_Spy1716</i>	<i>sof</i>	3.0	< 1.10E-16
<i>M28_Spy1717</i>	<i>grm</i>	3.6	< 1.10E-16
<i>M28_Spy1724</i>	<i>ropB</i>	-2.3	< 1.10E-16
<i>M28_Spy1725</i>	<i>mf</i>	-1.8	< 1.10E-16
<i>M28_Spy1728</i>	<i>gldA</i>	1.5	1.36E-02
<i>M28_Spy1729</i>	<i>mipB</i>	1.6	1.67E-02
<i>M28_Spy1731</i>	<i>M28_Spy1731</i>	-2.1	3.97E-03
<i>M28_Spy1736</i>	<i>M28_Spy1736</i>	-1.9	< 1.10E-16
<i>M28_Spy1739</i>	<i>pbp2A</i>	2.1	< 1.10E-16
<i>M28_Spy1740</i>	<i>M28_Spy1740</i>	2.2	< 1.10E-16
<i>M28_Spy1741</i>	<i>M28_Spy1741</i>	1.6	< 1.10E-16
<i>M28_Spy1742</i>	<i>M28_Spy1742</i>	1.6	< 1.10E-16
<i>M28_Spy1752</i>	<i>ahpC</i>	1.6	< 1.10E-16
<i>M28_Spy1753</i>	<i>ahpF</i>	1.6	< 1.10E-16
<i>M28_Spy1758</i>	<i>fhs.2</i>	-2.1	1.63E-02
<i>M28_Spy1760</i>	<i>M28_Spy1760</i>	-2.3	4.37E-05
<i>M28_Spy1761</i>	<i>hutH</i>	-2.3	5.13E-03
<i>M28_Spy1762</i>	<i>hutG</i>	-1.9	< 1.10E-16
<i>M28_Spy1763</i>	<i>M28_Spy1763</i>	-1.6	6.18E-07
<i>M28_Spy1766</i>	<i>pepO</i>	3.1	< 1.10E-16
<i>M28_Spy1767</i>	<i>dexS</i>	-1.5	< 1.10E-16
<i>M28_Spy1769</i>	<i>treR</i>	-1.5	2.33E-10
<i>M28_Spy1771</i>	<i>M28_Spy1771</i>	-1.5	2.47E-04
<i>M28_Spy1776</i>	<i>M28_Spy1776</i>	-1.5	< 1.10E-16
<i>M28_Spy1782</i>	<i>spxA2</i>	4.0	< 1.10E-16
<i>M28_Spy1818</i>	<i>uviB</i>	2.5	< 1.10E-16
<i>M28_Spy1826</i>	<i>cadD</i>	-1.6	4.02E-03
<i>M28_Spy1827</i>	<i>cadC</i>	-1.9	8.77E-13
<i>M28_Spy1828</i>	<i>M28_Spy1828</i>	-1.7	< 1.10E-16
<i>M28_Spy1829</i>	<i>M28_Spy1829</i>	-2.0	< 1.10E-16
<i>M28_Spy1830</i>	<i>M28_Spy1830</i>	-2.0	< 1.10E-16
<i>M28_Spy1835</i>	<i>ywzG</i>	-1.5	2.39E-03
<i>M28_Spy1866</i>	<i>M28_Spy1866</i>	-1.5	2.45E-04
<i>M28_Spy1875</i>	<i>M28_Spy1875</i>	-2.7	< 1.10E-16
<i>M28_Spy1881</i>	<i>M28_Spy1881</i>	2.0	< 1.10E-16
<i>M28_Spy1882</i>	<i>M28_Spy1882</i>	2.1	< 1.10E-16
<i>M28_Spy1884</i>	<i>hasA</i>	17.2	< 1.10E-16
<i>M28_Spy1885</i>	<i>hasB</i>	18.8	< 1.10E-16
<i>M28_Spy1886</i>	<i>hasC</i>	17.7	< 1.10E-16
<i>M28_Spy1891</i>	<i>trsA</i>	-1.5	2.19E-13
<i>M28_Spy1893</i>	<i>M28_Spy1893</i>	-1.7	< 1.10E-16

Bold font indicates significant differential expression in both growth phases.

^aLocus tag identified in the serotype M28 reference genome MGAS6180.

^bP value after Bonferroni correction.

Table B-2 Differentially expressed genes in the $\Delta rocA$ mutant strain compared to the wild-type (WT) strain at early-stationary growth phase.

Locus tag ^a	Gene	Fold change relative to WT	P value ^b
<i>M28_Spy0001</i>	<i>dnaA</i>	2.1	2.48E-10
<i>M28_Spy0003</i>	<i>M28_Spy0003</i>	2.1	3.84E-04
<i>M28_Spy0004</i>	<i>M28_Spy0004</i>	2.2	5.06E-08
<i>M28_Spy0005</i>	<i>pth</i>	3.2	< 1.10E-16
<i>M28_Spy0006</i>	<i>trcF</i>	2.4	2.19E-13
<i>M28_Spy0007</i>	<i>M28_Spy0007</i>	2.3	2.68E-08
<i>M28_Spy0009</i>	<i>M28_Spy0009</i>	2.5	2.50E-03
<i>M28_Spy0010</i>	<i>M28_Spy0010</i>	2.4	1.25E-10
<i>M28_Spy0011</i>	<i>tilS</i>	2.5	< 1.10E-16
<i>M28_Spy0012</i>	<i>hpt</i>	2.8	< 1.10E-16
<i>M28_Spy0013</i>	<i>ftsH</i>	1.6	3.43E-02
<i>M28_Spy0014</i>	<i>M28_Spy0014</i>	-1.9	6.04E-06
<i>M28_Spy0017</i>	<i>sibA</i>	-1.7	1.89E-02
<i>M28_Spy0019</i>	<i>recO</i>	1.8	1.30E-02
<i>M28_Spy0023</i>	<i>purL</i>	-2.0	3.72E-06
<i>M28_Spy0024</i>	<i>purF</i>	-2.0	3.79E-05
<i>M28_Spy0025</i>	<i>purM</i>	-2.0	2.96E-04
<i>M28_Spy0026</i>	<i>purN</i>	-2.9	7.89E-12
<i>M28_Spy0027</i>	<i>purH</i>	-2.9	< 1.10E-16
<i>M28_Spy0028</i>	<i>M28_Spy0028</i>	-2.4	2.86E-07
<i>M28_Spy0029</i>	<i>purD</i>	-3.2	< 1.10E-16
<i>M28_Spy0030</i>	<i>purE</i>	-3.4	< 1.10E-16
<i>M28_Spy0031</i>	<i>purK</i>	-3.2	< 1.10E-16
<i>M28_Spy0033</i>	<i>purB</i>	-1.6	1.25E-02
<i>M28_Spy0035</i>	<i>ruwB</i>	1.7	3.31E-02
<i>M28_Spy0044</i>	<i>rplD</i>	-1.7	1.38E-03
<i>M28_Spy0045</i>	<i>rplW</i>	-2.0	4.91E-10
<i>M28_Spy0047</i>	<i>rpsS</i>	-1.6	1.61E-04
<i>M28_Spy0048</i>	<i>rplV</i>	-1.9	< 1.10E-16
<i>M28_Spy0051</i>	<i>rpmC</i>	-1.8	5.90E-07
<i>M28_Spy0052</i>	<i>rpsQ</i>	-1.9	6.74E-06
<i>M28_Spy0053</i>	<i>rplN</i>	-2.1	4.65E-08
<i>M28_Spy0054</i>	<i>rplX</i>	-2.1	8.78E-09
<i>M28_Spy0055</i>	<i>rplE</i>	-1.8	1.53E-12
<i>M28_Spy0056</i>	<i>rpsN</i>	-1.8	2.28E-03
<i>M28_Spy0058</i>	<i>rplF</i>	-1.6	1.40E-02
<i>M28_Spy0059</i>	<i>rplR</i>	-1.6	1.08E-02
<i>M28_Spy0060</i>	<i>rpsE</i>	-1.7	3.79E-04
<i>M28_Spy0064</i>	<i>adk</i>	1.7	1.47E-03
<i>M28_Spy0078</i>	<i>M28_Spy0078</i>	-3.5	< 1.10E-16
<i>M28_Spy0079</i>	<i>tyrS</i>	-2.3	1.02E-09
<i>M28_Spy0082</i>	<i>rpoC</i>	-1.6	8.59E-03
<i>M28_Spy0091</i>	<i>M28_Spy0091</i>	2.5	4.22E-06
<i>M28_Spy0096</i>	<i>M28_Spy0096</i>	2.0	1.13E-02
<i>M28_Spy0097</i>	<i>M28_Spy0097</i>	2.5	3.15E-07
<i>M28_Spy0098</i>	<i>trx.1</i>	2.1	1.79E-03
<i>M28_Spy0105</i>	<i>sfb1</i>	1.9	7.77E-04
<i>M28_Spy0113</i>	<i>prtF2</i>	2.2	1.53E-07

Table B-2 Continued.

Locus tag ^a	Gene	Fold change relative to WT	P value ^b
M28_Spy0115	<i>atoE</i>	-1.8	1.28E-02
M28_Spy0137	<i>nga</i>	7.6	< 1.10E-16
M28_Spy0138	<i>ifs</i>	7.3	< 1.10E-16
M28_Spy0139	<i>slo</i>	7.2	1.15E-06
M28_Spy0140	<i>M28_Spy0140</i>	7.7	< 1.10E-16
M28_Spy0143	<i>M28_Spy0143</i>	4.4	< 1.10E-16
M28_Spy0144	<i>metB</i>	-2.7	< 1.10E-16
M28_Spy0145	<i>leuS</i>	-1.5	7.42E-03
M28_Spy0149	<i>M28_Spy0149</i>	-2.3	1.79E-04
M28_Spy0150	<i>M28_Spy0150</i>	-1.9	3.35E-02
M28_Spy0156	<i>opuABC</i>	-2.0	2.39E-06
M28_Spy0178	<i>M28_Spy0178</i>	2.0	7.43E-05
M28_Spy0187	<i>hasC.2</i>	1.6	4.48E-03
M28_Spy0196	<i>M28_Spy0196</i>	-1.9	4.44E-05
M28_Spy0206	<i>M28_Spy0206</i>	-2.5	1.16E-03
M28_Spy0207	<i>M28_Spy0207</i>	-2.4	1.90E-02
M28_Spy0208	<i>M28_Spy0208</i>	-2.1	1.18E-03
M28_Spy0225	<i>rpsG</i>	1.7	2.84E-02
M28_Spy0231	<i>M28_Spy0231</i>	-1.7	3.18E-02
M28_Spy0238	<i>M28_Spy0238</i>	1.8	2.00E-08
M28_Spy0239	<i>nifS3</i>	1.7	1.21E-09
M28_Spy0242	<i>M28_Spy0242</i>	1.8	6.46E-04
M28_Spy0244	<i>oppA</i>	-1.6	2.54E-02
M28_Spy0247	<i>oppD</i>	-1.6	2.94E-02
M28_Spy0248	<i>oppF</i>	-1.8	4.37E-04
M28_Spy0253	<i>M28_Spy0253</i>	2.6	4.34E-09
M28_Spy0255	<i>nadD</i>	2.2	2.12E-04
M28_Spy0256	<i>M28_Spy0256</i>	2.0	8.62E-05
M28_Spy0260	<i>M28_Spy0260</i>	2.5	4.81E-02
M28_Spy0267	<i>M28_Spy0267</i>	-3.3	< 1.10E-16
M28_Spy0270	<i>gidB</i>	2.1	1.12E-04
M28_Spy0276	<i>nrdR</i>	1.8	7.84E-03
M28_Spy0282	<i>murC</i>	1.7	4.63E-02
M28_Spy0283	<i>M28_Spy0283</i>	1.8	1.70E-02
M28_Spy0291	<i>M28_Spy0291</i>	1.8	1.32E-03
M28_Spy0302	<i>M28_Spy0302</i>	2.0	8.21E-04
M28_Spy0315	<i>M28_Spy0315</i>	1.6	5.87E-03
M28_Spy0328	<i>lctO</i>	-3.3	1.03E-04
M28_Spy0330	<i>M28_Spy0330</i>	2.1	4.99E-02
M28_Spy0333	<i>M28_Spy0333</i>	1.8	2.31E-02
M28_Spy0334	<i>nrdF.1</i>	1.8	5.97E-03
M28_Spy0338	<i>M28_Spy0338</i>	14.4	< 1.10E-16
M28_Spy0341	<i>M28_Spy0341</i>	7.8	< 1.10E-16
M28_Spy0342	<i>M28_Spy0342</i>	-1.7	1.08E-02
M28_Spy0359	<i>mtsC</i>	-1.5	2.54E-02
M28_Spy0366	<i>rrf</i>	-1.9	2.61E-02
M28_Spy0371	<i>M28_Spy0371</i>	-1.8	4.63E-02
M28_Spy0420	<i>M28_Spy0420</i>	-1.8	4.12E-04
M28_Spy0426	<i>acpA</i>	2.0	2.10E-03

Table B-2 Continued.

Locus tag ^a	Gene	Fold change relative to WT	P value ^b
<i>M28_Spy0427</i>	<i>smc</i>	1.6	8.26E-03
<i>M28_Spy0463</i>	<i>M28_Spy0463</i>	-1.8	1.30E-04
<i>M28_Spy0474</i>	<i>lysS</i>	1.7	4.61E-02
<i>M28_Spy0475</i>	<i>M28_Spy0475</i>	2.2	3.05E-05
<i>M28_Spy0482</i>	<i>gpoA</i>	-1.6	2.23E-04
<i>M28_Spy0493</i>	<i>M28_Spy0493</i>	1.7	7.40E-05
<i>M28_Spy0494</i>	<i>M28_Spy0494</i>	1.9	4.56E-03
<i>M28_Spy0506</i>	<i>kgdA</i>	-1.9	1.13E-03
<i>M28_Spy0514</i>	<i>dinG</i>	1.6	3.04E-02
<i>M28_Spy0515</i>	<i>aspC</i>	1.9	4.45E-09
<i>M28_Spy0516</i>	<i>asnS</i>	1.6	1.46E-03
<i>M28_Spy0531</i>	<i>M28_Spy0531</i>	2.4	1.15E-07
<i>M28_Spy0532</i>	<i>gyrB</i>	1.7	1.36E-04
<i>M28_Spy0533</i>	<i>M28_Spy0533</i>	1.9	5.73E-06
<i>M28_Spy0538</i>	<i>ralp3</i>	-1.8	3.41E-03
<i>M28_Spy0573</i>	<i>rexB</i>	1.5	3.08E-02
<i>M28_Spy0581</i>	<i>rmlD</i>	1.7	2.93E-02
<i>M28_Spy0625</i>	<i>M28_Spy0625</i>	-2.0	1.10E-06
<i>M28_Spy0626</i>	<i>M28_Spy0626</i>	-1.8	1.22E-05
<i>M28_Spy0632</i>	<i>M28_Spy0632</i>	2.6	< 1.10E-16
<i>M28_Spy0633</i>	<i>M28_Spy0633</i>	2.2	5.09E-07
<i>M28_Spy0634</i>	<i>czcD</i>	1.8	5.71E-03
<i>M28_Spy0636</i>	<i>rimM</i>	2.4	4.67E-07
<i>M28_Spy0637</i>	<i>trmD</i>	2.1	2.42E-04
<i>M28_Spy0682</i>	<i>M28_Spy0682</i>	-1.8	1.80E-03
<i>M28_Spy0693</i>	<i>bcaT</i>	-2.5	6.36E-12
<i>M28_Spy0694</i>	<i>M28_Spy0694</i>	2.7	8.55E-09
<i>M28_Spy0695</i>	<i>M28_Spy0695</i>	2.3	3.26E-02
<i>M28_Spy0697</i>	<i>M28_Spy0697</i>	1.7	4.92E-03
<i>M28_Spy0708</i>	<i>apt</i>	2.2	4.94E-05
<i>M28_Spy0709</i>	<i>dnaD</i>	2.4	4.26E-07
<i>M28_Spy0710</i>	<i>nth</i>	2.2	1.44E-04
<i>M28_Spy0742</i>	<i>femD</i>	-1.5	5.27E-06
<i>M28_Spy0744</i>	<i>hemN</i>	1.7	5.05E-03
<i>M28_Spy0764</i>	<i>gabD</i>	-1.9	6.24E-04
<i>M28_Spy0767</i>	<i>M28_Spy0767</i>	-1.6	1.76E-02
<i>M28_Spy0768</i>	<i>thdF</i>	2.2	9.94E-04
<i>M28_Spy0780</i>	<i>srtK</i>	1.7	1.06E-02
<i>M28_Spy0792</i>	<i>M28_Spy0792</i>	1.8	1.56E-02
<i>M28_Spy0801</i>	<i>folK</i>	1.6	1.84E-02
<i>M28_Spy0803</i>	<i>potA</i>	1.8	2.42E-06
<i>M28_Spy0804</i>	<i>potB</i>	1.8	5.25E-03
<i>M28_Spy0824</i>	<i>M28_Spy0824</i>	3.0	2.62E-10
<i>M28_Spy0825</i>	<i>M28_Spy0825</i>	2.8	9.47E-11
<i>M28_Spy0836</i>	<i>tdk2</i>	2.2	3.26E-04
<i>M28_Spy0838</i>	<i>hemK</i>	1.7	2.57E-02
<i>M28_Spy0848</i>	<i>gyrA</i>	1.7	8.34E-05
<i>M28_Spy0853</i>	<i>M28_Spy0853</i>	-2.4	2.19E-13
<i>M28_Spy0854</i>	<i>M28_Spy0854</i>	-3.7	< 1.10E-16

Table B-2 Continued.

Locus tag ^a	Gene	Fold change relative to WT	P value ^b
<i>M28_Spy0855</i>	<i>M28_Spy0855</i>	-3.7	< 1.10E-16
<i>M28_Spy0864</i>	<i>satD</i>	-1.8	2.22E-03
<i>M28_Spy0865</i>	<i>satE</i>	-2.0	3.60E-05
<i>M28_Spy0873</i>	<i>M28_Spy0873</i>	-4.2	< 1.10E-16
<i>M28_Spy0874</i>	<i>M28_Spy0874</i>	-2.7	1.04E-07
<i>M28_Spy0875</i>	<i>M28_Spy0875</i>	-3.1	6.58E-13
<i>M28_Spy0876</i>	<i>oadB</i>	-2.6	2.72E-07
<i>M28_Spy0877</i>	<i>M28_Spy0877</i>	-2.2	5.22E-03
<i>M28_Spy0878</i>	<i>citD</i>	-2.3	6.31E-05
<i>M28_Spy0879</i>	<i>citE</i>	-2.5	3.19E-07
<i>M28_Spy0880</i>	<i>citF</i>	-2.2	1.15E-05
<i>M28_Spy0881</i>	<i>citX</i>	-1.9	7.08E-03
<i>M28_Spy0882</i>	<i>oadA1</i>	-1.8	1.04E-02
<i>M28_Spy0884</i>	<i>M28_Spy0884</i>	1.8	2.02E-03
<i>M28_Spy0889</i>	<i>nagR</i>	2.8	4.46E-10
<i>M28_Spy0890</i>	<i>M28_Spy0890</i>	2.1	4.35E-03
<i>M28_Spy0891</i>	<i>guaA</i>	1.8	1.89E-02
<i>M28_Spy0896</i>	<i>pdxR</i>	1.8	1.14E-02
<i>M28_Spy0897</i>	<i>rnhB</i>	-1.6	9.39E-03
<i>M28_Spy0915</i>	<i>cdd</i>	1.6	3.81E-04
<i>M28_Spy0917</i>	<i>coaA</i>	2.4	1.93E-05
<i>M28_Spy0918</i>	<i>rpsT</i>	2.4	1.24E-05
<i>M28_Spy0919</i>	<i>ciaH</i>	2.1	2.63E-09
<i>M28_Spy0920</i>	<i>ciaR</i>	2.0	4.11E-06
<i>M28_Spy0949</i>	<i>pcrA</i>	1.7	4.19E-03
<i>M28_Spy0963</i>	<i>M28_Spy0963</i>	-1.7	1.20E-02
<i>M28_Spy0965</i>	<i>M28_Spy0965</i>	-1.6	3.36E-03
<i>M28_Spy1050</i>	<i>M28_Spy1050</i>	1.7	1.85E-02
<i>M28_Spy1051</i>	<i>dluD</i>	1.5	2.45E-02
<i>M28_Spy1070</i>	<i>M28_Spy1070</i>	2.3	8.88E-04
<i>M28_Spy1074</i>	<i>M28_Spy1074</i>	-2.1	2.20E-03
<i>M28_Spy1098</i>	<i>grab</i>	-8.7	< 1.10E-16
<i>M28_Spy1109</i>	<i>udk</i>	2.7	7.22E-07
<i>M28_Spy1111</i>	<i>M28_Spy1111</i>	2.1	6.13E-09
<i>M28_Spy1115</i>	<i>nrdH</i>	4.4	< 1.10E-16
<i>M28_Spy1116</i>	<i>nrdE.2</i>	2.2	1.07E-11
<i>M28_Spy1118</i>	<i>nrdF.2</i>	2.3	2.88E-10
<i>M28_Spy1127</i>	<i>surA</i>	1.9	3.05E-02
<i>M28_Spy1144</i>	<i>M28_Spy1144</i>	1.8	2.82E-02
<i>M28_Spy1147</i>	<i>kup</i>	-4.0	< 1.10E-16
<i>M28_Spy1148</i>	<i>deaD</i>	1.8	2.12E-03
<i>M28_Spy1149</i>	<i>prfC</i>	2.2	9.91E-09
<i>M28_Spy1151</i>	<i>murF</i>	2.1	3.57E-05
<i>M28_Spy1152</i>	<i>ddlA</i>	2.0	2.75E-02
<i>M28_Spy1154</i>	<i>M28_Spy1154</i>	2.5	1.13E-03
<i>M28_Spy1156</i>	<i>M28_Spy1156</i>	-1.7	2.78E-02
<i>M28_Spy1178</i>	<i>M28_Spy1178</i>	2.4	4.44E-04
<i>M28_Spy1206</i>	<i>M28_Spy1206</i>	1.7	9.31E-04
<i>M28_Spy1207</i>	<i>asnA</i>	-1.8	3.07E-02

Table B-2 Continued.

Locus tag ^a	Gene	Fold change relative to WT	P value ^b
M28_Spy1289	<i>cas2</i>	2.7	4.43E-10
M28_Spy1290	<i>cas1</i>	2.9	7.98E-06
M28_Spy1291	<i>cas4</i>	2.7	< 1.10E-16
M28_Spy1292	<i>cas7</i>	2.2	3.60E-07
M28_Spy1293	<i>cas8</i>	3.2	< 1.10E-16
M28_Spy1294	<i>cas5</i>	3.4	< 1.10E-16
M28_Spy1295	<i>cas3</i>	4.0	< 1.10E-16
M28_Spy1296	<i>valS</i>	-1.7	1.02E-04
M28_Spy1300	M28_Spy1300	1.6	5.00E-02
M28_Spy1338	M28_Spy1338	1.9	3.66E-02
M28_Spy1356	M28_Spy1356	-1.9	7.33E-04
M28_Spy1359	<i>rocA</i>	-193.2	< 1.10E-16
M28_Spy1370	<i>cysM</i>	-1.8	8.77E-13
M28_Spy1371	M28_Spy1371	-1.8	2.05E-05
M28_Spy1373	<i>liaR</i>	-1.7	1.12E-05
M28_Spy1382	<i>gmk</i>	1.9	2.82E-04
M28_Spy1388	M28_Spy1388	-1.7	1.77E-02
M28_Spy1392	M28_Spy1392	1.5	2.92E-02
M28_Spy1394	M28_Spy1394	2.5	8.55E-07
M28_Spy1409	<i>ftsL</i>	2.2	4.22E-05
M28_Spy1410	<i>mraW</i>	2.4	2.97E-06
M28_Spy1417	M28_Spy1417	1.7	2.83E-03
M28_Spy1420	M28_Spy1420	-2.0	3.80E-03
M28_Spy1421	M28_Spy1421	-1.7	1.25E-02
M28_Spy1425	M28_Spy1425	-2.0	2.63E-06
M28_Spy1426	M28_Spy1426	-1.8	6.30E-05
M28_Spy1430	M28_Spy1430	-1.9	2.73E-04
M28_Spy1441	<i>lacA.1</i>	-2.0	2.01E-03
M28_Spy1442	M28_Spy1442	-2.4	1.31E-05
M28_Spy1443	M28_Spy1443	-2.6	7.45E-03
M28_Spy1444	M28_Spy1444	-2.6	5.75E-03
M28_Spy1445	<i>lacR.1</i>	-2.3	6.85E-05
M28_Spy1450	<i>sse</i>	1.7	4.65E-02
M28_Spy1458	M28_Spy1458	1.6	1.89E-02
M28_Spy1465	M28_Spy1465	2.0	1.77E-03
M28_Spy1471	<i>manO</i>	2.2	3.76E-05
M28_Spy1473	<i>accD</i>	-1.9	3.62E-05
M28_Spy1476	<i>fabZ</i>	-1.9	3.17E-05
M28_Spy1477	<i>accB</i>	-2.1	2.16E-09
M28_Spy1478	<i>fabF</i>	-2.8	< 1.10E-16
M28_Spy1479	<i>fabG</i>	-2.8	< 1.10E-16
M28_Spy1480	<i>fabD</i>	-2.4	2.19E-13
M28_Spy1481	<i>fabK</i>	-2.0	1.45E-08
M28_Spy1493	M28_Spy1493	-1.8	4.18E-02
M28_Spy1495	<i>gatB</i>	-1.9	4.60E-06
M28_Spy1496	<i>gatA</i>	-1.5	6.41E-03
M28_Spy1506	M28_Spy1506	2.5	1.18E-09
M28_Spy1507	M28_Spy1507	2.6	3.25E-10
M28_Spy1520	<i>shr</i>	1.7	2.23E-04

Table B-2 Continued.

Locus tag^a	Gene	Fold change relative to WT	P value^b
<i>M28_Spy1526</i>	<i>scrK</i>	-1.8	5.68E-03
<i>M28_Spy1527</i>	<i>endoS</i>	-2.0	6.99E-07
<i>M28_Spy1528</i>	<i>M28_Spy1528</i>	-2.9	1.03E-11
<i>M28_Spy1529</i>	<i>scrA</i>	-3.2	< 1.10E-16
<i>M28_Spy1530</i>	<i>scrB</i>	-2.2	1.35E-07
<i>M28_Spy1531</i>	<i>scrR</i>	-1.6	4.61E-02
<i>M28_Spy1534</i>	<i>efp</i>	1.6	2.15E-03
<i>M28_Spy1538</i>	<i>corA</i>	1.9	7.14E-04
<i>M28_Spy1549</i>	<i>mutS2</i>	1.6	2.31E-03
<i>M28_Spy1552</i>	<i>M28_Spy1552</i>	1.8	1.66E-04
<i>M28_Spy1553</i>	<i>spi</i>	1.9	2.05E-05
<i>M28_Spy1558</i>	<i>M28_Spy1558</i>	1.8	4.05E-03
<i>M28_Spy1559</i>	<i>M28_Spy1559</i>	1.8	2.74E-02
<i>M28_Spy1564</i>	<i>srv</i>	3.1	< 1.10E-16
<i>M28_Spy1571</i>	<i>M28_Spy1571</i>	1.9	9.91E-04
<i>M28_Spy1578</i>	<i>deoC</i>	-2.1	1.84E-09
<i>M28_Spy1579</i>	<i>nupC</i>	-2.1	< 1.10E-16
<i>M28_Spy1580</i>	<i>udp</i>	-3.0	< 1.10E-16
<i>M28_Spy1583</i>	<i>M28_Spy1583</i>	1.8	5.40E-03
<i>M28_Spy1584</i>	<i>M28_Spy1584</i>	2.3	4.89E-07
<i>M28_Spy1585</i>	<i>M28_Spy1585</i>	2.1	1.20E-05
<i>M28_Spy1591</i>	<i>pgk</i>	-1.6	2.08E-02
<i>M28_Spy1598</i>	<i>M28_Spy1598</i>	1.7	7.26E-03
<i>M28_Spy1601</i>	<i>ropA</i>	2.5	6.15E-10
<i>M28_Spy1602</i>	<i>M28_Spy1602</i>	1.6	2.74E-02
<i>M28_Spy1615</i>	<i>salR</i>	1.8	8.45E-04
<i>M28_Spy1620</i>	<i>salB</i>	1.9	1.57E-04
<i>M28_Spy1636</i>	<i>M28_Spy1636</i>	-1.9	8.05E-04
<i>M28_Spy1670</i>	<i>msmK</i>	-2.7	< 1.10E-16
<i>M28_Spy1672</i>	<i>ska</i>	-7.4	< 1.10E-16
<i>M28_Spy1675</i>	<i>sclA</i>	4.1	< 1.10E-16
<i>M28_Spy1687</i>	<i>smeZ</i>	2.0	7.04E-04
<i>M28_Spy1689</i>	<i>dppA</i>	2.7	< 1.10E-16
<i>M28_Spy1694</i>	<i>M28_Spy1694</i>	-1.7	4.71E-03
<i>M28_Spy1695</i>	<i>htpA</i>	1.7	2.41E-12
<i>M28_Spy1696</i>	<i>lmb</i>	2.0	4.30E-08
<i>M28_Spy1699</i>	<i>fba</i>	2.3	< 1.10E-16
<i>M28_Spy1700</i>	<i>scpA</i>	3.7	< 1.10E-16
<i>M28_Spy1702</i>	<i>emm</i>	6.0	< 1.10E-16
<i>M28_Spy1703</i>	<i>mvp</i>	2.3	1.62E-07
<i>M28_Spy1704</i>	<i>mga</i>	2.0	7.01E-04
<i>M28_Spy1715</i>	<i>sfbX</i>	3.0	< 1.10E-16
<i>M28_Spy1716</i>	<i>sof</i>	3.4	< 1.10E-16
<i>M28_Spy1718</i>	<i>prsA</i>	-2.4	2.52E-06
<i>M28_Spy1719</i>	<i>M28_Spy1719</i>	-3.3	< 1.10E-16
<i>M28_Spy1720</i>	<i>spi</i>	-3.2	5.35E-07
<i>M28_Spy1721</i>	<i>speB</i>	-3.2	8.12E-07
<i>M28_Spy1722</i>	<i>M28_Spy1722</i>	-2.9	< 1.10E-16
<i>M28_Spy1723</i>	<i>M28_Spy1723</i>	-2.8	1.97E-12

Table B-2 Continued.

Locus tag ^a	Gene	Fold change relative to WT	P value ^b
M28_Spy1736	M28_Spy1736	-1.7	2.26E-02
M28_Spy1750	<i>ctsR</i>	2.7	2.85E-12
M28_Spy1762	hutG	-1.8	1.09E-05
M28_Spy1764	<i>rpsB</i>	2.8	< 1.10E-16
M28_Spy1765	<i>M28_Spy1765</i>	1.5	4.48E-04
M28_Spy1773	<i>nrdG</i>	1.7	4.33E-03
M28_Spy1774	<i>M28_Spy1774</i>	1.8	1.13E-04
M28_Spy1775	<i>M28_Spy1775</i>	1.6	4.01E-06
M28_Spy1776	M28_Spy1776	1.7	2.95E-03
M28_Spy1779	<i>M28_Spy1779</i>	1.9	3.60E-02
M28_Spy1780	<i>M28_Spy1780</i>	1.5	1.11E-06
M28_Spy1781	<i>M28_Spy1781</i>	1.6	1.63E-03
M28_Spy1824	<i>rpmF</i>	1.7	1.32E-03
M28_Spy1829	M28_Spy1829	-2.0	1.99E-05
M28_Spy1830	M28_Spy1830	-2.5	5.70E-12
M28_Spy1835	ywzG	-2.0	5.73E-05
M28_Spy1836	<i>M28_Spy1836</i>	-2.5	2.19E-09
M28_Spy1837	<i>M28_Spy1837</i>	-2.8	< 1.10E-16
M28_Spy1839	<i>pipR</i>	1.8	7.00E-04
M28_Spy1871	<i>M28_Spy1871</i>	3.1	4.39E-13
M28_Spy1872	<i>trmU</i>	2.8	< 1.10E-16
M28_Spy1875	M28_Spy1875	-2.8	< 1.10E-16
M28_Spy1878	<i>cbiO1</i>	2.1	5.02E-05
M28_Spy1879	<i>M28_Spy1879</i>	2.1	6.47E-05
M28_Spy1880	<i>M28_Spy1880</i>	2.3	5.19E-09
M28_Spy1881	M28_Spy1881	2.8	1.38E-11
M28_Spy1882	M28_Spy1882	4.1	< 1.10E-16
M28_Spy1887	<i>M28_Spy1887</i>	2.1	7.38E-06
M28_Spy1888	<i>recF</i>	2.0	1.66E-04
M28_Spy1889	<i>M28_Spy1889</i>	3.1	< 1.10E-16

Bold font indicates significant differential expression in both growth phases.

^aLocus tag identified in the serotype M28 reference genome MGAS6180.

^bP value after Bonferroni correction.

Table B-3 Differentially expressed genes in the *rocA* null mutant strain compared to the wild-type (WT) strain of serotype M1, M3, and M28 GAS at mid-exponential growth phase.

Locus tag ^a	Gene	Fold change relative to WT ^b		
		M1	M3	M28
M28_Spy0002	<i>dnaN</i>	-1.7		
M28_Spy0008	<i>divIC</i>		1.9	
M28_Spy0011	<i>tilS</i>	2.1	2.1	1.7
M28_Spy0012	<i>hpt</i>	2.3		1.7
M28_Spy0013	<i>ftsH</i>	1.8		2.1
M28_Spy0014	<i>M28_Spy0014</i>	-1.5	-1.6	-1.9
M28_Spy0015	<i>M28_Spy0015</i>	2.1		
M28_Spy0017	<i>sibA</i>	1.5	-2.0	
M28_Spy0019	<i>recO</i>			1.5
M28_Spy0020	<i>plsX</i>	1.5		

Table B-3 Continued.

Locus tag ^a	Gene	Fold change relative to WT ^b		
		M1	M3	M28
<i>M28_Spy0021</i>	<i>acpP.1</i>	1.6		
<i>M28_Spy0022</i>	<i>purC</i>	-3.6	-4.6	-2.5
<i>M28_Spy0023</i>	<i>purL</i>	-4.4	-5.6	-2.0
<i>M28_Spy0024</i>	<i>purF</i>	-3.2	-4.2	-1.8
<i>M28_Spy0025</i>	<i>purM</i>	-4.1	-3.5	-1.9
<i>M28_Spy0026</i>	<i>purN</i>	-3.4	-3.6	-1.9
<i>M28_Spy0027</i>	<i>purH</i>	-3.3	-7.5	-1.7
<i>M28_Spy0028</i>	<i>M28_Spy0028</i>	-7.0		-2.0
<i>M28_Spy0029</i>	<i>purD</i>	-4.5	-5.2	-2.6
<i>M28_Spy0030</i>	<i>purE</i>	-4.6	-4.3	-2.3
<i>M28_Spy0031</i>	<i>purK</i>	-4.0	-3.4	-2.3
<i>M28_Spy0032</i>	<i>M28_Spy0032</i>			-1.9
<i>M28_Spy0033</i>	<i>purB</i>	-1.6	-2.1	
<i>M28_Spy0034</i>	<i>comR</i>			-1.7
<i>M28_Spy0037</i>	<i>M28_Spy0037</i>			-1.5
<i>M28_Spy0038</i>	<i>M28_Spy0038</i>		-1.5	
<i>M28_Spy0039</i>	<i>M28_Spy0039</i>		1.9	2.6
<i>M28_Spy0042</i>	<i>rpsJ</i>	-1.5		
<i>M28_Spy0044</i>	<i>rplD</i>	-1.5		
<i>M28_Spy0046</i>	<i>rplB</i>	-1.5		
<i>M28_Spy0047</i>	<i>rpsS</i>	-1.5		
<i>M28_Spy0048</i>	<i>rplV</i>	-1.5		
<i>M28_Spy0049</i>	<i>rpsC</i>	-1.5		
<i>M28_Spy0053</i>	<i>rplN</i>	-1.7		
<i>M28_Spy0056</i>	<i>rpsN</i>	-2.0		
<i>M28_Spy0058</i>	<i>rplF</i>	-1.5		
<i>M28_Spy0071</i>	<i>M28_Spy0071</i>	2.4		
<i>M28_Spy0072</i>	<i>M28_Spy0072</i>	-1.6		-2.0
<i>M28_Spy0077</i>	<i>adcB</i>		-1.8	
<i>M28_Spy0078</i>	<i>M28_Spy0078</i>	-2.3		
<i>M28_Spy0080</i>	<i>pbp1b</i>			1.5
<i>M28_Spy0083</i>	<i>M28_Spy0083</i>	2.0		
<i>M28_Spy0091</i>	<i>M28_Spy0091</i>		-1.5	
<i>M28_Spy0104</i>	<i>rofA</i>			-1.9
<i>M28_Spy0105</i>	<i>sfb1</i>			-2.5
<i>M28_Spy0106</i>	<i>M28_Spy0106</i>	2.0		
<i>M28_Spy0107</i>	<i>cpa</i>			-2.7
<i>M28_Spy0108</i>	<i>lepA</i>			-2.4
<i>M28_Spy0109</i>	<i>M28_Spy0109</i>			-2.8
<i>M28_Spy0110</i>	<i>eflLSL.B</i>			-1.9
<i>M28_Spy0111</i>	<i>M28_Spy0111</i>			-1.8
<i>M28_Spy0114</i>	<i>M28_Spy0114</i>	13.3	16.8	7.7
<i>M28_Spy0115</i>	<i>atoE</i>	-1.8		
<i>M28_Spy0117</i>	<i>atoB.2</i>			-1.5
<i>M28_Spy0119</i>	<i>atoA.2</i>	-2.2		
<i>M28_Spy0121</i>	<i>M28_Spy0121</i>	-2.2	-1.5	
<i>M28_Spy0122</i>	<i>sloR</i>	-2.2	-2.2	
<i>M28_Spy0124</i>	<i>ntpI</i>	-2.1		
<i>M28_Spy0125</i>	<i>ntpK</i>	-2.9		

Table B-3 Continued.

Locus tag ^a	Gene	Fold change relative to WT ^b		
		M1	M3	M28
<i>M28_Spy0126</i>	<i>nipE</i>	-3.3		
<i>M28_Spy0127</i>	<i>nipC</i>	-2.5		
<i>M28_Spy0129</i>	<i>nipA</i>	-2.3		
<i>M28_Spy0130</i>	<i>nipB</i>	-1.7		
<i>M28_Spy0132</i>	<i>M28_Spy0132</i>			1.7
<i>M28_Spy0133</i>	<i>M28_Spy0133</i>			1.5
<i>M28_Spy0136</i>	<i>nusG</i>		-1.6	
<i>M28_Spy0137</i>	<i>nga</i>		13.0	6.3
<i>M28_Spy0138</i>	<i>ifs</i>		13.4	6.4
<i>M28_Spy0139</i>	<i>slo</i>		11.4	6.0
<i>M28_Spy0140</i>	<i>M28_Spy0140</i>			6.4
<i>M28_Spy0141</i>	<i>M28_Spy0141</i>	3.9	10.5	20.4
<i>M28_Spy0142</i>	<i>M28_Spy0142</i>			3.1
<i>M28_Spy0143</i>	<i>M28_Spy0143</i>			2.7
<i>M28_Spy0144</i>	<i>metB</i>	-3.6	-10.3	-3.0
<i>M28_Spy0146</i>	<i>M28_Spy0146</i>	-2.1		-2.8
<i>M28_Spy0147</i>	<i>M28_Spy0147</i>			-3.3
<i>M28_Spy0148</i>	<i>M28_Spy0148</i>			-2.6
<i>M28_Spy0149</i>	<i>M28_Spy0149</i>	-3.2		-4.0
<i>M28_Spy0150</i>	<i>M28_Spy0150</i>			-3.4
<i>M28_Spy0151</i>	<i>araD</i>			-3.3
<i>M28_Spy0153</i>	<i>sgaR</i>		-1.6	-1.5
<i>M28_Spy0155</i>	<i>opuAA</i>	-2.4	-2.1	-2.1
<i>M28_Spy0156</i>	<i>opuABC</i>	-2.1	-2.2	-1.7
<i>M28_Spy0157</i>	<i>polA</i>			1.5
<i>M28_Spy0164</i>	<i>M28_Spy0164</i>	-2.1		
<i>M28_Spy0167</i>	<i>M28_Spy0167</i>	-4.7		-1.7
<i>M28_Spy0168</i>	<i>nadC</i>	-1.9		
<i>M28_Spy0171</i>	<i>M28_Spy0171</i>		-2.0	
<i>M28_Spy0172</i>	<i>M28_Spy0172</i>			-1.8
<i>M28_Spy0173</i>	<i>tgt</i>		-1.5	
<i>M28_Spy0174</i>	<i>M28_Spy0174</i>			-1.6
<i>M28_Spy0175</i>	<i>M28_Spy0175</i>	-2.3		
<i>M28_Spy0178</i>	<i>M28_Spy0178</i>	1.5	1.9	1.9
<i>M28_Spy0180</i>	<i>speG</i>	1.9	2.1	
<i>M28_Spy0184</i>	<i>rivR</i>		3.8	2.4
<i>M28_Spy0187</i>	<i>hasC.2</i>			1.6
<i>M28_Spy0188</i>	<i>gpsA</i>			1.6
<i>M28_Spy0189</i>	<i>yjdR</i>	-1.9	-1.9	-2.3
<i>M28_Spy0190</i>	<i>M28_Spy0190</i>	-2.0	-1.6	-2.0
<i>M28_Spy0191</i>	<i>M28_Spy0191</i>	-2.0	-1.9	-2.0
<i>M28_Spy0193</i>	<i>M28_Spy0193</i>		-1.5	
<i>M28_Spy0196</i>	<i>M28_Spy0196</i>			1.6
<i>M28_Spy0197</i>	<i>glx</i>			1.5
<i>M28_Spy0206</i>	<i>M28_Spy0206</i>	-3.0		-2.1
<i>M28_Spy0207</i>	<i>M28_Spy0207</i>	-2.1		-1.7
<i>M28_Spy0208</i>	<i>M28_Spy0208</i>	-3.3		-1.9
<i>M28_Spy0209</i>	<i>M28_Spy0209</i>			-2.0
<i>M28_Spy0210</i>	<i>M28_Spy0210</i>	-2.0		-1.6

Table B-3 Continued.

Locus tag ^a	Gene	Fold change relative to WT ^b		
		M1	M3	M28
<i>M28_Spy0211</i>	<i>nanH</i>	-2.1		-1.8
<i>M28_Spy0212</i>	<i>M28_Spy0212</i>	-2.9		-1.6
<i>M28_Spy0216</i>	<i>ksgA</i>		-1.6	
<i>M28_Spy0229</i>	<i>M28_Spy0229</i>	-1.5		
<i>M28_Spy0233</i>	<i>bacA</i>			1.5
<i>M28_Spy0234</i>	<i>mecA</i>	1.5		
<i>M28_Spy0242</i>	<i>M28_Spy0242</i>		1.8	
<i>M28_Spy0243</i>	<i>dacA2</i>	1.8	2.7	
<i>M28_Spy0245</i>	<i>oppB</i>	-1.5		
<i>M28_Spy0246</i>	<i>oppC</i>		2.2	
<i>M28_Spy0248</i>	<i>oppF</i>		1.5	
<i>M28_Spy0252</i>	<i>M28_Spy0252</i>	1.5		
<i>M28_Spy0261</i>	<i>M28_Spy0261</i>	1.6		
<i>M28_Spy0262</i>	<i>M28_Spy0262</i>	1.6	1.5	
<i>M28_Spy0266</i>	<i>braB</i>		-2.5	-2.6
<i>M28_Spy0267</i>	<i>M28_Spy0267</i>		-1.9	-1.5
<i>M28_Spy0273</i>	<i>M28_Spy0273</i>	1.8	2.1	1.9
<i>M28_Spy0274</i>	<i>covR</i>		-1.8	
<i>M28_Spy0275</i>	<i>covS</i>		-1.8	
<i>M28_Spy0279</i>	<i>pgdA</i>		-1.5	
<i>M28_Spy0286</i>	<i>M28_Spy0286</i>			1.8
<i>M28_Spy0287</i>	<i>M28_Spy0287</i>	1.6	1.9	
<i>M28_Spy0289</i>	<i>M28_Spy0289</i>	1.7		
<i>M28_Spy0290</i>	<i>M28_Spy0290</i>	1.5		
<i>M28_Spy0297</i>	<i>M28_Spy0297</i>		1.5	
<i>M28_Spy0302</i>	<i>M28_Spy0302</i>			-1.8
<i>M28_Spy0306</i>	<i>hlyX</i>		-1.5	
<i>M28_Spy0307</i>	<i>pfIC</i>	1.5		
<i>M28_Spy0309</i>	<i>M28_Spy0309</i>		-1.7	
<i>M28_Spy0310</i>	<i>fhuG</i>	-2.2		-1.7
<i>M28_Spy0311</i>	<i>fhuB</i>	-2.1		-1.8
<i>M28_Spy0312</i>	<i>fhuD</i>	-2.4		-1.8
<i>M28_Spy0313</i>	<i>fhuA</i>	-1.8		-1.9
<i>M28_Spy0315</i>	<i>M28_Spy0315</i>			1.8
<i>M28_Spy0327</i>	<i>exoA</i>			1.8
<i>M28_Spy0329</i>	<i>spyCEP</i>	7.3	92.5	38.0
<i>M28_Spy0330</i>	<i>M28_Spy0330</i>	-1.8		-1.7
<i>M28_Spy0331</i>	<i>M28_Spy0331</i>	-2.5		-2.0
<i>M28_Spy0332</i>	<i>metS</i>	-1.6		
<i>M28_Spy0335</i>	<i>nrdI</i>			-1.5
<i>M28_Spy0337</i>	<i>spyA</i>	1.9	2.9	
<i>M28_Spy0338</i>	<i>M28_Spy0338</i>			13.3
<i>M28_Spy0341</i>	<i>M28_Spy0341</i>			13.0
<i>M28_Spy0342</i>	<i>M28_Spy0342</i>		-1.8	2.2
<i>M28_Spy0343</i>	<i>M28_Spy0343</i>			2.8
<i>M28_Spy0345</i>	<i>speJ</i>	3.0		
<i>M28_Spy0346</i>	<i>M28_Spy0346</i>			3.0
<i>M28_Spy0350</i>	<i>M28_Spy0350</i>	-1.5		
<i>M28_Spy0355</i>	<i>M28_Spy0355</i>			1.5

Table B-3 Continued.

Locus tag ^a	Gene	Fold change relative to WT ^b		
		M1	M3	M28
<i>M28_Spy0357</i>	<i>mtsA</i>	2.0		
<i>M28_Spy0367</i>	<i>M28_Spy0367</i>		-1.8	
<i>M28_Spy0368</i>	<i>msrA.2</i>		-1.8	
<i>M28_Spy0370</i>	<i>M28_Spy0370</i>		1.8	
<i>M28_Spy0371</i>	<i>M28_Spy0371</i>	1.7		2.0
<i>M28_Spy0372</i>	<i>phoH</i>			1.6
<i>M28_Spy0373</i>	<i>M28_Spy0373</i>			1.8
<i>M28_Spy0377</i>	<i>M28_Spy0377</i>			1.6
<i>M28_Spy0379</i>	<i>M28_Spy0379</i>	1.7		
<i>M28_Spy0380</i>	<i>M28_Spy0380</i>	1.7		
<i>M28_Spy0390</i>	<i>M28_Spy0390</i>			1.5
<i>M28_Spy0395</i>	<i>rgg2</i>	1.5		
<i>M28_Spy0396</i>	<i>lpg</i>			1.5
<i>M28_Spy0397</i>	<i>M28_Spy0397</i>			1.7
<i>M28_Spy0398</i>	<i>M28_Spy0398</i>			1.7
<i>M28_Spy0404</i>	<i>M28_Spy0404</i>	-1.5		
<i>M28_Spy0405</i>	<i>pcp</i>		-1.5	
<i>M28_Spy0407</i>	<i>M28_Spy0407</i>		-1.6	
<i>M28_Spy0409</i>	<i>gloA</i>			1.8
<i>M28_Spy0410</i>	<i>M28_Spy0410</i>			1.6
<i>M28_Spy0411</i>	<i>pepQ</i>			1.8
<i>M28_Spy0413</i>	<i>M28_Spy0413</i>	1.5		2.7
<i>M28_Spy0414</i>	<i>M28_Spy0414</i>	1.5		3.1
<i>M28_Spy0420</i>	<i>M28_Spy0420</i>	-1.6		
<i>M28_Spy0423</i>	<i>vicR</i>		1.6	
<i>M28_Spy0426</i>	<i>acpA</i>			1.6
<i>M28_Spy0427</i>	<i>smc</i>			1.6
<i>M28_Spy0433</i>	<i>metK1</i>		2.1	
<i>M28_Spy0444</i>	<i>M28_Spy0444</i>	1.9		
<i>M28_Spy0445</i>	<i>M28_Spy0445</i>	2.1		
<i>M28_Spy0446</i>	<i>M28_Spy0446</i>	2.0		
<i>M28_Spy0447</i>	<i>M28_Spy0447</i>	1.6		
<i>M28_Spy0448</i>	<i>M28_Spy0448</i>			1.5
<i>M28_Spy0449</i>	<i>M28_Spy0449</i>			1.5
<i>M28_Spy0454</i>	<i>M28_Spy0454</i>	-2.5	-3.2	-1.8
<i>M28_Spy0456</i>	<i>M28_Spy0456</i>	-1.6		
<i>M28_Spy0458</i>	<i>M28_Spy0458</i>			2.3
<i>M28_Spy0459</i>	<i>M28_Spy0459</i>			2.0
<i>M28_Spy0460</i>	<i>M28_Spy0460</i>	2.1	3.3	1.8
<i>M28_Spy0464</i>	<i>M28_Spy0464</i>	2.0		4.2
<i>M28_Spy0476</i>	<i>M28_Spy0476</i>		-1.9	-1.5
<i>M28_Spy0477</i>	<i>M28_Spy0477</i>			-1.7
<i>M28_Spy0479</i>	<i>M28_Spy0479</i>	2.1	2.0	1.5
<i>M28_Spy0480</i>	<i>M28_Spy0480</i>	1.8		1.5
<i>M28_Spy0481</i>	<i>M28_Spy0481</i>	1.8		1.7
<i>M28_Spy0482</i>	<i>gpoA</i>			1.6
<i>M28_Spy0483</i>	<i>pepF</i>			1.7
<i>M28_Spy0484</i>	<i>ppc</i>	1.8	-1.7	
<i>M28_Spy0494</i>	<i>M28_Spy0494</i>		-2.4	

Table B-3 Continued.

Locus tag ^a	Gene	Fold change relative to WT ^b		
		M1	M3	M28
M28_Spy0496	regR	1.6		
M28_Spy0501	M28_Spy0501	-2.9		-1.6
M28_Spy0507	M28_Spy0507			1.5
M28_Spy0513	M28_Spy0513	1.8		1.8
M28_Spy0517	M28_Spy0517			1.6
M28_Spy0519	M28_Spy0519			1.6
M28_Spy0520	pepD			1.5
M28_Spy0521	adcA			1.6
M28_Spy0522	agaR2	-2.4		-1.9
M28_Spy0523	agaS	-2.6	-3.6	-1.8
M28_Spy0524	rpmE		-2.0	
M28_Spy0527	M28_Spy0527	-2.0		
M28_Spy0528	M28_Spy0528	-1.9	-2.0	
M28_Spy0536	M28_Spy0536			-2.4
M28_Spy0537	M28_Spy0537			-2.3
M28_Spy0538	ralp3	-1.7		-2.3
M28_Spy0539	epf	-2.3		-2.2
M28_Spy0540	sagA	-3.5		-2.7
M28_Spy0541	sagB	-3.2		-3.4
M28_Spy0542	sagC	-3.2		-3.2
M28_Spy0543	sagD	-3.4		-3.5
M28_Spy0544	sagE	-3.2		-3.0
M28_Spy0545	sagF	-3.0		-2.5
M28_Spy0546	sagG	-2.6		-3.1
M28_Spy0547	sagH	-2.3		-2.9
M28_Spy0548	sagI	-2.4		-2.7
M28_Spy0549	spnA	-1.8	-1.9	-2.2
M28_Spy0552	M28_Spy0552		1.5	
M28_Spy0553	atpE		-2.2	
M28_Spy0555	atpF		1.6	
M28_Spy0572	M28_Spy0572			1.5
M28_Spy0573	rexB		1.6	1.9
M28_Spy0574	rexA		1.7	1.9
M28_Spy0575	M28_Spy0575			1.6
M28_Spy0576	rpsU		-7.5	
M28_Spy0586	rgpEc		1.6	
M28_Spy0592	M28_Spy0592		1.6	
M28_Spy0593	pepT		-1.5	
M28_Spy0595	M28_Spy0595			-1.5
M28_Spy0602	M28_Spy0602		-1.5	
M28_Spy0608	folC.2			1.6
M28_Spy0609	M28_Spy0609			1.6
M28_Spy0622	carA		-1.6	
M28_Spy0623	M28_Spy0623			-2.0
M28_Spy0625	M28_Spy0625			1.8
M28_Spy0626	M28_Spy0626		-1.5	2.0
M28_Spy0627	M28_Spy0627			1.9
M28_Spy0628	M28_Spy0628			1.9
M28_Spy0632	M28_Spy0632	-1.5	1.8	-2.1

Table B-3 Continued.

Locus tag ^a	Gene	Fold change relative to WT ^b		
		M1	M3	M28
<i>M28_Spy0633</i>	<i>M28_Spy0633</i>		1.8	-1.7
<i>M28_Spy0635</i>	<i>gczA</i>	1.7		
<i>M28_Spy0641</i>	<i>fruR</i>	1.9		
<i>M28_Spy0642</i>	<i>fruB</i>	1.5		
<i>M28_Spy0644</i>	<i>mur1.1</i>		2.2	
<i>M28_Spy0645</i>	<i>mur1.2</i>			-1.5
<i>M28_Spy0647</i>	<i>M28_Spy0647</i>	15.5		13.3
<i>M28_Spy0648</i>	<i>M28_Spy0648</i>	25.4		63.8
<i>M28_Spy0649</i>	<i>mac</i>	23.9	52.4	38.1
<i>M28_Spy0651</i>	<i>M28_Spy0651</i>		1.5	
<i>M28_Spy0652</i>	<i>M28_Spy0652</i>	1.5	1.7	
<i>M28_Spy0656</i>	<i>M28_Spy0656</i>			-2.2
<i>M28_Spy0657</i>	<i>fms</i>			-1.7
<i>M28_Spy0658</i>	<i>s5nA</i>		-5.2	-2.9
<i>M28_Spy0660</i>	<i>sptR</i>	1.6		
<i>M28_Spy0666</i>	<i>M28_Spy0666</i>			1.6
<i>M28_Spy0667</i>	<i>mvaS.1</i>			1.6
<i>M28_Spy0669</i>	<i>dyr</i>			1.6
<i>M28_Spy0671</i>	<i>clpX</i>		1.5	1.6
<i>M28_Spy0672</i>	<i>M28_Spy0672</i>			1.6
<i>M28_Spy0681</i>	<i>cpsY</i>			1.6
<i>M28_Spy0682</i>	<i>M28_Spy0682</i>		-1.7	-1.5
<i>M28_Spy0683</i>	<i>pyrF</i>	-1.6		-1.6
<i>M28_Spy0684</i>	<i>pyrE</i>	-1.6		-1.6
<i>M28_Spy0686</i>	<i>M28_Spy0686</i>	1.5	2.3	1.9
<i>M28_Spy0687</i>	<i>M28_Spy0687</i>	1.5	2.0	1.9
<i>M28_Spy0688</i>	<i>ung</i>		-1.7	
<i>M28_Spy0689</i>	<i>pyrC</i>		-1.5	
<i>M28_Spy0693</i>	<i>bcaT</i>	1.6		
<i>M28_Spy0696</i>	<i>M28_Spy0696</i>	1.9		
<i>M28_Spy0697</i>	<i>M28_Spy0697</i>	1.8		
<i>M28_Spy0701</i>	<i>M28_Spy0701</i>			2.1
<i>M28_Spy0709</i>	<i>dnaD</i>		1.7	
<i>M28_Spy0715</i>	<i>cpsFP</i>			1.6
<i>M28_Spy0716</i>	<i>cpsFQ</i>			1.5
<i>M28_Spy0719</i>	<i>M28_Spy0719</i>			1.5
<i>M28_Spy0722</i>	<i>M28_Spy0722</i>	-1.8		
<i>M28_Spy0724</i>	<i>M28_Spy0724</i>	-2.2		-1.5
<i>M28_Spy0725</i>	<i>M28_Spy0725</i>	-2.1		
<i>M28_Spy0730</i>	<i>acoA</i>			1.5
<i>M28_Spy0731</i>	<i>acoB</i>			1.7
<i>M28_Spy0732</i>	<i>acoC</i>			1.6
<i>M28_Spy0733</i>	<i>M28_Spy0733</i>			1.5
<i>M28_Spy0734</i>	<i>acoL</i>	1.5		1.6
<i>M28_Spy0748</i>	<i>cas9</i>			-1.6
<i>M28_Spy0749</i>	<i>cas1</i>			-1.5
<i>M28_Spy0752</i>	<i>M28_Spy0752</i>			-1.6
<i>M28_Spy0754</i>	<i>sclB</i>	2.5	8.7	2.4
<i>M28_Spy0755</i>	<i>msrB</i>	1.7	1.9	

Table B-3 Continued.

Locus tag ^a	Gene	Fold change relative to WT ^b		
		M1	M3	M28
<i>M28_Spy0757</i>	<i>ptsA</i>		2.7	1.8
<i>M28_Spy0758</i>	<i>ptsB</i>		3.9	2.1
<i>M28_Spy0759</i>	<i>ptsC</i>		2.2	2.1
<i>M28_Spy0760</i>	<i>ptsD</i>		2.7	2.2
<i>M28_Spy0762</i>	<i>M28_Spy0762</i>		2.0	
<i>M28_Spy0764</i>	<i>gabD</i>			1.7
<i>M28_Spy0765</i>	<i>uvrC</i>		1.5	2.1
<i>M28_Spy0766</i>	<i>M28_Spy0766</i>			1.9
<i>M28_Spy0767</i>	<i>M28_Spy0767</i>			1.9
<i>M28_Spy0768</i>	<i>thdF</i>	-1.6		-1.6
<i>M28_Spy0771</i>	<i>M28_Spy0771</i>			-1.6
<i>M28_Spy0772</i>	<i>M28_Spy0772</i>			-1.7
<i>M28_Spy0773</i>	<i>M28_Spy0773</i>			-1.6
<i>M28_Spy0774</i>	<i>M28_Spy0774</i>			-2.3
<i>M28_Spy0778</i>	<i>srtI</i>			-1.7
<i>M28_Spy0779</i>	<i>srtR</i>	1.8		
<i>M28_Spy0780</i>	<i>srtK</i>	1.7		
<i>M28_Spy0797</i>	<i>folC.1</i>	1.5		2.1
<i>M28_Spy0798</i>	<i>folE</i>	1.6		1.8
<i>M28_Spy0799</i>	<i>folP</i>	1.5		1.9
<i>M28_Spy0800</i>	<i>folQ</i>	1.5		1.9
<i>M28_Spy0801</i>	<i>folK</i>			2.0
<i>M28_Spy0811</i>	<i>M28_Spy0811</i>			-1.6
<i>M28_Spy0816</i>	<i>radC</i>	-1.8		
<i>M28_Spy0823</i>	<i>M28_Spy0823</i>	1.5		
<i>M28_Spy0831</i>	<i>guaC</i>		-3.7	
<i>M28_Spy0832</i>	<i>xpt</i>	-6.4		
<i>M28_Spy0833</i>	<i>M28_Spy0833</i>	-8.1	-1.9	-1.5
<i>M28_Spy0835</i>	<i>M28_Spy0835</i>			-1.5
<i>M28_Spy0846</i>	<i>nox</i>	2.1		1.7
<i>M28_Spy0852</i>	<i>M28_Spy0852</i>	1.9		1.5
<i>M28_Spy0853</i>	<i>M28_Spy0853</i>			1.6
<i>M28_Spy0858</i>	<i>smf</i>	-3.5		-1.8
<i>M28_Spy0862</i>	<i>M28_Spy0862</i>			-1.6
<i>M28_Spy0863</i>	<i>ddh</i>			-1.7
<i>M28_Spy0866</i>	<i>gid</i>		-2.0	
<i>M28_Spy0871</i>	<i>citG</i>	-1.8		-1.5
<i>M28_Spy0872</i>	<i>M28_Spy0872</i>			-1.8
<i>M28_Spy0873</i>	<i>M28_Spy0873</i>	-2.4		
<i>M28_Spy0882</i>	<i>oadA1</i>			1.5
<i>M28_Spy0883</i>	<i>citC</i>			1.7
<i>M28_Spy0884</i>	<i>M28_Spy0884</i>		1.9	1.6
<i>M28_Spy0885</i>	<i>xerD</i>	-1.9		-1.7
<i>M28_Spy0892</i>	<i>M28_Spy0892</i>	-2.0		
<i>M28_Spy0898</i>	<i>M28_Spy0898</i>	1.8		
<i>M28_Spy0899</i>	<i>fhs.1</i>	1.5		
<i>M28_Spy0900</i>	<i>lplA</i>	1.9	1.7	
<i>M28_Spy0901</i>	<i>M28_Spy0901</i>	1.5		
<i>M28_Spy0902</i>	<i>M28_Spy0902</i>	1.5		

Table B-3 Continued.

Locus tag ^a	Gene	Fold change relative to WT ^b		
		M1	M3	M28
<i>M28_Spy0903</i>	<i>M28_Spy0903</i>			1.5
<i>M28_Spy0915</i>	<i>cdt</i>	1.5	2.0	
<i>M28_Spy0916</i>	<i>M28_Spy0916</i>			-1.8
<i>M28_Spy0917</i>	<i>coaA</i>	1.9	2.4	2.4
<i>M28_Spy0919</i>	<i>ciaH</i>	1.5	1.7	
<i>M28_Spy0920</i>	<i>ciaR</i>	1.7		
<i>M28_Spy0923</i>	<i>phoU</i>	-1.7		-1.6
<i>M28_Spy0924</i>	<i>pstB</i>	-1.6	-2.3	-1.6
<i>M28_Spy0925</i>	<i>pstB2</i>	-2.0	-1.6	-1.5
<i>M28_Spy0926</i>	<i>pstA</i>	-1.9	-1.7	-1.5
<i>M28_Spy0927</i>	<i>pstC</i>	-1.9	-1.8	-1.6
<i>M28_Spy0928</i>	<i>pstS</i>	-1.9	-2.0	-1.5
<i>M28_Spy0933</i>	<i>mreA</i>		1.6	1.5
<i>M28_Spy0934</i>	<i>truB</i>			1.5
<i>M28_Spy0935</i>	<i>M28_Spy0935</i>			1.5
<i>M28_Spy0938</i>	<i>M28_Spy0938</i>		1.7	
<i>M28_Spy0942</i>	<i>M28_Spy0942</i>		1.7	
<i>M28_Spy0943</i>	<i>M28_Spy0943</i>	2.0	2.5	1.8
<i>M28_Spy0944</i>	<i>M28_Spy0944</i>	1.9	1.9	1.6
<i>M28_Spy0945</i>	<i>M28_Spy0945</i>	2.0	2.0	1.7
<i>M28_Spy0946</i>	<i>M28_Spy0946</i>	1.9	2.2	1.6
<i>M28_Spy0947</i>	<i>M28_Spy0947</i>	1.8	2.3	1.6
<i>M28_Spy0948</i>	<i>M28_Spy0948</i>	1.5		1.7
<i>M28_Spy0950</i>	<i>M28_Spy0950</i>		-2.3	
<i>M28_Spy0951</i>	<i>M28_Spy0951</i>			-1.5
<i>M28_Spy0953</i>	<i>cfa</i>	-2.9		-1.6
<i>M28_Spy0954</i>	<i>M28_Spy0954</i>	-1.7		
<i>M28_Spy0955</i>	<i>M28_Spy0955</i>	-2.0	-1.8	
<i>M28_Spy0956</i>	<i>M28_Spy0956</i>	-1.8		
<i>M28_Spy0957</i>	<i>M28_Spy0957</i>	-1.6		
<i>M28_Spy0958</i>	<i>glmS</i>	1.9		
<i>M28_Spy0962</i>	<i>dnaE</i>	1.5		
<i>M28_Spy0963</i>	<i>M28_Spy0963</i>			2.0
<i>M28_Spy0964</i>	<i>M28_Spy0964</i>			2.1
<i>M28_Spy0965</i>	<i>M28_Spy0965</i>			2.2
<i>M28_Spy0966</i>	<i>M28_Spy0966</i>	1.6		1.7
<i>M28_Spy1040</i>	<i>malF</i>	-1.7		
<i>M28_Spy1043</i>	<i>malA</i>	-1.5		
<i>M28_Spy1044</i>	<i>malD</i>	-1.7		
<i>M28_Spy1045</i>	<i>malC</i>	-1.6		
<i>M28_Spy1046</i>	<i>amyA</i>	-1.5		
<i>M28_Spy1050</i>	<i>M28_Spy1050</i>		1.6	2.4
<i>M28_Spy1051</i>	<i>dltD</i>		1.7	2.2
<i>M28_Spy1052</i>	<i>dltC</i>		2.3	2.0
<i>M28_Spy1053</i>	<i>dltB</i>		1.6	2.4
<i>M28_Spy1054</i>	<i>dltA</i>			2.2
<i>M28_Spy1055</i>	<i>M28_Spy1055</i>	1.9	2.3	2.0
<i>M28_Spy1056</i>	<i>uvrB</i>			1.6
<i>M28_Spy1067</i>	<i>M28_Spy1067</i>		-2.1	-1.9

Table B-3 Continued.

Locus tag ^a	Gene	Fold change relative to WT ^b		
		M1	M3	M28
<i>M28_Spy1074</i>	<i>M28_Spy1074</i>			2.0
<i>M28_Spy1075</i>	<i>M28_Spy1075</i>		-2.9	-1.9
<i>M28_Spy1076</i>	<i>M28_Spy1076</i>	-1.6	-1.6	
<i>M28_Spy1098</i>	<i>grab</i>	-2.8	-4.4	-5.5
<i>M28_Spy1099</i>	<i>murZ</i>		-1.6	
<i>M28_Spy1104</i>	<i>M28_Spy1104</i>		2.3	
<i>M28_Spy1106</i>	<i>M28_Spy1106</i>			1.5
<i>M28_Spy1107</i>	<i>M28_Spy1107</i>	1.5		1.6
<i>M28_Spy1112</i>	<i>gapN</i>			1.5
<i>M28_Spy1115</i>	<i>nrdH</i>			1.5
<i>M28_Spy1116</i>	<i>nrdE.2</i>			1.7
<i>M28_Spy1118</i>	<i>nrdF.2</i>			1.6
<i>M28_Spy1119</i>	<i>M28_Spy1119</i>	-1.6		
<i>M28_Spy1124</i>	<i>M28_Spy1124</i>	-1.5		
<i>M28_Spy1127</i>	<i>surA</i>	1.7	3.0	1.8
<i>M28_Spy1129</i>	<i>M28_Spy1129</i>	-1.7	-3.2	
<i>M28_Spy1131</i>	<i>M28_Spy1131</i>	-2.5		
<i>M28_Spy1132</i>	<i>M28_Spy1132</i>	-2.0		
<i>M28_Spy1133</i>	<i>nagB</i>	-5.8		
<i>M28_Spy1136</i>	<i>M28_Spy1136</i>	-1.9	-5.6	-1.7
<i>M28_Spy1138</i>	<i>M28_Spy1138</i>		-7.5	-1.7
<i>M28_Spy1139</i>	<i>sodA</i>	3.2		
<i>M28_Spy1147</i>	<i>kup</i>	-6.1	-11.4	-3.4
<i>M28_Spy1150</i>	<i>M28_Spy1150</i>			1.7
<i>M28_Spy1154</i>	<i>M28_Spy1154</i>	1.6		
<i>M28_Spy1155</i>	<i>M28_Spy1155</i>			-1.6
<i>M28_Spy1156</i>	<i>M28_Spy1156</i>	-1.6		
<i>M28_Spy1159</i>	<i>pyrD</i>	-2.0	-2.2	
<i>M28_Spy1161</i>	<i>pmtA</i>	-2.6	-2.0	
<i>M28_Spy1162</i>	<i>M28_Spy1162</i>			1.7
<i>M28_Spy1176</i>	<i>artP</i>	-1.9	-2.6	-1.9
<i>M28_Spy1177</i>	<i>artQ</i>	-1.8	-2.8	-1.6
<i>M28_Spy1179</i>	<i>clpE</i>			1.8
<i>M28_Spy1181</i>	<i>M28_Spy1181</i>		1.6	
<i>M28_Spy1183</i>	<i>divIVAS</i>		1.6	
<i>M28_Spy1189</i>	<i>ftsA</i>		1.6	
<i>M28_Spy1193</i>	<i>M28_Spy1193</i>			1.5
<i>M28_Spy1198</i>	<i>dpr</i>	2.2	1.5	1.9
<i>M28_Spy1207</i>	<i>asnA</i>	-3.0	-4.4	-3.3
<i>M28_Spy1208</i>	<i>arcC</i>	-2.6	7.4	1.8
<i>M28_Spy1209</i>	<i>M28_Spy1209</i>	-2.6	4.8	1.7
<i>M28_Spy1210</i>	<i>arcD</i>	-2.7	4.9	1.7
<i>M28_Spy1211</i>	<i>arcB</i>	-2.4	5.3	2.4
<i>M28_Spy1212</i>	<i>M28_Spy1212</i>	-2.4	6.4	1.9
<i>M28_Spy1213</i>	<i>arcA</i>	-2.2	4.9	2.2
<i>M28_Spy1289</i>	<i>cas2</i>			2.0
<i>M28_Spy1290</i>	<i>cas1</i>			1.8
<i>M28_Spy1291</i>	<i>cas4</i>			2.0
<i>M28_Spy1292</i>	<i>cas7</i>			2.1

Table B-3 Continued.

Locus tag ^a	Gene	Fold change relative to WT ^b		
		M1	M3	M28
<i>M28_Spy1293</i>	<i>cas8</i>			1.8
<i>M28_Spy1294</i>	<i>cas5</i>			1.7
<i>M28_Spy1295</i>	<i>cas3</i>	1.6		1.8
<i>M28_Spy1341</i>	<i>M28_Spy1341</i>			1.5
<i>M28_Spy1342</i>	<i>M28_Spy1342</i>			1.5
<i>M28_Spy1345</i>	<i>lacZ</i>	-2.0	-1.9	-1.8
<i>M28_Spy1346</i>	<i>trxR</i>	-1.7		-1.9
<i>M28_Spy1347</i>	<i>trxS</i>	-1.8		-2.0
<i>M28_Spy1352</i>	<i>M28_Spy1352</i>	-1.9		
<i>M28_Spy1359</i>	<i>rocA</i>	-135.9		-551.0
<i>M28_Spy1361</i>	<i>recX</i>			1.9
<i>M28_Spy1365</i>	<i>M28_Spy1365</i>	2.0		
<i>M28_Spy1366</i>	<i>M28_Spy1366</i>	2.0	1.5	1.7
<i>M28_Spy1367</i>	<i>comFC</i>			-1.5
<i>M28_Spy1374</i>	<i>liaS</i>	1.5		
<i>M28_Spy1375</i>	<i>liaF</i>	1.9		
<i>M28_Spy1380</i>	<i>priA</i>	-1.6		
<i>M28_Spy1384</i>	<i>atoR</i>			1.7
<i>M28_Spy1385</i>	<i>atoB</i>			2.0
<i>M28_Spy1386</i>	<i>atoD.1</i>			1.8
<i>M28_Spy1387</i>	<i>atoA</i>			1.6
<i>M28_Spy1388</i>	<i>M28_Spy1388</i>			1.8
<i>M28_Spy1389</i>	<i>M28_Spy1389</i>	-1.7		
<i>M28_Spy1390</i>	<i>luxS</i>		-2.0	
<i>M28_Spy1393</i>	<i>M28_Spy1393</i>	1.5		
<i>M28_Spy1394</i>	<i>M28_Spy1394</i>	1.7		
<i>M28_Spy1397</i>	<i>pepC</i>			2.0
<i>M28_Spy1400</i>	<i>M28_Spy1400</i>	1.5		
<i>M28_Spy1415</i>	<i>M28_Spy1415</i>	-1.5		1.6
<i>M28_Spy1417</i>	<i>M28_Spy1417</i>			1.5
<i>M28_Spy1423</i>	<i>glpO</i>	-2.0		
<i>M28_Spy1424</i>	<i>glpK</i>	-1.8		
<i>M28_Spy1425</i>	<i>M28_Spy1425</i>	2.4		
<i>M28_Spy1429</i>	<i>M28_Spy1429</i>	1.6	2.5	1.8
<i>M28_Spy1431</i>	<i>nagA</i>		-1.7	
<i>M28_Spy1434</i>	<i>M28_Spy1434</i>	2.1	2.4	4.1
<i>M28_Spy1438</i>	<i>lacD.1</i>	-2.3		
<i>M28_Spy1439</i>	<i>lacC.1</i>	-3.2		
<i>M28_Spy1440</i>	<i>lacB.1</i>	-2.7		-1.6
<i>M28_Spy1441</i>	<i>lacA.1</i>	-2.9		
<i>M28_Spy1442</i>	<i>M28_Spy1442</i>	-2.7		-2.0
<i>M28_Spy1443</i>	<i>M28_Spy1443</i>	-2.3		-1.6
<i>M28_Spy1444</i>	<i>M28_Spy1444</i>	-2.1		-1.8
<i>M28_Spy1447</i>	<i>copZ</i>	-1.7		
<i>M28_Spy1448</i>	<i>copA</i>	-1.7		-1.8
<i>M28_Spy1449</i>	<i>copY</i>			-2.4
<i>M28_Spy1450</i>	<i>sse</i>	2.9	26.2	3.6
<i>M28_Spy1459</i>	<i>M28_Spy1459</i>		1.5	
<i>M28_Spy1461</i>	<i>hit</i>			1.6

Table B-3 Continued.

Locus tag ^a	Gene	Fold change relative to WT ^b		
		M1	M3	M28
<i>M28_Spy1462</i>	<i>M28_Spy1462</i>		2.5	1.5
<i>M28_Spy1466</i>	<i>M28_Spy1466</i>	-1.8	-2.8	-1.9
<i>M28_Spy1468</i>	<i>manL</i>	-1.5	-1.6	
<i>M28_Spy1469</i>	<i>manM</i>	-1.5		
<i>M28_Spy1470</i>	<i>manN</i>	-1.7	-1.9	
<i>M28_Spy1475</i>	<i>accC</i>	-1.5		
<i>M28_Spy1478</i>	<i>fabF</i>	-1.5		
<i>M28_Spy1482</i>	<i>acpP.2</i>		2.2	
<i>M28_Spy1486</i>	<i>dnaJ</i>	-1.7		
<i>M28_Spy1488</i>	<i>grpE</i>	-1.7		
<i>M28_Spy1489</i>	<i>hrcA</i>	-1.5		
<i>M28_Spy1493</i>	<i>M28_Spy1493</i>			-1.6
<i>M28_Spy1498</i>	<i>M28_Spy1498</i>			-2.9
<i>M28_Spy1499</i>	<i>M28_Spy1499</i>			-3.8
<i>M28_Spy1500</i>	<i>M28_Spy1500</i>			-2.8
<i>M28_Spy1501</i>	<i>codY</i>	1.9		1.5
<i>M28_Spy1503</i>	<i>M28_Spy1503</i>	1.6		
<i>M28_Spy1505</i>	<i>asnB</i>		-1.5	1.6
<i>M28_Spy1506</i>	<i>M28_Spy1506</i>			4.3
<i>M28_Spy1507</i>	<i>M28_Spy1507</i>			4.3
<i>M28_Spy1513</i>	<i>M28_Spy1513</i>	1.5		
<i>M28_Spy1520</i>	<i>shr</i>		2.3	
<i>M28_Spy1522</i>	<i>acpS</i>	-2.1		
<i>M28_Spy1523</i>	<i>alr</i>	-2.0		
<i>M28_Spy1525</i>	<i>pmi</i>			2.3
<i>M28_Spy1526</i>	<i>scrK</i>	-8.4		-2.1
<i>M28_Spy1527</i>	<i>endoS</i>	-6.4		
<i>M28_Spy1529</i>	<i>scrA</i>	-5.6		
<i>M28_Spy1530</i>	<i>scrB</i>	-1.8		
<i>M28_Spy1531</i>	<i>scrR</i>	-1.9		
<i>M28_Spy1537</i>	<i>uvrA</i>			1.7
<i>M28_Spy1539</i>	<i>M28_Spy1539</i>	-1.6	-1.6	
<i>M28_Spy1543</i>	<i>M28_Spy1543</i>	3.9	5.3	3.4
<i>M28_Spy1544</i>	<i>mutY</i>	1.6	2.5	2.2
<i>M28_Spy1545</i>	<i>M28_Spy1545</i>			1.7
<i>M28_Spy1546</i>	<i>M28_Spy1546</i>			1.5
<i>M28_Spy1547</i>	<i>trx.2</i>	1.6		1.6
<i>M28_Spy1554</i>	<i>recD</i>	-1.6		
<i>M28_Spy1556</i>	<i>dinP</i>			2.0
<i>M28_Spy1557</i>	<i>pfl</i>	-2.2	-1.5	
<i>M28_Spy1559</i>	<i>M28_Spy1559</i>	1.7		
<i>M28_Spy1562</i>	<i>M28_Spy1562</i>			-2.7
<i>M28_Spy1563</i>	<i>norA</i>			-2.8
<i>M28_Spy1566</i>	<i>M28_Spy1566</i>			-2.5
<i>M28_Spy1567</i>	<i>M28_Spy1567</i>		1.6	
<i>M28_Spy1568</i>	<i>M28_Spy1568</i>			1.5
<i>M28_Spy1569</i>	<i>M28_Spy1569</i>	-1.6		-1.6
<i>M28_Spy1570</i>	<i>dnaQ</i>			-1.8
<i>M28_Spy1572</i>	<i>M28_Spy1572</i>			2.1

Table B-3 Continued.

Locus tag ^a	Gene	Fold change relative to WT ^b		
		M1	M3	M28
<i>M28_Spy1574</i>	<i>M28_Spy1574</i>			1.8
<i>M28_Spy1575</i>	<i>M28_Spy1575</i>			1.9
<i>M28_Spy1576</i>	<i>M28_Spy1576</i>			2.3
<i>M28_Spy1577</i>	<i>M28_Spy1577</i>		-1.8	
<i>M28_Spy1578</i>	<i>deoC</i>	1.5		
<i>M28_Spy1580</i>	<i>udp</i>			-1.5
<i>M28_Spy1585</i>	<i>M28_Spy1585</i>		-1.6	
<i>M28_Spy1592</i>	<i>lppC</i>		-1.5	
<i>M28_Spy1593</i>	<i>M28_Spy1593</i>			1.6
<i>M28_Spy1597</i>	<i>lba</i>		-1.8	
<i>M28_Spy1608</i>	<i>M28_Spy1608</i>	2.0		
<i>M28_Spy1615</i>	<i>salR</i>	1.6	2.2	
<i>M28_Spy1616</i>	<i>salK</i>		1.6	
<i>M28_Spy1618</i>	<i>salX</i>	-2.2		-1.5
<i>M28_Spy1620</i>	<i>salM</i>	-4.9		-1.6
<i>M28_Spy1622</i>	<i>lacG</i>	-3.3		
<i>M28_Spy1623</i>	<i>lacE</i>	-3.5		
<i>M28_Spy1624</i>	<i>lacF</i>	-5.3		
<i>M28_Spy1625</i>	<i>lacD.2</i>	-4.2		
<i>M28_Spy1626</i>	<i>lacC.2</i>	-4.1	1.9	-1.6
<i>M28_Spy1627</i>	<i>lacB.2</i>	-4.7	1.9	-1.6
<i>M28_Spy1628</i>	<i>lacA.2</i>	-4.6		
<i>M28_Spy1629</i>	<i>lacR.2</i>	1.5		
<i>M28_Spy1631</i>	<i>M28_Spy1631</i>			1.7
<i>M28_Spy1641</i>	<i>M28_Spy1641</i>	-1.5		
<i>M28_Spy1642</i>	<i>M28_Spy1642</i>		-1.6	
<i>M28_Spy1650</i>	<i>M28_Spy1650</i>	-3.4		
<i>M28_Spy1655</i>	<i>M28_Spy1655</i>	-4.4		
<i>M28_Spy1660</i>	<i>polC</i>			1.5
<i>M28_Spy1662</i>	<i>eep</i>		-1.5	
<i>M28_Spy1671</i>	<i>lrp</i>			-1.5
<i>M28_Spy1672</i>	<i>ska</i>	2.1	15.4	-2.2
<i>M28_Spy1673</i>	<i>M28_Spy1673</i>			1.5
<i>M28_Spy1674</i>	<i>relA</i>			1.5
<i>M28_Spy1675</i>	<i>sclA</i>	8.3		19.1
<i>M28_Spy1676</i>	<i>nrdI.1</i>		-1.7	
<i>M28_Spy1677</i>	<i>M28_Spy1677</i>			-1.5
<i>M28_Spy1678</i>	<i>malT</i>	-1.9		
<i>M28_Spy1682</i>	<i>M28_Spy1682</i>			1.6
<i>M28_Spy1683</i>	<i>trpG</i>	-1.7		1.5
<i>M28_Spy1684</i>	<i>M28_Spy1684</i>			1.7
<i>M28_Spy1686</i>	<i>flaR</i>			-1.6
<i>M28_Spy1689</i>	<i>dppA</i>		2.1	2.0
<i>M28_Spy1690</i>	<i>dppB</i>		1.7	2.1
<i>M28_Spy1691</i>	<i>dppC</i>			2.1
<i>M28_Spy1692</i>	<i>dppD</i>		1.7	2.0
<i>M28_Spy1693</i>	<i>dppE</i>		1.8	2.0
<i>M28_Spy1694</i>	<i>M28_Spy1694</i>			1.5
<i>M28_Spy1695</i>	<i>htpA</i>	-1.8		-1.6

Table B-3 Continued.

Locus tag ^a	Gene	Fold change relative to WT ^b		
		M1	M3	M28
<i>M28_Spy1696</i>	<i>lmb</i>	-1.8		-1.7
<i>M28_Spy1699</i>	<i>fba</i>			4.1
<i>M28_Spy1700</i>	<i>scpA</i>		8.6	4.1
<i>M28_Spy1701</i>	<i>enn</i>			1.6
<i>M28_Spy1702</i>	<i>emm</i>			3.5
<i>M28_Spy1704</i>	<i>mga</i>		1.8	2.2
<i>M28_Spy1706</i>	<i>M28_Spy1706</i>			1.7
<i>M28_Spy1707</i>	<i>isp</i>			1.5
<i>M28_Spy1708</i>	<i>ihk</i>			1.5
<i>M28_Spy1710</i>	<i>M28_Spy1710</i>			1.8
<i>M28_Spy1711</i>	<i>M28_Spy1711</i>			1.6
<i>M28_Spy1712</i>	<i>M28_Spy1712</i>			1.7
<i>M28_Spy1713</i>	<i>M28_Spy1713</i>			1.8
<i>M28_Spy1714</i>	<i>M28_Spy1714</i>			1.7
<i>M28_Spy1715</i>	<i>sfbX</i>			3.4
<i>M28_Spy1716</i>	<i>sof</i>			3.0
<i>M28_Spy1717</i>	<i>grm</i>			3.6
<i>M28_Spy1719</i>	<i>M28_Spy1719</i>	-3.7		
<i>M28_Spy1720</i>	<i>spi</i>	-3.7		
<i>M28_Spy1721</i>	<i>speB</i>	-3.5	-3.3	
<i>M28_Spy1723</i>	<i>M28_Spy1723</i>	-4.9		
<i>M28_Spy1724</i>	<i>ropB</i>	-1.9	-2.8	-2.3
<i>M28_Spy1725</i>	<i>mf</i>	-2.5		-1.8
<i>M28_Spy1728</i>	<i>gldA</i>			1.5
<i>M28_Spy1729</i>	<i>mipB</i>			1.6
<i>M28_Spy1731</i>	<i>M28_Spy1731</i>	-5.5		-2.1
<i>M28_Spy1733</i>	<i>M28_Spy1733</i>	-4.6		
<i>M28_Spy1734</i>	<i>M28_Spy1734</i>	-1.7		
<i>M28_Spy1736</i>	<i>M28_Spy1736</i>	-2.7		-1.9
<i>M28_Spy1739</i>	<i>pbp2A</i>		1.6	2.1
<i>M28_Spy1740</i>	<i>M28_Spy1740</i>	1.8	3.2	2.2
<i>M28_Spy1741</i>	<i>M28_Spy1741</i>	1.5		1.6
<i>M28_Spy1742</i>	<i>M28_Spy1742</i>			1.6
<i>M28_Spy1744</i>	<i>M28_Spy1744</i>		-1.8	
<i>M28_Spy1747</i>	<i>groEL</i>	1.9		
<i>M28_Spy1748</i>	<i>groES</i>	1.9		
<i>M28_Spy1751</i>	<i>csp</i>	-2.0		
<i>M28_Spy1752</i>	<i>ahpC</i>	1.5		1.6
<i>M28_Spy1753</i>	<i>ahpF</i>	1.6		1.6
<i>M28_Spy1758</i>	<i>fhs.2</i>	-3.0		-2.1
<i>M28_Spy1760</i>	<i>M28_Spy1760</i>			-2.3
<i>M28_Spy1761</i>	<i>hutH</i>	-2.6		-2.3
<i>M28_Spy1762</i>	<i>hutG</i>	-1.7	-2.0	-1.9
<i>M28_Spy1763</i>	<i>M28_Spy1763</i>			-1.6
<i>M28_Spy1766</i>	<i>pepO</i>	1.8	2.6	3.1
<i>M28_Spy1767</i>	<i>dexS</i>	-1.8	-2.2	-1.5
<i>M28_Spy1768</i>	<i>M28_Spy1768</i>		-2.2	
<i>M28_Spy1769</i>	<i>treR</i>			-1.5
<i>M28_Spy1770</i>	<i>M28_Spy1770</i>	-1.9		

Table B-3 Continued.

Locus tag ^a	Gene	Fold change relative to WT ^b		
		M1	M3	M28
<i>M28_Spy1771</i>	<i>M28_Spy1771</i>	-2.1		-1.5
<i>M28_Spy1773</i>	<i>nrdG</i>	-1.8		
<i>M28_Spy1774</i>	<i>M28_Spy1774</i>	-1.7		
<i>M28_Spy1775</i>	<i>M28_Spy1775</i>	-1.7		
<i>M28_Spy1776</i>	<i>M28_Spy1776</i>			-1.5
<i>M28_Spy1779</i>	<i>M28_Spy1779</i>		2.5	
<i>M28_Spy1780</i>	<i>M28_Spy1780</i>	1.8		
<i>M28_Spy1781</i>	<i>M28_Spy1781</i>	1.8		
<i>M28_Spy1782</i>	<i>spxA2</i>	2.7	2.2	4.0
<i>M28_Spy1815</i>	<i>M28_Spy1815</i>	1.5		
<i>M28_Spy1818</i>	<i>uviB</i>			2.5
<i>M28_Spy1821</i>	<i>M28_Spy1821</i>		-1.7	
<i>M28_Spy1826</i>	<i>cadD</i>			-1.6
<i>M28_Spy1827</i>	<i>cadC</i>			-1.9
<i>M28_Spy1828</i>	<i>M28_Spy1828</i>			-1.7
<i>M28_Spy1829</i>	<i>M28_Spy1829</i>	-2.2		-2.0
<i>M28_Spy1830</i>	<i>M28_Spy1830</i>	-2.1	-1.7	-2.0
<i>M28_Spy1835</i>	<i>ywzG</i>			-1.5
<i>M28_Spy1836</i>	<i>M28_Spy1836</i>	-1.8		
<i>M28_Spy1837</i>	<i>M28_Spy1837</i>	-1.8		
<i>M28_Spy1838</i>	<i>M28_Spy1838</i>	-1.7	-2.1	
<i>M28_Spy1866</i>	<i>M28_Spy1866</i>		2.8	-1.5
<i>M28_Spy1873</i>	<i>sdhB</i>	-1.8		
<i>M28_Spy1874</i>	<i>sdhA</i>	-2.1		
<i>M28_Spy1875</i>	<i>M28_Spy1875</i>		-1.7	-2.7
<i>M28_Spy1881</i>	<i>M28_Spy1881</i>		2.2	2.0
<i>M28_Spy1882</i>	<i>M28_Spy1882</i>	1.7	2.2	2.1
<i>M28_Spy1884</i>	<i>hasA</i>	18.8	250.6	17.2
<i>M28_Spy1885</i>	<i>hasB</i>	18.0	181.4	18.8
<i>M28_Spy1886</i>	<i>hasC</i>	16.3	97.2	17.7
<i>M28_Spy1889</i>	<i>M28_Spy1889</i>		1.8	
<i>M28_Spy1890</i>	<i>guaB</i>	-1.7	-1.8	
<i>M28_Spy1891</i>	<i>trsA</i>	-1.6		-1.5
<i>M28_Spy1893</i>	<i>M28_Spy1893</i>	-2.4		-1.7
<i>M28_Spy1895</i>	<i>M28_Spy1895</i>	-2.2		

Bold font indicates transcription regulators regulated by RocA.

^aLocus tag identified in the serotype M28 reference genome MGAS6180.

^bEmpty cells: the gene does not satisfy the *P* value and/or fold change requirement.

Table B-4 Primers used to construct the isogenic *rocA* deletion mutant strain.

Primer	Sequence	Remarks
rocA-DEL-1	5' - GCGTGGATCCGAATTGACTAAGGCATTCCTCAGGT - 3'	<i>Bam</i> HI site underlined
rocA-DEL-2	5' - TGAGTGATTATTAATACCTTTAACATTCAAAATATGTTATCACATCTCGA - 3'	
rocA-DEL-3	5' - TCGAGATGTGATAACATATTTGAATGTTAAAGGTATTAATAATCACTCA - 3'	
rocA-DEL-4	5' - GCGTGGATCCCCAAGAGAACCTTCCGAGAACCTT - 5'	<i>Bam</i> HI site underlined

Table B-5 Clinical isolates with naturally-occurring *rocA* polymorphisms and the phylogenetically-matched wild-type (WT) strains.

Strain	Subclade	RocA polymorphism	Mutations in other global regulators‡
MGAS28166	1A	V104G	
MGAS28204	1A	E256*	
MGAS28245	1A	Q223*	
MGAS28411	1A	-9del(6nt)	
MGAS28426	1A	WT†	
MGAS28941	1A	195del(8nt)	RopB N108D
MGAS7893	1A-mga	T442P	Mga I479T, TrxR A289V, FasB S28F
MGAS7895	1A-mga	T442P	Mga I479T, TrxR A289V, DpiA T141I
MGAS7904	1A-mga	T442P	Mga I479T, TrxR A289V, RopB K71E, FasA 532del(6nt)
MGAS7909	1A-mga	T442P	Mga I479T, TrxR A289V, CcpA G202D, FasA 532del(6nt)
MGAS7966	1A-mga	T442P	Mga I479T, TrxR A289V, FasA 532del(6nt)
MGAS7967	1A-mga	T442P	Mga I479T, TrxR A289V, FasA 532del(6nt)
MGAS7995	1A-mga	T442P	Mga I479T, TrxR A289V
MGAS8020	1A-mga	T442P	Mga I479T, TrxR A289V
MGAS10816	1A-mga	E3K	Mga I479T, RofA K141R, CcpA K108N, M28_Spy0762 A108V
MGAS12250	1A-mga	T442P	Mga I479T, TrxR A289V
MGAS28330	1A-mga	WT	Mga I479T
MGAS11107	1B	WT	
MGAS28101	1B	T442I	RopB S143N
MGAS28253	1B	P58S	
MGAS28652	1B	T442I	RopB I156T, CovR G35A, Mga 567ins(1nt)
MGAS28706	1B	T442I	CcpA D106G, CovR R66C, FasB 134ins(1nt)
MGAS28742	1B	Y81*	RopB M76I, YesN V177I
MGAS29146	1B	A55T	CovS Q8*
MGAS29160	1B	419del(1nt)	
MGAS29250	1B	Q443*	
MGAS29251	1B	Q225*	
MGAS29298	1B	Q157*	
MGAS29336	1B	Q146*	
MGAS29395	1B	644del(1nt)	
MGAS29454	1B	R106*	
MGAS29460	1B	-9del(6nt)	
MGAS29475	1B	V420I	RopB A245T, CovR G61S, CovS M391I, VicK R83C/T319I
MGAS29555	1B	419del(1nt)	
MGAS29562	1B	-9del(6nt) + H60Y	
MGAS29596	1B	-9del(6nt)	
MGAS31960	1B	A164V	RivR R195H
MGAS31968	1B	A164V	RivR R195H
MGAS31971	1B	A164V	RivR R195H
MGAS31997	1B	P97L	
MGAS32013	1B	A164V	RivR R195H, CovR R66H
MGAS32014	1B	A164V	RivR R195H, CovR R66H
MGAS32031	1B	A164V	RivR R195H, RopB I195F, CovS 1206del(5nt)
MGAS12241	2A	S202P	
MGAS27961	2A	WT	M28_Spy0761 T380M
MGAS28050	2A	R258K	CovS I332L
MGAS28299	2A	Y131H	
MGAS28553	2A	F53L	
MGAS28632	2A	-9del(6nt)	
MGAS28677	2A	G184W	CovS 98ins(1nt)
MGAS28689	2A	K105N	FasB A414V, CovS 75del(1nt)
MGAS28912	2A	H149Y	CovS R216C

†WT: Wild-type allele. These strains are the phylogenetically-matched WT strains used in the clinical isolate RNA-seq analysis.

‡All strains have a mutation in RopB (K11R) compared to the reference strain MGAS6180, and this is the wild-type allele. All subclade 1B strains have two RivR mutations (Q278R + R279Q), and all subclade 2A strains have a RivR (M91V), in addition to the other mutations listed (46).

Table B-6 RNA-seq analysis at the mid-exponential (ME) growth phase of clinical isolates with naturally-occurring *rocA* polymorphisms. Differential expression was conducted for each strain against its phylogenetically-matched wild-type (WT) strain (see Table B-5). Included as a separate file (Table B-6.xlsx).

Table B-7 RNA-seq analysis at the early-stationary (ES) growth phase of clinical isolates with naturally-occurring *rocA* polymorphisms. Differential expression was conducted for each strain against its phylogenetically-matched wild-type (WT) strain (see Table B-5). Included as a separate file (Table B-7.xlsx).

Table B-8 RNA-seq analysis at the mid-exponential (ME) growth phase of isogenic $\Delta rocA$ deletion mutant and *rocA* mutant strains. Differential expression was conducted for each strain against the parental wild-type (WT) strain.

Strain		$\Delta rocA$	RocA VNTR + H60Y	RocA P97L	RocA G184W	RocA R258K	RocA T442P
Locus Tag	Gene						
M28_Spy0017	<i>sibA</i>	2.0	1.9	1.6			1.8
M28_Spy0029	<i>purD</i>	-1.7	-1.6	-2.2			-1.8
M28_Spy0030	<i>purE</i>	-1.6	-1.5	-2.1			-1.6
M28_Spy0031	<i>purK</i>			-1.9			
M28_Spy0104	<i>rofA</i>	-2.6	-2.5	-1.9			-1.7
M28_Spy0105	<i>sfb1</i>	-2.4	-2.5	-1.9			
M28_Spy0107	<i>cpa</i>	-2.0	-1.9	-1.6			
M28_Spy0108	<i>lepA</i>	-1.9	-1.9	-1.6			
M28_Spy0109	M28_Spy0109	-1.7	-1.6	-1.5			
M28_Spy0113	<i>prtF2</i>	1.5					1.9
M28_Spy0114	M28_Spy0114	2.6	2.7	2.6			2.6
M28_Spy0117	<i>atoB.2</i>	-1.5		-1.6			
M28_Spy0118	<i>atoD.2</i>			-1.6			
M28_Spy0119	<i>atoA.2</i>	-1.5		-1.5			
M28_Spy0137	<i>nga</i>	2.5	2.5	2.5	-2.5		2.3
M28_Spy0138	<i>ifs</i>	2.5	2.5	2.5	-2.6		2.3
M28_Spy0139	<i>slo</i>	2.4	2.4	2.4	-2.6		2.2
M28_Spy0140	M28_Spy0140	3.7	3.5	3.5	-2.1		3.6
M28_Spy0141	M28_Spy0141	11.8	13.1	9.0	-1.9		9.7
M28_Spy0142	M28_Spy0142	5.6	6.2	4.3			4.9
M28_Spy0143	M28_Spy0143	2.3	2.1	2.1	-1.6		6.9
M28_Spy0144	<i>metB</i>	-2.2	-2.1	-1.8			-1.8
M28_Spy0146	M28_Spy0146	-1.7					
M28_Spy0148	M28_Spy0148			-2.0			
M28_Spy0149	M28_Spy0149			-2.0			
M28_Spy0151	<i>araD</i>	-1.8	-1.7	-2.0			
M28_Spy0167	M28_Spy0167	-1.5		-1.5			
M28_Spy0184	<i>rivR</i>				-1.7		
M28_Spy0189	<i>yjdR</i>	-1.7	-1.6	-1.7			
M28_Spy0190	M28_Spy0190	-1.7	-1.6	-1.7			-1.5
M28_Spy0191	M28_Spy0191	-1.8	-1.7	-1.8			-1.6
M28_Spy0206	M28_Spy0206	-1.7	-1.6	-1.8			-1.5
M28_Spy0207	M28_Spy0207	-1.5		-1.7			
M28_Spy0208	M28_Spy0208	-1.5		-1.7			
M28_Spy0209	M28_Spy0209	-1.6		-1.5			
M28_Spy0210	M28_Spy0210	-1.5	-1.6	-1.5			
M28_Spy0211	<i>nanH</i>	-1.5		-1.5			
M28_Spy0212	M28_Spy0212	-1.5		-1.6			
M28_Spy0262	M28_Spy0262						1.6
M28_Spy0273	M28_Spy0273	2.0	2.0	1.9			1.9
M28_Spy0329	<i>spyCEP</i>	11.2	11.5	9.5	-2.4		10.7
M28_Spy0338	M28_Spy0338	4.6	4.5	4.3	-2.8		5.1

Table B-8 Continued.

Strain		$\Delta rocA$	RocA VNTR + H60Y	RocA P97L	RocA G184W	RocA R258K	RocA T442P
Locus Tag	Gene						
<i>M28_Spy0341</i>	<i>M28_Spy0341</i>	6.1	5.4	5.5	-2.5		6.1
<i>M28_Spy0342</i>	<i>M28_Spy0342</i>	4.0	3.8	3.7	-1.6		4.0
<i>M28_Spy0343</i>	<i>M28_Spy0343</i>	2.5	2.5	2.3			2.3
<i>M28_Spy0346</i>	<i>M28_Spy0346</i>	1.6	6.9	6.0		2.3	
<i>M28_Spy0413</i>	<i>M28_Spy0413</i>			1.6			
<i>M28_Spy0414</i>	<i>M28_Spy0414</i>			1.6			
<i>M28_Spy0454</i>	<i>M28_Spy0454</i>	-1.5					
<i>M28_Spy0464</i>	<i>M28_Spy0464</i>			1.6			
<i>M28_Spy0476</i>	<i>M28_Spy0476</i>	-1.5					
<i>M28_Spy0477</i>	<i>M28_Spy0477</i>	-1.6	-1.5	-1.5			
<i>M28_Spy0501</i>	<i>M28_Spy0501</i>	-1.5		-1.7			
<i>M28_Spy0502</i>	<i>M28_Spy0502</i>	-1.5		-1.8			
<i>M28_Spy0521</i>	<i>adcA</i>	1.9	1.8	1.5			1.6
<i>M28_Spy0523</i>	<i>agaS</i>	-1.7	-1.6	-1.7			
<i>M28_Spy0528</i>	<i>M28_Spy0528</i>	-1.5		-1.5			-1.5
<i>M28_Spy0536</i>	<i>M28_Spy0536</i>	-2.3	-2.1	-2.2			-1.7
<i>M28_Spy0537</i>	<i>M28_Spy0537</i>	-2.2	-2.0	-2.4			-1.8
<i>M28_Spy0538</i>	<i>ralp3</i>	-2.8	-2.4	-2.5			-2.0
<i>M28_Spy0539</i>	<i>epf</i>	-1.8	-1.6	-1.6			
<i>M28_Spy0540</i>	<i>sagA</i>	-2.3	-2.3	-2.5			-2.2
<i>M28_Spy0541</i>	<i>sagB</i>	-2.0	-2.0	-2.2			-1.9
<i>M28_Spy0542</i>	<i>sagC</i>	-2.1	-2.0	-2.3			-1.9
<i>M28_Spy0543</i>	<i>sagD</i>	-2.1	-2.1	-2.3			-1.9
<i>M28_Spy0544</i>	<i>sagE</i>	-2.1	-2.0	-2.2			-1.9
<i>M28_Spy0545</i>	<i>sagF</i>	-1.9	-1.9	-2.0			-1.7
<i>M28_Spy0546</i>	<i>sagG</i>	-2.0	-1.8	-2.1			-1.7
<i>M28_Spy0547</i>	<i>sagH</i>	-2.0	-1.9	-2.1			-1.8
<i>M28_Spy0548</i>	<i>sagI</i>	-2.0	-1.9	-2.1			-1.8
<i>M28_Spy0593</i>	<i>pepT</i>	-1.5	-1.5				
<i>M28_Spy0594</i>	<i>ebsA</i>	-1.6	-1.5				
<i>M28_Spy0595</i>	<i>M28_Spy0595</i>	-1.6	-1.5				
<i>M28_Spy0596</i>	<i>M28_Spy0596</i>	-1.6	-1.6				
<i>M28_Spy0597</i>	<i>cmk</i>	-1.7	-1.6	-1.5			-1.5
<i>M28_Spy0625</i>	<i>M28_Spy0625</i>	2.1	2.0	1.7			2.1
<i>M28_Spy0626</i>	<i>M28_Spy0626</i>	2.3	2.2	1.8			2.2
<i>M28_Spy0627</i>	<i>M28_Spy0627</i>	2.3	2.2	1.8			2.2
<i>M28_Spy0628</i>	<i>M28_Spy0628</i>	2.3	2.3	1.8			2.2
<i>M28_Spy0647</i>	<i>M28_Spy0647</i>	11.3	12.9	7.1			9.5
<i>M28_Spy0648</i>	<i>M28_Spy0648</i>	18.3	20.4	11.3			14.5
<i>M28_Spy0649</i>	<i>mac</i>	23.5	25.7	14.1			18.4
<i>M28_Spy0683</i>	<i>pyrF</i>			-1.5			
<i>M28_Spy0684</i>	<i>pyrE</i>			-1.5			
<i>M28_Spy0754</i>	<i>sclB</i>	2.1	2.0	2.0			1.9
<i>M28_Spy0833</i>	<i>M28_Spy0833</i>						-1.5
<i>M28_Spy0851</i>	<i>M28_Spy0851</i>						1.5
<i>M28_Spy0871</i>	<i>citG</i>	-1.5	-1.5				
<i>M28_Spy0873</i>	<i>M28_Spy0873</i>	-2.3	-2.0	-2.5			-1.9
<i>M28_Spy0874</i>	<i>M28_Spy0874</i>	-1.9		-2.1			
<i>M28_Spy0875</i>	<i>M28_Spy0875</i>	-2.3	-2.1	-2.4			-1.8

Table B-8 Continued.

Strain		$\Delta rocA$	RocA VNTR + H60Y	RocA P97L	RocA G184W	RocA R258K	RocA T442P
Locus Tag	Gene						
M28_Spy0876	<i>oadB</i>	-1.9	-1.9	-2.0			-1.7
M28_Spy0877	M28_Spy0877	-2.3	-2.1	-2.3			-2.0
M28_Spy0878	<i>citD</i>	-1.9	-1.9	-1.9			-1.6
M28_Spy0879	<i>citE</i>	-1.9	-1.8	-2.1			-1.7
M28_Spy0880	<i>citF</i>	-1.9	-1.7	-1.9			-1.6
M28_Spy0881	<i>citX</i>			-1.6			
M28_Spy0882	<i>oadA1</i>	-1.7	-1.7	-1.7			-1.5
M28_Spy0885	<i>xerD</i>	-1.9	-1.7	-2.1			-1.6
M28_Spy0903	M28_Spy0903	1.5		1.5			
M28_Spy0904	M28_Spy0904	1.5		1.5			
M28_Spy0905	M28_Spy0905	1.5					
M28_Spy0906	M28_Spy0906	1.5					
M28_Spy0917	<i>coaA</i>	1.5		1.5			1.5
M28_Spy0923	<i>phoU</i>	-1.5	-1.5	-1.5			
M28_Spy0924	<i>pstB</i>	-1.5	-1.5				
M28_Spy0925	<i>pstB2</i>	-1.5	-1.5				
M28_Spy0926	<i>pstA</i>	-1.5					
M28_Spy0943	M28_Spy0943			1.5			1.5
M28_Spy0944	M28_Spy0944			1.5			1.5
M28_Spy0945	M28_Spy0945			1.5			1.5
M28_Spy0946	M28_Spy0946						1.5
M28_Spy0947	M28_Spy0947						1.5
M28_Spy0953	<i>cfa</i>	-2.0	-1.8	-2.1			-1.9
M28_Spy0963	M28_Spy0963	2.4	2.2	2.0			2.2
M28_Spy0964	M28_Spy0964	2.4	2.3	2.0			2.3
M28_Spy0965	M28_Spy0965	2.5	2.3	2.0			2.3
M28_Spy0966	M28_Spy0966			1.5			
M28_Spy0968	<i>spdI</i>	-8.9	-8.2	-7.1			-7.4
M28_Spy0969	<i>speC</i>	-9.5	-8.2	-7.0			-7.6
M28_Spy0970	M28_Spy0970	-2.9	-2.5	-2.8			-2.7
M28_Spy0973	M28_Spy0973			-1.7			-1.6
M28_Spy0975	M28_Spy0975	-1.6		-1.6			-1.5
M28_Spy0978	M28_Spy0978	-1.6		-1.6			-1.5
M28_Spy0979	M28_Spy0979			-1.6			
M28_Spy0980	M28_Spy0980	-1.6		-1.7			-1.6
M28_Spy0983	M28_Spy0983			-1.6			
M28_Spy0986	M28_Spy0986						-1.7
M28_Spy0987	M28_Spy0987	-1.8		-1.6			
M28_Spy0988	M28_Spy0988			-1.7			
M28_Spy0989	M28_Spy0989	-1.6		-1.6			-1.6
M28_Spy0995	M28_Spy0995			-1.5			
M28_Spy0996	M28_Spy0996			-1.6			
M28_Spy0999	M28_Spy0999	-2.0	-1.7	-2.1			-1.7
M28_Spy1000	M28_Spy1000	-1.6		-1.7			-1.5
M28_Spy1001	M28_Spy1001	-3.1	-2.7	-2.9			-2.4
M28_Spy1002	M28_Spy1002	-3.0	-2.5	-3.1			-2.4
M28_Spy1003	M28_Spy1003	-2.7	-2.1	-2.6			-2.2
M28_Spy1004	M28_Spy1004	-2.1	-1.7	-2.0			-1.7
M28_Spy1005	M28_Spy1005	-1.9	-1.6	-1.8			-1.7

Table B-8 Continued.

Strain		$\Delta rocA$	RocA VNTR + H60Y	RocA P97L	RocA G184W	RocA R258K	RocA T442P
Locus Tag	Gene						
M28_Spy1006	M28_Spy1006	-1.7		-1.6			
M28_Spy1007	M28_Spy1007	-2.0					
M28_Spy1008	M28_Spy1008	-1.9					
M28_Spy1009	M28_Spy1009	-1.9	-1.7	-1.8			-1.7
M28_Spy1011	M28_Spy1011	-1.7		-1.8			-1.5
M28_Spy1012	M28_Spy1012	-1.8	-1.5	-1.9			-1.7
M28_Spy1013	M28_Spy1013	-2.3	-1.7	-2.2			-1.8
M28_Spy1014	M28_Spy1014	-2.2	-1.7	-2.2			-1.8
M28_Spy1015	M28_Spy1015	-1.8		-2.0			-1.8
M28_Spy1016	M28_Spy1016	-2.0		-2.0			
M28_Spy1017	M28_Spy1017			-1.9			
M28_Spy1018	M28_Spy1018	-2.0	-1.7	-2.1			-1.7
M28_Spy1020	M28_Spy1020	-2.0		-2.0			
M28_Spy1023	M28_Spy1023						-1.5
M28_Spy1026	M28_Spy1026	-1.6					
M28_Spy1049	M28_Spy1049	1.5					
M28_Spy1052	<i>dltC</i>	1.5					
M28_Spy1053	<i>dltB</i>	1.5					
M28_Spy1054	<i>dltA</i>	1.5					
M28_Spy1055	M28_Spy1055	1.5	1.5	1.5			
M28_Spy1098	<i>grab</i>	-3.0	-1.8	-2.5	2.5		-2.1
M28_Spy1127	<i>surA</i>	1.6	1.5	1.6			1.5
M28_Spy1132	M28_Spy1132	-1.7	-1.5	-1.7			-1.6
M28_Spy1133	<i>nagB</i>	-2.7	-2.1	-2.9			-2.1
M28_Spy1137	M28_Spy1137	-1.6	-1.6	-1.8			-1.6
M28_Spy1138	M28_Spy1138	-1.9	-1.8	-1.6			-1.7
M28_Spy1141	<i>comEC.1</i>	-1.5					
M28_Spy1150	M28_Spy1150			1.5			
M28_Spy1161	<i>pmtA</i>	-1.5		-1.6			
M28_Spy1207	<i>asnA</i>	-2.5	-2.1	-2.3			-2.1
M28_Spy1208	<i>arcC</i>	2.1	1.9	2.1			1.9
M28_Spy1209	M28_Spy1209	2.1	1.9	2.2			1.9
M28_Spy1210	<i>arcD</i>	2.1	1.8	2.3			1.9
M28_Spy1211	<i>arcB</i>	2.7	2.2	3.1			2.3
M28_Spy1212	M28_Spy1212	2.7	2.1	3.2			2.4
M28_Spy1213	<i>arcA</i>	2.8	2.2	3.4			2.4
M28_Spy1308	M28_Spy1308	-1.8		-1.8			-1.5
M28_Spy1314	M28_Spy1314	-1.7		-1.6			
M28_Spy1322	M28_Spy1322	-1.5		-1.6			
M28_Spy1325	<i>aspA</i>	-1.6		-1.5			
M28_Spy1326	M28_Spy1326	-2.2	-2.2	-1.9			-1.9
M28_Spy1330	M28_Spy1330						-1.5
M28_Spy1331	M28_Spy1331			-1.5			-1.5
M28_Spy1336	M28_Spy1336	-1.6	-1.6	-2.0			-1.6
M28_Spy1345	<i>lacZ</i>	-1.8	-1.8	-1.7			-1.5
M28_Spy1346	<i>trxR</i>	-1.7	-1.6	-1.6			
M28_Spy1347	<i>trxS</i>	-1.7	-1.5	-1.5			
M28_Spy1348	M28_Spy1348	-1.5					
M28_Spy1359	<i>rocA</i>	-184.8	-1.9				

Table B-8 Continued.

Strain		$\Delta rocA$	RocA VNTR + H60Y	RocA P97L	RocA G184W	RocA R258K	RocA T442P
Locus Tag	Gene						
M28_Spy1415	M28_Spy1415	2.1	2.0	1.6			1.8
M28_Spy1416	M28_Spy1416	2.2	2.1	1.7			2.0
M28_Spy1417	M28_Spy1417	2.4	2.3	1.9			2.1
M28_Spy1429	M28_Spy1429	2.3	2.2	1.8			1.8
M28_Spy1430	M28_Spy1430	-1.8	-1.5	-1.8			-1.5
M28_Spy1431	nagA			-1.5			
M28_Spy1433	M28_Spy1433	1.5		1.6			
M28_Spy1434	M28_Spy1434	2.2	1.9	2.2	-1.5		1.9
M28_Spy1443	M28_Spy1443	-1.7		-1.8			
M28_Spy1447	copZ	-1.8	-1.7	-2.1			-1.6
M28_Spy1448	copA	-2.6	-2.3	-2.8			-2.1
M28_Spy1449	copY	-3.2	-2.5	-3.1			-2.5
M28_Spy1450	sse	2.0	1.8	2.1	-1.6		1.7
M28_Spy1486	dnaJ			-1.8			
M28_Spy1487	dnaK			-1.7			
M28_Spy1488	grpE			-2.0			-1.5
M28_Spy1489	hrcA	-1.6	-1.5	-2.2			-1.7
M28_Spy1505	asnB	2.2	2.2	1.9			1.9
M28_Spy1506	M28_Spy1506	4.7	4.6	3.8			3.7
M28_Spy1507	M28_Spy1507	4.6	4.5	3.7	-1.5		3.7
M28_Spy1520	shr	1.6	1.6				
M28_Spy1521	isp2	-1.6	-1.5	-1.5			
M28_Spy1526	scrK	-2.9	-2.7	-3.0			-2.6
M28_Spy1527	endoS	-1.7	-1.6	-1.9			-1.6
M28_Spy1528	M28_Spy1528	-1.9	-1.7	-2.3			-1.9
M28_Spy1529	scrA	-2.6	-2.3	-2.8			-2.2
M28_Spy1530	scrB	-1.6	-1.5				
M28_Spy1543	M28_Spy1543	1.8	2.0	1.6			1.8
M28_Spy1544	mutY	1.7	1.6	1.7			1.6
M28_Spy1570	dnaQ			-1.5			
M28_Spy1572	M28_Spy1572	2.4	2.5	2.1			2.1
M28_Spy1573	M28_Spy1573	2.4	2.4	2.1			1.9
M28_Spy1574	M28_Spy1574	2.1	2.4	2.1			2.0
M28_Spy1575	M28_Spy1575	2.5	2.5	2.2			2.1
M28_Spy1576	M28_Spy1576	2.8	2.6	2.2			2.1
M28_Spy1593	M28_Spy1593	2.1	1.9	1.7			1.8
M28_Spy1623	lacE	-2.2	-2.0	-2.7			-2.0
M28_Spy1624	lacF			-1.9			
M28_Spy1625	lacD.2	-3.2	-2.7	-3.8			-2.7
M28_Spy1626	lacC.2	-3.0	-2.2	-3.0			-2.3
M28_Spy1627	lacB.2	-2.8	-2.4	-3.2			-2.7
M28_Spy1628	lacA.2	-4.3	-3.6	-5.1			-3.9
M28_Spy1672	ska						-2.4
M28_Spy1675	sclA	6.1	6.2	5.6	-2.6		6.3
M28_Spy1686	flaR			-1.5			
M28_Spy1689	dppA	1.7	1.6	1.6			1.5
M28_Spy1699	fba	2.4	2.5	2.4	-1.8		2.3
M28_Spy1700	scpA	2.5	2.6	2.5	-1.8		2.4
M28_Spy1701	emm				-1.7		

Table B-8 Continued.

Strain		$\Delta rocA$	RocA VNTR + H60Y	RocA P97L	RocA G184W	RocA R258K	RocA T442P
Locus Tag	Gene						
M28_Spy1702	<i>emm</i>	1.7	1.6	1.8	-1.8		1.6
M28_Spy1703	<i>mrp</i>						2.3
M28_Spy1704	<i>mga</i>	1.9	1.9	1.9			1.7
M28_Spy1715	<i>sfbX</i>	1.5	1.5	1.5			1.5
M28_Spy1716	<i>sof</i>	1.7	1.7	1.7			1.7
M28_Spy1718	<i>prsA</i>	1.9	2.0				1.6
M28_Spy1721	<i>speB</i>	-1.6		-1.7			
M28_Spy1724	<i>ropB</i>	-2.6	-2.4	-2.4			-2.1
M28_Spy1725	<i>mf</i>		-1.5	-1.5			
M28_Spy1726	M28_Spy1726	-2.1					
M28_Spy1731	M28_Spy1731	-1.7					
M28_Spy1736	M28_Spy1736	-1.8	-1.6	-2.0			-1.7
M28_Spy1745	M28_Spy1745	-1.6	-1.5	-1.6			
M28_Spy1746	M28_Spy1746	-1.8	-1.6	-1.8			
M28_Spy1748	<i>groES</i>			-1.8			
M28_Spy1751	<i>csp</i>			2.0			
M28_Spy1755	<i>hutU</i>	-1.6	-1.7	-1.7			-1.5
M28_Spy1761	<i>hutH</i>	-1.8					
M28_Spy1766	<i>pepO</i>	1.7	1.6	1.7			1.6
M28_Spy1770	M28_Spy1770	-1.7		-1.8			-1.6
M28_Spy1771	M28_Spy1771	-1.9	-1.8	-1.9			-1.6
M28_Spy1777	<i>nrdD</i>	-1.5		-1.5			
M28_Spy1782	<i>spxA2</i>			1.5	-1.5		
M28_Spy1789	M28_Spy1789			-1.5			
M28_Spy1790	M28_Spy1790			-1.5			
M28_Spy1793	M28_Spy1793	-2.1					
M28_Spy1794	M28_Spy1794	-2.0		-1.9			
M28_Spy1796	M28_Spy1796	-1.9	-1.6	-1.9			-1.5
M28_Spy1798	M28_Spy1798	-1.5		-1.6			-1.5
M28_Spy1799	M28_Spy1799	-1.7		-1.8			-1.6
M28_Spy1800	M28_Spy1800	-1.9		-2.0			
M28_Spy1804	M28_Spy1804	-1.9		-2.0			
M28_Spy1805	M28_Spy1805			-1.6			
M28_Spy1809	M28_Spy1809			-1.7			
M28_Spy1813	M28_Spy1813	3.4	3.3	3.0	-2.1		2.4
M28_Spy1830	M28_Spy1830			-1.5			
M28_Spy1838	M28_Spy1838	-1.9	-1.7	-2.0			-1.7
M28_Spy1839	<i>pipR</i>	-1.5	-1.5	-1.5			
M28_Spy1846	M28_Spy1846	-1.6					
M28_Spy1848	M28_Spy1848	-1.6		-1.5			
M28_Spy1849	M28_Spy1849	-1.9	-1.9	-2.1			-1.7
M28_Spy1850	M28_Spy1850	-1.9		-1.7			-1.6
M28_Spy1861	M28_Spy1861			-1.7			
M28_Spy1875	M28_Spy1875	1.9					1.9
M28_Spy1881	M28_Spy1881	1.5		1.5			
M28_Spy1882	M28_Spy1882	1.7	1.5	1.7			1.6
M28_Spy1884	<i>hasA</i>	48.0	49.6	31.1			26.1
M28_Spy1885	<i>hasB</i>	54.4	56.8	35.7			30.0
M28_Spy1886	<i>hasC</i>	46.3	46.7	30.3			25.5

Table B-9 RNA-seq analysis at the early-stationary (ES) growth phase of isogenic $\Delta rocA$ deletion mutant and *rocA* mutant strains. Differential expression was conducted for each strain against the parental wild-type (WT) strain.

Strain		$\Delta rocA$	RocA VNTR + H60Y	RocA P97L	RocA G184W	RocA R258K	RocA T442P
Locus Tag	Gene						
M28_Spy0005	<i>pth</i>			1.5			
M28_Spy0012	<i>hpt</i>			1.7			
M28_Spy0013	<i>ftsH</i>			1.5			
M28_Spy0014	M28_Spy0014	-1.7	-1.8	-1.5			-1.7
M28_Spy0018	<i>prsA2</i>	-1.6	-1.6				
M28_Spy0023	<i>purL</i>						-1.5
M28_Spy0024	<i>purF</i>			-1.5			
M28_Spy0027	<i>purH</i>			-1.5			
M28_Spy0029	<i>purD</i>	-1.8	-1.7	-1.8			-1.9
M28_Spy0030	<i>purE</i>	-1.6	-1.6	-1.7			-1.9
M28_Spy0031	<i>purK</i>	-1.7	-1.8	-1.9			-1.8
M28_Spy0032	M28_Spy0032	-1.5					
M28_Spy0033	<i>purB</i>	-1.7	-1.6	-1.7			-1.5
M28_Spy0034	<i>comR</i>	-1.5	-1.5				
M28_Spy0036	M28_Spy0036	-1.6	-1.6	-1.5			-1.6
M28_Spy0037	M28_Spy0037	-2.2	-2.2	-2.1			-1.9
M28_Spy0038	M28_Spy0038	-2.2	-2.1	-2.1			-1.9
M28_Spy0039	M28_Spy0039			-2.3			
M28_Spy0044	<i>rplD</i>				-1.6		
M28_Spy0045	<i>rplW</i>				-1.6		
M28_Spy0046	<i>rplB</i>				-1.6		
M28_Spy0047	<i>rpsS</i>				-1.6		
M28_Spy0048	<i>rplV</i>				-1.6		
M28_Spy0049	<i>rpsC</i>				-1.7		
M28_Spy0050	<i>rplP</i>				-1.6		
M28_Spy0051	<i>rpmC</i>				-1.7		
M28_Spy0052	<i>rpsQ</i>				-1.6		
M28_Spy0053	<i>rplN</i>				-1.7		
M28_Spy0054	<i>rplX</i>				-1.6		
M28_Spy0055	<i>rplE</i>				-1.6		
M28_Spy0056	<i>rpsN</i>				-1.6		
M28_Spy0057	<i>rpsH</i>				-1.6		
M28_Spy0058	<i>rplF</i>				-1.6		
M28_Spy0059	<i>rplR</i>				-1.5		
M28_Spy0060	<i>rpsE</i>				-1.6		
M28_Spy0064	<i>adk</i>	1.7	1.9	1.7			1.8
M28_Spy0065	<i>infA</i>		1.5	1.5			1.6
M28_Spy0066	<i>rpmJ</i>			1.5			1.6
M28_Spy0067	<i>rpsM</i>		1.5	1.5			1.5
M28_Spy0068	<i>rpsK</i>			1.5			1.5
M28_Spy0069	<i>rpoA</i>		1.5				1.5
M28_Spy0070	<i>rplQ</i>		1.5				1.5
M28_Spy0083	M28_Spy0083	-1.9	-2.0	-1.7			-1.9
M28_Spy0099	M28_Spy0099			1.6			
M28_Spy0103	M28_Spy0103			1.5			
M28_Spy0105	<i>sfb1</i>			1.7			
M28_Spy0113	<i>prtF2</i>	2.0	1.7	2.0			1.8
M28_Spy0120	M28_Spy0120	-1.5	-1.5				

Table B-9 Continued.

Strain		$\Delta rocA$	RocA VNTR + H60Y	RocA P97L	RocA G184W	RocA R258K	RocA T442P
Locus Tag	Gene						
<i>M28_Spy0137</i>	<i>nga</i>	6.1	5.9	4.1			5.1
<i>M28_Spy0138</i>	<i>ifs</i>	7.3	7.0	4.7			5.8
<i>M28_Spy0139</i>	<i>slo</i>	4.8	4.9	3.1			4.0
<i>M28_Spy0142</i>	<i>M28_Spy0142</i>			-1.8			
<i>M28_Spy0143</i>	<i>M28_Spy0143</i>	3.0	2.4	2.7			2.9
<i>M28_Spy0144</i>	<i>metB</i>	-2.3	-2.0	-2.1			-1.7
<i>M28_Spy0155</i>	<i>opuAA</i>		-1.7				-2.0
<i>M28_Spy0156</i>	<i>opuABC</i>		-1.6	-1.5			-1.8
<i>M28_Spy0167</i>	<i>M28_Spy0167</i>	1.7					
<i>M28_Spy0184</i>	<i>rivR</i>			-1.6			-1.7
<i>M28_Spy0191</i>	<i>M28_Spy0191</i>	-1.5		-1.8			-1.5
<i>M28_Spy0195</i>	<i>M28_Spy0195</i>			1.5			
<i>M28_Spy0196</i>	<i>M28_Spy0196</i>	-2.5	-2.5	-2.4			-2.1
<i>M28_Spy0223</i>	<i>prgA</i>	-1.6	-1.5	-1.6			
<i>M28_Spy0224</i>	<i>rpsL</i>	1.5		1.7			
<i>M28_Spy0225</i>	<i>rpsG</i>	1.6		1.7			
<i>M28_Spy0227</i>	<i>plr</i>	-1.5					
<i>M28_Spy0242</i>	<i>M28_Spy0242</i>	1.8	1.5	1.8			1.5
<i>M28_Spy0244</i>	<i>oppA</i>	-1.9	-1.9	-1.8			-1.7
<i>M28_Spy0245</i>	<i>oppB</i>	-1.9	-1.8	-2.0			-1.6
<i>M28_Spy0246</i>	<i>oppC</i>	-1.7	-1.6	-1.9			-1.5
<i>M28_Spy0247</i>	<i>oppD</i>	-1.7	-1.5	-1.8			
<i>M28_Spy0248</i>	<i>oppF</i>	-1.6	-1.5	-1.7			
<i>M28_Spy0257</i>	<i>M28_Spy0257</i>	1.5		1.6			
<i>M28_Spy0262</i>	<i>M28_Spy0262</i>	-2.5	-2.2	-2.1			-1.6
<i>M28_Spy0263</i>	<i>M28_Spy0263</i>	-1.8	-1.5	-1.6			
<i>M28_Spy0264</i>	<i>M28_Spy0264</i>	-1.6		-1.6			
<i>M28_Spy0265</i>	<i>M28_Spy0265</i>	-1.5		-1.6			
<i>M28_Spy0271</i>	<i>lemA</i>	-1.5					
<i>M28_Spy0272</i>	<i>M28_Spy0272</i>	-1.6					
<i>M28_Spy0300</i>	<i>M28_Spy0300</i>			-1.5			
<i>M28_Spy0307</i>	<i>pflC</i>	-1.8	-1.6	-1.5			
<i>M28_Spy0310</i>	<i>fhuG</i>	1.5					
<i>M28_Spy0313</i>	<i>fhuA</i>	1.8		1.9			
<i>M28_Spy0316</i>	<i>upp</i>			1.6			
<i>M28_Spy0317</i>	<i>clpP</i>	-1.8	-1.9	-1.6			-1.6
<i>M28_Spy0332</i>	<i>metS</i>	1.5					
<i>M28_Spy0337</i>	<i>spyA</i>	2.1	1.8	1.7			1.6
<i>M28_Spy0338</i>	<i>M28_Spy0338</i>	2.6	2.6	2.1			2.7
<i>M28_Spy0339</i>	<i>M28_Spy0339</i>	-1.5		-1.6	-1.5	-1.6	-1.7
<i>M28_Spy0341</i>	<i>M28_Spy0341</i>	1.8	1.7				1.8
<i>M28_Spy0343</i>	<i>M28_Spy0343</i>	1.5	1.5	1.5			
<i>M28_Spy0344</i>	<i>M28_Spy0344</i>		1.6				
<i>M28_Spy0345</i>	<i>speJ</i>	1.7	1.6	1.6			1.5
<i>M28_Spy0346</i>	<i>M28_Spy0346</i>	1.5	2.6	2.5		1.5	
<i>M28_Spy0356</i>	<i>mtsR</i>	-1.7	-1.7	-1.5			
<i>M28_Spy0357</i>	<i>mtsA</i>	-1.8	-1.9				-1.6
<i>M28_Spy0365</i>	<i>pyrH</i>		-1.5				
<i>M28_Spy0366</i>	<i>rrf</i>	-1.6	-1.7				

Table B-9 Continued.

Strain		$\Delta rocA$	RocA VNTR + H60Y	RocA P97L	RocA G184W	RocA R258K	RocA T442P
Locus Tag	Gene						
<i>M28_Spy0371</i>	<i>M28_Spy0371</i>	-2.0	-1.7	-1.7			
<i>M28_Spy0386</i>	<i>M28_Spy0386</i>	1.5					
<i>M28_Spy0420</i>	<i>M28_Spy0420</i>	1.5	1.5				
<i>M28_Spy0421</i>	<i>M28_Spy0421</i>	1.6	1.5				
<i>M28_Spy0423</i>	<i>vicR</i>	-1.5		-1.5			
<i>M28_Spy0424</i>	<i>vicK</i>	-1.5		-1.5			
<i>M28_Spy0425</i>	<i>vicX</i>	-1.5		-1.5			
<i>M28_Spy0426</i>	<i>acpA</i>			1.6			
<i>M28_Spy0428</i>	<i>rgg3</i>	-1.8	-2.1	-1.8			-1.9
<i>M28_Spy0451</i>	<i>M28_Spy0451</i>	-1.8	-1.6	-1.7			
<i>M28_Spy0452</i>	<i>M28_Spy0452</i>	-1.6	-1.5	-1.6			
<i>M28_Spy0453</i>	<i>ftsY</i>	-1.5		-1.6			
<i>M28_Spy0465</i>	<i>ptsK</i>	-1.5	-1.5				-1.5
<i>M28_Spy0466</i>	<i>lgt</i>	-1.5	-1.5	-1.5			-1.5
<i>M28_Spy0467</i>	<i>M28_Spy0467</i>	-1.6	-1.6	-1.5			-1.5
<i>M28_Spy0468</i>	<i>M28_Spy0468</i>	-1.7	-1.5	-1.7			-1.5
<i>M28_Spy0479</i>	<i>M28_Spy0479</i>	-1.5	-1.5	-1.5			-1.5
<i>M28_Spy0498</i>	<i>agaD</i>	2.0					
<i>M28_Spy0499</i>	<i>agaW</i>	1.9					
<i>M28_Spy0500</i>	<i>agaV</i>	1.9					
<i>M28_Spy0501</i>	<i>M28_Spy0501</i>	1.8					
<i>M28_Spy0505</i>	<i>M28_Spy0505</i>	1.5					
<i>M28_Spy0508</i>	<i>M28_Spy0508</i>	-1.5					
<i>M28_Spy0513</i>	<i>M28_Spy0513</i>	-2.1	-1.8	-2.0			-1.6
<i>M28_Spy0521</i>	<i>adcA</i>	2.9	2.8	2.1			2.3
<i>M28_Spy0532</i>	<i>gyrB</i>		-1.5				
<i>M28_Spy0539</i>	<i>epf</i>	1.5					
<i>M28_Spy0543</i>	<i>sagD</i>	1.5	1.6				
<i>M28_Spy0544</i>	<i>sagE</i>	1.6	1.7				
<i>M28_Spy0545</i>	<i>sagF</i>	1.7	1.7	1.5			
<i>M28_Spy0546</i>	<i>sagG</i>	1.7	1.7				
<i>M28_Spy0547</i>	<i>sagH</i>	1.7	1.7	1.6			
<i>M28_Spy0548</i>	<i>sagI</i>	1.7	1.7				
<i>M28_Spy0549</i>	<i>spnA</i>	1.5	1.5				
<i>M28_Spy0550</i>	<i>M28_Spy0550</i>	1.5	1.5				
<i>M28_Spy0571</i>	<i>M28_Spy0571</i>	-1.5		-1.5			
<i>M28_Spy0572</i>	<i>M28_Spy0572</i>	-1.6	-1.5	-1.5			
<i>M28_Spy0574</i>	<i>rexA</i>						1.5
<i>M28_Spy0575</i>	<i>M28_Spy0575</i>						1.5
<i>M28_Spy0599</i>	<i>rpl36</i>			1.6			
<i>M28_Spy0607</i>	<i>gor</i>	-1.5	-1.5	-1.5			
<i>M28_Spy0625</i>	<i>M28_Spy0625</i>			-1.5			
<i>M28_Spy0632</i>	<i>M28_Spy0632</i>	2.1	2.1	1.9			1.8
<i>M28_Spy0633</i>	<i>M28_Spy0633</i>	2.1	2.3	1.7			2.0
<i>M28_Spy0635</i>	<i>gczA</i>	1.5	1.5	1.5			
<i>M28_Spy0637</i>	<i>trmD</i>			1.6			
<i>M28_Spy0638</i>	<i>trxB</i>			1.6			
<i>M28_Spy0641</i>	<i>fruR</i>	-2.8	-2.1				
<i>M28_Spy0642</i>	<i>fruB</i>	-2.5	-1.9	-1.8			

Table B-9 Continued.

Strain		$\Delta rocA$	RocA VNTR + H60Y	RocA P97L	RocA G184W	RocA R258K	RocA T442P
Locus Tag	Gene						
M28_Spy0643	<i>fruA</i>	-1.8		-1.7			
M28_Spy0648	M28_Spy0648	2.4	2.3				
M28_Spy0649	<i>mac</i>	2.1	1.9				
M28_Spy0657	<i>fms</i>		-2.0				-2.2
M28_Spy0670	M28_Spy0670			1.5			
M28_Spy0673	M28_Spy0673	1.5		1.5			
M28_Spy0674	<i>clpL</i>	-1.7	-2.0	-2.0			-2.4
M28_Spy0682	M28_Spy0682	-1.6	-1.5	-1.5			
M28_Spy0696	M28_Spy0696	-1.5	-1.5				
M28_Spy0703	<i>hflX</i>	1.5		1.6			
M28_Spy0704	M28_Spy0704	1.6	1.5	1.6			1.5
M28_Spy0705	<i>elaC</i>	1.6	1.5				1.5
M28_Spy0706	M28_Spy0706	1.5					
M28_Spy0707	<i>recJ</i>	1.6	1.6				1.6
M28_Spy0708	<i>apt</i>	1.5		1.6			
M28_Spy0709	<i>dnaD</i>	1.7		1.9			1.5
M28_Spy0710	<i>nth</i>	1.8	1.5	1.9			1.6
M28_Spy0711	M28_Spy0711	1.5		1.6			
M28_Spy0712	M28_Spy0712			1.5			
M28_Spy0722	M28_Spy0722	2.4	2.3	2.2			
M28_Spy0723	M28_Spy0723	2.7	2.8	2.3			
M28_Spy0724	M28_Spy0724	2.6	2.8	2.1			
M28_Spy0725	M28_Spy0725	2.0	2.3				
M28_Spy0755	<i>msrB</i>	-1.8	-1.7	-1.6			-1.5
M28_Spy0758	<i>ptsB</i>	-1.8		-1.8			
M28_Spy0759	<i>ptsC</i>			-1.7			
M28_Spy0760	<i>ptsD</i>			-1.6			
M28_Spy0768	<i>thdF</i>			1.6			
M28_Spy0772	M28_Spy0772	1.7		1.8			
M28_Spy0782	<i>srtT</i>		1.5				
M28_Spy0783	<i>srtC</i>		1.6				1.5
M28_Spy0784	<i>srtB</i>		1.6				1.5
M28_Spy0785	<i>srtF</i>		1.5				
M28_Spy0786	<i>srtE</i>		1.5				
M28_Spy0802	<i>murB</i>			1.5			
M28_Spy0803	<i>potA</i>	1.6		1.6			
M28_Spy0804	<i>potB</i>	1.6	1.5	1.5			
M28_Spy0805	<i>potC</i>	1.6	1.5	1.5			
M28_Spy0809	<i>malP</i>	1.8	1.7	1.6			1.5
M28_Spy0810	<i>malE</i>	1.6	1.5				
M28_Spy0823	M28_Spy0823			1.5			
M28_Spy0824	M28_Spy0824			1.7			1.5
M28_Spy0825	M28_Spy0825	1.6	1.6	1.8			1.6
M28_Spy0826	<i>pta</i>	-1.7	-1.6				
M28_Spy0827	M28_Spy0827	-1.7					
M28_Spy0828	M28_Spy0828	-1.6					
M28_Spy0830	M28_Spy0830	-1.6					
M28_Spy0834	<i>apbE</i>			1.8			
M28_Spy0845	M28_Spy0845	1.6	1.6				1.5

Table B-9 Continued.

Strain		$\Delta rocA$	RocA VNTR + H60Y	RocA P97L	RocA G184W	RocA R258K	RocA T442P
Locus Tag	Gene						
<i>M28_Spy0851</i>	<i>M28_Spy0851</i>	-2.5	-2.0	-2.0			-1.7
<i>M28_Spy0852</i>	<i>M28_Spy0852</i>	-2.3	-2.0	-2.1			-1.9
<i>M28_Spy0853</i>	<i>M28_Spy0853</i>	-2.2	-2.2	-2.2			-2.1
<i>M28_Spy0854</i>	<i>M28_Spy0854</i>	-2.6	-2.7	-2.9			-2.7
<i>M28_Spy0855</i>	<i>M28_Spy0855</i>	-2.3	-2.4	-2.4			-2.3
<i>M28_Spy0862</i>	<i>M28_Spy0862</i>	2.3	1.8				
<i>M28_Spy0863</i>	<i>ddh</i>	1.6					
<i>M28_Spy0866</i>	<i>gid</i>	1.8		1.8			
<i>M28_Spy0867</i>	<i>oadA2</i>	1.5					
<i>M28_Spy0873</i>	<i>M28_Spy0873</i>	-2.0	-1.8	-1.9			-1.8
<i>M28_Spy0874</i>	<i>M28_Spy0874</i>	-2.1	-2.1	-2.9			
<i>M28_Spy0875</i>	<i>M28_Spy0875</i>	-2.4	-2.2	-2.6			-1.9
<i>M28_Spy0876</i>	<i>oadB</i>	-2.1	-2.0	-2.2			-1.9
<i>M28_Spy0877</i>	<i>M28_Spy0877</i>	-2.0	-2.0	-2.2			-1.9
<i>M28_Spy0878</i>	<i>citD</i>	-2.0	-1.9	-2.2			-1.8
<i>M28_Spy0879</i>	<i>citE</i>	-1.9	-1.8	-2.0			-1.8
<i>M28_Spy0880</i>	<i>citF</i>	-1.8	-1.7	-2.0			-1.9
<i>M28_Spy0881</i>	<i>citX</i>	-1.7	-1.7	-1.9			-1.8
<i>M28_Spy0882</i>	<i>oadA1</i>	-1.7	-1.7	-1.9			-1.9
<i>M28_Spy0891</i>	<i>guaA</i>			1.5			
<i>M28_Spy0892</i>	<i>M28_Spy0892</i>			1.6			
<i>M28_Spy0893</i>	<i>M28_Spy0893</i>			1.9			
<i>M28_Spy0896</i>	<i>M28_Spy0896</i>	1.6		1.6			
<i>M28_Spy0910</i>	<i>pgmA</i>	-1.7	-1.5	-1.6			
<i>M28_Spy0917</i>	<i>coaA</i>						1.6
<i>M28_Spy0919</i>	<i>ciaH</i>	1.5	1.5	1.5			1.5
<i>M28_Spy0932</i>	<i>spxA1</i>	-1.5	-1.5				
<i>M28_Spy0936</i>	<i>M28_Spy0936</i>	1.5		1.5			
<i>M28_Spy0943</i>	<i>M28_Spy0943</i>						-1.7
<i>M28_Spy0944</i>	<i>M28_Spy0944</i>						-1.7
<i>M28_Spy0945</i>	<i>M28_Spy0945</i>						-1.7
<i>M28_Spy0946</i>	<i>M28_Spy0946</i>						-1.6
<i>M28_Spy0948</i>	<i>M28_Spy0948</i>						-1.9
<i>M28_Spy0949</i>	<i>pcrA</i>	1.6		1.5			
<i>M28_Spy0951</i>	<i>M28_Spy0951</i>	-1.7	-2.0				-1.7
<i>M28_Spy0953</i>	<i>cfa</i>	-1.7	-1.7	-1.5			-1.5
<i>M28_Spy0962</i>	<i>dnaE</i>	-1.5		-1.6			
<i>M28_Spy0973</i>	<i>M28_Spy0973</i>			-1.8			
<i>M28_Spy0983</i>	<i>M28_Spy0983</i>			-1.8			
<i>M28_Spy0985</i>	<i>M28_Spy0985</i>			-1.9			
<i>M28_Spy0987</i>	<i>M28_Spy0987</i>			-1.9			
<i>M28_Spy0988</i>	<i>M28_Spy0988</i>			-2.0			
<i>M28_Spy0989</i>	<i>M28_Spy0989</i>			-2.3			
<i>M28_Spy0990</i>	<i>M28_Spy0990</i>			-1.9			
<i>M28_Spy0991</i>	<i>M28_Spy0991</i>			-1.9			
<i>M28_Spy0994</i>	<i>M28_Spy0994</i>	-1.8		-1.9			
<i>M28_Spy1001</i>	<i>M28_Spy1001</i>	-2.3	-2.4	-2.6			-2.7
<i>M28_Spy1002</i>	<i>M28_Spy1002</i>	-1.9	-1.9	-2.4			-2.2
<i>M28_Spy1003</i>	<i>M28_Spy1003</i>			-1.6			-1.6

Table B-9 Continued.

Strain		$\Delta rocA$	RocA VNTR + H60Y	RocA P97L	RocA G184W	RocA R258K	RocA T442P
Locus Tag	Gene						
<i>M28_Spy1004</i>	<i>M28_Spy1004</i>			-1.5			
<i>M28_Spy1014</i>	<i>M28_Spy1014</i>						-1.5
<i>M28_Spy1019</i>	<i>M28_Spy1019</i>						-1.8
<i>M28_Spy1020</i>	<i>M28_Spy1020</i>						-1.9
<i>M28_Spy1021</i>	<i>M28_Spy1021</i>			-1.8			
<i>M28_Spy1022</i>	<i>M28_Spy1022</i>	-2.0	-1.9	-1.6			-1.8
<i>M28_Spy1023</i>	<i>M28_Spy1023</i>						-1.5
<i>M28_Spy1024</i>	<i>M28_Spy1024</i>						-1.7
<i>M28_Spy1025</i>	<i>M28_Spy1025</i>	-1.7	-1.6	-1.8			
<i>M28_Spy1027</i>	<i>M28_Spy1027</i>	-1.6	-1.5	-1.6			-1.5
<i>M28_Spy1043</i>	<i>malA</i>	2.5	2.3				
<i>M28_Spy1044</i>	<i>malD</i>	2.4	2.3				
<i>M28_Spy1045</i>	<i>malC</i>	2.4	2.3				
<i>M28_Spy1049</i>	<i>M28_Spy1049</i>	1.5	1.7				
<i>M28_Spy1050</i>	<i>M28_Spy1050</i>	1.7	1.7	1.5			1.6
<i>M28_Spy1051</i>	<i>dltD</i>	1.6	1.6	1.5			1.5
<i>M28_Spy1052</i>	<i>dltC</i>	1.6	1.6				
<i>M28_Spy1053</i>	<i>dltB</i>	1.6	1.6	1.5			
<i>M28_Spy1054</i>	<i>dltA</i>	1.6	1.5	1.5			
<i>M28_Spy1055</i>	<i>M28_Spy1055</i>			1.5			
<i>M28_Spy1057</i>	<i>glnH</i>	2.8	2.2	3.2			2.3
<i>M28_Spy1058</i>	<i>glnQ.2</i>	2.4	2.0	2.4			2.1
<i>M28_Spy1059</i>	<i>M28_Spy1059</i>	1.6	1.6	1.5			
<i>M28_Spy1067</i>	<i>pmuC</i>	1.9	1.7	1.6			
<i>M28_Spy1068</i>	<i>M28_Spy1068</i>	1.6					
<i>M28_Spy1069</i>	<i>obg</i>			1.5			
<i>M28_Spy1076</i>	<i>M28_Spy1076</i>						1.5
<i>M28_Spy1098</i>	<i>grab</i>	-2.4	-2.0	-1.9			-2.7
<i>M28_Spy1099</i>	<i>murZ</i>			1.6			
<i>M28_Spy1101</i>	<i>inlA</i>	2.2	2.3	1.6			2.0
<i>M28_Spy1109</i>	<i>udk</i>			2.0			
<i>M28_Spy1111</i>	<i>M28_Spy1111</i>	1.7	1.5	1.6			1.6
<i>M28_Spy1115</i>	<i>nrdH</i>			2.0			
<i>M28_Spy1116</i>	<i>nrdE.2</i>			1.7			
<i>M28_Spy1127</i>	<i>surA</i>						1.5
<i>M28_Spy1128</i>	<i>M28_Spy1128</i>			1.9			
<i>M28_Spy1130</i>	<i>pepB</i>	1.5					
<i>M28_Spy1131</i>	<i>M28_Spy1131</i>	1.8					
<i>M28_Spy1139</i>	<i>sodA</i>	-2.1	-1.8	-1.8			-1.5
<i>M28_Spy1144</i>	<i>M28_Spy1144</i>			1.7			
<i>M28_Spy1148</i>	<i>deaD</i>			1.9			
<i>M28_Spy1149</i>	<i>prfC</i>			1.5			
<i>M28_Spy1151</i>	<i>murF</i>			1.6			
<i>M28_Spy1152</i>	<i>ddlA</i>			1.7			
<i>M28_Spy1153</i>	<i>recR</i>			1.6			
<i>M28_Spy1154</i>	<i>M28_Spy1154</i>			1.5			
<i>M28_Spy1173</i>	<i>folD</i>			1.5			
<i>M28_Spy1179</i>	<i>clpE</i>	-2.1	-2.2	-2.1			-1.8
<i>M28_Spy1198</i>	<i>dpr</i>	-1.6					

Table B-9 Continued.

Strain		$\Delta rocA$	RocA VNTR + H60Y	RocA P97L	RocA G184W	RocA R258K	RocA T442P
Locus Tag	Gene						
M28_Spy1200	M28_Spy1200			1.5			
M28_Spy1201	M28_Spy1201	1.5		1.6			
M28_Spy1216	M28_Spy1216	-1.7	-1.6	-1.7			
M28_Spy1289	cas2	1.6	1.6				1.7
M28_Spy1290	cas1	1.6	1.6				1.7
M28_Spy1291	cas4	1.6	1.6				1.7
M28_Spy1292	cas7		1.5				1.7
M28_Spy1293	cas8						1.8
M28_Spy1294	cas5						1.7
M28_Spy1295	cas3	1.7		1.6			1.7
M28_Spy1297	M28_Spy1297		-1.6				
M28_Spy1298	M28_Spy1298		-1.5				
M28_Spy1306	M28_Spy1306			-1.6			-1.8
M28_Spy1308	M28_Spy1308						-1.7
M28_Spy1309	M28_Spy1309				-1.6	-1.6	-1.8
M28_Spy1310	M28_Spy1310						-1.6
M28_Spy1311	M28_Spy1311						-1.6
M28_Spy1314	M28_Spy1314						-1.7
M28_Spy1316	M28_Spy1316						-2.0
M28_Spy1318	M28_Spy1318						-1.8
M28_Spy1321	M28_Spy1321						-1.7
M28_Spy1322	M28_Spy1322	-1.5		-1.7			-1.9
M28_Spy1323	M28_Spy1323			-1.5			-1.8
M28_Spy1324	M28_Spy1324						-1.6
M28_Spy1325	aspA						-1.5
M28_Spy1326	M28_Spy1326	-1.7	-1.6	-1.6			
M28_Spy1329	M28_Spy1329				1.6		
M28_Spy1333	M28_Spy1333	-1.5	-1.5				
M28_Spy1334	M28_Spy1334	-1.6	-1.6				-1.5
M28_Spy1336	M28_Spy1336	-2.7	-2.2	-2.6			-1.7
M28_Spy1338	M28_Spy1338	1.8		2.0			
M28_Spy1339	aroB	1.7		1.7			
M28_Spy1340	M28_Spy1340	1.8					
M28_Spy1359	rocA	-18.3	-1.7				
M28_Spy1366	M28_Spy1366	-1.6					
M28_Spy1368	comFA	2.3	1.9	1.9			1.7
M28_Spy1371	M28_Spy1371	-1.6		-1.6			
M28_Spy1372	M28_Spy1372	-1.5					
M28_Spy1393	M28_Spy1393		-1.5				
M28_Spy1394	M28_Spy1394			1.8			
M28_Spy1402	aapA	1.5		1.5			
M28_Spy1409	ftsL	1.9	1.6	2.1			
M28_Spy1410	mraW			1.7			
M28_Spy1411	M28_Spy1411			-1.5			
M28_Spy1412	M28_Spy1412			-1.5			
M28_Spy1413	proA	-1.5		-1.5			
M28_Spy1425	M28_Spy1425	-2.2	-2.0	-2.1			-1.9
M28_Spy1426	M28_Spy1426	-1.6		-1.7			
M28_Spy1427	glyS	-1.7	-1.5	-1.8			

Table B-9 Continued.

Strain		$\Delta rocA$	RocA VNTR + H60Y	RocA P97L	RocA G184W	RocA R258K	RocA T442P
Locus Tag	Gene						
<i>M28_Spy1428</i>	<i>glyQ</i>	-1.6	-1.5	-1.5			
<i>M28_Spy1430</i>	<i>M28_Spy1430</i>	-1.9		-2.1			
<i>M28_Spy1449</i>	<i>copY</i>						-1.9
<i>M28_Spy1450</i>	<i>sse</i>	1.6		1.5			
<i>M28_Spy1472</i>	<i>serS</i>	-2.8	-2.4	-2.2			-1.9
<i>M28_Spy1473</i>	<i>accD</i>	2.8	3.2	2.5			3.2
<i>M28_Spy1474</i>	<i>accA</i>	2.7	3.1	2.4			3.2
<i>M28_Spy1475</i>	<i>accC</i>	2.8	3.2	2.6			3.3
<i>M28_Spy1476</i>	<i>fabZ</i>	3.0	3.5	2.7			3.5
<i>M28_Spy1477</i>	<i>accB</i>	3.1	3.6	2.9			3.6
<i>M28_Spy1478</i>	<i>fabF</i>	3.2	3.6	2.9			3.5
<i>M28_Spy1479</i>	<i>fabG</i>	3.6	4.1	3.4			3.9
<i>M28_Spy1480</i>	<i>fabD</i>	3.7	4.0	3.5			3.7
<i>M28_Spy1481</i>	<i>fabK</i>	4.1	4.3	4.1			4.0
<i>M28_Spy1482</i>	<i>acpP.2</i>	2.8	3.3	3.0			2.9
<i>M28_Spy1483</i>	<i>fabH</i>	3.3	3.6	3.6			3.1
<i>M28_Spy1484</i>	<i>fabT</i>	3.4	3.5	3.7			3.1
<i>M28_Spy1485</i>	<i>phaB</i>	3.3	3.3	3.7			2.9
<i>M28_Spy1486</i>	<i>dnaJ</i>	-1.6	-1.8	-1.7			-1.9
<i>M28_Spy1487</i>	<i>dnaK</i>	-2.3	-2.6	-2.4			-2.9
<i>M28_Spy1488</i>	<i>grpE</i>	-2.3	-2.7	-2.5			-3.0
<i>M28_Spy1489</i>	<i>hrcA</i>	-2.7	-3.0	-2.8			-3.3
<i>M28_Spy1495</i>	<i>gatB</i>			-1.5			
<i>M28_Spy1501</i>	<i>codY</i>	-1.8	-1.8	-1.7			-1.7
<i>M28_Spy1503</i>	<i>M28_Spy1503</i>	-1.7					
<i>M28_Spy1506</i>	<i>M28_Spy1506</i>	1.6	1.5				
<i>M28_Spy1507</i>	<i>M28_Spy1507</i>	1.6	1.5				
<i>M28_Spy1514</i>	<i>M28_Spy1514</i>	1.8	1.5				
<i>M28_Spy1515</i>	<i>M28_Spy1515</i>	2.3	1.8				
<i>M28_Spy1516</i>	<i>fhuC</i>	2.1	1.7				
<i>M28_Spy1517</i>	<i>M28_Spy1517</i>	1.9	1.7				
<i>M28_Spy1518</i>	<i>M28_Spy1518</i>	1.7					
<i>M28_Spy1519</i>	<i>shp</i>	1.7	1.6				
<i>M28_Spy1521</i>	<i>isp2</i>	-1.9	-1.7	-1.8			-1.6
<i>M28_Spy1526</i>	<i>scrK</i>	-1.5	-1.6	-1.7			-1.8
<i>M28_Spy1537</i>	<i>uvrA</i>	-1.6		-1.6			
<i>M28_Spy1544</i>	<i>mutY</i>			1.5			
<i>M28_Spy1545</i>	<i>M28_Spy1545</i>	1.5		1.5			
<i>M28_Spy1546</i>	<i>M28_Spy1546</i>	1.5		1.5			1.5
<i>M28_Spy1555</i>	<i>M28_Spy1555</i>	-1.7	-1.5	-1.5			
<i>M28_Spy1562</i>	<i>M28_Spy1562</i>	-1.6					-1.6
<i>M28_Spy1571</i>	<i>M28_Spy1571</i>		-1.5				
<i>M28_Spy1580</i>	<i>udp</i>			-1.7			
<i>M28_Spy1582</i>	<i>rpsN2</i>	1.6	1.5	1.5			1.5
<i>M28_Spy1588</i>	<i>glnA</i>	1.9	1.8	1.8			
<i>M28_Spy1589</i>	<i>M28_Spy1589</i>	2.0	1.8	1.8			1.6
<i>M28_Spy1591</i>	<i>pgk</i>	-1.6					
<i>M28_Spy1596</i>	<i>rpmB</i>	1.6	1.5	1.8			
<i>M28_Spy1599</i>	<i>pyrG</i>	1.8	1.6	1.7			

Table B-9 Continued.

Strain		$\Delta rocA$	RocA VNTR + H60Y	RocA P97L	RocA G184W	RocA R258K	RocA T442P
Locus Tag	Gene						
<i>M28_Spy1609</i>	<i>M28_Spy1609</i>	1.6		1.6			
<i>M28_Spy1611</i>	<i>hsdS</i>			-1.5			
<i>M28_Spy1635</i>	<i>rplM</i>			1.8			
<i>M28_Spy1636</i>	<i>M28_Spy1636</i>	2.0	1.9				1.7
<i>M28_Spy1637</i>	<i>M28_Spy1637</i>	2.0	2.0	1.7			1.8
<i>M28_Spy1641</i>	<i>M28_Spy1641</i>		1.5				
<i>M28_Spy1642</i>	<i>M28_Spy1642</i>		1.6				1.5
<i>M28_Spy1643</i>	<i>cysS</i>	1.5	1.6				1.5
<i>M28_Spy1644</i>	<i>M28_Spy1644</i>	1.6	1.6				1.5
<i>M28_Spy1647</i>	<i>M28_Spy1647</i>	1.5	1.5				
<i>M28_Spy1648</i>	<i>M28_Spy1648</i>	1.5					
<i>M28_Spy1666</i>	<i>M28_Spy1666</i>						-1.6
<i>M28_Spy1669</i>	<i>dexB</i>			-1.9			
<i>M28_Spy1670</i>	<i>msmK</i>	-1.9	-1.9	-1.9			-1.7
<i>M28_Spy1672</i>	<i>ska</i>	-2.8	-2.5	-2.5			-7.8
<i>M28_Spy1673</i>	<i>M28_Spy1673</i>	-1.6	-1.5	-1.7			-1.5
<i>M28_Spy1675</i>	<i>sclA</i>	4.6	4.6	2.6			4.1
<i>M28_Spy1679</i>	<i>M28_Spy1679</i>	-1.7	-2.0	-1.8			-1.8
<i>M28_Spy1680</i>	<i>M28_Spy1680</i>	-1.9	-2.1	-2.0			-1.9
<i>M28_Spy1681</i>	<i>M28_Spy1681</i>	-2.0	-2.0	-2.0			-1.9
<i>M28_Spy1689</i>	<i>dppA</i>	1.6	1.7				1.6
<i>M28_Spy1690</i>	<i>dppB</i>	1.9	2.0	1.5			1.6
<i>M28_Spy1691</i>	<i>dppC</i>	2.0	2.0	1.5			1.6
<i>M28_Spy1692</i>	<i>dppD</i>	2.1	2.1	1.5			1.7
<i>M28_Spy1693</i>	<i>dppE</i>	2.0	2.0				1.6
<i>M28_Spy1695</i>	<i>htpA</i>	1.9	1.8	1.5			1.5
<i>M28_Spy1696</i>	<i>lmb</i>	1.5					
<i>M28_Spy1699</i>	<i>fba</i>	1.5	1.5				
<i>M28_Spy1700</i>	<i>scpA</i>	2.0	1.8	1.5	-1.6		
<i>M28_Spy1702</i>	<i>emm</i>	4.3	4.1	3.1	-1.5		3.9
<i>M28_Spy1703</i>	<i>mrp</i>	1.5		1.6			2.1
<i>M28_Spy1704</i>	<i>mga</i>	1.7		1.8			
<i>M28_Spy1711</i>	<i>M28_Spy1711</i>				1.8		
<i>M28_Spy1712</i>	<i>M28_Spy1712</i>				1.7	1.5	
<i>M28_Spy1713</i>	<i>M28_Spy1713</i>				1.6	1.5	
<i>M28_Spy1715</i>	<i>sfbX</i>	2.2	2.1				1.8
<i>M28_Spy1716</i>	<i>sof</i>	1.9	1.8				1.7
<i>M28_Spy1718</i>	<i>prsA</i>	-5.6	-4.3	-3.5			-3.4
<i>M28_Spy1719</i>	<i>M28_Spy1719</i>	-5.5	-4.0	-3.2			-3.0
<i>M28_Spy1720</i>	<i>spi</i>	-5.2	-3.6	-2.9			-2.9
<i>M28_Spy1721</i>	<i>speB</i>	-5.3	-3.9	-3.0			-2.9
<i>M28_Spy1722</i>	<i>M28_Spy1722</i>	-5.6	-3.9	-3.2			-2.9
<i>M28_Spy1723</i>	<i>M28_Spy1723</i>	-5.5	-3.9	-3.1			-2.8
<i>M28_Spy1724</i>	<i>ropB</i>	-1.5					
<i>M28_Spy1725</i>	<i>mf</i>	2.1	2.1	1.9			1.8
<i>M28_Spy1727</i>	<i>M28_Spy1727</i>	-1.6	-1.6	-1.6			
<i>M28_Spy1734</i>	<i>M28_Spy1734</i>						-1.5
<i>M28_Spy1735</i>	<i>M28_Spy1735</i>						-1.5
<i>M28_Spy1739</i>	<i>pbp2A</i>	-1.5	-1.5	-1.5			

Table B-9 Continued.

Strain		$\Delta rocA$	RocA VNTR + H60Y	RocA P97L	RocA G184W	RocA R258K	RocA T442P
Locus Tag	Gene						
<i>M28_Spy1740</i>	<i>M28_Spy1740</i>	-1.5	-1.5	-1.5			
<i>M28_Spy1747</i>	<i>groEL</i>	-3.2	-3.2	-3.6			-3.5
<i>M28_Spy1748</i>	<i>groES</i>	-4.0	-3.7	-4.1			-3.6
<i>M28_Spy1749</i>	<i>clpC</i>	-2.3	-2.2	-2.4			-2.0
<i>M28_Spy1750</i>	<i>ctsR</i>		-1.8				
<i>M28_Spy1751</i>	<i>csp</i>	-2.2	-2.0	-1.8			-1.9
<i>M28_Spy1755</i>	<i>hutU</i>	1.9					
<i>M28_Spy1756</i>	<i>M28_Spy1756</i>	2.0					
<i>M28_Spy1758</i>	<i>fhs.2</i>	1.9	1.6				
<i>M28_Spy1759</i>	<i>M28_Spy1759</i>	1.9					
<i>M28_Spy1760</i>	<i>M28_Spy1760</i>	1.9					
<i>M28_Spy1761</i>	<i>hutH</i>	1.8	1.7				
<i>M28_Spy1776</i>	<i>M28_Spy1776</i>						-1.7
<i>M28_Spy1784</i>	<i>cinA</i>	-1.5					
<i>M28_Spy1785</i>	<i>tag</i>			-1.6			-1.5
<i>M28_Spy1786</i>	<i>ruvA</i>			-1.6			-1.5
<i>M28_Spy1787</i>	<i>lmrP</i>			-1.7			-1.5
<i>M28_Spy1788</i>	<i>mutL</i>			-1.6			-1.5
<i>M28_Spy1797</i>	<i>M28_Spy1797</i>						-1.7
<i>M28_Spy1799</i>	<i>M28_Spy1799</i>						-1.7
<i>M28_Spy1823</i>	<i>hisS</i>	-1.6	-1.5	-1.5			
<i>M28_Spy1829</i>	<i>M28_Spy1829</i>			-1.5			
<i>M28_Spy1838</i>	<i>M28_Spy1838</i>			-1.5			-1.7
<i>M28_Spy1840</i>	<i>M28_Spy1840</i>	-1.6	-1.8	-1.8			-1.8
<i>M28_Spy1841</i>	<i>M28_Spy1841</i>	-1.6	-1.8	-1.8			-1.8
<i>M28_Spy1848</i>	<i>M28_Spy1848</i>			-1.9			
<i>M28_Spy1849</i>	<i>M28_Spy1849</i>	-2.3		-2.4			
<i>M28_Spy1860</i>	<i>M28_Spy1860</i>			-1.9			
<i>M28_Spy1861</i>	<i>M28_Spy1861</i>			-1.6			
<i>M28_Spy1870</i>	<i>gidA</i>	1.8	1.7	1.6			1.7
<i>M28_Spy1871</i>	<i>M28_Spy1871</i>	1.8	1.8	1.7			1.7
<i>M28_Spy1872</i>	<i>trmU</i>	1.7	1.7	1.6			1.7
<i>M28_Spy1881</i>	<i>M28_Spy1881</i>	1.5		1.6			1.5
<i>M28_Spy1882</i>	<i>M28_Spy1882</i>	1.5		1.8			
<i>M28_Spy1884</i>	<i>hasA</i>	6.5	5.6	3.2			3.1
<i>M28_Spy1885</i>	<i>hasB</i>	7.5	6.5	3.6			3.7
<i>M28_Spy1886</i>	<i>hasC</i>	4.2	3.6	2.2			2.2
<i>M28_Spy1897</i>	<i>M28_Spy1897</i>	-1.7	-1.8	-1.7			-1.7
<i>M28_Spy1898</i>	<i>htrA</i>	-1.8	-1.8	-1.7			-1.8

Table B-10 Differential expression of proven virulence factor genes.

Strain		$\Delta rocA$	RocA VNTR + H60Y	RocA P97L	RocA G184W	RocA R258K	RocA T442P
Locus Tag	Gene						
<i>M28_Spy0137</i>	<i>nga</i>	2.5/6.1	2.5/5.9	2.5/4.1	-2.5/NS	NS/NS	2.3/5.1
<i>M28_Spy0139</i>	<i>slo</i>	2.4/4.8	2.4/4.9	2.4/3.1	-2.6/NS	NS/NS	2.2/4.0
<i>M28_Spy0329</i>	<i>spyCEP</i>	11.2/NS	11.5/NS	9.5/NS	-2.4/NS	NS/NS	10.7/NS
<i>M28_Spy0649</i>	<i>mac</i>	23.5/2.1	25.7/1.9	14.1/NS	NS/NS	NS/NS	18.4/NS
<i>M28_Spy1450</i>	<i>sse</i>	2.0/1.6	1.8/NS	2.1/1.5	-1.6/NS	NS/NS	1.7/NS
<i>M28_Spy1672</i>	<i>ska</i>	NS/-2.8	NS/-2.5	NS/-2.5	NS/NS	NS/NS	-2.4/-7.8
<i>M28_Spy1675</i>	<i>sclA</i>	6.1/4.6	6.2/4.6	5.6/2.6	-2.6/NS	NS/NS	6.3/4.5
<i>M28_Spy1699</i>	<i>fba</i>	2.4/1.5	2.5/1.5	2.4/NS	-1.8/NS	NS/NS	2.3/NS
<i>M28_Spy1700</i>	<i>scpA</i>	2.5/2.0	2.6/1.8	2.5/1.5	-1.8/-1.6	NS/NS	2.4/NS
<i>M28_Spy1701</i>	<i>enn</i>	NS/NS	NS/NS	NS/NS	-1.7/NS	NS/NS	NS/NS
<i>M28_Spy1702</i>	<i>emm</i>	1.7/4.3	1.6/4.1	1.8/3.1	-1.8/-1.5	NS/NS	1.6/3.9
<i>M28_Spy1703</i>	<i>mrp</i>	NS/1.5	NS/NS	NS/1.6	NS/NS	NS/NS	2.3/2.1
<i>M28_Spy1715</i>	<i>sfbX</i>	1.5/2.2	1.5/2.1	1.5/NS	NS/NS	NS/NS	1.5/1.8
<i>M28_Spy1716</i>	<i>sof</i>	1.7/1.9	1.7/1.8	1.7/NS	NS/NS	NS/NS	1.7/1.7
<i>M28_Spy1721</i>	<i>speB</i>	-1.6/-5.3	NS/-3.9	-1.7/-3.0	NS/NS	NS/NS	NS/-2.9

Data are shown fold change compared to the parental wild-type strain at mid-exponential (ME) and early-stationary (ES) growth phases, ME/ES. NS, the gene did not reach statistical significance.

Table B-11 RNA-seq analysis at the mid-exponential (ME) and early-stationary (ES) growth phases of isogenic P97L mutant strain compared to the isogenic $\Delta rocA$, VNTR + H60Y, and T442P mutant strains.

Growth Phase	Locus Tag	Gene	Fold Change
ME	<i>M28_Spy0647</i>	<i>M28_Spy0647</i>	-1.8
ME	<i>M28_Spy0649</i>	<i>mac</i>	-1.8
ME	<i>M28_Spy1718</i>	<i>prsA</i>	-1.5
ES	<i>M28_Spy0139</i>	<i>slo</i>	-1.5
ES	<i>M28_Spy0141</i>	<i>M28_Spy0141</i>	-1.7
ES	<i>M28_Spy0832</i>	<i>xpt</i>	2.6
ES	<i>M28_Spy0833</i>	<i>M28_Spy0833</i>	2.4
ES	<i>M28_Spy0973</i>	<i>M28_Spy0973</i>	-1.5
ES	<i>M28_Spy0989</i>	<i>M28_Spy0989</i>	-1.7
ES	<i>M28_Spy1675</i>	<i>sclA</i>	-1.7

Table B-12 Comparison of genes differentially regulated by RocA and RocA polymorphism mutants and genes identified as important for fitness in transposon mutagenesis studies. Included as a separate file (Table B-12.xlsx).

Table B-13 List of strains and plasmids used in this study.

Strain or Plasmid	Use/Description	Ref
Strains		
<i>E. coli</i>		
DH5 α	Cloning and protein fusion membrane topology studies	(94)
DHM1	Bacterial adenylate cyclase-based two hybrid (BACTH) studies	Euromedex
BTH101	Bacterial adenylate cyclase-based two hybrid (BACTH) studies	Euromedex
<i>S. pyogenes</i>		
MGAS28426	Serotype M28 parental wild-type strain	(57)
Δ rocA	MGAS28426 with deletion of the entire rocA gene	(57)
RocA P97L	MGAS28426 in which the rocA allele has been replaced with an allele with a P97L substitution	(25)
RocA G184W	MGAS28426 in which the rocA allele has been replaced with an allele with a G184W substitution	(25)
RocA R258K	MGAS28426 in which the rocA allele has been replaced with an allele with a R258K substitution	(25)
RocA V420I	MGAS28426 in which the rocA allele has been replaced with an allele with a V420I substitution	This study
RocA T442I	MGAS28426 in which the rocA allele has been replaced with an allele with a T442I substitution	This study
RocA T442P	MGAS28426 in which the rocA allele has been replaced with an allele with a T442P substitution	(25)
RocA Q443*	MGAS28426 in which the rocA allele has been replaced with an allele that has a stop codon at codon 443	This study
Plasmids		
pKTop	Protein fusion membrane topology vector expressing dual reporter PhoA ₂₂₋₄₇₂ /LacZ ₄₋₆₀ , p15A ori; kanamycin resistance	(77)
pKTop-RocA-K24	pKTop derivative expressing RocA ₁₋₂₄ /PhoA ₂₂₋₄₇₂ /LacZ ₄₋₆₀	This study
pKTop-RocA-L34	pKTop derivative expressing RocA ₁₋₃₄ /PhoA ₂₂₋₄₇₂ /LacZ ₄₋₆₀	This study
pKTop-RocA-L44	pKTop derivative expressing RocA ₁₋₄₄ /PhoA ₂₂₋₄₇₂ /LacZ ₄₋₆₀	This study
pKTop-RocA-H60	pKTop derivative expressing RocA ₁₋₆₀ /PhoA ₂₂₋₄₇₂ /LacZ ₄₋₆₀	This study
pKTop-RocA-K88	pKTop derivative expressing RocA ₁₋₈₈ /PhoA ₂₂₋₄₇₂ /LacZ ₄₋₆₀	This study
pKTop-RocA-S121	pKTop derivative expressing RocA ₁₋₁₂₁ /PhoA ₂₂₋₄₇₂ /LacZ ₄₋₆₀	This study
pKTop-RocA-Q160	pKTop derivative expressing RocA ₁₋₁₆₀ /PhoA ₂₂₋₄₇₂ /LacZ ₄₋₆₀	This study
pKTop-RocA-C181	pKTop derivative expressing RocA ₁₋₁₈₁ /PhoA ₂₂₋₄₇₂ /LacZ ₄₋₆₀	This study
pKTop-RocA-L192	pKTop derivative expressing RocA ₁₋₁₉₂ /PhoA ₂₂₋₄₇₂ /LacZ ₄₋₆₀	This study
pKTop-RocA-R201	pKTop derivative expressing RocA ₁₋₂₀₁ /PhoA ₂₂₋₄₇₂ /LacZ ₄₋₆₀	This study
pKTop-RocA-Q225	pKTop derivative expressing RocA ₁₋₂₂₅ /PhoA ₂₂₋₄₇₂ /LacZ ₄₋₆₀	This study
pKTop-RocA-A360	pKTop derivative expressing RocA ₁₋₃₆₀ /PhoA ₂₂₋₄₇₂ /LacZ ₄₋₆₀	This study
pKTop-RocA-D451	pKTop derivative expressing RocA ₁₋₄₅₁ /PhoA ₂₂₋₄₇₂ /LacZ ₄₋₆₀	This study
pKNT25	BACTH vector designed to express T25 fused to the C-terminus of an inserted polypeptide; p15A ori; kanamycin resistance	Euromedex
pKNT25-CovR	pKNT25 derivative expressing CovR fused to T25	This study
pKNT25-CovS	pKNT25 derivative expressing CovS fused to T25	This study
pKNT25-RocA	pKNT25 derivative expressing RocA fused to T25	This study
pKNT25-RocA-P97L	pKNT25 derivative expressing RocA with a P97L substitution fused to T25	This study
pKNT25-RocA-G184W	pKNT25 derivative expressing RocA with a G184W substitution fused to T25	This study
pKNT25-RocA-R258K	pKNT25 derivative expressing RocA with a R258K substitution fused to T25	This study
pKNT25-RocA-V420I	pKNT25 derivative expressing RocA with a V420I substitution fused to T25	This study
pKNT25-RocA-T442I	pKNT25 derivative expressing RocA with a T442I substitution fused to T25	This study
pKNT25-RocA-T442P	pKNT25 derivative expressing RocA with a T442P substitution fused to T25	This study
pKNT25-RocA-Q443*	pKNT25 derivative expressing the first 442 amino acids of RocA fused to T25	This study
pKT25	BACTH vector designed to express T25 fused to the N-terminus of an inserted polypeptide; p15A ori; kanamycin resistance	Euromedex
pKT25-CovR	pKT25 derivative expressing CovR fused to T25	This study
pKT25-CovS	pKT25 derivative expressing CovS fused to T25	This study
pKT25-RocA	pKT25 derivative expressing RocA fused to T25	This study
pKT25-zip	pKT25 derivative expressing leucine zipper of GCN4 fused to T25	Euromedex
pUT18	BACTH vector designed to express T18 fused to the C-terminus of an inserted polypeptide; ColE1 ori; ampicillin resistance	Euromedex
pUT18-CovR	pUT18 derivative expressing CovR fused to T18	This study
pUT18-CovS	pUT18 derivative expressing CovS fused to T18	This study
pUT18-RocA	pUT18 derivative expressing RocA fused to T18	This study
pUT18-RocA-P97L	pUT18 derivative expressing RocA with a P97L substitution fused to T18	This study
pUT18-RocA-G184W	pUT18 derivative expressing RocA with a G184W substitution fused to T18	This study
pUT18-RocA-R258K	pUT18 derivative expressing RocA with a R258K substitution fused to T18	This study
pUT18-RocA-V420I	pUT18 derivative expressing RocA with a V420I substitution fused to T18	This study
pUT18-RocA-T442I	pUT18 derivative expressing RocA with a T442I substitution fused to T18	This study
pUT18-RocA-T442P	pUT18 derivative expressing RocA with a T442P substitution fused to T18	This study
pUT18-RocA-Q443*	pUT18 derivative expressing the first 442 amino acids of RocA fused to T18	This study

Table B-13 Continued.

Strain or Plasmid	Use/Description	Ref
Plasmids		
pUT18C	BACTH vector designed to express T18 fused to the N-terminus of an inserted polypeptide; ColE1 ori; ampicillin resistance	Euromedex
pUT18C-CovR	pUT18C derivative expressing CovR fused to T18	This study
pUT18C-CovS	pUT18C derivative expressing CovS fused to T18	This study
pUT18C-RocA	pUT18C derivative expressing RocA fused to T18	This study
pUT18C-zip	pKT18C derivative expressing leucine zipper of GCN4 fused to T18	Euromedex
pDC123-RocA	pDC123 in which PhoA has been replaced with RocA and its native promoter	This study
pDC123-RocA-FLAG	pDC123 in which PhoA has been replaced with RocA with a C-terminal FLAG-tag and its native promoter	This study
pDC123-RocA-E3C-FLAG	pDC123 in which PhoA has been replaced with RocA with a E3C substitution and a C-terminal FLAG-tag and its native promoter	This study
pDC123-RocA-L34C-FLAG	pDC123 in which PhoA has been replaced with RocA with a L34C substitution and a C-terminal FLAG-tag and its native promoter	This study
pDC123-RocA-H60C-FLAG	pDC123 in which PhoA has been replaced with RocA with a H60C substitution and a C-terminal FLAG-tag and its native promoter	This study
pDC123-RocA-K88C-FLAG	pDC123 in which PhoA has been replaced with RocA with a K88C substitution and a C-terminal FLAG-tag and its native promoter	This study
pDC123-RocA-S121C-FLAG	pDC123 in which PhoA has been replaced with RocA with a S121C substitution and a C-terminal FLAG-tag and its native promoter	This study
pDC123-RocA-Q160C-FLAG	pDC123 in which PhoA has been replaced with RocA with a Q160C substitution and a C-terminal FLAG-tag and its native promoter	This study
pDC123-RocA-L192C-FLAG	pDC123 in which PhoA has been replaced with RocA with a L192C substitution and a C-terminal FLAG-tag and its native promoter	This study
pDC123-RocA-Q225C-FLAG	pDC123 in which PhoA has been replaced with RocA with a Q225C substitution and a C-terminal FLAG-tag and its native promoter	This study

Table B-14 List of primers used in this study.

Name	Sequence (5' to 3')	Use	Ref
pDC123-fwd1	TGACAAATGATCAGAACTTAAGGCGATTAAG	pDC123-RocA-FLAG plasmid construction	This study
pDC123-fwd2	GCGTACTGATCAGAACTTAAGGCGATTAAG	pDC123-RocA plasmid construction	This study
pDC123-rev	TGCCACTCAATTATAAAAGCCAGTCATTAGG	pDC123 plasmid construction	This study
RocA-FLAG-fwd	GCTTTTATAATTGAGTGGCAATAACAAC	pDC123 plasmid construction	This study
RocA-FLAG-rev1	TAAGTTCGTATCATTTGTATCGTCGTC	pDC123-RocA-FLAG plasmid construction	This study
RocA-FLAG-rev2	TAAGTTCGTATCAGTCAGGCTTAGCTATT	pDC123-RocA plasmid construction	This study
FLAGRocA-F	TTGAGTGGCAATAACAACACTCAAG	RocA-FLAG flanking primer	This study
FLAGRocA-R	TCATTTGTCATCGTCGTCCTTGTAGTCGTCAGGCTTAGCTATTCTATTAAGT	RocA-FLAG flanking primer	This study
RocA-E3C-F	GAAGGATAAATGTTATGTGATTTCTTC	pDC123-RocA-E3C-FLAG plasmid construction	This study
RocA-E3C-R	GAAGAAAATCACATAACATTTATCCTTC	pDC123-RocA-E3C-FLAG plasmid construction	This study
RocA-L34C-F	CAATTCCGTGTCGCTGAAAAAT	pDC123-RocA-L34C-FLAG plasmid construction	This study
RocA-L34C-R	ATTTTTCAGGCGACACGGAATTG	pDC123-RocA-L34C-FLAG plasmid construction	This study
RocA-H60C-F	CTTTCAGACTGTTTCATTTCTTG	pDC123-RocA-H60C-FLAG plasmid construction	This study
RocA-H60C-R	CAAGAATGAAACAGTCTGGAAG	pDC123-RocA-H60C-FLAG plasmid construction	This study
RocA-K88C-F	GGTAAATCAATAAAAGCTTGTTTTTTAATG	pDC123-RocA-K88C-FLAG plasmid construction	This study
RocA-K88C-R	CATTAATAAACCAAGCTTTTATTGATTACC	pDC123-RocA-K88C-FLAG plasmid construction	This study
RocA-S121C-F	GGTATGCCTTATTGTGTTGTTAAAC	pDC123-RocA-S121C-FLAG plasmid construction	This study
RocA-S121C-R	GTTTAAACAACAATAAAGGCATACC	pDC123-RocA-S121C-FLAG plasmid construction	This study
RocA-Q160C-F	CGCCAATATTTTTGTTACACATAGAG	pDC123-RocA-Q160C-FLAG plasmid construction	This study
pKTop1	TCAGCGGTGTTGGC	pKTop plasmid sequencing	This study

Table B-14 Continued.

Name	Sequence (5' to 3')	Use	Ref
RocA-Q160C-R	CTCTATGTGAACAAAAATATTGGCG	pDC123-RocA-Q160C-FLAG plasmid construction	This study
RocA-L192C-F	CGCCTTCTTGTTCAGGACTTG	pDC123-RocA-L192C-FLAG plasmid construction	This study
RocA-L192C-R	CAAGTCCTGAACAAGAAGGCG	pDC123-RocA-L192C-FLAG plasmid construction	This study
RocA-Q225C-F	GGGTTATGTAAAAATGAACCTCTATTG	pDC123-RocA-Q225C-FLAG plasmid construction	This study
RocA-Q225C-R	CAATAGAGTTACATTTTACATAACGC	pDC123-RocA-Q225C-FLAG plasmid construction	This study
rocA-VNTR-seq	CTGTTAGAATGACAGAAGCTTATGATA	RocA-FLAG plasmid sequencing	(53)
rocA-P97L-seq	GCTCTATGTGATTGAAAATATTGGCGCCAGG	RocA-FLAG and pKTop plasmid sequencing	(25)
rocA-seq1	TTTGCTACACCGGCTTTGA	BACTH, RocA-FLAG, and pKTop plasmid sequencing	This study
rocA-seq2	TCTGCGAGCTAATTGTGAGATAG	RocA-FLAG and pKTop plasmid sequencing	This study
rocA-seq3	CTTTGAATGACTATGACAAGTTTATGGTTTTG	RocA-FLAG plasmid sequencing	This study
Flag-seq	CAATAGCTTGACATAGTAGGGATG	RocA-FLAG plasmid sequencing	This study
pKTop-RocA-fwd	GGCTGCAGGTCGACTCTAGAGGATCCCATGTTAGAAGATTTCTTCAATTTTAGGA	pKTop-, pKNT25-, and pUT18-RocA plasmid construction	This study
pKTop-K24	GGGCCGAGCTCGGTACCCGGGGATCCTTTAACGTTAACATAATTTCAAT	pKTop-RocA-K24 plasmid construction	This study
pKTop-L34	GGGCCGAGCTCGGTACCCGGGGATCAAGCGAATTGCACTTACA	pKTop-RocA-L34 plasmid construction	This study
pKTop-L44	GGGCCGAGCTCGGTACCCGGGGATCAAGTGATAAATAAAAAATATTTTTTCAGG	pKTop-RocA-L44 plasmid construction	This study
pKTop-H60	GGGCCGAGCTCGGTACCCGGGGATCATGGTCTGGAAAGAAAGCC	pKTop-RocA-H60 plasmid construction	This study
pKTop-K88	GGGCCGAGCTCGGTACCCGGGGATCCTTAGCTTTTATTGATTTACCATAGTATAGG	pKTop-RocA-K88 plasmid construction	This study
pKTop-S121	GGGCCGAGCTCGGTACCCGGGGATCTGAATAAGGCATACCAACAATGG	pKTop-RocA-S121 plasmid construction	This study
pKTop-Q160	GGGCCGAGCTCGGTACCCGGGGATCTTGAATAATTTGGCGCCAGG	pKTop-RocA-Q160 plasmid construction	This study
pKTop-C181	GGGCCGAGCTCGGTACCCGGGGATCACACAAGTAATATAGAGCC	pKTop-RocA-C181 plasmid construction	This study
pKTop-L192	GGGCCGAGCTCGGTACCCGGGGATCTAAAGAAGCGCATCACATC	pKTop-RocA-L192 plasmid construction	This study
pKTop-R201	GGGCCGAGCTCGGTACCCGGGGATCAGCAGCAGTCGTT	pKTop-RocA-R201 plasmid construction	This study
pKTop-Q225	GGGCCGAGCTCGGTACCCGGGGATCTTGTTTTACATAACGCTC	pKTop-RocA-Q225 plasmid construction	This study
pKTop-A360	GGGCCGAGCTCGGTACCCGGGGATCAGCATTATCTAACAAAAATGACAAATAGC	pKTop-RocA-A360 plasmid construction	This study
pKTop-D451	GGGCCGAGCTCGGTACCCGGGGATCGTCAGGCTTAGCTATTCTATTAAGTC	pKTop-RocA-D451 plasmid construction	This study
M13-fwd	GTAACACGACGCCAGT	BACTH and pKTop plasmid sequencing	This study
M13-rev	CAGGAAACAGCTATGAC	BACTH and pKTop plasmid sequencing	This study
pKTop1	TCAGCGGGTGTGGC	pKTop plasmid sequencing	This study
pKTop2	CAACCGGTGTCAAAACCT	pKTop plasmid sequencing	This study
pKTop3	CTGCCTCACTGAATTCGG	pKTop plasmid sequencing	This study
pKTop4	TCTCGCCAATTTGCCAC	pKTop plasmid sequencing	This study
pKTop6	GGTAAGCGGTAAGGCATCTATAC	pKTop plasmid sequencing	This study
rocA-H60Y-seq	AACCAACTAATAGACACTAGTGGAAAAAGGC	BACTH and pKTop plasmid sequencing	(25)
rocA-R258K-seq	CTAAACAAGTTAAATCAAGTCTGTCATCTTTAGC	BACTH and pKTop plasmid sequencing	(25)
pKNT25-CovR-fwd	GGCTGCAGGTCGACTCTAGAGGATCCCATGACAAAGAAAATTTAATTATTGAAGATGAAAAG	pKNT25- and pUT18-CovR plasmid construction	This study
pKNT25-CovR-rev	AATTCGAGCTCGGTACCCGGGGATCTTCTCACGAATAACGTATCCC	pKNT25-, pUT18-, and pUT18C-CovR plasmid construction	This study
pKNT25-CovS-fwd	GGCTGCAGGTCGACTCTAGAGGATCCCATGGAAAATCAGAAACAAAACAGGAG	pKNT25- and pUT18-CovS plasmid construction	This study

Table B-14 Continued.

Name	Sequence (5' to 3')	Use	Ref
pKNT25-CovS-rev	AATTCGAGCTCGGTACCCGGGGATCACTCTCTTTAGACTGGGCC	pKNT25-, pUT18-, and pUT18C-CovS plasmid construction	This study
pKNT25-RocA-rev	AATTCGAGCTCGGTACCCGGGGATCGTCAGGCTTAGCTATTTCTATTAAGT	pKNT25-, pUT18-, and pUT18C-RocA plasmid construction	This study
pKNT25-Q443-rev	AATTCGAGCTCGGTACCCGGGGATCGTTAAAAATGCCATCATGAATCTG	pKNT25- and pUT18-RocA-Q443* plasmid construction	This study
pKT25-CovR-fwd	GCTGCAGGGTCGACTCTAGAGGATCCCATGACAAAAGAAAATTTAATTATTGAAGATGAAAAG	pKT25-CovR plasmid construction	This study
pKT25-CovR-rev	TTACTTACTTAGGTACCCGGGGATCTTCTCACGAATAACGTATCCC	pKT25-CovR plasmid construction	This study
pKT25-CovS-fwd	GCTGCAGGGTCGACTCTAGAGGATCCCATGAAAATCAGAAAACAAAACAGAAG	pKT25-CovS plasmid construction	This study
pKT25-CovS-rev	TTACTTACTTAGGTACCCGGGGATCACTCTCTTTAGACTGGGCC	pKT25-CovS plasmid construction	This study
pKT25-RocA-fwd	GCTGCAGGGTCGACTCTAGAGGATCCCATGTTAGAAGATTTTCTTCAATTTTAGGA	pKT25-RocA plasmid construction	This study
pKT25-RocA-rev	TTACTTACTTAGGTACCCGGGGATCGTCAGGCTTAGCTATTTCTATTAAGT	pKT25-RocA plasmid construction	This study
pUT18C-CovR-fwd	CACTGCAGGGTCGACTCTAGAGGATCCCATGACAAAAGAAAATTTAATTATTGAAGATGAAAAG	pUT18C-CovR plasmid construction	This study
pUT18C-CovS-fwd	CACTGCAGGGTCGACTCTAGAGGATCCCATGAAAATCAGAAAACAAAACAGAAG	pUT18C-CovS plasmid construction	This study
pUT18C-RocA-fwd	CACTGCAGGGTCGACTCTAGAGGATCCCATGTTAGAAGATTTTCTTCAATTTTAGGA	pUT18C-RocA plasmid construction	This study
pKTop5	AGTGAGCGCAACGC	BACTH plasmid sequencing	This study
pKNT25-seq	TCGGGGCTGGCTTAAC	BACTH plasmid sequencing	This study
T25-seq1	GCCTGGCCGATGG	BACTH plasmid sequencing	This study
T25-seq2	GTGGAATGGGGTTGAC	BACTH plasmid sequencing	This study
T18-seq1	TCGGTGCCCACTGC	BACTH plasmid sequencing	This study
T18-seq2	ACTGAGCAGAACAACTCTTTC	BACTH plasmid sequencing	This study
covR-seq1	GATGACTGCGCGTGATTCTA	BACTH plasmid sequencing	This study
covR-seq2	ACGGGCAAGTAGTTCTTCAAT	BACTH plasmid sequencing	This study
covS-seq1	GGTCTCTTACAACGTTGGG	BACTH plasmid sequencing	This study
covS-seq2	GGGATTGGCTTGTCTATTCTC	BACTH plasmid sequencing	This study
covS-seq3	GCGTGGATCCGTCCTCAAATGAGCCTTGTACGCG	BACTH plasmid sequencing	This study
covS-seq4	GAAAGGGCAGTCGAGTCATTAG	BACTH plasmid sequencing	This study
covS-seq5	GCCAGGAGATGATCTTCTCGTTAT	BACTH plasmid sequencing	This study
rocA-T442P-1	GCGTGGATCCGGACTCTCCCAATCTTTCCAAGTCA	Construction of isogenic C-terminal <i>rocA</i> polymorphism strains; BamHI site underlined	(25)
rocA-T442P-2	GCGTGGATCCCAATATAGAAAAGTTACTTAATCAAG	Construction of isogenic C-terminal <i>rocA</i> polymorphism strains; BamHI site underlined	(25)
rocA-T442P-seq	CCAACTTGGCAAAGCTGAAATTTTAACTCTAGC	Sanger sequencing V420I, T442I, and Q443* RocA mutations	(25)